

# Notional Permeability of breakwaters

*“Experimental research on the permeability factor  $P$ ”*



**Msc. Thesis**

Author: ing. Rémon Kik  
Date: 19 September 2011  
Version: 1.3



# Notional Permeability of breakwaters

*“Experimental research on the permeability factor  $P$ ”*

**Author:**

ing. R. Kik

**Date:**

19/09/2011

**Committee:**

Prof. dr. ir. M.J.F. Stive

Prof. dr. ir. W.S.J. Uijtewaald

ir. H.J. Verhagen

ir. J.P. van den Bos

dr. ir. J.W. van der Meer

ir. J. Maertens

**Commissioned by:**

Royal Boskalis Westminster N.V.

Hydronamic

Rosmolenweg 20

3350 AE Papendrecht

**Studentnumber:**

1539566

**Company:**

TU Delft

TU Delft

TU Delft

Royal Boskalis Westminster / TU Delft

Van der Meer consulting

DEME

**Educational institute:**

TU Delft Faculty Civil Engineering

Department of Hydraulic Engineering

Stevinweg 1

2628 CN Delft



## Preface

You are about to read the final closure works of my study Civil Engineering at the Technical University of Delft. This master thesis with the subject Notional Permeability was commissioned by Boskalis Westminster n.v. and was executed both at the head office of Boskalis at Papendrecht and at the Laboratory of Fluid Mechanics of the Faculty of Civil Engineering and Geo sciences.

The experiment were conducted together with Dimitrios Papadopoulos who investigated the measure of spreading in accuracy of repetitive tests with respect to the occurring damage. I would like to thank Dimitrios for his help of rebuilding and measuring the breakwater several times a day for about two months. His help made it possible to conduct almost twice as much tests as was originally planned.

Furthermore I would like to thank all the members of the graduation committee for taking the time to read and point out points of improvement of this thesis.

Finally I would like to thank my parents, brothers and sister, girlfriend and friends who supported me during my entire study period. A period, especially after starting the Master phase in Delft, of long and laborious hours of studying in the Royal Library at The Hague. Special thanks to Erwin and Christiaan who joined me during these weeks of studying at the Royal Library and made it a lot more fun.



## Abstract

All over the world manmade structures are built to protect coastal areas. Some of these structures are revetments, breakwaters and groins. These coastal structures often consist of natural rock (when present in the vicinity) to withstand the impact of waves. These structures are often constructed in different layers with different properties. Within this research the stability of rock slopes and its under layers is investigated.

Different layer design of a rock slope has a big effect on the loads on the rock slope itself. In the stability formula developed by Van der Meer in 1988 this effect is represented by the term "Notional Permeability". A more open, or permeable, structure has the ability to dissipate more wave energy and therefore requires less weight of the outer layer. The influence of this parameter is thus very important in economic sense. Up until now only 3 configurations have been tested. In practice often intermediate structures were designed which do not correspond to the standard situations. Therefore there is the demand for more values of the notional permeability representing other structures.

Producing other values for the notional permeability can be done in two ways. Namely by determining it with means of a theoretical model or by determining it empirically thus by means of scale model tests. A theoretical model recently developed is the Volume Exchange model of Jumelet. This model describes the interaction of fluids between the incoming wave and the structure. The wave run up in combination with the water containment capacity of the structure was assumed to be a measure of the notional permeability of the structure. However this model is not yet complete and not yet validated with new structures. Within this study the second method, determining the value empirically is used.

When conducting physical scale model tests scaling laws have to be taken into account. Basically these scaling laws can be subdivided into three main laws. The first one is the geometrically scaling, which implies that all the length scales must be scaled with the same factor to guarantee a geometrically undistorted model. The second requirement is that the Froude number, representing the ratio between gravitational forces and the inertial forces, must be the same. The third requirement is that the Reynolds number, representing the ratio between viscous and the inertial forces, must be in the same order as the prototype. It is however impossible to achieve both the Froude and the Reynolds scaling at the same time, therefore it is said that the scaling effects are neglectable when the flow is still considered turbulent, which is the case in real life breakwaters. Scaling down the breakwaters can have the effect that internal flow inside the core reduces to laminar flow. Burcharth proposed a method to scale the core with a different factor in comparison to the entire structure to ensure turbulent flow inside the core.

One of the most important parameters in the Van der Meer stability formulae is the Iribarren number, sometimes also described as the breaker parameter. Which describes the way a wave reacts when it encounters a structure, this is done on the basis of wave steepness and slope of the structure. During the experiments a variation in wave steepness and therefore Iribarren number is applied to investigate the behaviour of the structure under these circumstances.

To arrive at a value for the notional permeability all the variables in the formulae were fixed or measured, resulting in one unknown value, namely the notional permeability. The damage was determined by measuring the initial and the final profile every 5 cm. When these profiles were averaged and subtracted from each other the total eroded surface was determined, dividing this eroded area by the cross sectional area of one single representative armour unit results into the damage number  $S$ . The performance of the stability formula with a specific value of the notional permeability was assessed by comparing the calculated damage with the actual measured damage. The difference was squared and summed, at the end the squared root of this summed value was taken ending up with a value also known as the root mean squared error. The value for which this difference between measured and calculated damage was lowest was considered to be the best value for the notional permeability.

First of all two reference structures were tested to ensure that the test method and the method of analysis result into the same value for the notional permeability as defined by Van der Meer. The first structure was a structure with a permeable core, which according to Van der Meer has a value of  $P=0.5$ . After analysis of the tests executed within this study a value of  $P=0.55$  was found. The second structure had an impermeable core and therefore a very low permeability. According to Van der Meer the value of the notional permeability is 0.1. After the tests a value of  $P=0.08$  was found. Overall the conclusion was drawn that the method of testing and analysis results in similar outcomes as the research of Van der Meer in 1988. Therefore it is safe to draw conclusions from similar tests on new structures.

This new structure consists out of an impermeable core, covered by a thick filter layer with a relatively small stone size, followed by a coarse filter layer and finally an armour layer. This structure represents the real life situation in which a core of sand is placed and covered by a geo-textile. Then quarry run is used to create the desired slope of the structure and the coarser filter layer is used to make the filter geometrically closed. Finally, like all the other structures, the double armour layer is used to withstand the wave impact. After conducting all the tests on the 1:2 slope the analysis showed a value for the notional permeability of  $P=0.37$ . Because only a limited number of tests on only one slope angle have been conducted it is advised to use the value of  $P=0.35$  for design practice, until further data is available.

Together with the profile and wave measurements also recordings were made of the pressure differences inside the structure and the wave run up below the armour layer. The aim was to gain insight into the processes that play a role when considering the notional permeability of a specific structure. Broekhoven showed in his research that the theoretical model to describe the notional permeability should be based on the wave run up below the armour layer. Therefore this parameter was measured during all the tests. It was however not possible to derive the value of  $P$  on the basis of these measurements because of the fact that they were executed with irregular waves. The reference run up level to which the run up of a more permeable structure was compared to was not able to produce correct results for the irregular wave spectra. The pressure difference was hard to analyse under irregular wave conditions. The regular waves applied on the third structure did give some additional information regarding the water motion inside the structure. The flow in the armour layer and the first filter layer appeared to be turbulent, in the last filter layer close to the impermeable core there was hardly any motion observed. This could possibly induce scaling effect regarding the Reynolds scaling.

Besides the Van der Meer formula, which requires more detailed information about the structure and hydraulic loads, there is the much older stability formula of Hudson. This formula uses a lot less parameters and is therefore considered to be much easier to apply, but also considered to be much less acute as compared to the Van der Meer formula. Within this study also a comparison is made between the two formulae, but now introducing a different coefficient representing the permeability of the structure. Using three different coefficients for the three different structures gave similar results with respect to the accuracy as the Van der Meer formula. When applied to the tests conducted by Van der Meer on other slopes than the 1:2 slopes the deviation became larger. This indicates that the slope effect of Hudson formula is not well represented.



# Contents

1.	Introduction.....	1
1.1	Problem definition .....	3
1.2	Objective .....	3
1.3	Structure of report .....	3
2.	Literature review .....	4
2.1	Background of the Notional Permeability .....	4
2.1.1	Basics of armour layer stability .....	4
2.1.2	Van der Meer in detail .....	10
2.2	Scaling laws .....	18
2.2.1	Geometrical scale .....	18
2.2.2	Froude scale .....	19
2.2.3	Reynolds scale.....	19
2.2.4	Porous flow .....	20
2.2.5	Burcharth .....	25
2.2.6	Conclusion.....	27
2.3	Hypotheses about the Notional Permeability .....	28
2.3.1	Volume exchange model .....	28
2.3.2	Numerical HADEER model .....	32
3.	Test matrix .....	33
3.1	Environmental variations .....	33
3.1.1	Surging/plunging.....	33
3.1.2	Duration .....	33
3.1.3	Spectral shape.....	33
3.1.4	Wave height/ period.....	34
3.2	Structural variations.....	35
3.2.1	Type of structures .....	35
3.2.2	Layer thickness.....	36
3.2.3	Slope angle.....	36
3.2.4	Grading rock.....	36
3.2.5	Final model designs .....	37
3.3	Combined test matrix.....	38
3.4	Test equipment .....	40
3.4.1	Wave flume.....	40
3.4.2	Measuring damage .....	40

3.4.3	Measuring core velocity.....	41
3.4.4	Wave measurements.....	42
3.4.5	Wave run up .....	42
4.	Data analysis: damage level.....	43
4.1	Determine damage level .....	43
4.2	Structure 1 .....	47
4.2.1	Conclusion.....	50
4.3	Structure 2 .....	51
4.3.1	Conclusion.....	53
4.4	Structure 3 .....	54
4.4.1	Conclusion.....	56
4.5	Repetition tests .....	57
4.6	Stone balance.....	58
5.	Additional data .....	59
5.1	Wave run up.....	59
5.2	Pressure distribution .....	64
6.	Discussion .....	69
6.1	P as a function of the Iribarren number.....	69
6.2	Other stability formulae .....	75
6.2.1	Hudson type formula .....	75
6.2.2	Van Gent formula .....	78
7.	Conclusions and recommendations.....	82
7.1	Conclusions .....	82
7.2	Recommendations .....	84
7.3	Points of attention .....	86
	References .....	87
Appendix A	Rock properties	
Appendix B	Calibration and signal data	
Appendix C	Method of determining damage level	
Appendix D	Test planning	
Appendix E	Damage lines per test	
Appendix F	Specifications Laser and Echo sounder	

## List of figures

Figure 1 Typical rubble mound breakwater.....	1
Figure 2 Notional permeability as described by VAN DER MEER [1988].....	2
Figure 3 Schematization as by Iribarren [1938] From Breakwaters & Closure dams 2009 .....	4
Figure 4 Breaker type based on Iribarren number .....	9
Figure 5 Tested structure by VAN DER MEER [1988] with impermeable core .....	12
Figure 6 Tested structure by VAN DER MEER [1988] with permeable core .....	12
Figure 7 Tested structure by VAN DER MEER [1988] homogenous structure .....	12
Figure 8 Concept of damage.....	13
Figure 9 Results of VAN DER MEER [1988] with different notional permeabilities.....	16
Figure 10 Influence of permeability coefficient on armour layer design .....	17
Figure 11 Flow regimes in porous media FROM Burcharth and Andersen [1995] .....	20
Figure 12 Contribution of coefficients by Van Gent [1993].....	21
Figure 13 Core pressures by BURCHARTH.....	25
Figure 14 pressure distribution in the breakwater core.....	26
Figure 15 Locations of pressure calculations from Burcharth [1999].....	26
Figure 16 Pore velocities.....	27
Figure 17 Scheme volume exchange model from Jumelet 2010.....	28
Figure 18 Results HADEER model from Van der Meer [1988] .....	32
Figure 19 Resulting P by Van der Meer [1988] .....	32
Figure 20 Scatter plot measured/calculated damage with P=0.5 data of Van der Meer[1988].....	35
Figure 21 Scatter plot measured/calculated damage with P=0.6 data of Van der Meer[1988].....	35
Figure 22 Damage vs. Iribarren for different permeabilities .....	37
Figure 23 Test structure 1, P=0.5.....	39
Figure 24 Test structure 2, P=0.1.....	39
Figure 25 Test structure 3, P=0.3.....	39
Figure 26 Measuring below water level with echo-sounder .....	40
Figure 27 Measuring profile above water line with laser .....	40
Figure 28 Location of pressure difference gauges.....	41
Figure 29 Laser and Echo sounder of one cross section .....	44
Figure 30 Combined and corrected signal of one cross section .....	44
Figure 31 3d presentation of a measured structure.....	44
Figure 32 Average profiles discrete .....	45
Figure 33 Average profiles continuous .....	45
Figure 34 $S_{\text{calculated}}/S_{\text{measured}}$ plot structure 1 P=0.55 .....	48
Figure 35 Measured stability structure 2 with Van der Meer formula P=0.55.....	49
Figure 36 $S_{\text{calculated}}/S_{\text{measured}}$ plot structure 2 P=0.08 .....	52
Figure 37 Measured stability structure 2 with Van der Meer formula p=0.08.....	53
Figure 38 $S_{\text{calculated}}/S_{\text{measured}}$ plot structure 3 P=0.37 .....	55
Figure 39 Measured stability structure 3 with Van der Meer formula p=0.37.....	56
Figure 40 Results damages repetition tests Papadopoulos.....	57
Figure 41 location of the run-up gauge .....	59
Figure 42 Run-up under armour layer test#4 .....	60
Figure 43 cumulative distribution function wave run up test#4 .....	60
Figure 44 Measured wave run-up below the armour layer T=3.2s .....	62
Figure 45 Measured wave run-up below armour layer .....	63
Figure 46 Location of pressure gauges .....	64
Figure 47 Pressure difference in time T=3.2s .....	65
Figure 48 Pressure differences in time T=1.2s.....	65
Figure 49 Measured pressure differences inside structure 3 T=1.2s.....	66
Figure 50 Measured pressure difference inside structure 3 T=3.2s .....	66
Figure 51 H max regular waves T3.2.....	68
Figure 52 H min regular waves T3.2 .....	68
Figure 53 H min regular waves T1.2 .....	68
Figure 54 H max regular waves T1.2.....	68

Figure 55 P as a function of Iribarren .....	71
Figure 56 Energy scheme from JUMELET 2010 .....	72
Figure 57 Measured reflection coefficient .....	74
Figure 58 Stability Hudson with difference $K_D$ values. Slope 1:2 .....	76
Figure 59 Stability Hudson with difference $K_D$ values. Slope 1:1.5 ~ 1:6 .....	77
Figure 60 Comparison different stability formulae .....	79
Figure 61 $S_{\text{calculated}} / S_{\text{measured}}$ for impermeable structures comparison Van Gent and Van der Meer formulae ...	80
Figure 62 $S_{\text{calculated}} / S_{\text{measured}}$ for permeable structures comparison Van Gent and Van der Meer formulae .....	80
Figure 63 $S_{\text{calculated}} / S_{\text{measured}}$ for all structures comparison Modified Van Gent, original Van Gent and Van der Meer formulae.....	81

## List of tables

Table 1 Iribarren friction and N parameters From BREAKWATERS & CLOSURE DAMS [2009] .....	6
Table 2 Considered parameters by Van der Meer [1988] .....	10
Table 3 Executed tests by Van der Meer [1988] .....	11
Table 4 Tested slopes by Van der Meer.....	11
Table 5 Damage number with actual state from VAN DER MEER [1988] .....	13
Table 6 Flow regimes on the basis of $Re_p$ .....	22
Table 7 Summarized flow constants from Troch [2000].....	23
Table 8 Flow constants from Burcharth and Christensen.....	23
Table 9 Stone dimension and ratios needed .....	37
Table 10 Test matrix .....	38
Table 11 Test data structure 1 with calculated results for $P=0.5$ .....	47
Table 12 Statistical performance Van der Meer formula for different P values structure 1 .....	48
Table 13 Test data structure 2 with calculated results for $P=0.1$ .....	51
Table 14 Statistical performance Van der Meer formula for different P values structure 2 .....	51
Table 15 Test data structure 3 with calculated results for $P=0.3$ .....	54
Table 16 Statistical performance Van der Meer formula for different P values structure 3 .....	54
Table 17 Spreading of repetition test .....	58
Table 18 Measured run up 2% and significant below armour layer structure1 .....	61
Table 19 Measured run up 2% and significant below armour layer structure2 .....	61
Table 20 Measured run up 2% and significant below armour layer structure3 .....	62
Table 21 Measured run-up below armour layer with calculated $Cr$ and $P$ for regular waves .....	63
Table 22 Pressure and velocities structure 3 regular waves $H=0.1$ $T=3.2$ .....	67
Table 23 Pressure and velocities structure 3 regular waves $H=0.1$ $T=1.2$ .....	67
Table 24 $P$ determined for each individual test structure 1 .....	69
Table 25 $P$ determined for each individual test structure 2 .....	70
Table 26 $P$ determined for each individual test structure 3 .....	70
Table 27 Mean and standard deviation of $P$ , data Kik[2011] .....	70
Table 28 Measured reflection coefficients structure 1 .....	72
Table 29 Measured reflection coefficients structure 2 .....	73
Table 30 Measured reflection coefficients structure 3 .....	73
Table 31 Wave height factor as a function of damage: From Rock Manual 2007 .....	75
Table 32 Modified coefficients Van der Meer formulae .....	78
Table 33 Statistical performance stability formulae.....	79

## List of symbols

### Greek symbols

$\alpha$	Slope angle
$\alpha_f$	Laminar flow constant
$\beta$	Turbulent flow coefficient
$V_{Ru}$	Core run up factor
$V_{cr}$	Reduction coefficient Cr
$\Delta$	Relative density
$\delta$	Damping coefficient
$\lambda$	Scale factor
$\mu$	Friction factor
$\nu$	Dynamic viscosity
$\xi$	Iribarren number
$\rho_s$	Density of rock
$\rho_w$	Density of water
$\phi$	Natural angle of repose
$\psi$	Angle of wave attack
$\kappa$	Spectral shape

### Roman symbols

$A_{eroded}$	Total eroded area
$b$	Turbulent Forchheimer constant
$c$	Time dependent Forchheimer constant
$C_{pl}$	Plunging waves constant Van der Meer
$C_r$	Run up reduction coefficient
$C_s$	Surging waves constant Van der Meer
$D$	Seepage length coefficient
$d_{50}$	Mean stone size diameter
$d_{n50}$	Mean nominal stone size diameter
$Fr$	Froude number
$g$	Gravitational acceleration
$H$	Wave height
$I$	Hydraulic gradient
$k$	Permeability
$KC$	Keulegan-Carpenter number
$K_D$	Hudson coefficient
$L$	Wave length
$l$	Length
$L'$	Wavelength inside the core
$N$	Number of waves

$n$	Porosity
$N_i$	Dustbin coefficient Iribarren
$P$	Notional permeability
$q$	Flow
$R_c$	Crest height
$Re$	Reynolds number
$RU_{;c}$	Run up at the core
$RU_{2\%;c}$	Run up at the core exceeded by 2%
$RU_{;c;imp}$	Run up at the core, impermeable core
$RU_{;c;r}$	Run up at the core, with friction and inflow
$RU_{;s;f}$	Run up at surface with friction
$RU_{;s;r}$	Run up at surface with friction and inflow
$S$	Damage number
$s$	Wave steepness
$T$	Wave period
$t_a$	Thickness of armour layer
$u$	Velocity
$V_{b;1}$	Internal volume capacity
$V_{b;2}$	Volume forced into the core by waves
$V_{b;N}$	Resulting internal volume
$V_{ru}$	Volume run up wedge
$W_c$	Crest width
$x$	Horizontal distance
$X_i$	Calculated results
$Y_i$	Measured results

## Abbreviations

BIAS	Mean difference between measured and calculated value
MAE	Mean absolute error
RMSE	Root mean squared error
VEM	Volume exchange model

## 1. Introduction

When looking at coastlines all around the world one can immediately recognize numerous of manmade interventions, all trying to exploit certain properties of the coastal area. One of these structures is a breakwater, which is often used to protect ports from wave attack and to serve as a method to influence the sediment distribution along a coastline.

Breakwaters come in different types and sizes. According to structural features we can subdivide the breakwaters into different categories:

**Mound types (stable or dynamic):** consist out of a large heap of loose elements like: gravel, quarry stone or concrete elements. For the design of stable breakwaters little movement of the armour units is allowed. This is contrary to the dynamic breakwater, which is based on the idea that with some extra quantity of materials the breakwater can reshape its profile under extreme conditions.

**Monolithic types:** consist out of one single element, for instance a caisson.

**Composite types:** this is a combination of mound type and monolithic type breakwaters.

**Special types:** one should think of floating or pneumatic breakwaters.

Within this study the statically stable rubble mound type breakwater is considered.

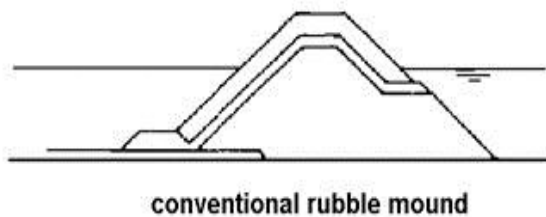


Figure 1 Typical rubble mound breakwater

For the design of the armour layer of randomly placed rubble mound breakwaters usually the choice is made between two formulas; the Hudson formula which is the result of studies in 1953, 1959 and 1961, or the other one which is the well-known formula of Van der Meer introduced in 1988. The Hudson type formulae is, besides natural rock, also used for the design of breakwaters consisting of concrete elements.

The Van der Meer formula has a lot of differences with respect to the Hudson formula. The main difference is in the number of coefficients used, which indicates that the Van der Meer formula is much more detailed. The Van der Meer formula takes the Iribarren number, number of waves and damage level into account. It also contains a factor  $P$  which describes the “notional permeability” of the breakwater. This factor is based on the fact that a more permeable structure dissipates more energy and hence requires less heavy armouring. Its value depends on the different layer designs of the breakwater.

The notional permeability ( $P$ ) was empirically determined by VAN DER MEER [1988] for three different standard situations, to be exact the  $P=0.1$ ,  $P=0.5$  and  $P=0.6$ . The fourth one with a filter layer and a core is determined by interpolation of the tested configurations ( $P=0.4$ ). The figure below shows these four standard situations.

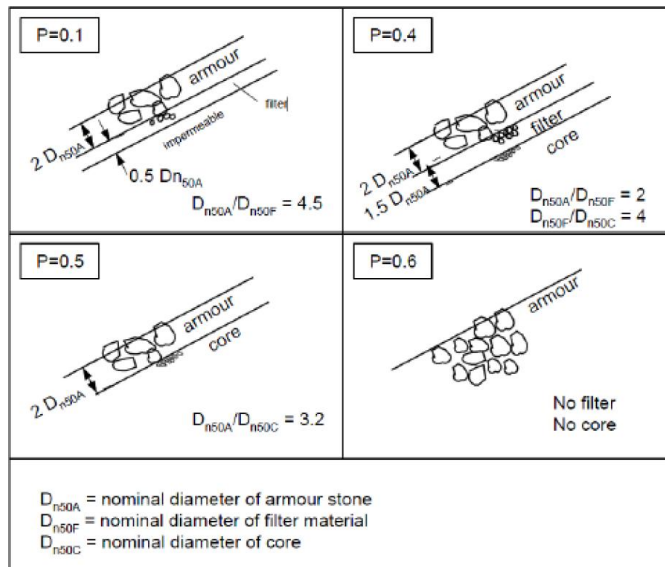


Figure 2 Notional permeability as described by VAN DER MEER [1988]

In practice however these standard situations from the figure above do not always apply. Often intermediate configurations between the first and the second are designed (structures with a thick filter layer and an impermeable core with geo-textile) which do not completely correspond with one of the four standard configurations for which the  $P$  value is known. Despite the fact that the influence of the permeability of the structure is very large, there is still no easy way to calculate the notional permeability of a given cross-section of a rubble mound breakwater.



## 1.1 Problem definition

At this moment the notional permeability for only four situations is given. In practice these situations not always occur.

The problem definition is:

*“How to determine the notional permeability of a given cross-section of a rubble mound breakwater?”*

## 1.2 Objective

Considering the topic regarding the notional permeability the distinction can be made between the long term objective and the objective achievable within this specific thesis. The main “overall” objective is to provide a physically based method to easily determine the permeability coefficient of an arbitrary cross section.

To arrive at this point however smaller steps have to be taken. In the past there have been some studies regarding a hypothesis to describe the coefficient analytically, but these hypotheses aren’t proven yet.

At this moment only three structures are known and a fourth one is assumed. To gain more insight into the matter and to provide more data for a possible calculation method it is valuable to have a bigger data set. Furthermore it is useful for practical situations to know what the P value of an often applied structure is.

Within this study the method to determine the notional permeability coefficient empirically is investigated.

In other words the goal is:

*“To come up with and execute an experiment plan to empirically determine the notional permeability for situations other than the three known situations”*

## 1.3 Structure of report

At the beginning of this master thesis a literature study was carried out, in this literature study the basics of breakwater stability is discussed and the recent studies regarding the notional permeability were summarized. Besides this it also contains the governing scaling rules to be used for physical scale modelling of hydraulic structures. All the relevant items from this literature study can be found in chapter 2 of this report.

In chapter 3 the focus is on the physical modelling. The test location will be described, and a detailed work method for the tests is elaborated. Furthermore the test matrix with all the executed tests will be given.

In the fourth chapter of this report the results of the executed test will be presented. The results will be analysed on; the functionality of the test method and the effects of the variables on the notional permeability.

The fifth chapter is devoted to the additional data, besides the damage, measured during this study. The additional data consists out of the pressure distribution in the structure and the wave run up below the armour layer.

After that a discussion chapter involving the basics of the current theories regarding breakwater stability can be found. At the end of this report the conclusions and recommendations can be found.

## 2. Literature review

### 2.1 Background of the Notional Permeability

In this section the background of the notional permeability is discussed. First of all the basics of stability formula of armour layer design is given. After that, the improvements of the stability formula done by VAN DER MEER [1988] are presented and the term “*Notional permeability*” is introduced. Finally the notional permeability will be further elaborated, one should think of the influence on the stability, the way to determine its value and the parameters which can have an influence on the notional permeability.

#### 2.1.1 Basics of armour layer stability

##### *Iribarren*

The first one who mathematically tried to describe the physical processes that take place on a rock slope was IRIBARREN in [1938].

He considered rocks on a slope and described four forces that would govern the stability of the armour layer.

- Weight of the armour unit
- Buoyancy of the armour unit
- Wave forces (lift and drag)
- Friction forces

The stability formula is the result of a force balance of the above mentioned forces.

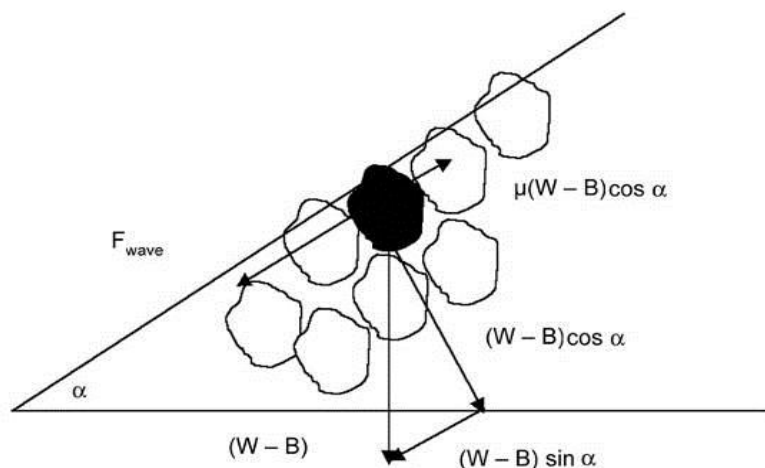


Figure 3 Schematization as by Iribarren [1938] From Breakwaters & Closure dams 2009

Iribarren assumed the following relation to express the wave forces on the armour blocks.

$$F_{wave} = \rho_w g d_n^2 H \quad 2-1$$

The weight of one block is:

$$W = d_n^3 \rho_s g \quad 2-2$$

The submerged weight of a block then becomes:

$$W - B = (\rho_s - \rho_w) d_n^3 g \quad 2-3$$

To assure stability the wave force must be smaller than the sum of the friction and the gravity forces. Iribarren split the process of wave attack into two components, namely the up rush and the down rush. For the down rush the stability condition becomes:

$$F_{wave} < (\mu((W - B) \cos \alpha - (W - B) \sin \alpha)) \quad 2-4$$

$$\rho_w g d_n^2 H < ((\rho_s - \rho_w) d_n^3 g (\mu \cos(\alpha) - \sin(\alpha))) \quad 2-5$$

In term of block weight the requirement becomes:

$$W > \frac{H^3 \rho_s g}{\Delta^3 (\mu \cos(\alpha) - \sin(\alpha))} \quad 2-6$$

Iribarren introduced a dustbin coefficient N which takes other influences into account who are not described explicitly in the formulae. The original stability formulae of Iribarren are:

$$W > \frac{N \rho_s H^3 g}{\Delta^3 (\mu \cos(\alpha) - \sin(\alpha))} \quad \text{(down rush)} \quad 2-7$$

$$W > \frac{N \rho_s H^3 g}{\Delta^3 (\mu \cos(\alpha) + \sin(\alpha))} \quad \text{(up rush)} \quad 2-8$$

The modern presentation of the formulae in terms of  $\frac{H}{\Delta d_n}$  results into the following equations for stability:

$$\frac{H}{\Delta d_n} < N_i(\mu \cos \alpha - \sin \alpha) \quad (\text{down rush}) \quad 2-9$$

$$\frac{H}{\Delta d_n} < N_i(\mu \cos \alpha + \sin \alpha) \quad (\text{up rush}) \quad 2-10$$

In which:

H	=	wave height	[m]
$\Delta$	=	relative density ( $\rho_s - \rho_w / \rho_w$ )	[-]
$\rho_s$	=	density of rock	[kg/m <sup>3</sup> ]
$\rho_w$	=	density of water	[kg/m <sup>3</sup> ]
$d_n$	=	characteristic size of stone	[m]
$N_i$	=	dustbin coefficient	[-]
$\mu$	=	friction factor	[-]
$\alpha$	=	angle of slope	[-]

The factor N is determined experimentally and represents things like the shape of the blocks and all the other influences not explicitly named in the formula.

The friction factor  $\mu$  depends on the natural angle of repose of the material.

$$\mu = \tan(\varphi) \quad 2-11$$

IRIBARREN [1965] recommended the following values for  $\mu$  and  $N_i$ , taken from BREAKWATERS & CLOSURE DAMS [2009].

	$\mu$	N
<b>Downward stability</b>	2.38	0.430
<b>Upward stability</b>	2.38	0.849

**Table 1 Iribarren friction and N parameters From BREAKWATERS & CLOSURE DAMS [2009]**

In the report of DE HEIJ [2001] it is mentioned that the transition slope is 1:3.64. For slopes steeper than this value the downward stability has to be considered, milder slopes should be calculated using the upward stability relation.

**Hudson**

HUDSON [1953] did a comparable research and found the following relation for the stability of rubble mound slopes.

$$W \geq \frac{\rho_s g H^3}{K_D \Delta^3 \cot(\alpha)} \quad 2-12$$

Written in terms of  $\frac{H}{\Delta d_n}$  the relation becomes:

$$\frac{H}{\Delta d_n} = \sqrt[3]{K_D \cot \alpha} \quad 2-13$$

The original experiments were carried out with regular waves. When applied for a significant wave height the SHORE PROTECTION MANUAL edition [1984] describes that the formula becomes:

$$\frac{H_s}{\Delta d_n} = \sqrt[3]{(K_D \cot \alpha)} * \frac{1}{1.27} \quad 2-14$$

In which:

$K_D$  = dustbin factor of Hudson [-]

However  $K_D$  is more detailed described than the  $N$  in the Iribarren formula but it still has a lot of shortcomings for a good breakwater design. The main item missing in the above formulae is the lack of the influence of the wave period. Furthermore there is no clear definition of damage and it has a limited range of slope angles of which the formula is valid ( $\cot 1.5 \sim 4$ ).

### Van der Meer

In 1988 Van der Meer conducted another research to the subject of rock slope stability under wave attack. He tried to link the environmental parameters and the structural parameters to finally predict the damage that will occur to the initial profile of the breakwater.

First of all Van der Meer described variables that possibly could play a role in the stability of the breakwater. Afterwards these variables were presented in a dimensionless way and an extensive amount of tests were carried out to cover a wide range of conditions as possible. With the physics of the occurring processes in mind a method of curve fitting was applied to describe the observed damage.

The method used by Van der Meer is a so called a grey-box method. Parts of the load and strengths are known but not fully understood like in a white-box method on the other hand it is not completely unknown like in a black-box method.

With means of curve fitting the acquired data was used to formulate relations for statically stable rock slopes.

Finally it led to the following two original versions of the stability relations:

$$\frac{H_s}{\Delta d_{n50}} = 6.2 P^{0.18} \left( \frac{S}{\sqrt{N}} \right)^{0.2} \xi_m^{-0.5} \quad (\text{plunging waves}) \quad 2-15$$

$$\frac{H_s}{\Delta d_{n50}} = 1.0 P^{-0.13} \left( \frac{S}{\sqrt{N}} \right)^{0.2} \xi_m^P \sqrt{\cot a} \quad (\text{surging waves}) \quad 2-16$$

The transition between the two formulae is according to the following relation found by VAN DER MEER [1988].

$$\xi_{critical} = \left( 6.2 * P^{0.31} \sqrt{\tan(\alpha)} \right)^{\frac{1}{P+0.5}} \quad 2-17$$

If  $\xi_m < \xi_c \rightarrow$  formula 2-15

If  $\xi_m > \xi_c \rightarrow$  formula 2-16

In modern literature (ROCK MANUAL [2007] and BREAKWATERS AND CLOSURE DAMS [2009]) the stability formulae are often written with the coefficients 6.2 and 1.0 as the stochastic variables  $c_{pl}$  and  $c_s$ .

$$\frac{H_s}{\Delta d_{n50}} = c_{pl} P^{0.18} \left( \frac{S}{\sqrt{N}} \right)^{0.2} \xi_m^{-0.5} \quad (\text{plunging waves})$$

$$\frac{H_s}{\Delta d_{n50}} = c_s P^{-0.13} \left( \frac{S}{\sqrt{N}} \right)^{0.2} \xi_m^P \sqrt{\cot a} \quad (\text{surging waves})$$

The transition relation is then described as:

$$\xi_{critical} = \left( \frac{c_{pl}}{c_s} * P^{0.31} \sqrt{\tan(\alpha)} \right)^{\frac{1}{P+0.5}} \quad 2-18$$

In which:

$H_s$	=	Significant wave height
$C_{pl}$	=	Parameter for plunging waves $\mu = 6.2$ $\sigma = 0.4$
$C_s$	=	Parameter for surging waves $\mu = 1.0$ $\sigma = 0.08$
$P$	=	Notional permeability
$S$	=	Damage number
$N$	=	Number of waves
$\xi_m$	=	$\frac{\tan(\alpha)}{\sqrt{s_m}}$ Iribarren number or Breaker parameter
$s_m$	=	Wave steepness calculated with the mean wave period

Van der Meer was also the first one who made a distinct difference between two types of breaking waves with respect to the stability of the breakwater. Namely plunging and surging waves. The classification between the different types of breaking waves is made on the basis of the Iribarren number, which on its turn depends on the wave steepness and the slope of the structure. In the figure below the different breaker types are shown. Up until  $\xi < 3$  the waves are considered to be plunging, above this value one can speak of surging waves.

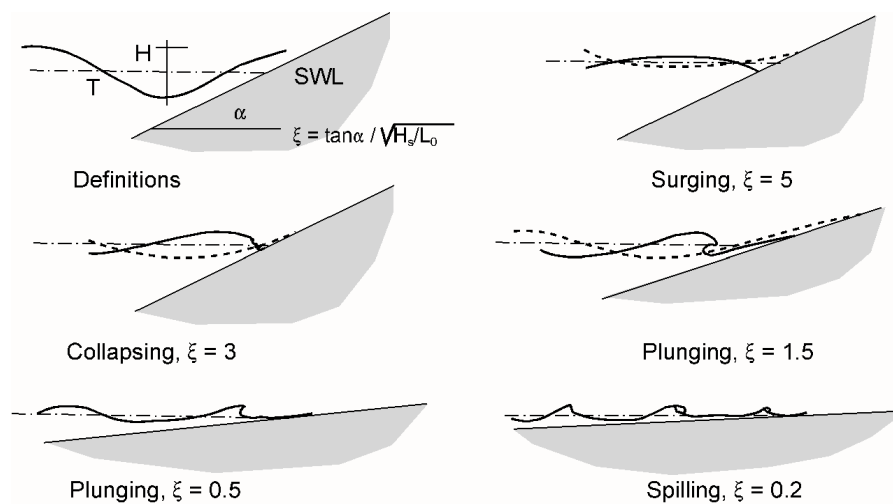


Figure 4 Breaker type based on Iribarren number

### 2.1.2 Van der Meer in detail

As mentioned before Van der Meer first defined a list of variables that could possibly influence the armour layer stability. In order to compare results of different tests and to formulate a relation for the stability which is widely applicable the variables are made dimensionless. Once the variables that could possibly influence the stability are known, then their influence was assessed by means of physical scale model tests. In this section the variables, the method of testing and the found influence will be discussed.

#### Parameters

The parameters affecting the stability of a certain breakwater can be separated into two types; the environmental variables and the structural variables.

Environmental parameters		Structural parameters	
Wave height	$H_s$	Nominal diameter	$d_{n50}$
Wave period	$T_m$	Grading of the stone	$d_{85}/d_{15}$
Spectral shape	$\kappa$	Mass density stone	$\rho_s$
Number of waves	$N$	Natural angle of repose	$\phi$
Angle of wave attack	$\psi$	Shape of the stone	-
Water depth	$h$	Mechanical strength of stone	-
Mass density water	$\rho_w$	Ratio $D_{50\text{armour}}/D_{50\text{filter}}$	-
Kinematic viscosity	$\nu$	Grading of the filter	$d_{85}/d_{15}$
Acceleration of gravity	$g$	Slope angle	$\cot \alpha$
		Thickness of armour layer	$t_a$
		Crest height	$R_c$
		Crest width	$W_c$
		Permeability	$P$
		Construction method	-

Table 2 Considered parameters by Van der Meer [1988]

The final list of governing **dimensionless variables** considered by Van der Meer is:

Wave height parameter	$H_s/\Delta d_{n50}$
Wave-period steepness	$s_m$
and surf similarity parameter	$\xi_m$
Damage with respect to number of waves	$S/N^{0.5}$
Slope angle	$\cot \alpha$
Grading of armour stone	$d_{85}/d_{15}$
Notional Permeability factor	$P$
Spectral shape	$\kappa$
Crest height	$R_c/H_s$



### Test set-up

In order to cover a wide range of different conditions as possible with the study of Van der Meer a lot of different configurations were tested. A lot of apparently similar tests but with one single difference were carried out to determine the influence of the individual parameters. In order to eliminate the effects of scaling some tests are repeated on a larger scale in the Delta flume, if those tests show the same results the scale effects are assumed to be insignificant. In the table below the test matrix of Van der Meer is given.

Slope angle	Grading armour	Spectral shape	Core permeability	Relative mass density	Number of tests	Range $H_s/\Delta d_{n50}$	Range $s_m$
2	2.25	PM	None	1.63	19	0.8-1.6	0.005-0.016
3	2.25	PM	None	1.63	20	1.2-2.3	0.006-0.024
4	2.25	PM	None	1.63	21	1.2-3.3	0.005-0.059
6	2.25	PM	None	1.63	26	1.2-4.4	0.004-0.063
3*	1.25	PM	None	1.62	21	1.4-2.9	0.006-0.038
4	1.25	PM	None	1.62	20	1.2-3.4	0.005-0.059
3	2.25	Narrow	None	1.63	19	1.0-2.8	0.004-0.054
3	2.25	Wide	None	1.63	20	1.0-2.4	0.004-0.043
3*	1.25	PM	Permeable	1.62	19	1.6-3.2	0.008-0.060
2	1.25	PM	Permeable	1.62	20	1.5-2.8	0.007-0.056
1.5	1.25	PM	Permeable	1.62	21	1.5-2.6	0.008-0.050
2	1.25	PM	Homogeneous	1.62	16	1.8-3.2	0.008-0.059
2	1.25	PM	Permeable	0.95	10	1.7-2.7	0.016-0.037
2	1.25	PM	Permeable	2.05	10	1.6-2.5	0.016-0.032
2**	1.25	PM	Permeable	1.62	16	1.6-2.5	0.014-0.031
2***	1.25	PM	Permeable	1.63	31	1.4-5.9	0.010-0.046

Table 3 Executed tests by Van der Meer [1988]

PM	=	Pierson Moskowitz spectrum
*	=	Some tests repeated in Delta flume
**	=	Foreshore 1:30
***	=	Low crested structure with foreshore 1:30

The small scale model test were all executed with the same size armour units  $d_{n50} = 0.036\text{m}$ . The filter material had a diameter of  $d_{n50} = 0.008\text{ m}$  and the core in the case of a permeable core had a diameter of  $0.011\text{ m}$ .

Two different grading widths of the armour layer were applied during the experiments of Van der Meer. The grading width of the filter and core material was kept constant. The filter material used in the experiments had a grading of  $d_{85}/d_{15} = 2.25$ . For the permeable core a grading of  $d_{85}/d_{15} = 1.25$  was used.

In table 3 it can be seen that not every slope- permeability combination is tested. In a clear way this is:

Slope [cot $\alpha$ ]	Structure
1.5	Permeable
2	Homogeneous/Permeable/Impermeable
3	Permeable/Impermeable
4	Impermeable
6	Impermeable

Table 4 Tested slopes by Van der Meer

On the next page the tested structures by Van der Meer can be seen. In all the tests (except the homogeneous structure) a double armour layer is applied.

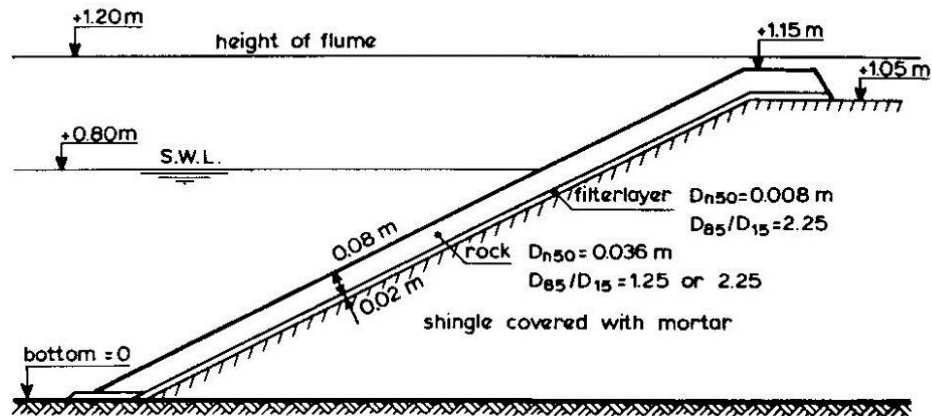


Figure 5 Tested structure by VAN DER MEER [1988] with impermeable core

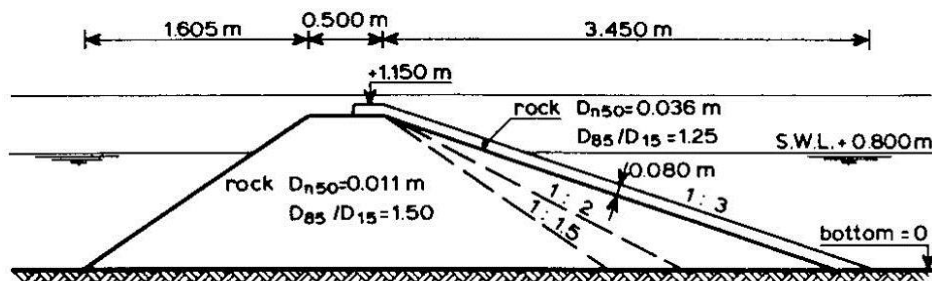


Figure 6 Tested structure by VAN DER MEER [1988] with permeable core

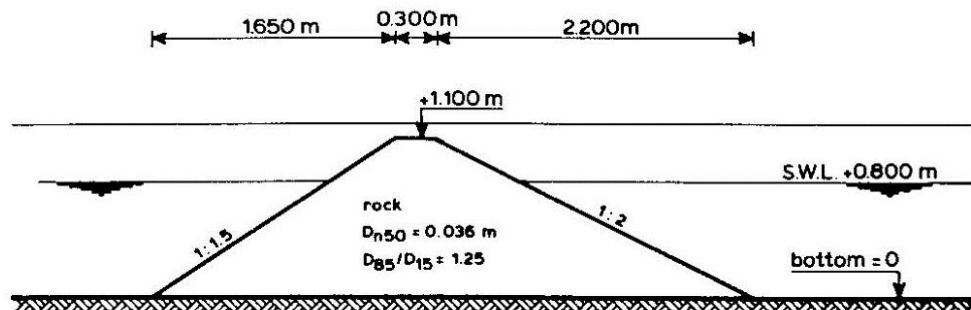


Figure 7 Tested structure by VAN DER MEER [1988] homogenous structure

One can see in the figures above that the thickness of the armour layer tested by VAN DER MEER [1988] is twice the  $d_{50}$  of the armour material. However in Figure 2 with the 4 standard situations of VAN DER MEER [1988] regarding the permeability the layer thickness is described as twice the  $d_{n50}$ . This should in fact be  $2 \cdot d_{50}$ , which with a double armour layer is already common design practice.

### Damage

In the previous sections damage was already mentioned with relation to the stability of rock slopes. Based on the environmental and structural parameters Iribarren and Hudson found a relation for the stability of the armour layer. Stability or just the opposite; failure of the armour layer is a subjective statement. Generally the incipient of motion of an armour unit doesn't necessarily imply failure of the structure. Therefore the damage is divided into different stages of damage/failure. A better way to describe damage is to define it as the amount of displacement. In this way the damage becomes a measurable variable.

There are two common ways to determine damage; to count the number of displaced armour units ( $N_{od}$ ) or to determine the total eroded area  $A_e$ . HUDSON [1559] determined the damage using rods equipped with a circular foot. Also AHRENS [1975] and THOMPSON AND SHUTTLE [1975] used rods to measure the damaged profile. Thomson and Shuttle used the total eroded area to calculate an estimated number of displaced stones, to calculate this damage parameter ( $N_d$ ) the bulk density of the material as placed on the slope and the sieve curve of the stones have to be known. The disadvantage of the method of Thomson and Shuttle is the determination of the bulk density, secondly the use of the sieve curve instead of the actual mass is considered to be a disadvantage. BRODERICK [1984] defined the damage as the eroded area divided by the square of the median stone mass divided by the stone density  $d_{n50}$ . This finally leads to the damage number  $S$ . This definition is also used by VAN DER MEER [1988].

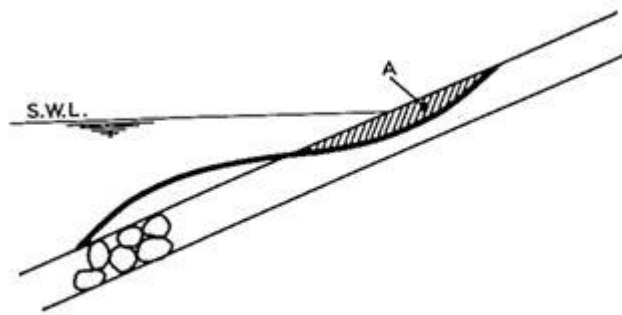


Figure 8 Concept of damage

The theoretical description of damage becomes:

$$S_d = \frac{A_e}{d_{n50}^2} \quad 2-19$$

The damage level  $S$ , with respect to the slope of the structure represents the following visual damage:

Slope	Initial damage (needs no repair)	Intermediate damage (needs repair)	Failure (core exposed)
1:1.5	2	3-5	8
1:2	2	4-6	8
1:3	2	6-9	12
1:4	3	8-12	17
1:6	3	8-12	17

Table 5 Damage number with actual state from VAN DER MEER [1988]

### *Test procedure*

Van der Meer conducted his test at Delft Hydraulics (Deltares) and used a wave flume of 50 m long, 1 m wide and 1.2 m deep. The structure was placed 44 m from the random wave generator, which was equipped with a reflection compensator to avoid the occurrence of standing waves in the basin. In front of the structure two wave gauges were placed  $\frac{1}{4} L$  apart to measure the incident significant wave height, both incoming as well as reflected.

The damage was measured using nine measuring rods each 0.10 m apart, measuring the profile every 0.04 m. The measurements of the nine individual measuring rods were averaged to construct a profile.

Every test consisted out of a series of 3000 waves. The initial profile prior to the test was measured, at 1000 waves an intermediate measurement took place and finally after 3000 waves the final measurement was conducted.

### *Influence of general parameters*

After conducting all the tests mentioned before, Van der Meer analysed the results and found the following influence of the dimensionless parameters. The, for this research, most interesting influence of the permeability will be discussed in the next section.

Below a brief summary of the influences of the variables tested by Van der Meer is given.

The relation of storm duration and damage as described by the parameter  $S/N^{0.5}$  is the result of the study of THOMPSON AND SHUTTLE [1975]. They examined the amount of damage after 1000 waves and kept repeating the measurements up until 5000 waves. This led eventually to a relation describing the influence of the duration by  $S/N^{0.5}$ . Van der Meer found in his test a similar relation and concluded that  $S/N^{0.5}$  is a proper way to describe the influence.

When Van der Meer analysed the combined influence of the wave characteristics and slope angle by plotting the results in an  $H_s/\Delta d_{n50} - \xi_m$  plot, a strong distinction between surging and plunging waves was observed. He explained this by the fact that the fast run up in the plunging region is governing for the stability. In the surging region the run down is the most important contributor for instability. Thus for different Iribarren numbers different processes influence the stability.

Van der Meer tested two different kinds of armour grading, namely a uniform grading ( $d_{85}/d_{15} = 1.25$ ) and a widely graded riprap ( $d_{85}/d_{15} = 2.25$ ), the value of  $d_{n50}$  was used to compare the results. In the resulting damage for two identical configurations but with different grading no significant difference could be discovered.

Also narrow and wide spectral shapes were tested. After analysis no clear difference was found. The only difference was the influence of choosing the mean period or the peak period. In the plots shown by Van der Meer the least amount of difference caused by spectral shape was found when using the mean period.

The effect of the water depth is related to the breaking of waves on the shallow foreshore. In the case of a shallow foreshore waves start breaking which makes a Rayleigh distribution of the waves no longer valid. In these situations the usage of  $H_{2\%}$  gives a better representation of the wave height at the toe of the structure.

The influence of the relative density was determined by testing three different densities. Namely light stones with a density of  $1950 \text{ kg/m}^3$ , normal stones with a density of  $2620 \text{ kg/m}^3$  and heavy stones with a density of  $3050 \text{ kg/m}^3$ . It appears to be that the light and the heavy stones were a bit more stable with respect to the normal density. This was explained by Van der Meer by the fact that the shape did not correspond. The lighter and heavier stones were more angular, which resulted into a higher stability. Overall he concluded that the influence of the mass density was correctly described by  $H_s/\Delta d_{n50}$ .

### Influence of permeability

The most important structural parameter influence in this report is the influence of the permeability. In the research of Van der Meer tests were carried out on three different types of structures. The idea of the permeability of a structure is that it dissipates more energy as the permeability increases and therefore requires less weight for stability of the armour layer. The boundaries of this value thus should be a complete homogenous structure on one hand and a complete impermeable structure on the other hand. Van der Meer conducted tests on three different kind of structures; the earlier mentioned theoretical limits namely the homogenous and impermeable structures and in addition a structure with a permeable under layer.

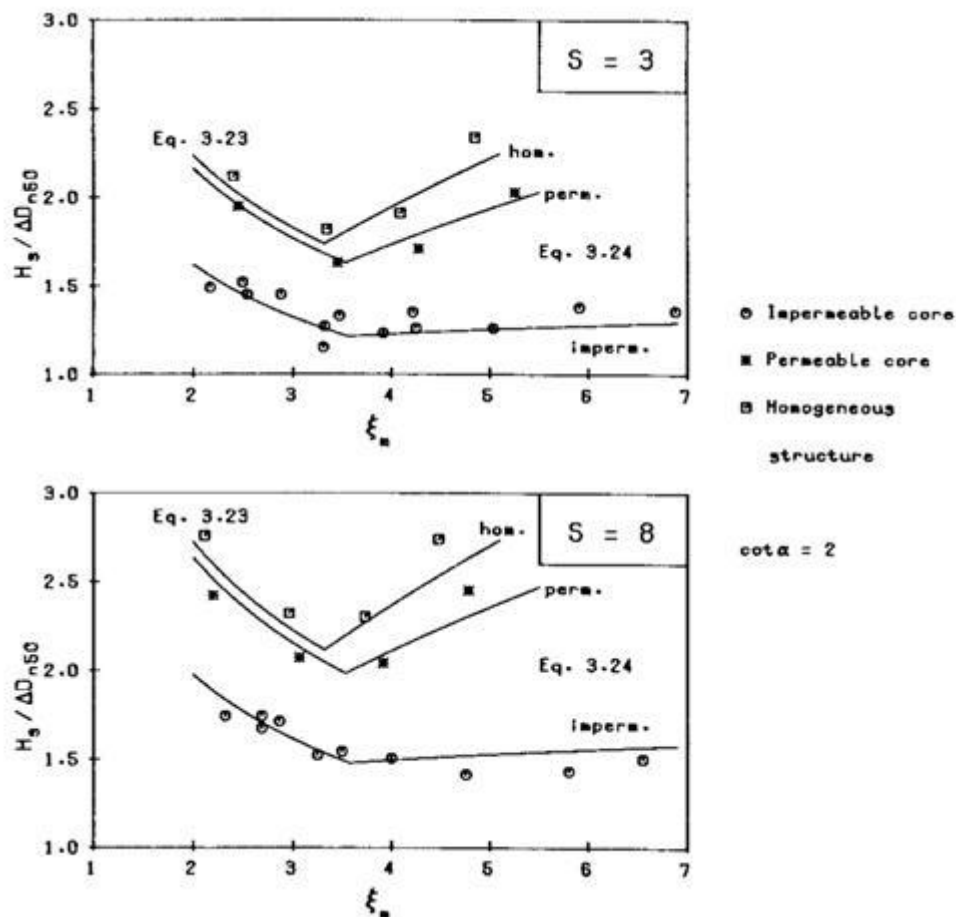
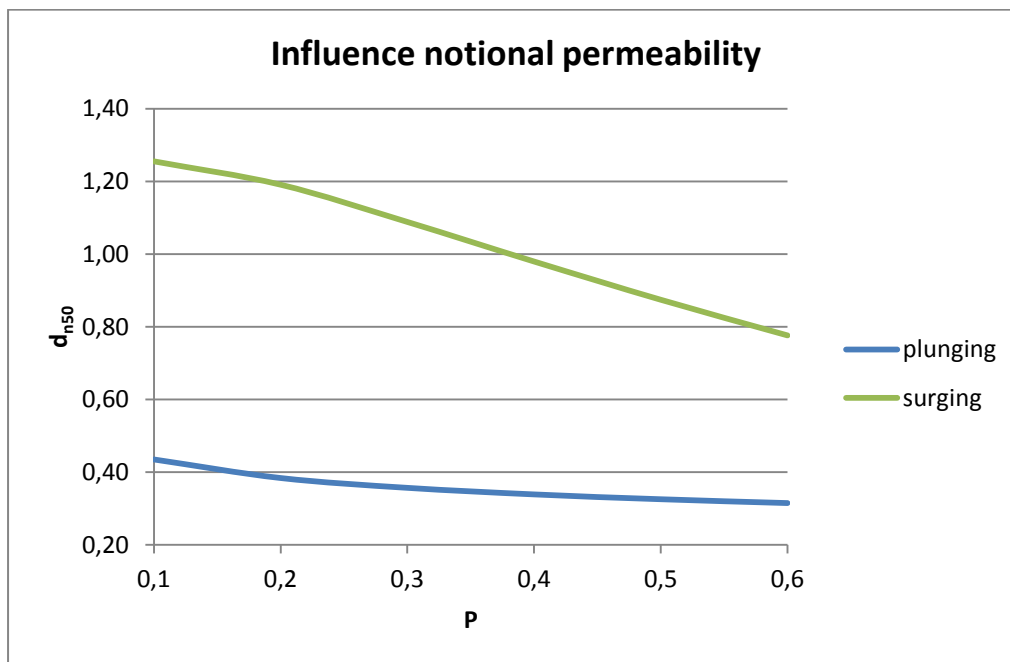


Figure 9 Results of VAN DER MEER [1988] with different notional permeabilities

In the figure above made by VAN DER MEER [1988] we can see the influence of the different permeabilities of the structures. At first sight one can easily recognise that the stability of the permeable structures is higher than the impermeable structure. A second observation that can be made is that the stability increases (in the surging region) when the Iribarren number increases. This is explained by the fact that with surging waves and thus larger periods more time is available for the water to flow through the pores towards the core of the structure, which gives more opportunity to dissipate energy. Furthermore this increasing effect of the stability is stronger in the case of a more permeable structure. The three values of  $P$  were extracted from the dataset by Van der Meer by means of curve fitting. He considered the surging region and assumed that the stability was a power function of the Iribarren number. The fact that the stability increases faster for a more permeable core indicates a higher power as compared to the impermeable structure. The curve fitting led to the powers of equations through the data points of  $P=0.6$ ,  $P=0.5$  and  $P=0.1$ .

The influence of the permeability according to the resulting formulae of Van der Meer can easily be shown by calculating the required nominal stone size for constant parameters except the permeability parameter  $P$ .



**Figure 10 Influence of permeability coefficient on armour layer design**

The calculations were made with a wave height of 1 m, a damage number of 3, 3000 waves, a 1:3 slope and wave periods of 6 and 10 seconds. In the range starting at  $P=0.1$  until  $P=0.6$  a reduction of 28% was found in the plunging area and even 38% in the surging area. This clearly states the importance of the permeability and the advantage of knowing the value for more than three structures.

## 2.2 Scaling laws

Using scale models of coastal structures can serve several goals. Usually a prototype is scaled and subjected to design conditions to analyse its behaviour under extreme conditions. In this thesis the purpose is to investigate the structure characteristics, and more specifically the damage as a result of different notional permeabilities. In order to use the results of the model tests in real life situations, the test results must represent the reality in a good way. Several physical properties must be scaled correctly to avoid deviations when applying them in 1:1 situations, in other words to avoid scale effects. In this section the governing scaling laws will be mentioned and the problems with regard to these laws will be discussed.

Dimensionless variables which reappear in the stability formula of Van der Meer are:

Dimensionless wave height	$H_s/d_{n50}$
Relative density $\Delta$	$(\rho_s - \rho_w) / \rho_w$
Wave-period steepness	$S_m$
and surf similarity parameter	$\xi_m$
Damage with respect to number of waves	$S/N^{0.5}$
Slope angle	$\cot \alpha$
Grading of armour stone	$d_{85}/d_{15}$
Permeability	$P$

The values used in real life situations must be represented correctly in the scale model in order to produce valid and useful outcomes of the model tests. In this study there is no real case of scale ratio because there is no real prototype that will be built to scale in the laboratory. The method of scaling used in this study is just the other way around. The structure that will be used during the tests, from which conclusions are drawn, will be up scaled in order to use the same conclusions in the design practice. In the following sections the index m and p represent the model conditions and respectively the prototype or large scale conditions.

### 2.2.1 Geometrical scale

The most basic and straight forward scale law is that the structure must be geometrically undistorted in length scale, no motion of any kind is involved only similarity in shape. All the vertical and horizontal length scales are the same. This implies that the dimensionless variables named above result in:

$$\begin{aligned}
 (H_s/d_{n50})_p &= (H_s/d_{n50})_m \\
 (S_m)_p &= (S_m)_m \\
 (\cot \alpha)_p &= (\cot \alpha)_m \\
 (d_{85}/d_{15})_p &= (d_{85}/d_{15})_m
 \end{aligned}$$



### 2.2.2 Froude scale

The second requirement for scale model test is that the Froude number of the model corresponds with the Froude number of the prototype or real life situation.

$$Fr_m = Fr_p = \frac{u}{\sqrt{gh}} \quad 2-20$$

This actually represents the ratio of inertial forces and gravitational forces. If the Froude scale is correct the processes dominated by gravity are correctly scaled.

This results in the following length scaling:

$$l_m = \frac{l_p}{\lambda} \quad 2-21$$

And for time scaling the following relation can be derived:

$$t_m = \frac{t_p}{\sqrt{\lambda}} \quad 2-22$$

In which:

$\lambda$  = scale factor

### 2.2.3 Reynolds scale

The third scale law is that the ratio of inertial forces and viscous forces must be correctly scaled.

This ratio is represented by the Reynolds number:

$$Re = \frac{uL}{\nu} \quad 2-23$$

The Reynolds scale is especially important when the processes involved are dominated by viscous forces.

It is not possible to fulfill all the scale requirements at the same time, therefore the transition of turbulent to laminar flow is said to be the starting point for Reynolds related scale effects. THOMPSON AND SHUTTLE [FROM VAN DER MEER [1988] showed no influence of the Reynolds number as long as it is larger than  $1 \cdot 10^4 \sim 4 \cdot 10^4$ . Usually the pore velocities in the first two armour layers is sufficiently large to assure turbulent flow, but sometimes in the filter layer and in the core the velocities can drop below the critical value of Thompson and Shuttle and the flow becomes laminar, which is a wrong representation of the reality.

In this study the flow between the pores, this is related to energy dissipation and therefore on the notional permeability of the structure, plays an important role. Hence it has to be scaled as good as possible, keeping the scale effects as small as possible.

### 2.2.4 Porous flow

Flow through a porous media induced by pressure differences can have three different flow regimes, subdivided on the basis of Reynolds number.

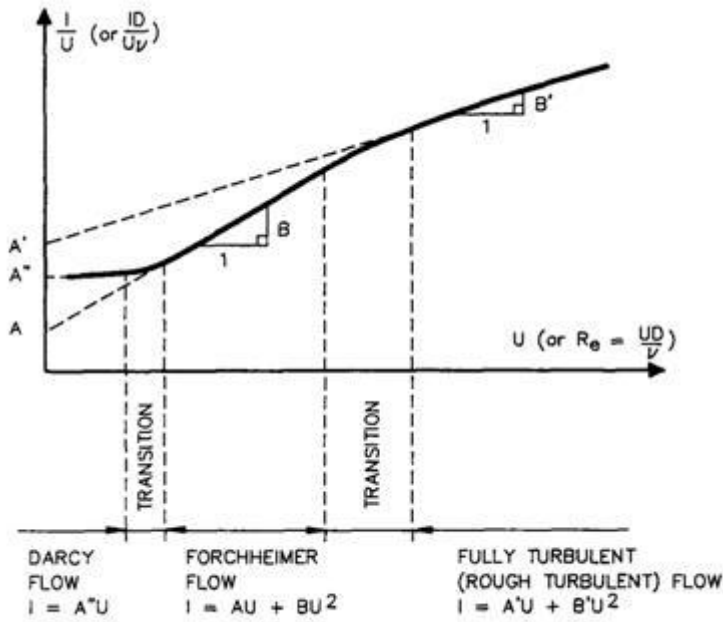


Figure 11 Flow regimes in porous media FROM Burcharth and Andersen [1995]

The most basic equation is that of Darcy which describes the groundwater flow in laminar conditions.

$$q = kI$$

2-24

In which:

q = flow  
k = permeability  
I = hydraulic gradient

In the situation of larger pores/grains or high flow velocities this relations is no longer valid. In that case we have to use a more advanced method, the formula of Forchheimer gives a good relation of flow and resistance in non-laminar conditions.

The Forchheimer relation [1902] (FROM VAN GENT [1995]) reads:

$$I = au + bu|u|$$

2-25

The first term is the laminar contribution, the second term is the turbulent part of the flow. This relation is valid for stationary flow. POLUBARINOVA AND KOCHINA [1952] (FROM VAN GENT 1995) extended the formula with an extra time depended part.

This extended Forchheimer equations becomes:

$$I = au + bu|u| + c \frac{\partial u}{\partial t} \quad 2-26$$

VAN GENT [1995] did experiments with stationary and oscillatory flows to find a way to determine the different coefficients present in the extended Forchheimer equation, and to test the influence of the oscillatory water motion. His tests showed that the value  $b$  has the largest contribution to the flow. In the oscillatory flow test the value of  $b$  appeared to be larger than in the situation with stationary flow. Van Gent found a relation for the value  $b$  which depends on the stationary coefficient  $\beta$  plus an extra factor accounting for the oscillating flow which depends on the Keulegan-Carpenter number (KC).

He defined a stationary contribution of  $\beta_c$  added with an extra effect of the oscillatory motion. Analysing different types of rock and different flows resulted in the following variation of the Forchheimer formula. The major difference with the formula above is the introduction of the Keulegan-Carpenter number KC.

The coefficient  $b$  becomes:

$$b = \beta_c \left(1 + \frac{7.5}{KC}\right) \frac{1-n}{n^3} \frac{1}{gd_{n50}} \quad 2-27$$

Where:

$$KC = \frac{\hat{u} T}{n d_{n50}} \quad 2-28$$

In the test with small velocity amplitudes, the coefficient  $c$  didn't contributed to a better representation of the pressure gradient and was therefore set to zero. In the next figure the contribution of the individual coefficients found by Van Gent is shown.

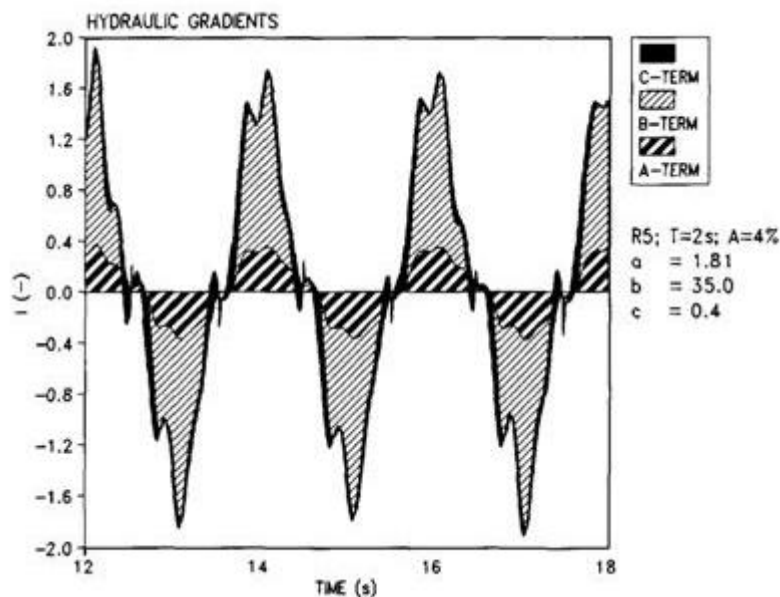


Figure 12 Contribution of coefficients by Van Gent [1993]

In the report of VAN GENT [1995] an estimate of the values  $\alpha$  and  $\beta$  is given in the situation in which no information about the material is known. In these situations it is recommended to use:  $\alpha = 1000$  and  $\beta=1.1$ .

P. TROCH [2000] did an experimental and numerical study on the interaction between waves and rubble mound breakwaters. In his study the different flow regimes (figure 11) depended on the Reynolds particle number were presented. The source of this description is the work of ANDERSEN [1994] FROM TROCH [2000].

Type	Name	Limits	Formula
I	Darcy flow	$Re_p < 1$	$I = a''V$
II	Laminar Forchheimer flow	$1 < 10 < Re_p < 150$	$I = aV + bV^2$
IV	Fully turbulent flow	$Re_p > 300$	$I = a'V + b'V^2$

Table 6 Flow regimes on the basis of  $Re_p$

Especially between the laminar Forchheimer flow and the turbulent flow there is a wide transition zone ( $150 < Re_p < 300$ ) which could not be described correctly. Based on measurements on the breakwater at Zeebrugge it was found that the flow inside the core of a breakwater is fully turbulent. The tests of Van Gent were executed with high Reynolds numbers ( $2000 \sim 66000$ ), therefore we can conclude that these results are valid for the fully turbulent region.

Many authors tried to quantify the flow through porous media. The fact that many author tried to do this indicates the uncertainties which still exist in the different flow formula. This is caused by the empirical character of these relations.

TROCH [2000] concluded that the best way to determine permanent laminar Forchheimer flow with:

$$I_x = \alpha_f \left( \frac{1-n}{n} \right)^2 \frac{v}{gd_{50}^2} \left( \frac{u}{n} \right) + \beta \frac{1-n}{n} \frac{1}{gd_{50}} \left( \frac{u}{n} \right)^2 \quad 2-29$$

In the table on the next page flow constants for a number of porous media found by different authors are presented.

From	Material	Porosity	D <sub>50</sub> [mm]	Re	α <sub>f</sub>	β
<b>Fand et al [1987]</b>	Uniform glass spheres	0.0360	2-4	5-80	~182	~1.92
<b>Lindquist [1933]</b>	Shot	0.383	1-5	4-263	184	1.82
<b>Dudgeon [1966]</b>	Uniform glass spheres	0.415	16	<400	164	1.7
		0.385	29	<180	193	2.4
	River gravel	0.367	16	<85	329	4.7
		0.406	110	<7000	922	2.0
	Angular rock	0.455	16	<400	622	5.4
		0.515	14	<200	479	4.0
		0.438	25	<400	425	5.3
		0.483	37	<500	92	10.8
<b>Engelund [1953]</b>	Flinty, calcareous sand uniform size	0.395	1.4-2.6	25-150	335	3.57

**Table 7 Summarized flow constants from Troch [2000]**

In the situation with a fully turbulent flow the influence of the laminar term should physically be neglected. BURCHARTH AND CHRISTENSEN [1991] proposed a method which eventually led to:

$$I_x = \beta' \frac{1-n}{n} \frac{1}{g d_{50}} \left( \frac{u}{n} \right)^2 \quad 2-30$$

In the table below taken from Burcharth and Christensen one can find some values for β'.

Material	d <sub>85</sub> /d <sub>15</sub>	β'	from
<b>Glass spheres</b>	1	1.4	Dundgeon and Fand
<b>Very rounded stones</b>	1.4	2.2	Burcharth
<b>Very rounded stones</b>	1.7	2.7	Dundgeon
<b>Semi rounded stones</b>	1.9	2.7	Burcharth
<b>Angular stones</b>	1.3-1.4	2.7	Shih
<b>Angular stones</b>	1.4-1.8	2.9	Burcharth
<b>Angular stones</b>	1.6-1.8	4.1	Dundgeon

**Table 8 Flow constants from Burcharth and Christensen**

The non-stationary flow, which is the case in wave induced pore flow, should according to the extended Forchheimer equation be calculated using the coefficient c. However Van Gent showed that this coefficient had little contribution to the total velocity. Therefore in this study the coefficient c will be neglected.

The goal of calculating the velocity in the pores is to make sure the flow regimes which will occur in the model tests resemble the actual situation. In the next section the method of Burcharth to calculate the pressure difference in the structure is used to calculate the flow in the pores.

Because no clear method of determining the pore velocity in the core under oscillating flow conditions is given both the method of Van Gent and the method of Burcharth (with β' but without c) will be used to calculate the flow in the pores.

A difference that must be kept in mind but is often overlooked is the different notations / descriptions of the rock sizes. In the research of VAN GENT [1993/1995] the definition  $d_{n50}$  is used which is the diameter representing the  $M_{50}$  (median weight of the stones). BURCHARTH [1991] used the definition  $d_{50}$  which is the median stone size based on sieving of the material. The relation between the  $d_{50}$  and  $d_{n50}$  is determined by the shape factor of the material. LAAN [1981] showed that the shape factor of rock is almost always in between 0.7 and 0.9. In The ROCK MANUAL [2007] the value of 0.84 is recommended.

The relation then becomes:

$$d_{n50} = 0.84d_{50} \quad 2-31$$

It must be kept in mind that this relation has a very empirical character and can vary a lot depending on different origins of the material. During the research of VAN DER MEER [1988] the same sieve size of the material as the research of THOMPSON AND SHUTTLE [1975] was used, namely a  $d_{50}$  of 4 cm. However the resulting  $d_{n50}$  appeared to be twice as large.

### 2.2.5 Burcharth

Burcharth found a way to determine the pore velocities in a rubble mound breakwater induced by waves. Combined with the scale modelling problems with regard to the scaling of core material he applied a method of scaling the core in such a way that it still represents a turbulent flow regime.

With means of model tests and with in-situ measurements on the breakwater of Zeebrugge an empirical relation for the pressure as a function of distance  $x$  was derived.

$$p_{max}(x) = p_{0,max} e^{-\delta \frac{2\pi}{L'} x} \quad 2-32$$

In which:

$x$	=	horizontal coordinate
$p_{0,max}$	=	reference pressure
$\delta$	=	damping coefficient
$L'$	=	wave length in the core ( $L' = L/D^{0.5}$ )
$L$	=	wave length
$D$	=	coefficient to account for seepage length, LE MEHAUTE [1957] found the empirical value 1.4, Biesel [1950] found a theoretical value of 1.5

Burcharth showed with the tests of Bürger et al [1988] and the measurement of Zeebrugge that the maximum reference pressure reasonably can be estimated with:

$$p_{0,max} = \rho_w g \frac{H_s}{2} \quad 2-33$$

With means of the same dataset the empirical expression for the damping coefficient was derived by Burcharth.

$$\delta = 0.0141 \frac{n^{0.5} L^2}{H_s b} \quad 2-34$$

In which:

$n$	=	core porosity
-----	---	---------------

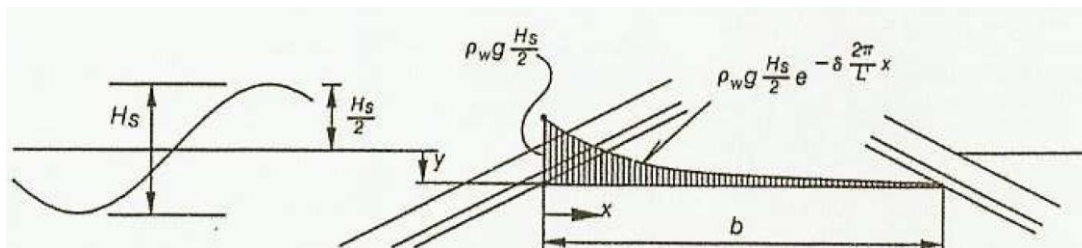


Figure 13 Core pressures by BURCHARTH

When assuming a harmonic oscillating water motion the final expression for the pressure in the structure becomes.

$$p(x, t) = \rho_w g \frac{H_s}{2} e^{-\delta \frac{2\pi}{L'} x} \cos\left(\frac{2\pi}{L'} x + \frac{2\pi}{T_p} t\right) \quad 2-35$$

$$I_x = \frac{1}{\rho g} \frac{dp(x, t)}{dx} = -\frac{\pi H_s}{L'} e^{-\delta \frac{2\pi}{L'} x} \left[ \delta \cos\left(\frac{2\pi}{L'} x + \frac{2\pi}{T_p} t\right) + \sin\left(\frac{2\pi}{L'} x + \frac{2\pi}{T_p} t\right) \right]$$

2-36

This is combined with the equation for pore velocity, given in the previous section, to compute the pore velocities for given wave conditions.

Burcharth proposed a method to scale the core materials with a different ratio than the rest of the scale model. The result will be that the new scale ratio for the core material represents the correct pore velocity of the model on the basis of Froude scaling of the entire structure.

The pressure in the core at the two different distances from the waterline is calculated, a wave height of 0.24 m and a peak period of 3.9 s results in the following pressure distribution in the cross section of the breakwater.

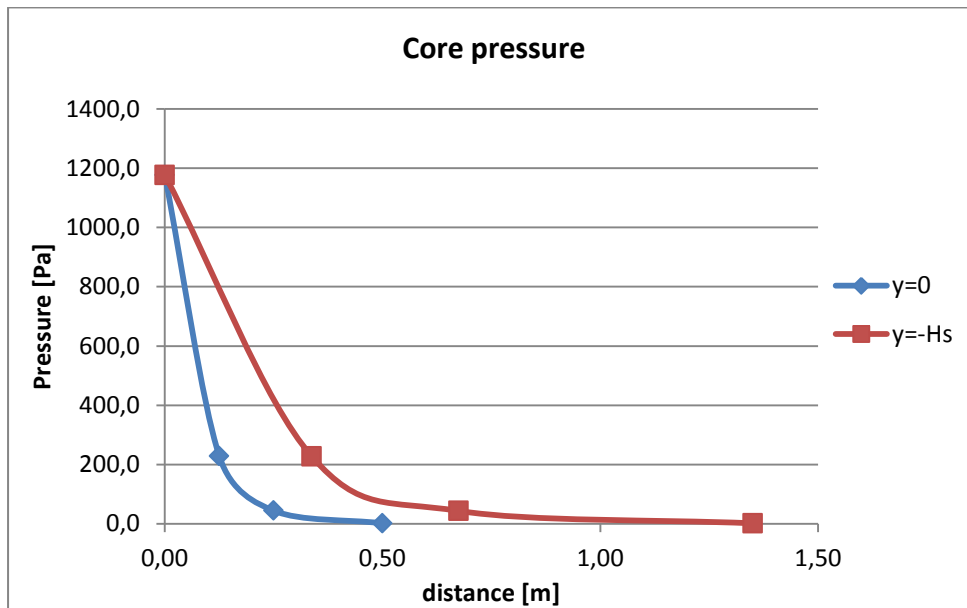


Figure 14 pressure distribution in the breakwater core

The pressures were calculated at six different locations as described by Burcharth and can be seen in the following figure. Starting with 3 points positioned around the water level and secondly three points positioned one wave height below the water level.

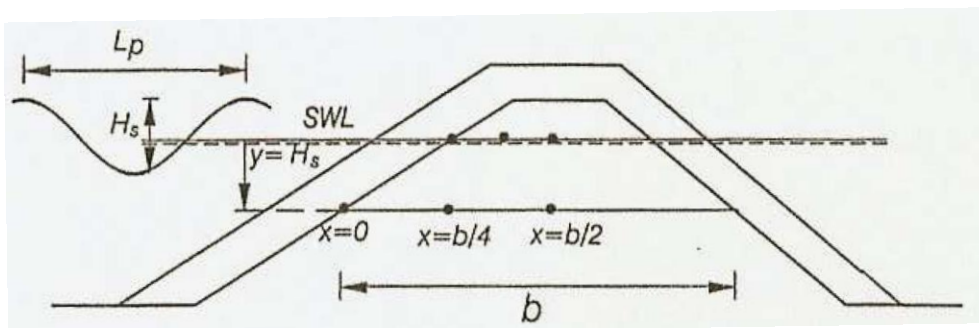


Figure 15 Locations of pressure calculations from Burcharth [1999]



Based on these pressures the gradient can be calculated, with this gradient the resulting velocities in the core can be determined. As mentioned before the velocities were determined both with the Burcharth and the Van Gent expressions. In the figure below the outcome of both methods are presented. The first three distances along the x axis were used to determine the average velocity at that height, the same was done at one wave height below the water level. Those six points were time averaged and said to be the representative core velocity on which Burcharth determined his scaling factor. These same six points were used in this study to assess whether the flow in the core is in the fully turbulent region, thus  $Re_p > 300$ .

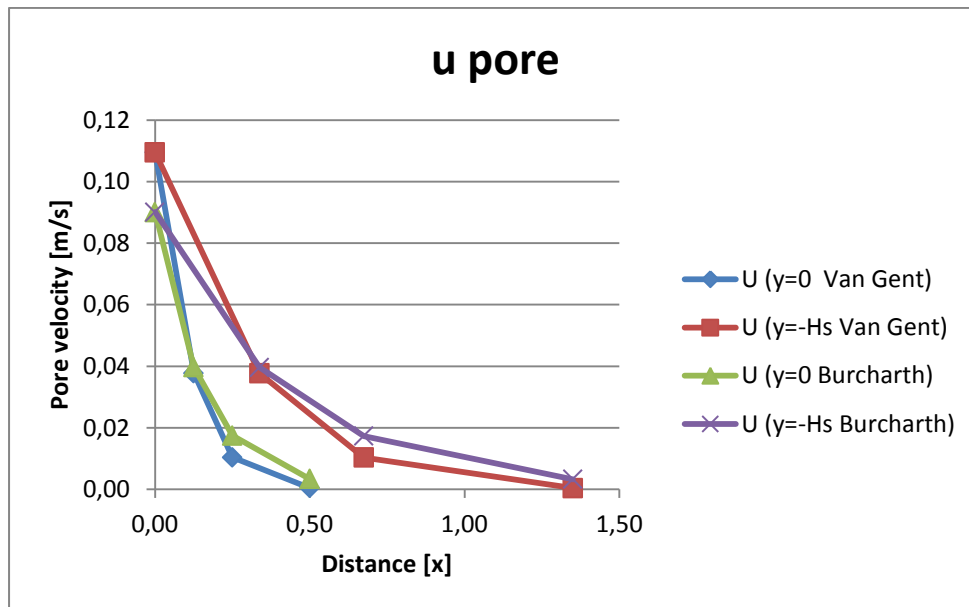


Figure 16 Pore velocities

The figure above indicated that the method of calculating the pore velocity with the formula of Van Gent and the one of Burcharth don't show remarkable differences.

If a structure with a permeable core and an armour / core ratio similar to the described ratio by Van der Meer for a structure with  $P=0.5$  is calculated, the resulting Reynolds particle value is in the order of 240. This implies a transition between laminar Forchheimer and a fully turbulent flow in model circumstances. Therefore it is assumed that the scale effects are limited.

When the same velocity is calculated for structures with a  $P$  of 0.4 the stone diameter and the applied wave height are much smaller. This results in a Reynolds particle value in the order of 60. This implies laminar Forchheimer flow and not a turbulent flow. This could lead to scale effects. The same holds for the new structure that is tested during this study, which has the same ratio with respect to the different stone sizes of the different layers.

### 2.2.6 Conclusion

Based on statements of Burcharth which describe the pressure distribution and the flow in the core of a breakwater a pore velocity is calculated. These calculated values showed laminar flow regimes for structures with small diameter core material, where the occurrence of errors due to wrong Reynolds scaling is highly likely.

## 2.3 Hypotheses about the Notional Permeability

In the recent past several studies concerning the notional permeability have taken place. The main aim of those studies was to gain more insight into the physical background of the notional permeability and the influence of the permeability on the armour layer stability. Finally the goal is to easily determine the factor 'P' for any arbitrary cross section of a rock slope without conducting scale model tests.

JUMELET [2010] tried to describe the process with a numerical model. This section starts with the description of the hypotheses of Jumelet. Later VILAPLANA [2010] evaluated the model of Jumelet with the test data of VAN DER MEER [1988]. The most recent improvement to this model is done by BROEKHOVEN [2011]. Finally the numerical model HADEER used by Van der Meer was briefly described.

### 2.3.1 Volume exchange model

The basic idea of the volume exchange model is the coupling of the internal and external processes that take place in and around a breakwater. Surging waves that encounter a breakwater on their path will result in a change of water level in front of and inside the breakwater, in other words wave run-up and run-down. The amount of wave run-up is affected by the type and thickness of the armour material. A rougher material results in more friction and therefore in a lower wave run-up. The same holds for a thicker construction, which is able to contain more water than a smooth impermeable surface and therefore also reduces the wave run-up.

The model of JUMELET [2010] assumes that the inflow of water into the structure takes place in a time span of  $\frac{1}{4}$  of the wave period. The volume of water able to flow in to the core of the structure during this period determines the reduced wave run-up. The run-up reduction coefficient derived by Jumelet is written as:

$$c_r = \frac{R_{u;s,r}}{R_{u;s,f}} \quad 2-37$$

Which represents the run-up reduced by friction and inflow ( $R_{u;s,r}$ ) divided by the run-up reduced by friction ( $R_{u;s,f}$ ).

The maximum wave run-up is reached on an impermeable smooth slope. On these slopes it is assumed that there is no energy dissipation and therefore all the wave energy is transferred to potential energy.

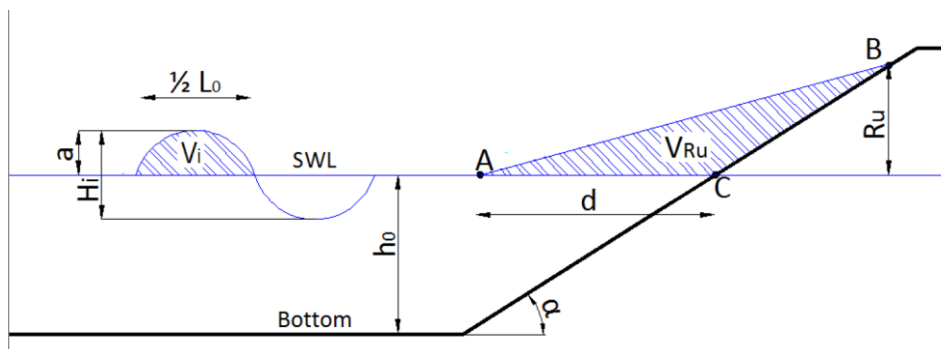


Figure 17 Scheme volume exchange model from Jumelet 2010

$$V_{ru} = \frac{2}{3} \frac{L_0}{\pi^2} R_u \quad 2-38$$

$$R_u = \frac{3}{4} \pi H \quad 2-39$$

In the case of a rough impermeable slope a reduction factor  $\gamma_f$  for the run up is assumed, which leads to  $R_{u,f}$ . The run up at the core was assumed to be half the run up at the armour layer.

$$R_{u;c} = R_u * \gamma_f * 0.5 \quad 2-40$$

The internal body of water can be described by the formulas for porous medium flow of Forchheimer with the constants for turbulent flow as can be seen in the previous chapter.

The internal volume capacity of water was assumed as a triangle which can be described by:

$$V_{b,1} = \frac{1}{2} n \left( \frac{1}{I} \right) R_{u;c}^2 \quad 2-41$$

$I$  is the hydraulic gradient calculated, with equation 2-26 from chapter 2.

$$I_x = \beta' \frac{1-n}{n} \frac{1}{g d_{50}} \left( \frac{u}{n} \right)^2 \quad 2-42$$

The inflow was estimated to take place in about  $\frac{1}{4}$  of the wave period, the total volume of inflow depends on the period and the magnitude of the flow into the core. With a sinusoidal wave and the mentioned inflow period this results into:

$$V_{b,2} = \frac{1}{\omega} \sqrt{I/b} * \frac{R_{u;c}}{\sin(\alpha)} \left( 1 - \cos\left(\omega * \frac{T_0}{4}\right) \right) \quad 2-43$$

The water level gradient is an interaction between the internal volume capacity and the volume flowed into the core driven by a sinusoidal wave. The gradient  $I$  can iteratively be determined with the condition that both volumes  $V_{b,1}$  and  $V_{b,2}$  are equal.

With the found hydraulic gradient a new reduced run up can be calculated and thus a new run up volume. The amount of reduction caused by the porous flow is presented relative to the volume of surface run up in the case of an impermeable rough slope  $V_{ru,f}$

$$V_{b;N} = \frac{1}{\omega} \sqrt{I_N/b} * \frac{R_{u;c;(N-1)}}{\sin(\alpha)} \left( 1 - \cos\left(\omega * \frac{T_0}{4}\right) \right) \quad 2-44$$

$$V_{Ru;s;r} = V_{Ru;s;f} - V_{b;N} \quad 2-45$$

$$R_{u;s;r} = \frac{V_{Ru;s;r}}{V_{Ru;s;f}} * R_{u;s;f} \quad 2-46$$

The run up reduction factor becomes

$$cr = \frac{R_{u;s;r}}{R_{u;s;f}} \quad 2-47$$

After curve fitting JUMELET [2010] found the following equation for the notional permeability, based on the run up reduction factor Cr and the wave steepness.

$$P = 3.1 * s^{-0.3} (1 - cr)^{0.8} \quad 2-48$$

### *Modifications by VILAPLANA [2010]*

VILAPLANA [2010] reviewed some parts of the Volume Exchange Model, the analysis executed in that additional thesis consisted out of 3 parts. In the first part a generalization of the notional permeability was made, using the measured data of VAN DER MEER [1988], which resulted into an adjusted equation for the notional permeability. In the second part some assumptions made by JUMELET [2010] were varied, leading to a sensitivity analysis of these parameters. Finally the adjusted equation for the permeability was compared to the measured data of VAN DER MEER [1988].

The most important outcome of the work of Vilaplana is the adjusted equation for the permeability. In this adjusted formula the influence of the slope of the structure and the dimensions of the armour layer are added. This resulted into the following new equation:

$$P = 1.38 * \cot(\alpha)^{-0.9} * s^{-0.66} * (1 - cr)^{1.44} * \left(2.5 * \frac{d_{n50a}}{t_a}\right)^{8.44} \quad 2-49$$

### *Broekhoven [2011]*

BROEKHOVEN [2011] continued where JUMELET [2010] and VILAPLANA [2010] stopped. In the research done in 2011 a number of assumptions made by Jumelet were investigated with means of scale model tests, conducted in the laboratory of fluid mechanics at the faculty of civil engineering in Delft. The main focus was to measure the effect of the stone diameters, grading and most important the effect of the permeability on the surface run up.

JUMELET [2010] made the assumption that the surface roughness reduced the wave run up with the constant factor:  $\gamma_f = 0.75$ . The other main assumption in the original Volume Exchange Model is the reduction of wave run up at the core with respect to the run up at the surface, which was assumed to be a factor 0.5.

The findings of BROEKHOVEN [2011] are very remarkable. After analysis of the tests he found no difference in the wave run up at the surface for different permeabilities, which is the foundation of the Volume exchange model. The main difference in wave run up however was found at the core. This implies that an adjustment to the model was necessary.

The adjustments proposed by BROEKHOVEN [2011] are:

- Adjustment to the assumption of a triangular wedge shape incoming wave
- Core run up factor

$$\gamma_{Ru} = 1.0 * \tanh(0.31 * \xi) \quad \text{valid for } 1.8 \leq \xi \leq 8.8 \quad 2-50$$

- Cr is the reduction of the run up at the core instead of the surface

$$cr = \frac{R_{u;c;r}}{R_{u;c;imp}} \quad 2-51$$

- For the reference level  $R_{u;c;imp}$  BROEKHOVEN[2011] found:

$$\frac{R_u}{H} = 1.63 * \tanh(0.14 * \xi) \quad 2-52$$

- The assumed inflow doesn't take place during the run up period of about ¼ of the wave period, but during a part of the run-down period. The inflow starts from the moment the maximum run up is reached, until the point where the water level outside has reached a level below the internal water level. The period was estimated to be in the range of 1/5 to 1/8 of the wave period.

The expression for the reduced run up at the core becomes

$$R_{u;c;r} = \frac{V_{Ru;c} - V_{b;N}}{V_{Ru;c}} * R_{u;c;imp} \quad 2-53$$

Based on curve fitting he found another extra reduction factor.

$$\gamma_{cr} = 1.60 * (1 - n) \xi^{-0.25} \quad 2-54$$

With means of the formulae and the measured data of Van der Meer Broekhoven found a different relationship between the run up reduction factor Cr and the notional permeability P.

$$P = 0.37 \xi^{-0.8} Cr^{-3.4} \quad 2-55$$

A remark must be made regarding the definition run up at the core made by BROEKHOVEN [2011]. During the tests executed by BROEKHOVEN [2011] no filter layer was used and all the measured run up at the core was measured direct below the armour layer. In real life a structure without filter layer underneath the armour layer hardly ever occurs. Therefore the mentioned run up at the core should in fact be the wave run up below the armour layer, this implies that the filter layers can be seen as a part of the core and thus affect the permeability of the structure and respectively the wave run up below the armour layer.

### 2.3.2 Numerical HADEER model

Van der Meer used the numerical HADEER model to describe the internal flow pattern of a breakwater under wave attack. The model was calibrated with means of scale model tests with mono chromatic waves and measuring the maximum wave run up and wave run down.

The output of the model is the dissipation of water into the core as a function of core stone diameter and wave period. The figure below shows the result of the calculation done by VAN DER MEER [1988].

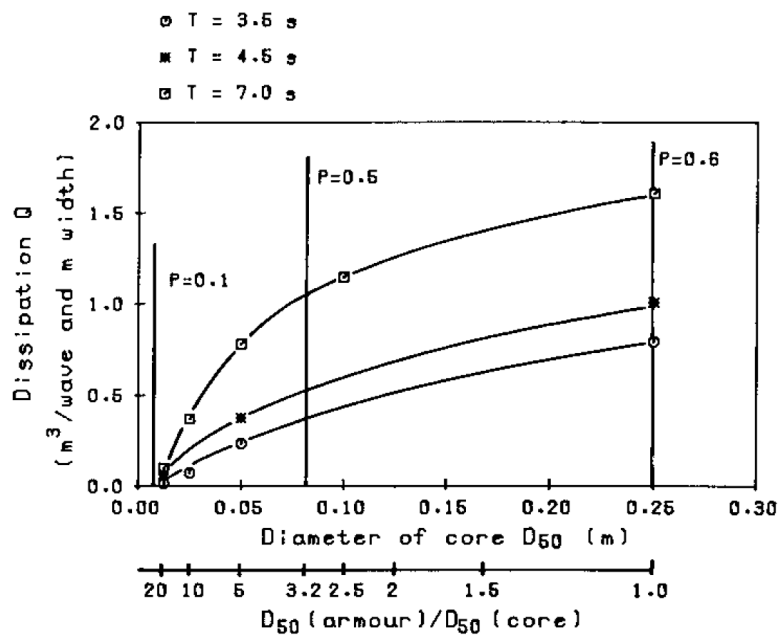


Figure 18 Results HADEER model from Van der Meer [1988]

The dissipation of water was related to the maximum dissipation created by the homogenous structure representing a notional permeability of  $P = 0.6$ .

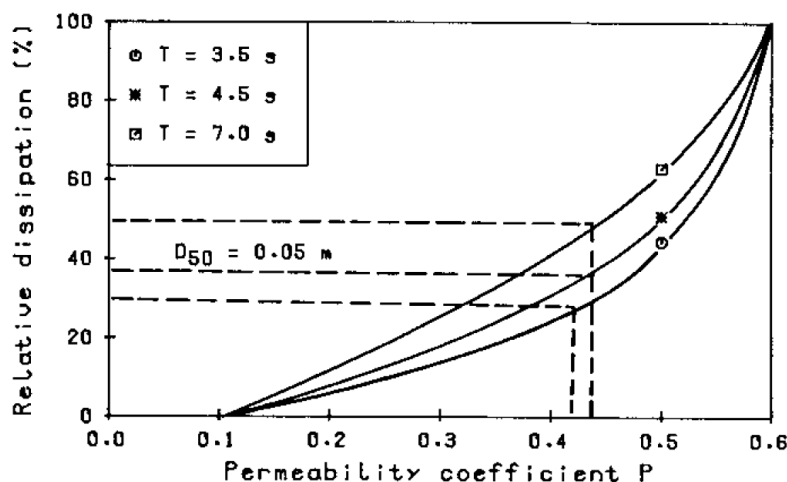


Figure 19 Resulting P by Van der Meer [1988]

Van der Meer concluded that the HADEER model can be used to make an assumption of the notional permeability of a structure. In a specific case the computations should be made for a homogenous structure, a permeable structure ( $d_{n50;armour}/d_{n50;core}=3.2$ ) and for the particular case of interest. The computations should be done for various wave conditions and can be plotted in a similar ways as figure 19.

### 3. Test matrix

This chapter will concern the considerations made to produce the test matrix and the test method. First of all the choice of the range of environmental and structural parameters is explained. This leads to a final design of the structures and the test matrix. Furthermore the work method and the measurement equipment are discussed.

#### 3.1 Environmental variations

With regards to the environmental variation the main consideration have to do with the wave characteristics, the number of waves and spectral shape. These parameters are chosen in such a way that they produce material which can be compared with results of previous studies. This basically means that the major environmental aspects used in the experiments of VAN DER MEER [1988] will also be used in the test series in this study.

##### 3.1.1 Surging/plunging

When the stability equations 2-15 and 2-16 are analysed with respect to the influence of the notional permeability, it can be concluded that the influence of the permeability on the stability of the armour layer in the case of surging waves is larger than the influence in the case of plunging waves. For that reason this study will focus on the surging region. It is however also recommended that there will also be tests with plunging waves to compare the results for the notional permeability.

##### 3.1.2 Duration

VAN DER MEER [1988] concluded that the influence of the number of waves can properly be described with the factor  $N/V(S)$ . Thompson and Shuttler already found this relation who tested until 5000 waves and even did some long duration test until 15000 waves. They found that the range of which the relation  $S/\sqrt{N}$  is valid is when  $N < 7.000 \sim 10.000$ . Because Van der Meer did his experiments up until 3000 waves, this value will also be used in this study.

##### 3.1.3 Spectral shape

During the experiments in this study the structures will be attacked by a Pierson-Moskowitz wave spectrum. Van der Meer did tests with three different spectra and found, as already mentioned in the previous chapter, no distinct difference between the spectra, as long as the mean period was used. Because the majority of his tests were performed with Pierson- Moskowitz spectrum this will also be used in this study.

### 3.1.4 Wave height/ period

The wave height is chosen in such a way that the highest possible waves in the flume will be tested. Smaller waves imply smaller armour stones and thus smaller filter and core materials. The reason for the fact that the wave height deviates from the research of VAN DER MEER [1988] is that the third structure has a second filter layer with a relative small  $d_{n50}$ . According to the formulae of porous flow in chapter two implying the high risk of scale effects when this porous flow becomes laminar led to an initially bigger armour layer and therefore a higher wave height in comparison to the work of VAN DER MEER [1988]. On page 27 one can read that the structures with this risk are the structure with  $P=0.4$  and the third structure tested in this study with equal stone weight ratios as the  $P=0.4$  structure. Van der Meer didn't had this problem because he did not tested the  $P=0.4$  structure, the  $P=0.5$  and  $P=0.6$  structures tested by Van der Meer have sufficiently large core materials resulting in turbulent flow even in scaled conditions.

With respect to wave breaking and wave run-up the maximum wave height will be 0.27 m. The maximum wave height occurring in this spectrum is in the order of twice the significant wave height. To avoid wave breaking we require a water depth in the order of 0.7 m. The run up (2%) is about 0.4 m therefore the final height of the breakwater will be 1.1 m.

However it appeared that the wave height of 0.27 m is not a practical value, after one test it was clear that the reflection compensator in combination with this large wave height gave errors which led to an abrupt stop of the experiment. Reducing the wave height to about 0.1 m to 0.15 m resolved the problem with the reflection compensator. During one test series the wave height will be kept constant and a variation with wave period is made.

A wide variation of wave height and period is beneficial for the fit of the notional permeability factor  $P$ , especially larger periods which result in large Iribarren numbers. These large periods should visualise the trend of increasing stability and make the fit of  $P$  more reliable. However during this thesis some concessions had to be made regarding the test matrix. Because of limited time available in the laboratory only a limited number of tests could be conducted. It is therefore assumed that the definition that describes the increase / decrease of the stability with regard to the wave height is correct.

Therefore the main focus in the test matrix is on the variation in Iribarren number which is the main parameter in the stability formulae. With a constant wave height this results in variation in wave period. Per structure about six different tests are possible supplemented with six repetition tests per structure. This research has the attempt to produce empirical values for the notional permeability which can be used in practice. For that reason the wave steepness will be between about 1% and 5%, which are the " bounds" of commonly occurring waves.



## 3.2 Structural variations

The most interesting structures within this study are those which have not yet been tested before. It is however not wise to only test these structures without having a good reference case. Therefore some structures already tested by VAN DER MEER [1988] will also be tested in this research. For this master thesis only a limited amount of time is available, therefore a selection of tests have to be made in order to not exceed the available time.

### 3.2.1 Type of structures

One outer edge of the notional permeability scale is a homogeneous structure. This should result into a notional permeability of  $P=0.6$ .

A method to determine the correlation of the formula of Van der Meer with the measured data is to make a scatter plot in which the measured damage and the calculated damage are presented. With the information about the experiments the expected damage is calculated using the formulae for both plunging as well as surging waves. A perfect formula with the correct parameters would give exactly the same calculated and measured results. Considering the graph this should lead to a trend line with a slope of 1:1. In the figure below we can see both the scatter plots for the  $P=0.6$  and  $P=0.5$  situation. The red line represents the perfect fit.

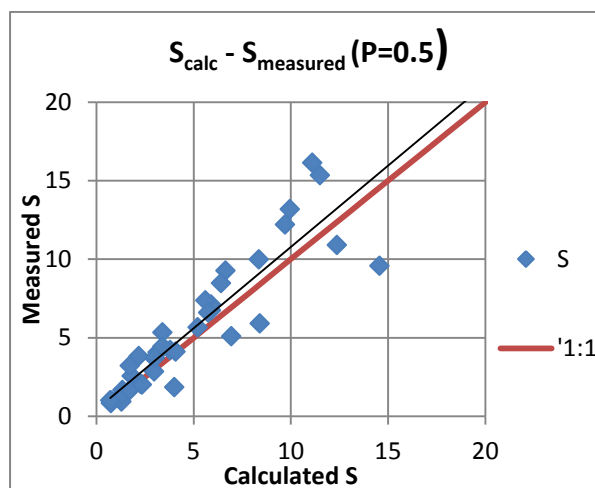


Figure 20 Scatter plot measured/calculated damage with  $P=0.5$  data of Van der Meer[1988]

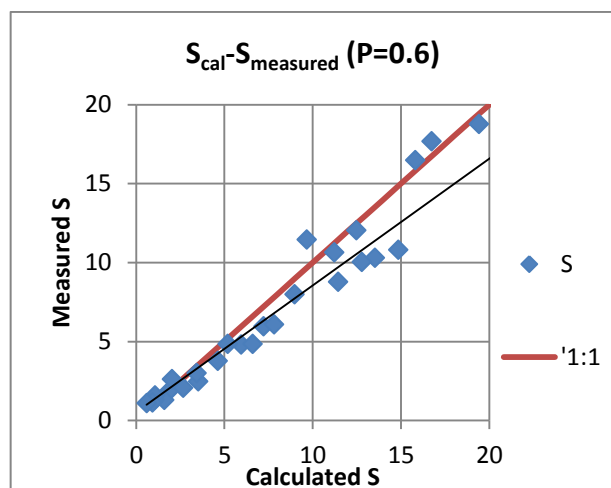


Figure 21 Scatter plot measured/calculated damage with  $P=0.6$  data of Van der Meer[1988]

In the reference scenario the value of  $P$  defined by Van der Meer has to be found to confirm that the method of testing is correct and resembles the experiments conducted by Van der Meer himself. As we can see in the previous figures is the general trend of the  $P=0.5$  structure closer to the 1:1 perfect fit. It is therefore easier to find the  $P=0.5$  from experiments, furthermore a lot more experiments are conducted on the  $P=0.5$  structure. Therefore the  $P=0.5$  situation will be used as a reference case.

The other reference case is the construction with an armour layer on a thin filter and an impermeable core as defined by Van de Meer. This structure should result in a notional permeability of 0.1.

Another structure which is often applied in practice but has no tested  $P$ -value is a structure with an impermeable core, like sand + geo-textile, but with an extra thick (double) filter layer. This “new” structure has the same stone ratio's as the  $P=0.4$  structure. One should think of a  $p$ -value in the order of 0.3.

Although validating the structure defined by Van de Meer as having a notional permeability of 0.4 is a very interesting one, it will not be executed during this thesis. In the experiences of *Hydronamic* the structure with an expected notional permeability of 0.3 is more often applied.

### 3.2.2 Layer thickness

The armour layer will consist in every test out of a double layer. This is common design practice, in this way there is a better protection of the layers underneath the armour layer. Also in the experiments of VAN DER MEER [1988] a double armour layer was applied. The thickness of the filter layer will be the same as specified by Van der Meer, which can be found in figure 2.

The structure with an expected  $P$  of 0.3 has dimensions based on experiences of *Hydronamic*. Often a core of dredged material is placed, which is covered by a geo-textile. The next layer is usually quarry-run to create the desired slope of the structure. On top of that layer the under layer is placed on which the armour layer will be situated. The first filter layer (directly under the armour layer) has a layer thickness of  $2 \cdot d_{50;f1}$ . The second filter layer with a smaller diameter has the same layer thickness as the armour layer, about  $2 \cdot d_{50;A}$ .

### 3.2.3 Slope angle

As can be seen in the previous chapter Van der Meer only tested all the different types of structures on a 1:2 slope. He tested other slopes as well but not with all the different structures. It is recommended that also on different slopes experiments will be executed. In this study however the focus will be on the 1:2 slopes in order to have good reference material.

### 3.2.4 Grading rock

Van der Meer found no relation between stability and the grading of the armour layer. Therefore the usual grading of quarry rock for armour layers will be applied. This implies  $d_{85}/d_{15} < 1.5$ . With respect to the filter layer and the core of the breakwater one can imagine that the grading of these elements do have an influence.

A wider grading results in smaller pores, and thus a smaller permeability. It is recommended that a variation of grading of the filter layer- and the core material will be tested.

### 3.2.5 Final model designs

Based on the choices made on the previous pages a  $d_{n50}$  of the armour layer can be calculated. This was done using the Van der Meer formulae for stability. In the environmental parameters discussed in the previous section it was found that the wave height will be in the order of 0.15 m.

Additionally there is the requirement that the damage must be at least above  $S=2$  to have initial damage but preferably be in the range of  $S=3\sim 10$  to have real damage that can be measured. In the figure below we see the stability formula for three different structures ( $P=0.1$ ,  $P=0.3$  and  $P=0.5$ ), on the horizontal axis the Iribarren number is given. On the vertical axis the expected damage can be seen.

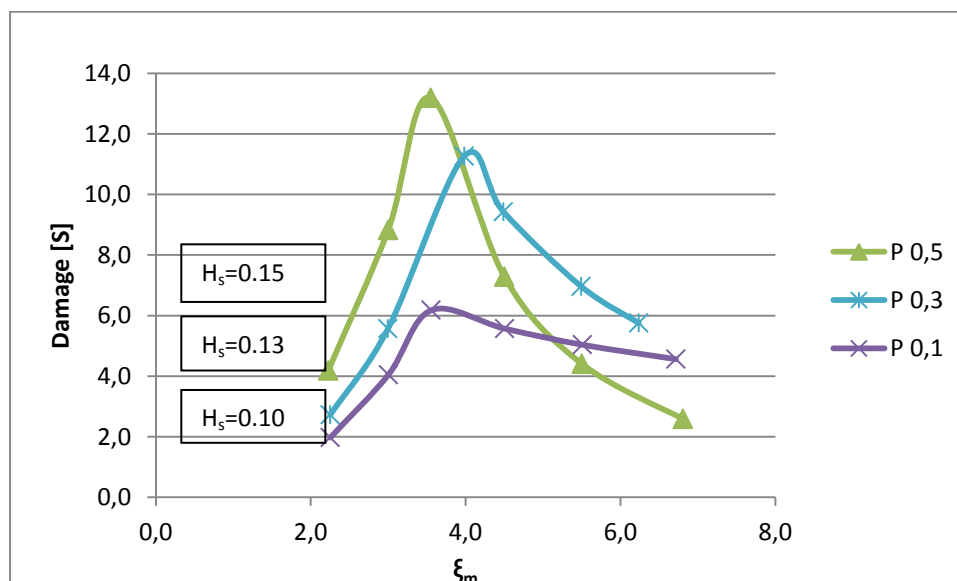


Figure 22 Damage vs. Iribarren for different permeabilities

This figure has been made for different armour stone diameters, wave heights and wave periods to finally end up at configurations for which the desired damages are reached. The final calculation was done with a  $d_{n50}$  of 0.04 m for the armour layer. The highest waves of  $H_s=0.15$  m will be applied in the situation with  $P=0.5$ , for the other two situation lower wave heights can be applied to arrive at the desired damage levels.

Structure	$d_{n50A}$ [m]	$d_{n50f}$ [m]	$d_{n50c}$ [m]	$d_{n50A}/d_{n50f}$	$d_{n50A}/d_{n50c}$
<b>P=0.6<sup>1</sup></b>	0.04	-	-	-	-
<b>P=0.5</b>	0.04		0.0125		3.2
<b>P=0.4<sup>1</sup></b>	0.04	0.02	0.005	2	8
<b>P=0.3</b>	0.04	0.02	0.005	2	8
<b>P=0.1</b>	0.04	0.009	-	4.5	-

Table 9 Stone dimension and ratios needed

<sup>1</sup> Will not be executed because of too the limited time available

### 3.3 Combined test matrix

Finally this results in the following test matrix that has been executed during this master thesis.

Testnr	Structure	P	H <sub>s</sub> [m]	T <sub>m</sub> [s]	T <sub>p</sub> [s]	Steepness [-]	Expected damage
1	I	0.5	0,15	1,39	1,82	4,97%	3,5
2	I	0.5	0,15	1,8	2,35	2,97%	6,6
3	I	0.5	0,15	2,22	2,90	1,95%	10,5
4	I	0.5	0,15	2,8	3,66	1,23%	5,9
5	I	0.5	0,15	3,3	4,31	0,88%	3,9
6	I	0.5	0,15	3,6	4,71	0,74%	3,1
7	II	0.1	0,1	1,13	1,48	5,02%	1,9
8	II	0.1	0,1	1,5	1,96	2,85%	3,9
9	II	0.1	0,1	1,8	2,35	1,98%	6,2
10	II	0.1	0,1	2,4	3,14	1,11%	5,4
11	II	0.1	0,1	2,9	3,79	0,76%	4,9
12	II	0.1	0,1	3,4	4,44	0,55%	4,6
13	III	0.3?	0,13	1,3	1,70	4,93%	2,7
14	III	0.3?	0,13	1,7	2,22	2,88%	5,3
15	III	0.3?	0,13	2,3	3,01	1,57%	11,3
16	III	0.3?	0,13	2,8	3,66	1,06%	8,4
17	III	0.3?	0,13	3,2	4,18	0,81%	6,9
18	III	0.3?	0,13	3,6	4,71	0,64%	5,8

Table 10 Test matrix

The first two series of tests will deal with the reference scenarios. Because the stability parameter  $H_s/\Delta d_{n50}$  is a power function of the Iribarren number a range of Iribarren numbers will be tested. The Iribarren number, which in this case only depends on the wave steepness, is chosen in such a way that a wide range is tested in order to fit a curve through the data points. Also a variation of occurring damages is necessary to assure a valid outcome for a range of damages.

In the surging region an increase of stability is expected when the Iribarren number increases, this in contrary to the plunging region where the stability decreases for growing Iribarren numbers.

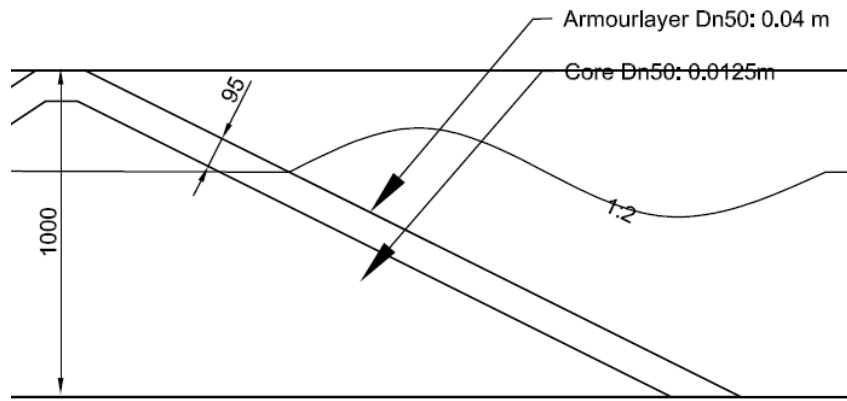


Figure 23 Test structure 1, P=0.5

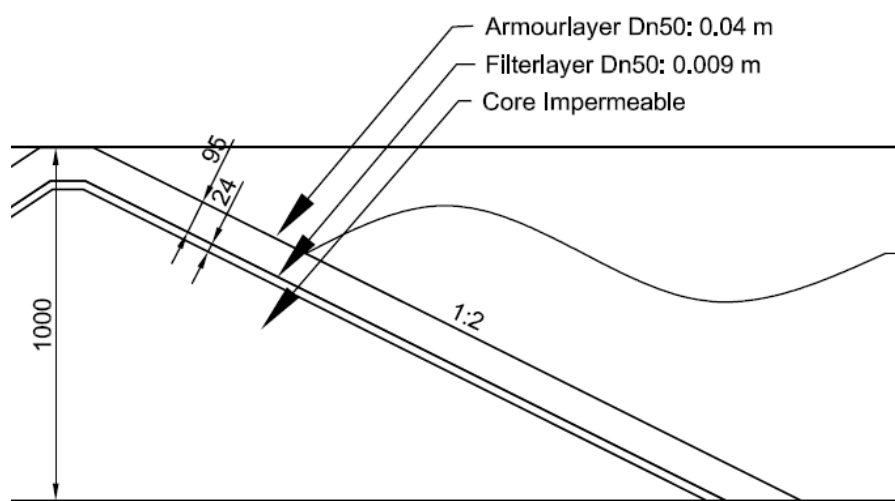


Figure 24 Test structure 2, P=0.1

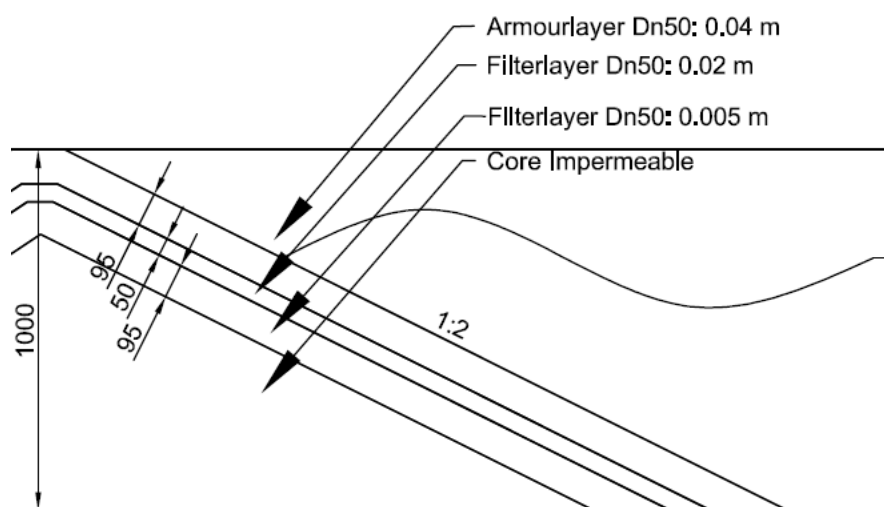


Figure 25 Test structure 3, P=0.3

## 3.4 Test equipment

During the experiments several items will be measured. The most important outcome of the experiments is the damage that will occur. Furthermore the wave height is measured at two different locations. And with regards to the physics behind the notional permeability the pressures inside the core of the breakwater will be measured.

### 3.4.1 Wave flume

The physical model tests will be executed in the Laboratory of Fluid mechanics of the Delft University of Technology. The wave flume has a length of about 40 m, a width of 0.8 m and a height of 1 m the water depth during these model tests is 0.65 m. The flume is equipped with a wave generator capable of generating regular and irregular waves, and contains an automatic reflection compensator to avoid the occurrence of standing waves in the closed basin.

### 3.4.2 Measuring damage

The damage is measured using both laser and echo-sounding equipment. Because this equipment measures the distance with a high frequency the result will be a continuous profile. Profiles are taken at thirteen different locations, each 5 centimetres apart from each other. The first and the last measurement is 0.1 m from the side of the wave flume. The profile below the water level is measured using the echo-sounder, the area above the water level is measured with the laser.

The area around the water level is the most critical area because the most amount of damage is expected in that region. Due to the clarity of the water the laser was able to measure through the water surface, which in combination with the echo sounder provided an overlap in the measured profile.

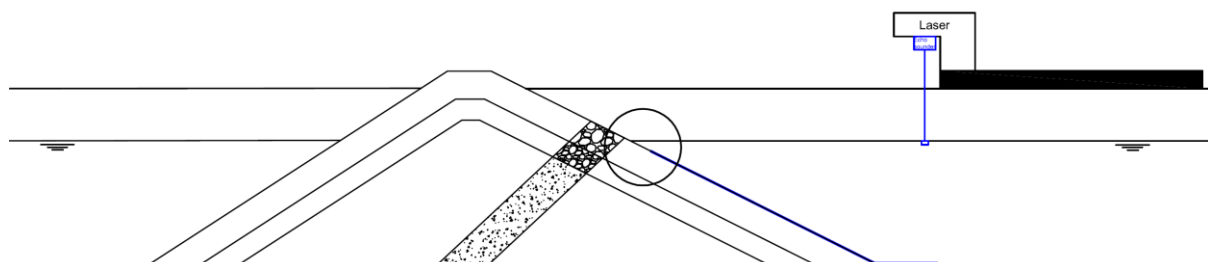


Figure 26 Measuring below water level with echo-sounder

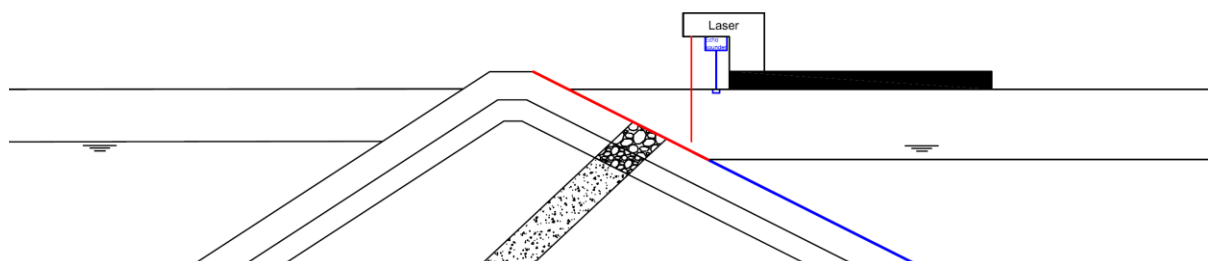


Figure 27 Measuring profile above water line with laser

### 3.4.3 Measuring core velocity

Regarding the notional permeability the flow and therefore the permeability of the structure is important. Measuring the velocities inside the pores is very difficult and will therefore not be attempted within this thesis. The velocities however are not completely unknown, measuring the difference in pressure at specific points in the structure is a very easy method to derive enough data to calculate the velocities. The measured pressure difference initiates the flow of water in the core of the breakwater. With additional testing on the core material the coefficients  $\alpha$  and  $\beta$  can be found which are needed for the formulas presented in section of porous flow to finally calculate the occurring velocities.

In the formula of Burcharth the pressure is calculated at six different positions based on that the velocities at those locations are calculated. The average velocity of those six is said to be the representative core velocity.

The first points are on the waterline, the second three are one significant wave height below the water level. The pressure difference sensors will be dry about 50% of the time when placed on the waterline. Therefore the choice is made to place them on the second position, 10 cm below the waterline.

In total four tubes will be installed inside the core of the structure. These tubes are connected to three pressure difference gauges and measure the pressure difference over three zones. All the tubes will be 0.25 m apart and are positioned about 0.46 m from the bottom of the flume. The structure in which the pressures and the flow in the core is the most relevant is the structure with a permeable core. In addition to the gauges inside the core, an extra pressure difference gauge is placed on the interface between the filter layer and the core.

At the first location the pressure gauge will be connected to the atmosphere, in combination with the pressure difference gauges the decrease of pressure can be determined.

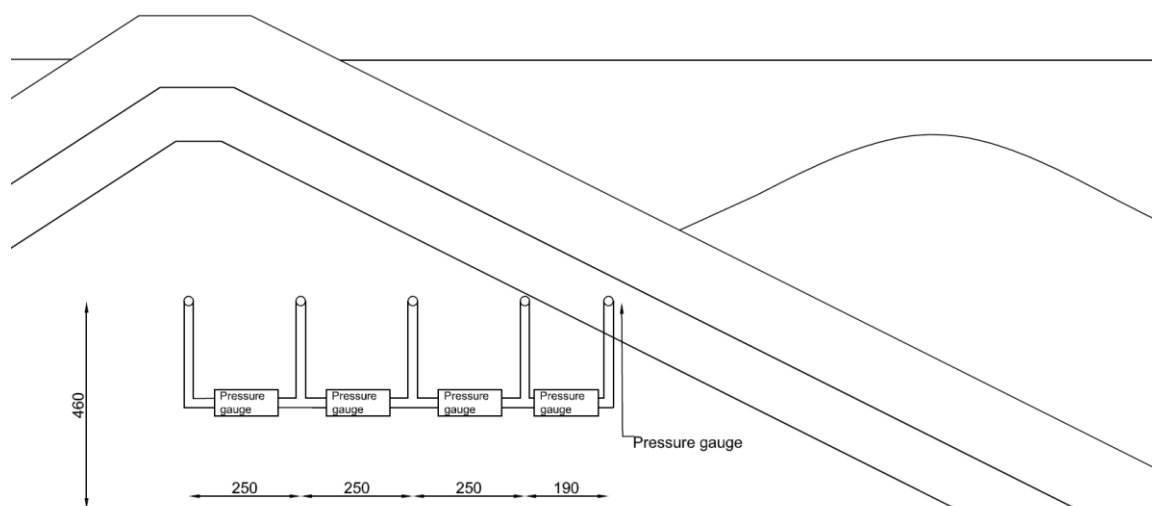


Figure 28 Location of pressure difference gauges

### 3.4.4 Wave measurements

To assure that the right wave height is produced by the wave generator two sets of gauges are placed in the flume. The first one is placed close to the wave generator, recording the produced wave. The second set is placed near the structure, measuring the income and reflected wave. In this way a very accurate record of the occurring wave height in the flume is known, which is very important for the stability of the breakwater.

### 3.4.5 Wave run up

The study of BROEKHOVEN [2011] showed that the most important factor for the volume exchange model is the wave run up at the core. As mentioned before in section 2.3 it is physically better to describe the run up below the armour layer. To possibly support the findings of BROEKHOVEN [2011] the wave run up below the armour layer was measured during the experiments conducted in this research. The wave run up was measured using a resistance wire.



## 4. Data analysis: damage level

A way to empirically determine the “notional permeability” factor  $P$  is to fix or measure all the variables in the Van der Meer formula's 2-15 and 2-16, except those of interest. The two remaining variables are the damage factor  $S$ , and the permeability factor  $P$ . After conducting a test one can rather accurately determine the damage level by comparing the initial profile with the final profile (after  $N$  waves). Finally the coefficient  $P$  can be calculated using all the measured data. In this chapter the analysis of the different structures based on the resulting damage is presented.

### 4.1 Determine damage level

In the previous chapter the method to measure the profile of the breakwater was already described. To process the data a number of manipulations have to be made, especially regarding the laser.

The first correction that had to be made was regarding the breaking index of water. When the laser is measuring below the water level a correction factor has to be applied to the section below the water level accounting for the different speed the laser is travelling over that specific distance. The total distance measured is the distance through the air plus the distance through water. Since the position of the laser is fixed the distance from the device until the water surface can be considered constant. When the measured distance is larger than this constant distance the correction factor will be applied to that specific section. Resulting in a correctly measured height of the profile both below as above the waterline. Combining the signal from the echo-sounder and the laser was done with means of a bar check. A metal bar was positioned inside the flume at a height where both the devices could measure the bar. The shift of the laser signal was done in such a way that both signals plotted the bar in exactly the same position.

When measuring through the water level often errors in the laser signal arises. The errors which are caused by small waves and dirt on the water surface lead to a bad reflection of the laser. These errors have a very short duration which leads to short peaks in the measured signal. During this research a filter for the laser signal has been made, which basically deletes the errors and fills in the deleted data points with interpolated values from neighbouring correct measurements. In this way a smooth signal was created where after it is possible to determine the eroded area of the cross section. In the figures below the difference between the signals can be seen. Around  $x=140$  there are some errors in measured signal from the laser profile (red) in the second figure these data is replaced by a smooth line.

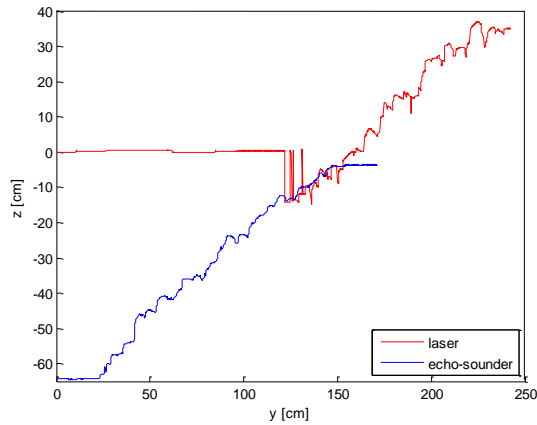


Figure 29 Laser and Echo sounder of one cross section

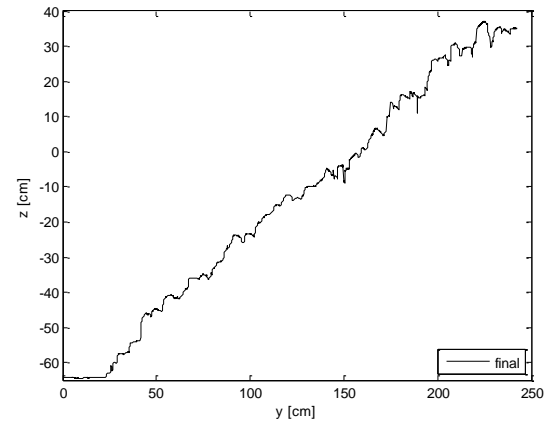


Figure 30 Combined and corrected signal of one cross section

The resulting damage of one test can be determined in a number of ways. During the research of VAN DER MEER [1988] the profile was measured in cross sections each 10 cm apart. The profiles were constructed by measuring the slope of the structure with measuring rods, measuring every 4 cm. Finally all the profiles of the structure were averaged and used to calculate the damage.

As presented in the previous figures the profile measured in this research is done by more modern measuring equipment. This has the result that the measured profile is not a discrete signal with data points every 4 cm but a “continuous” signal. To end up with comparable data the damage was determined by averaging all the cross sections (13 cross sections). In the figure below the measured profiles of the breakwater are presented, the red lines represent the breakwater after conducting a test, the black line is the initial profile.

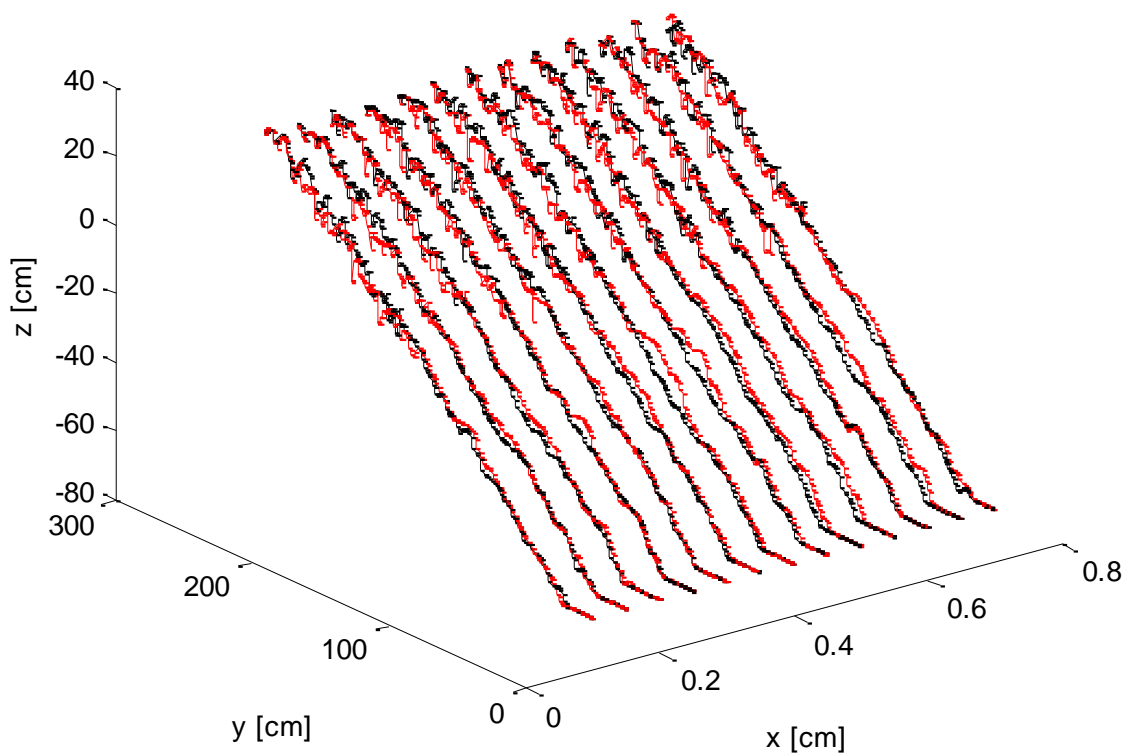


Figure 31 3d presentation of a measured structure

Because the damage is the most important outcome of the experiments the method to come to this damage number is very important. To analyse whether there is a big difference between the discrete measurement (data points every 4 cm) done by Van der Meer and the continuous measurement done in this research this continuous signal is reduced to a discrete signal. In the figures 32 and 33 both the discrete signal and the continuous signal can be seen. With the corrected and averaged measurement the final damage is calculated by determining the eroded area and dividing that area by  $d_{n50}^2$ . The difference in resulting damage appeared to be very small (see Appendix C). Therefore the continuous profile, thus without deleting data to make it discrete, was used to determine the damage.

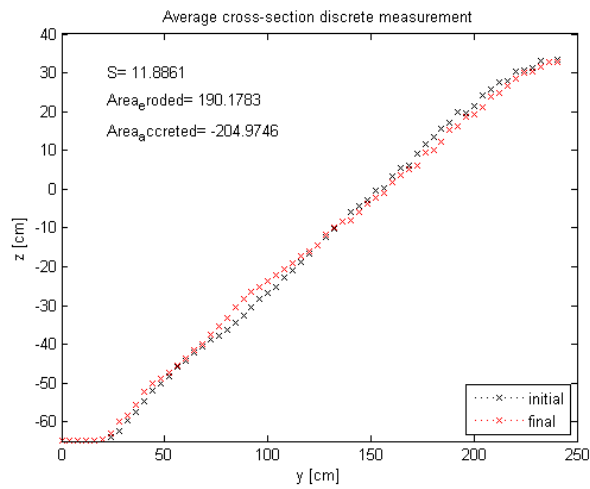


Figure 32 Average profiles discrete

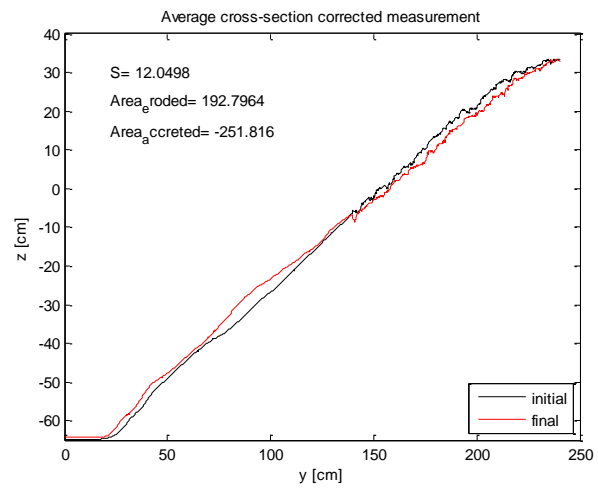


Figure 33 Average profiles continuous

When comparing the measured results with the calculated results on the basis of the stability formula 2-15 and 2-16 a number of statistical performance parameters can be used. Within this report 3 definitions will be used to describe the performance of the equation namely the BIAS (mean error), the MAE (mean absolute error) and the RMSE (root mean square error).

The remark must be made that the performance should not be based on the BIAS, this index has the possibility that equal but opposing errors cancel each other out. The BIAS can be used to assess whether the model generally under- or over-estimates the damage, a positive BIAS means that the calculated result is larger than the measured result and vice versa. The MAE is a linear score which gives every error the same weight. The RMSE on the other hand is a quadratic score, which gives more weight to larger errors. In general the RMSE is most favourable in situation where large errors are undesired. When the MAE and the RMSE are used simultaneously they tell something about the variance in the occurring error. When the difference is very large then the variance in errors is also very large. When the MAE and the RMSE are equal then the errors are of the same magnitude. Within this study the RMSE is used to assess which value of P has the best overall performance.

$$BIAS = \frac{1}{N} \sum_{i=1}^N (X_i - Y_i) \quad 4-1$$

$$MAE = \frac{1}{N} \sum_{i=1}^N |X_i - Y_i| \quad 4-2$$

$$RMSE = \sqrt{\frac{1}{N} \sum_{i=1}^N (X_i - Y_i)^2} \quad 4-3$$

Where:

$X_i$  = calculated result

$Y_i$  = measured result

## 4.2 Structure 1

The first structure is a structure already tested by VAN DER MEER[1988] and resulted during that research in a notional permeability of  $P=0.5$ . A similar structure during this research should produce results in the same range. When this is the case, the conclusion can be drawn that the work method produces reliable and comparable results.

In the table below the measured wave conditions together with the calculated damage and the measured damage are presented. The wave conditions of this matrix deviate slightly from the intended wave conditions as presented in table 10 in chapter 3, therefore the calculated damage contains less experiments with low damage numbers (between  $S=2\sim3$ ). This change was caused by a difference between the steer file of the wave generator and the finally resulting wave conditions.

Test	$H_{m,0}$ [m]	$T_m$ [s]	s	$\xi_m$ [-]	S calculated [-]	S measured [-]
<b>1b</b>	0.161	3.82	0.7%	5.95	5.08	7.71
<b>2</b>	0.142	1.49	4.1%	2.47	4.12	5.00
<b>3</b>	0.153	3.39	0.9%	5.42	5.01	13.03
<b>4</b>	0.150	2.79	1.2%	4.50	7.26	9.11
<b>5</b>	0.147	1.91	2.6%	3.12	8.68	6.33
<b>6</b>	0.138	2.22	1.8%	3.73	7.67	5.09
<b>6b</b>	0.150	2.23	1.9%	3.60	12.55	8.27
<b>7</b>	0.180	2.42	2.0%	3.55	32.97	10.33
<b>6a</b>	0.158	2.24	2.0%	3.52	17.05	8.45
<b>6b</b>	0.163	2.31	2.0%	3.57	19.51	8.65
<b>6c</b>	0.158	2.34	1.8%	3.68	15.66	7.89
<b>6d</b>	0.158	2.23	2.0%	3.51	16.66	6.74
<b>6e</b>	0.159	2.26	2.0%	3.55	17.50	9.46
<b>3a</b>	0.175	3.27	1.0%	4.89	12.71	17.79
<b>3b</b>	0.174	3.26	1.1%	4.88	12.58	16.98
<b>3c</b>	0.175	3.25	1.1%	4.85	13.05	18.61

**Table 11 Test data structure 1 with calculated results for  $P=0.5$**

Choosing the value of which gives the best results is done in the following way. The value of  $P$ , used to calculate the damage is adjusted gradually to finally end up at the lowest statistical error. In this study the RMSE between the measured and the calculated damage was chosen to be the decisive statistical parameter. The RMSE contains the error of the entire dataset of this specific structure, as presented in table 11. This means that initially all the 16 data points are used to determine the best value of  $P$ .

The value of 0.5 for the notional permeability as found by VAN DER MEER [1988] results according to table 12 into an RMSE (root mean square error) of 6.31. To increase the accuracy of the factor P the value is adjusted resulting in different average differences and standard deviations. This evaluation can be found in the table 12.

As described at the beginning of this chapter, the most important statistical parameter is the RMSE. The lowest value of the RMSE is found at  $P=0.55$ .

P	BIAS	MAE	RMSE
0.48	2.83	5.53	6.67
0.49	2.28	5.55	6.49
0,5	1.73	5.52	6.31
0.51	1.18	5.46	6.15
0.52	0.61	5.35	5.98
0.53	0.06	5.24	5.86
0.54	-0.46	5.12	5.80
0.55	-0.96	5.01	5.78
0.56	-1.43	4.89	5.82

Table 12 Statistical performance Van der Meer formula for different P values structure 1

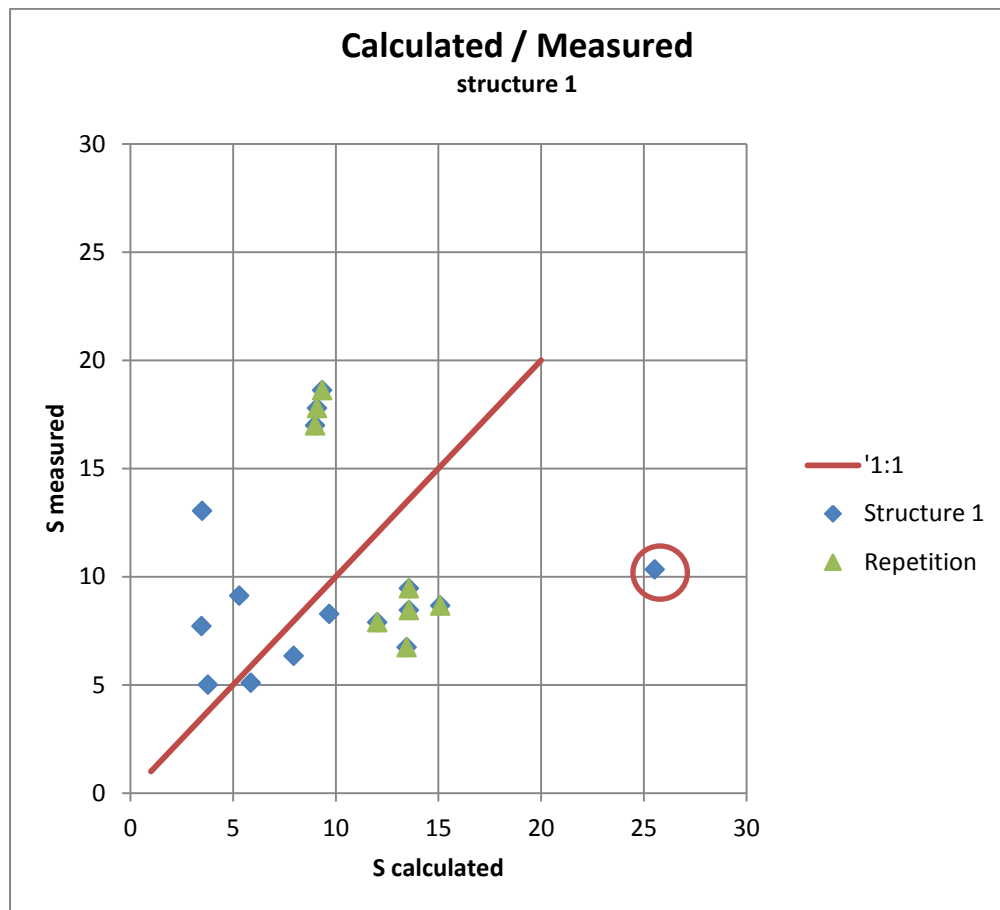


Figure 34  $S_{\text{calculated}}/S_{\text{measured}}$  plot structure 1  $P=0.55$

The analysis of the results has been made visual in the figure above. The data point of test#7 (within the red circle) was left out of the analysis because of the big deviation from the calculated value in combination with the very high calculated damage, which is not realistic.

In the following plot all the measured data of structure 1 is presented. On the y-axis the stability parameter  $\frac{H_s}{\Delta d_{n50}}$  is supplemented with an extra term to represent the damage  $\left(\frac{s}{\sqrt{N}}\right)^{0.2}$ . In this way the data acquired from the tests with different damage values can easily be compared to each other. On the x-axis one can see the Iribarren number, representing the wave data. According to the stability formulae derived by Van der Meer the stability should decrease in the plunging section of the Iribarren axis and increase for increasing Iribarren values in the area with surging waves. This has been visualized using the mean and the standard deviation of the plunging and surging coefficients from VAN DER MEER [1988] representing the 10 and 90% confidence intervals of the stability formulae. The mean value (50% confidence interval) of the stability formulae is positioned exactly in between the two lines. The test results of this research are represented with a diamond, the data of VAN DER MEER [1988] is represented by a +. The blue triangle symbolises the repetition tests executed by D. PAPADOPOULOS [2011].

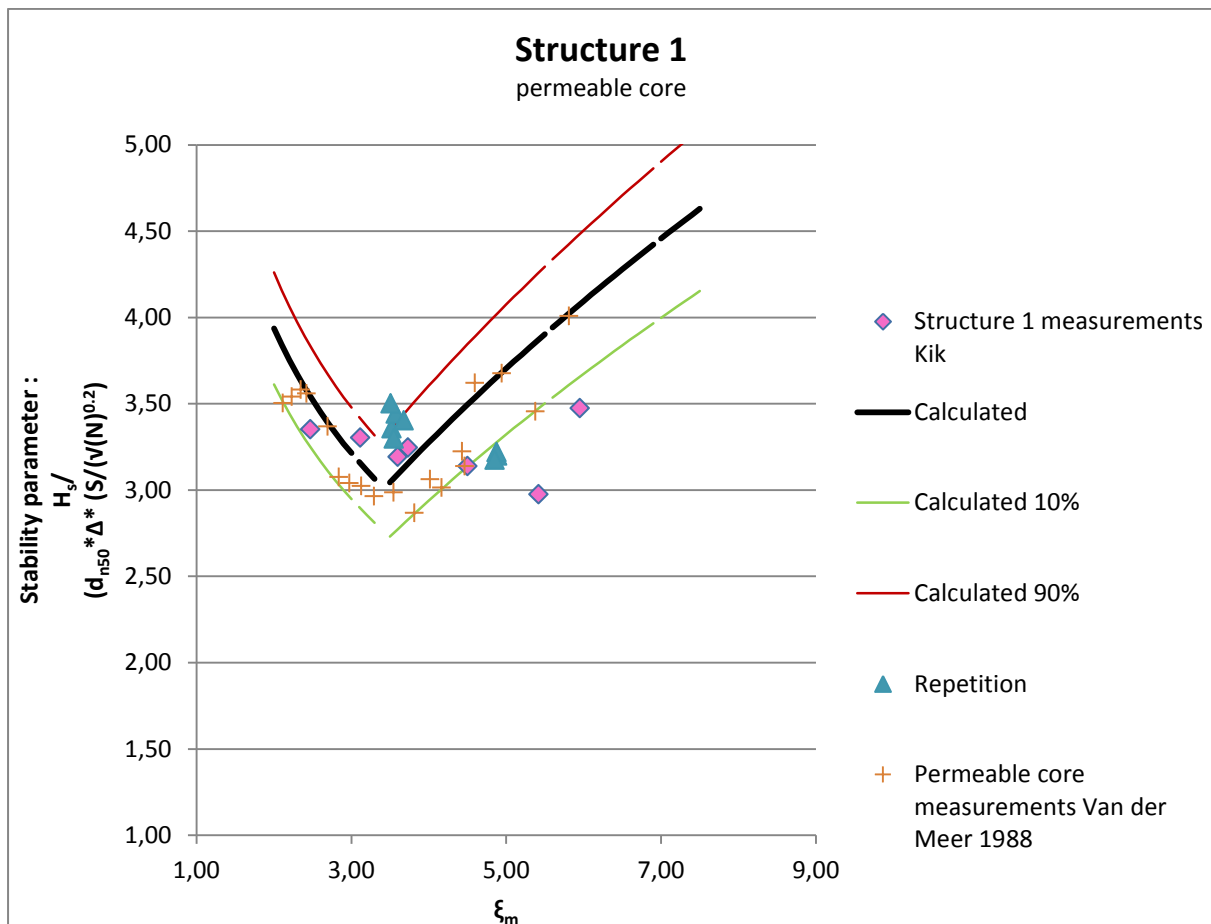


Figure 35 Measured stability structure 1 with Van der Meer formula P=0.55

The general trend is that the measured values are within the scatter of the original measurements.

#### 4.2.1 Conclusion

The value of  $P$  which gives the lowest statistical error (RMSE) between the calculated and measured damage is  $P=0.55$ . The lowest BIAS is found at  $P=0.53$ .

Several different analysis show small differences for the value of  $P$  to be used in the Van der Meer stability formula. All these possible values for  $P$  are very close to the definition of  $P=0.5$  made by VAN DER MEER [1988].

When considering the data points plotted on the basis of stability (figure 35) one can see that almost all the data points of this study are within the scatter of the original measurements.

From these findings the conclusion can be made that the tests executed in this research produce comparable results with the research of VAN DER MEER [1988]. Furthermore the value of  $P=0.5$  for this kind of structures is a realistic value to use.



### 4.3 Structure 2

The second structure, which is just like the first structure, is also a reference case. This structure has an expected value for the notional permeability of  $P=0.1$ . The structure consists out of an impermeable core with a thin filter layer and the same armour layer as the other structures. The expectation is to have relatively more damage because of the lower permeability.

In the table below the actual wave data together with the calculated damage and the measured damage is presented.

Test	$H_{m,0}$ [m]	$T_m$ [s]	s	$\xi_m$ [-]	S calculated [-]	S measured [-]
8	0.091	1.18	4.2%	2.44	1.84	1.74
9	0.100	1.81	2.0%	3.57	7.66	3.20
10	0.112	4.18	0.4%	7.80	9.14	9.47
11	0.104	3.59	0.5%	6.96	6.58	10.20
12	0.098	2.42	1.1%	4.83	5.96	5.56
13	0.098	2.11	1.4%	4.21	6.29	3.83
14	0.094	1.16	4.5%	2.36	1.99	2.22
15a	0.096	1.36	3.3%	2.74	3.19	2.16
15b	0.096	1.39	3.2%	2.79	3.41	3.44
15c	0.097	1.40	3.2%	2.81	3.57	3.65
16a	0.111	4.21	0.4%	7.89	8.68	12.06
16b	0.111	4.21	0.4%	7.89	8.68	10.98
16c	0.110	4.21	0.4%	7.93	8.28	12.53

Table 13 Test data structure 2 with calculated results for  $P=0.1$

The possible value of  $P$  is determined in the same way as for structure 1. A range of values are used to calculate different statistical parameters describing the accuracy of the stability formulae.

P	BIAS	MAE	RMSE
0.05	0.45	2.23	2.51
0.06	0.37	2.06	2.34
0.07	0.18	1.88	2.24
0.08	-0.01	1.77	2.24
0.09	-0.22	1.70	2.30
0.10	-0.44	1.74	2.40
0.11	-0.72	1.84	2.46
0.12	-0.99	1.96	2.57

Table 14 Statistical performance Van der Meer formula for different  $P$  values structure 2

The general trend of the damage measurements against the calculated damage is that the formulae underestimate the damage (negative BIAS). When attempting to adjust this underestimation using only the factor for the notional permeability, it logically should result into a lower value of  $P$ . When looking at table 14 with varying  $P$  values this statement can be validated. Reducing the value of  $P$  results into a lower difference between the measured and calculated damage. The lowest RMSE is found at  $P=0.08$ . The evaluation of  $P$  on the basis of RMSE results into figure 36.

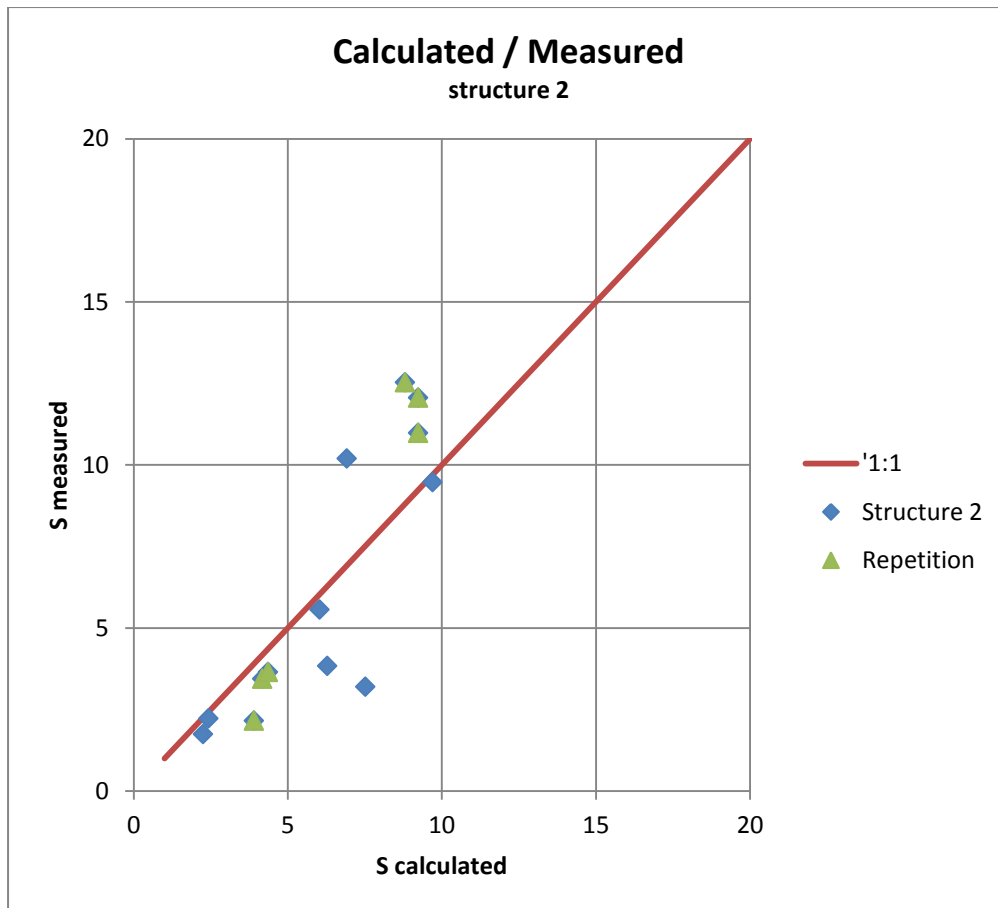


Figure 36  $S_{\text{calculated}} / S_{\text{measured}}$  plot structure 2  $P=0.08$

The figure above shows the relation between calculated and measured damage. No large deviations from the 1:1 line are observed.

Comparing the data points of VAN DER MEER [1988], THOMPSON AND SHUTTLE [1975], this research and the stability formulae is done with means of the plot with the stability parameter. In this plot it can clearly be seen whether the measured data point are positioned within the scatter of the original measurements or not. The dataset of VAN DER MEER [1988] was supplemented with the data of Thomson & Shuttle because Van der Meer did not conduct plunging wave tests on the impermeable structure, instead he used the data acquired by THOMPSON AND SHUTTLE [1975].

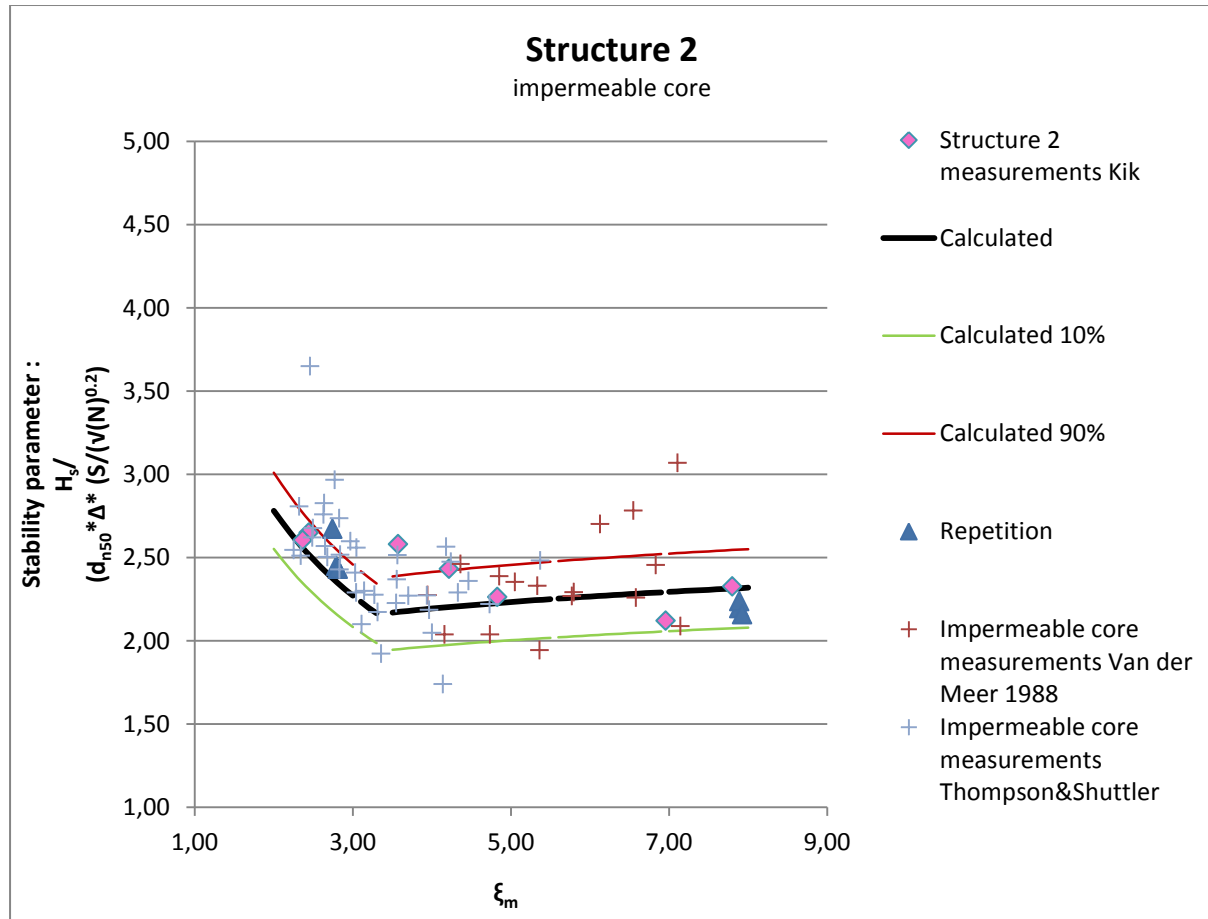


Figure 37 Measured stability structure 2 with Van der Meer formula  $p=0.08$

All the data points from this study are positioned within the scatter of the original measurements. Also the increasing stability for lower Iribarren numbers is recognized. This second structure shows a better trend with respect to the calculated and original results when compared to the first structure, which is also clear when both RMSE values are compared.

#### 4.3.1 Conclusion

After analysis of the data a P-value of 0.08 resulted into the lowest RMSE. However the practical value of  $P=0.1$  does not give large deviations from the best fit of  $P=0.08$  and together with figure 37 can the conclusion be drawn that the acquired data is within the expectation and the test method resembles the methods used in previous studies regarding the stability of breakwaters.

#### 4.4 Structure 3

The structure with no validated P-value of the three tested structures is the third one. This “new” structure has never been tested considering the permeability of the structure, but is often applied all over the world. The structure, as mentioned before, consists out of an impermeable core with two filter layers and an armour layer.

For structure 1 and 2 nearly the same value for the notional permeability P was found as stated by Van der Meer, namely  $P=0.1$  and  $P=0.5$ . Therefore the conclusion can be drawn that the test method and data analysis produce reliable results regarding the occurring damage. A value for the new structure could therefore be considered as a valid value, though further research improves the reliability of its value especially under other slope angles and a wider range of wave height and periods. Within this research the Iribarren number was between 1.74 and 6.11. The calculated damage S in the table below is based on an estimated value of  $P=0.3$ , this value of P will be considered in table 16.

Test	$H_{m,0}$ [m]	$T_m$ [s]	s	$\xi_m$ [-]	S calculated [-]	S measured [-]
17	0.125	1.77	2.6%	3.12	6.18	4.92
18	0.122	1.49	3.5%	2.67	3.72	2.20
19	0.144	3.71	0.7%	6.11	12.11	12.09
20	0.128	2.27	1.6%	3.96	12.67	5.35
21	0.125	2.80	1.0%	4.95	8.13	5.74
22	0.138	3.42	0.8%	5.74	10.75	9.65
23	0.110	1.27	4.4%	2.39	1.68	2.31
24	0.120	2.53	1.2%	4.56	7.56	4.03
25	0.120	2.01	1.9%	3.62	7.32	6.17
26	0.106	1.18	4.9%	2.26	1.21	1.83
31	0.158	1.11	8.2%	1.74	4.65	7.09
28	0.136	2.30	4.3%	4.06	11.02	4.02
29	0.134	2.29	4.3%	4.12	8.86	3.06
30	0.131	2.25	4.2%	4.06	8.92	4.67
27a	0.128	1.42	1.5%	2.41	4.91	4.16
27b	0.120	1.42	1.5%	2.42	4.69	5.16
27c	0.120	1.41	1.5%	2.43	4.26	4.18

Table 15 Test data structure 3 with calculated results for  $P=0.3$

Similar as for the earlier discussed structures 1 and 2, the predictive skills of the model are assessed for structure 3. This results in the following table with possible values of P.

P	BIAS	MAE	RMSE
0.29	2.21	2.65	3.59
0.3	1.88	2.37	3.31
0.31	1.57	2.20	3.07
0.32	1.27	2.07	2.83
0.33	0.98	1.98	2.64
0.34	0.70	1.90	2.49
0.35	0.44	1.82	2.37
0.36	0.19	1.75	2.30
0.37	-0.05	1.74	2.27
0.38	-0.28	1.73	2.27

Table 16 Statistical performance Van der Meer formula for different P values structure 3

The lowest RMSE was found with a P-value of 0.37. Based on this, one could imply that the estimated value of about 0.3 can be considered as a conservative value for this type of structure.

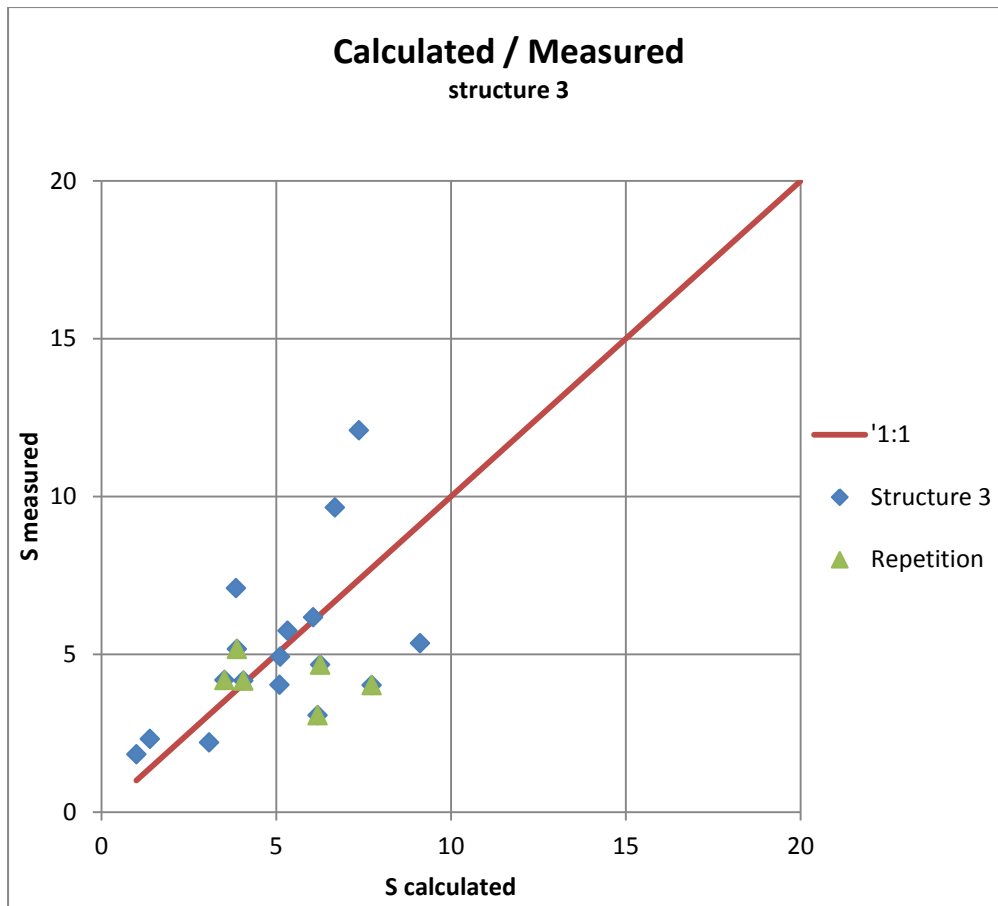


Figure 38  $S_{\text{calculated}} / S_{\text{measured}}$  plot structure 3  $P=0.37$

In the analysis presented in table 16 the best value of  $P$  was found at  $P=0.37$ . This value is much larger than the expected  $P$  value of 0.3 and very close to  $P=0.4$ . This result raises questions concerning the  $P=0.4$  structure. It could imply that the value of  $P=0.4$  is too low, or the effect of an impermeable core is no longer felt after a certain distance. This finding makes testing the  $P=0.4$  structure even more interesting.

In figure 39 the measured data points are presented together with the result of the formulae and the two confidence intervals of the stability formulae 2-15 and 2-16. The results are almost all within the two confidence intervals, and the decreasing trend in the plunging regions is observed clearly.

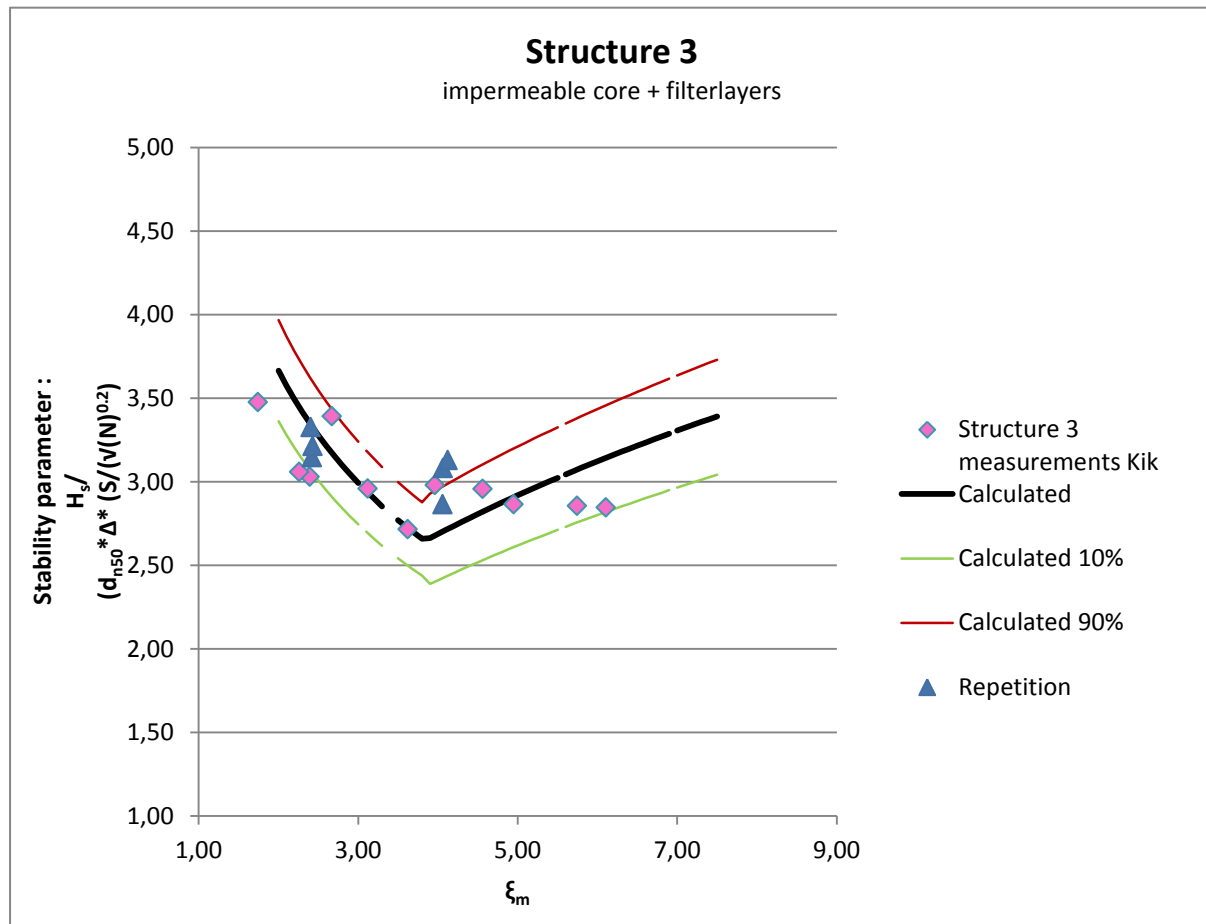


Figure 39 Measured stability structure 3 with Van der Meer formula  $p=0.37$

#### 4.4.1 Conclusion

The estimated value of  $P=0.3$  appears to be a conservative value. Optimising this value results in a value of  $P=0.37$  for the lowest BIAS and RMSE.

For practical applications at this moment the advised value for  $P$ , based on the limited number of tests executed in this research, is  $P=0.35$ . With a larger number of tests this empirical value could be determined more accurately, but at the time being it is best to remain at the conservative edge of the possible  $p$  values for this kind of structures.

## 4.5 Repetition tests

As an addition to this thesis DIMITRIOS PAPADOPOULOS repeated two individual tests three times for each tested structure. Furthermore he examined the effect on the accuracy of measuring the profile every 5 or 10 cm. In this section a short recap of the results of this additional thesis is given.

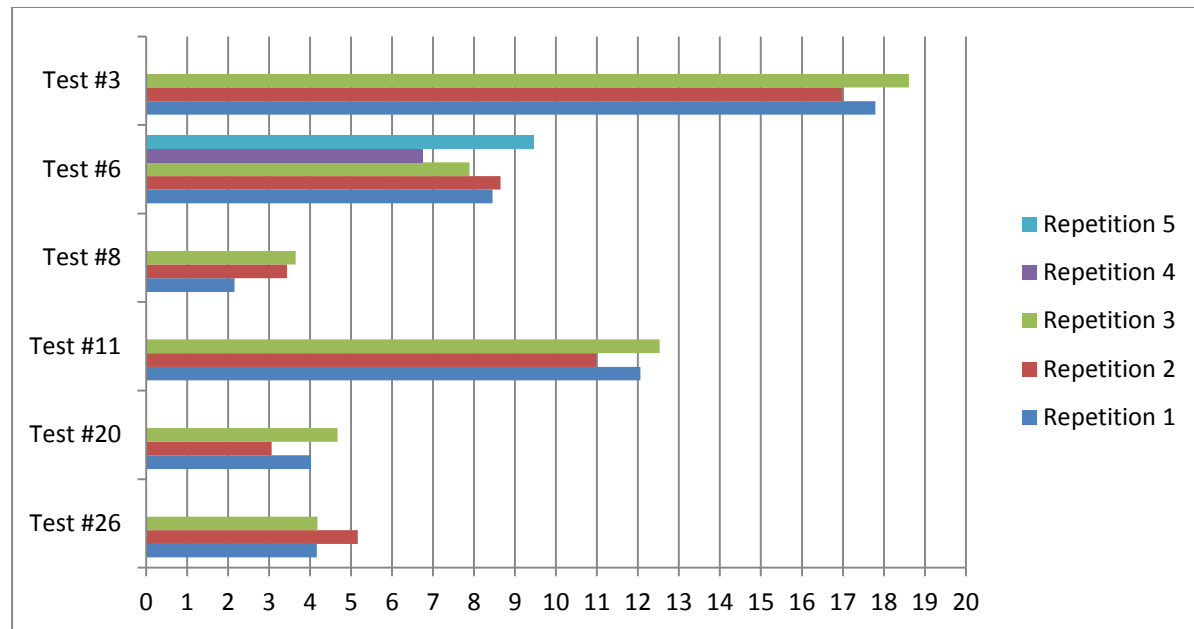


Figure 40 Results damages repetition tests Papadopoulos

In the chart above the resulting damage of the repeated tests is presented. Almost all the repetition series show a low spreading around their mean value. During the repetition tests of tests #3 and the first three repetitions of #6 no wave reflection compensator was used, the last two repetition tests of test #6 did have the reflection compensator turned on again. This should however not influence the outcome of the experiments because earlier research (VAN DER MEER [1988] and MERTENS [2007]) showed that the spectral shape has a neglectable influence.

The effect of measuring every 5 cm instead of every 10 cm is quite trivial. Additional measurements decrease the interval length of the confidence interval with a factor in the order of 20-40%. In absolute damage values the additional measurements did not affect the resulting damage very much. The advantage of measurements closer to each other is that the deformation of the rock slope can better be made visual. With a nominal stone diameter much smaller than the measuring distance the possibility can occur that movement of stones is not observed.

Another observation made by PAPADOPOULOS was that the spreading in damage between the individual measurements was slightly larger in the situations with plunging waves. This is probably caused by the more chaotic character of the plunging waves resulting in a less even reaction of the structure. For more detailed results the reference is made to the report of PAPADOPOULOS *Damage on rock slopes under wave attack* [2011].

Analysing the spreading occurring in the repetition tests provides the following standard deviations. As one can see in table 17 the difference in spreading of the repetition series is very small. The reason that different damage values occur can be caused by two facts. The first one is the natural variability of the material used. There are natural varieties in rock density present in the material that is used, besides the density there are also variations in shape which could affect the stability. The second cause is the construction method. Before every test the armour layer was placed by dumping a bucket of rocks on the slope, afterwards the slope was lightly compacted by hand. This manual process can result into small differences of structural initial conditions.

However the spreading in damage shows that the effect of these reasons is very small. The final standard deviation of the repetition tests is 0.8.

Test	Standard deviation
Test #3	$\sigma = 0.82$
Test #6	$\sigma = 1.01$
Test #8	$\sigma = 0.81$
Test #11	$\sigma = 0.79$
Test #20	$\sigma = 0.81$
Test #26	$\sigma = 0.57$
Average	$\sigma = 0.80$

Table 17 Spreading of repetition test

## 4.6 Stone balance

At the beginning of chapter four the method of determining the damage is presented. The way to define the resulting damage is done by measuring the eroded area. Besides the eroded area also the accreted area was measured. In theory these values should be equal to each other because no stones are lost during an experiment. However analysing the eroded and accreted areas showed that these areas were not always equal to each other. In general the accreted area was about 30% smaller compared to the eroded area.

A possible explanation for this is that the armour layer is not fully compacted prior to the experiment. Therefore during the wave series compaction of the armour layer could occur resulting into a smaller cross sectional area.

In a few cases the ratio between the eroded area and the accreted area became really large. This was however always in situations with small damage numbers and thus small eroded areas.



## 5. Additional data

New theories about the notional permeability as elaborated by JUMELET [2010] require a lot of data in order to be validated. This data provides insight in the processes that take place during a storm, and more specifically during the in- and out- flow of water driven by waves. To allow further research in the line of the physical background of the notional permeability with the tests executed during this research additional data was recorded which is not directly necessary to empirically determine the coefficient  $P$ . The measured data is the pressure distribution in the structure. Besides this, based on the work of BROEKHOVEN [2011], the wave run up below the armour layer is measured.

### 5.1 Wave run up

After the experiments conducted by BROEKHOVEN [2011] it became clear that not the wave run up on top of the armour layer is important but the run up below the armour layer. Therefore during the test series executed in this thesis the wave run-up under the armour layer was measured. The method used to measure the wave run-up was similar to the method used by Broekhoven, namely a resistance wire measuring the voltage over the two wires. This gauge is in fact a modified wave height gauge.



Figure 41 location of the run-up gauge

During the first two test series ( $P=0.5$  and  $P=0.1$ ) only the irregular pierson-moskowitz wave spectrum was applied. From this irregular wave spectrum it is difficult to extract the correct data required for the volume exchange model. At this moment the volume exchange model is only based on regular waves, further research is required to adapt it to  $H_s$  and  $Ru_{2\%}$  values. During the last test series also some tests with regular waves were executed.

In the next figure a small section of the recorded run-up below the armour layer is shown. Here one can easily recognize the irregular pattern of a wave spectrum. To extract amplitude information from such a signal often a Fourier analysis is used. For the wave run up however we are not particularly interested in the amplitude but

in the height of the peaks with respect to the still water level ( $y=0$ ). The only useful information a Fourier analysis could give is information regarding the frequency of the water level variations under the armour layer and a possible frequency shift between the external water motion and the internal water motion.

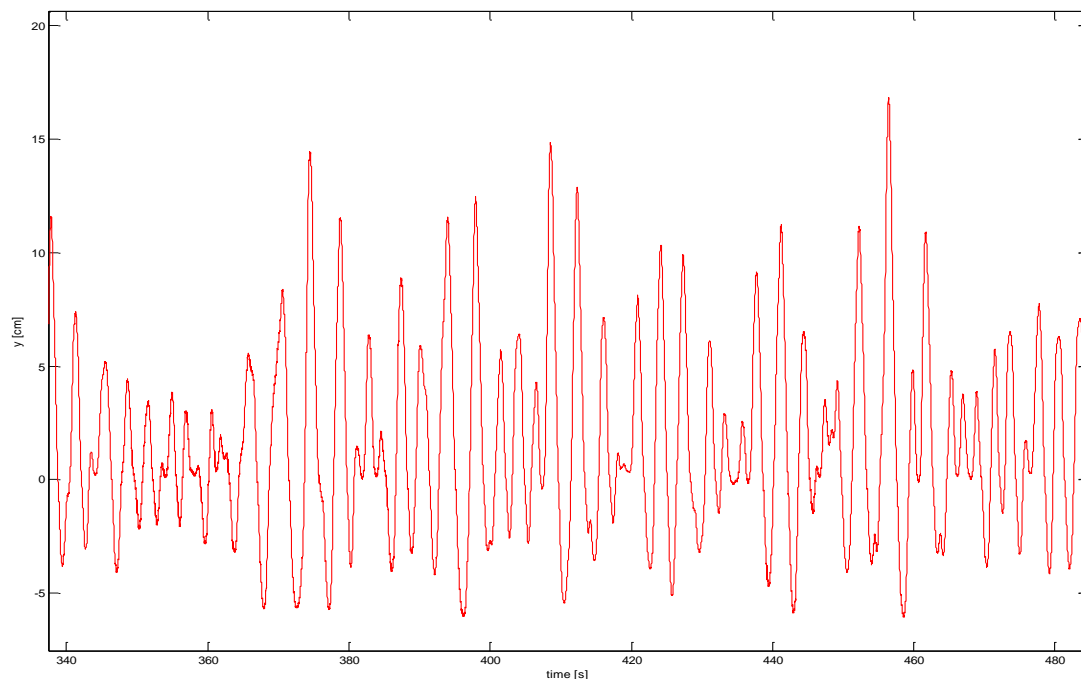


Figure 42 Run-up under armour layer test#4

Determining the run-up level from this signal was done by locating peaks in the signal and thereby finding the maximum value of a specific peak. This is done for the entire signal which leads to a list of peak locations and peak heights. This information is used to create a cumulative distribution function (CDF) of the run up height of a specific test. Based on this cumulative distribution function the run up height which is exceeded by only 2% of the wave is extracted, in other words the  $Ru_{c;2\%}$ .

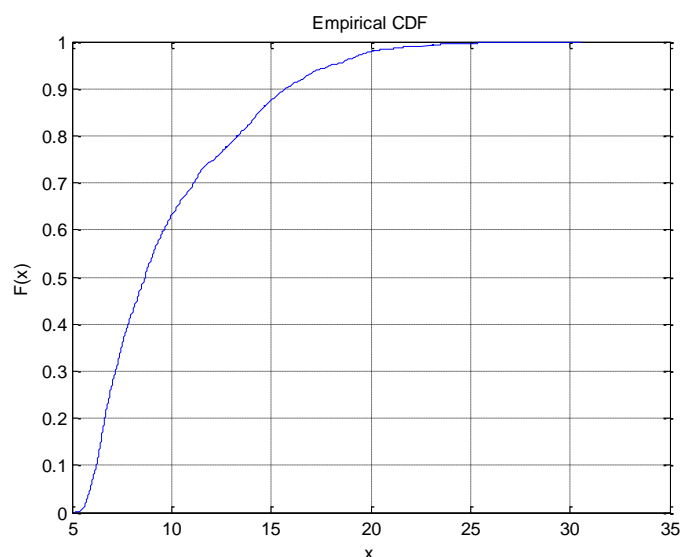


Figure 43 cumulative distribution function wave run up test#4

In the table below the wave run up per test can be found together with the measured  $H_s$ . Using this measured run up in combination with the definition from JUMELET & BROEKHOVEN the value of the run up reduction

coefficient can be calculated. The only remaining unknown data is the run up on an impermeable core. BROEKHOVEN found for this reference level the following relation with the Iribarren number.

$$\frac{R_u}{H} = 1.63 * \tanh(0.14 * \xi)$$

5-1

This definition describes the direct response of the water level to an external force (one regular wave). When the H in this formula is replaced by the  $H_{2\%}$  or  $H_s$  then the outcome is assumed to result into a  $R_{u_{2\%}}$  or  $R_{u_s}$ . If this assumption is applied to the formula stated above, then the reference level can be calculated. In the following analysis the mean period is used in the Iribarren number.

Test	$H_{m;0}$	$\xi_m$	$R_{u_{2\%};c}$	$R_{u_s;c}$	$R_{u_{imp};c}$	Cr
<b>1b</b>	0.161	4.74	0.302	0.1972	0.152	1.29
<b>2</b>	0.142	2.32	0.208	0.1753	0.073	2.41
<b>3</b>	0.153	4.76	0.318	0.2364	0.145	1.62
<b>4</b>	0.150	4.03	0.202	0.1467	0.125	1.17
<b>5</b>	0.147	2.97	0.254	0.1784	0.094	1.89
<b>6</b>	0.138	3.55	*	*	0.103	0
<b>6b</b>	0.150	3.36	0.1888	0.1487	0.107	1.38
<b>7</b>	0.180	2.71	*	*	0.106	0
<b>6a</b>	0.158	3.27	0.2239	0.1676	0.110	1.52
<b>6b</b>	0.163	3.31	0.2565	0.1904	0.115	1.66
<b>6c</b>	0.158	3.36	0.2260	0.1746	0.113	1.55
<b>6d</b>	0.158	3.31	0.2007	0.1518	0.111	1.36
<b>6e</b>	0.159	3.29	0.1978	0.1557	0.112	1.39
<b>3a</b>	0.175	4.19	0.4534	0.3081	0.150	2.05
<b>3b</b>	0.174	4.24	0.3801	0.2557	0.151	1.69
<b>3c</b>	0.175	4.23	0.3823	0.2658	0.152	1.75

Table 18 Measured run up 2% and significant below armour layer structure 1

Test	$H_{m;0}$	$\xi_m$	$R_{u_{2\%};c}$	$R_{u_s;c}$	$R_{u_{imp};c}$	Cr
<b>8</b>	0.091	2.76	0.1062	0.0823	0.055	1.51
<b>9</b>	0.100	3.48	*	*	0.074	
<b>10</b>	0.112	6.98	*	*	0.137	
<b>11</b>	0.104	6.71	*	*	0.125	
<b>12</b>	0.098	5.27	*	*	0.100	
<b>13</b>	0.098	4.14	0.2934**	0.2032	0.083	2.44
<b>14</b>	0.094	2.37	0.1143	0.0875	0.049	1.78
<b>15a</b>	0.096	2.68	0.1058	0.0798	0.056	1.42
<b>15b</b>	0.096	2.68	0.1167	0.0788	0.056	1.40
<b>15c</b>	0.097	2.67	0.0963	0.0680	0.056	1.20
<b>16a</b>	0.111	7.03	*	*	0.137	
<b>16b</b>	0.111	7.03	*	*	0.137	
<b>16c</b>	0.110	7.06	*	*	0.136	

Table 19 Measured run up 2% and significant below armour layer structure 2

Test	$H_{m;0}$	$\xi_m$	$Ru_{2\%;c}$	$Ru_{s;c}$	$Ru_{imp;c}$	Cr
17	0.125	2.93	0.0931	0.0674	0.079	0.85
18	0.122	2.38	0.0887	0.0736	0.064	1.15
19	0.144	5.32	*	*	0.148	
20	0.128	3.84	0.1477	0.1093	0.102	1.07
21	0.125	4.60	*	*	0.116	
22	0.138	5.06	0.1891	0.1291	0.137	0.94
23	0.110	2.20	0.0636	0.0485	0.054	0.91
24	0.120	4.15	*	*	0.102	
25	0.120	3.48	0.1285	0.0983	0.088	1.11
26	0.106	2.19	0.0563	0.0440	0.051	0.86
31	0.158	3.89	*	*	0.128	
28	0.136	2.31	0.0874	0.0692	0.069	1.00
29	0.134	2.37	0.1156	0.0897	0.070	1.28
30	0.131	2.41	0.0999	0.0815	0.069	1.17
27a	0.128	2.15	0.1455	0.1118	0.061	1.83
27b	0.120	3.98	0.1190	0.0882	0.099	0.89
27c	0.120	4.01	0.1564	0.1212	0.100	1.22

Table 20 Measured run up 2% and significant below armour layer structure 3

When the measured run up is divided by the calculated reference level as defined by BROEKHOVEN the run up reduction factor (Cr) is obtained. It however appears that almost all the Cr values are larger than one. Theoretically this value should be smaller than one. A number of explanations are possible; the first one is an error in the data from the measurements in the test series executed within this research. After every test the top layer was removed and thus the run up gauge exposed. This could lead to movement of the gauge and induce errors. However when looking at the repetition tests this error seems to be neglectable.

The second explanation is the applicability of the relation found by BROEKHOVEN for regular waves to irregular waves. It is advised to do additional research about the applicability under irregular wave spectra. On the third structure also regular waves were applied. Thus the type of waves wherefrom the relation was deducted. Analysing this can help to see what the problem is with the recorded run up.

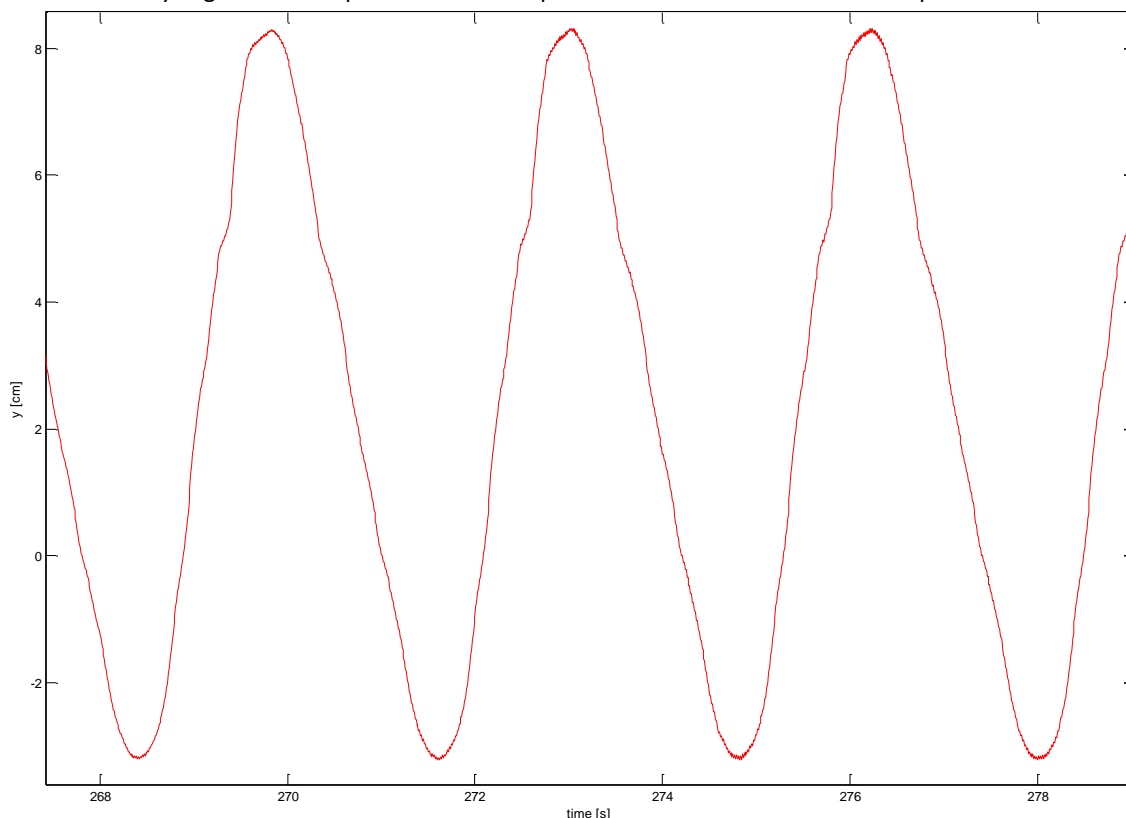


Figure 44 Measured wave run-up below the armour layer T=3.2s

The recorded wave run up with a regular wave with wave height of 8 cm and a period of 3.2 seconds is about 8.3 cm. The calculated reference run up level is about 9.80 cm. This results into a run up reduction factor of 0.85. When the same analysis is done for the test with a wave period of 1.2 seconds the run up reduction factor is in the order of 0.65. These values seem to be at first sight realistic values. Implying that the method of measuring and the reference relation produce better result for regular waves.

On the basis of damage analysis the factor for the notional permeability is determined empirically, namely  $P=0.35$ . With this data a brief analysis of the relation between  $Cr$  and  $P$  (as found by BROEKHOVEN) can be made.

According to equation 2-45 the  $P$  value should be:

H	T	$\xi$	$Ru_{\text{measured}}$	$Ru_{\text{reference}}$	$Cr$	$P$
0.1	1.2	2.34	0.03	0.05	0.6	1.06
0.1	3.18	6.24	0.083	0.11	0.75	0.227
0.085	4.50	9.51	0.10	0.12	0.83	0.115
0.14	2.40	3.95	0.092	0.11	0.83	0.23
0.10	1.57	3.06	0.045	0.066	0.68	0.56

Table 21 Measured run-up below armour layer with calculated  $Cr$  and  $P$  for regular waves

The first value in the table above is clearly a wrong value. The other values are within the range of individual values found from the experiments on structure 3. When these values are averages, except the first value, an average value of  $P=0.28$  is acquired. Nevertheless is this dataset of regular waves too limited to draw valid conclusions from. It is advised to do additional research to the effect of the irregular waves to the run up reduction coefficient and the volume exchange model.

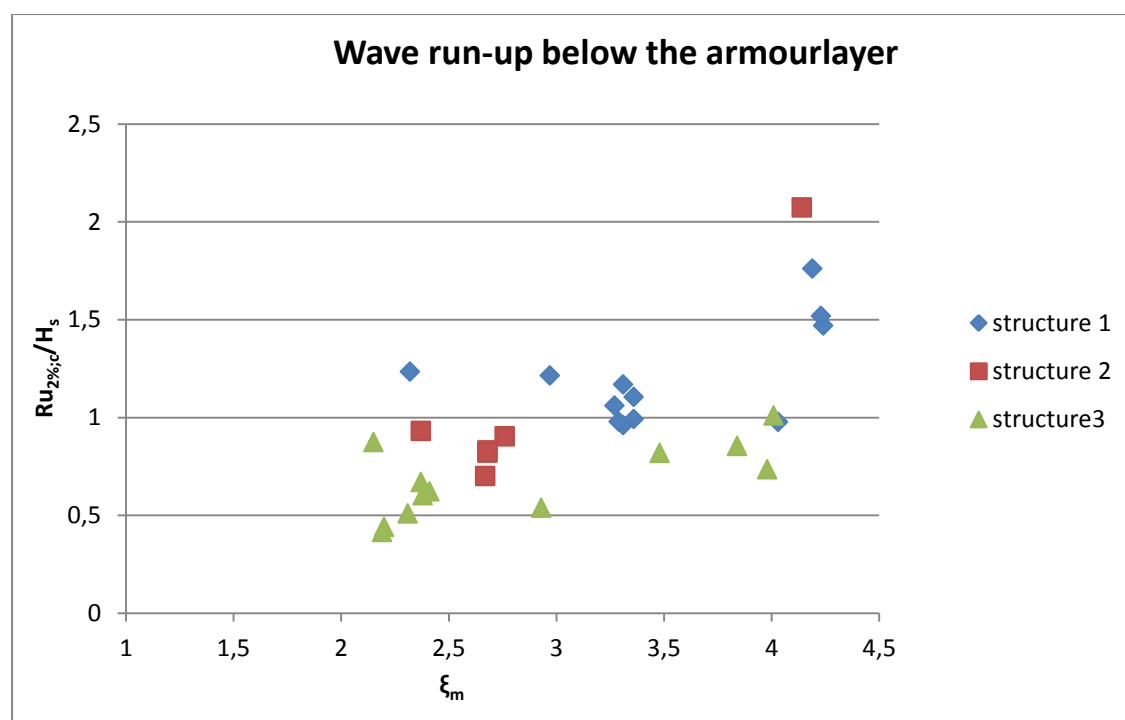


Figure 45 Measured wave run-up below armour layer

According to the theory elaborated by JUMELET the run up should be the largest for structure 2 where the core is completely impermeable. The third structure, which has filter layers and an impermeable core, should produce a slightly lower run up at the core and structure 1 with a permeable core should result into the lowest run up. This is however not observed during this research.

## 5.2 Pressure distribution

During every test of this thesis the pressure difference was measured. The initial intention of this measurement was to derive a pore velocity driven by the external forcing of the waves. This can provide insight in possible scale effect with respect to turbulent or laminar flow inside the structure. Burcharth proposed a method for scale models of breakwaters, as already presented in chapter 3. The probability of problems with the scaling with respect to porous flow is biggest for the structure defined by Van der Meer with a notional permeability of 0.4 and the new structure tested within the scope of this thesis.

Because of the fact that regular waves were only applied to the third structure and that this structure has a risk of laminar flow in the pores will this structure be considered in this section.

In total five pressure gauges were installed at a depth of about 55 cm. The first tube is connected to the open air and acts as a reference measuring the atmospheric pressure. The second tube is positioned inside the armour layer. All the other tubes are positioned at the interfaces between the individual layers. Each measuring the pressure difference occurring in a layer.

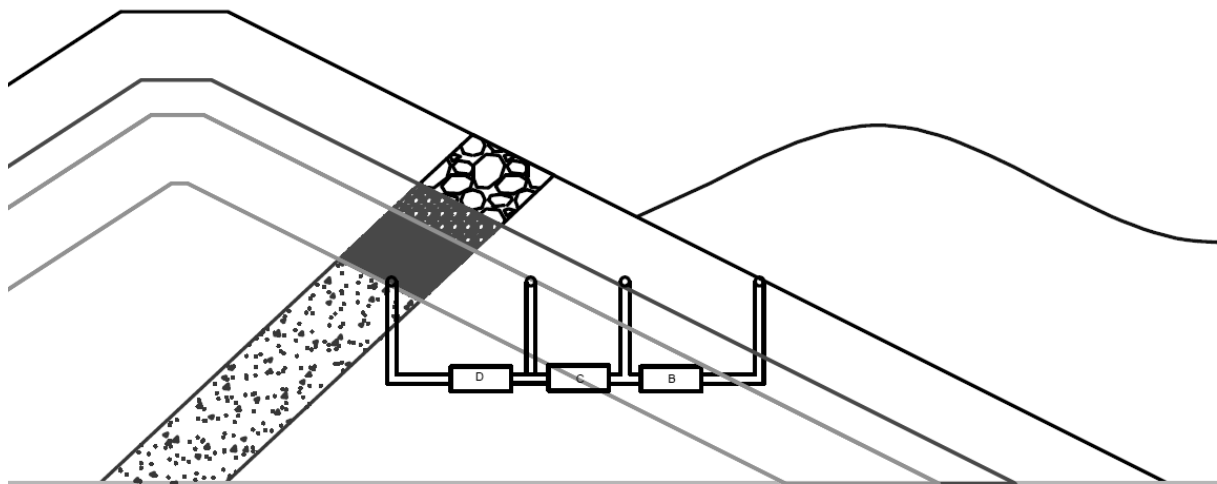


**Figure 46** Location of pressure gauges

In this figure the pressure differences as described has been made visual. With A as the difference between atmosphere and armour layer, B difference between armour layer and first filter layer and C is the difference over the first filter layer, D is the difference over the second filter layer.

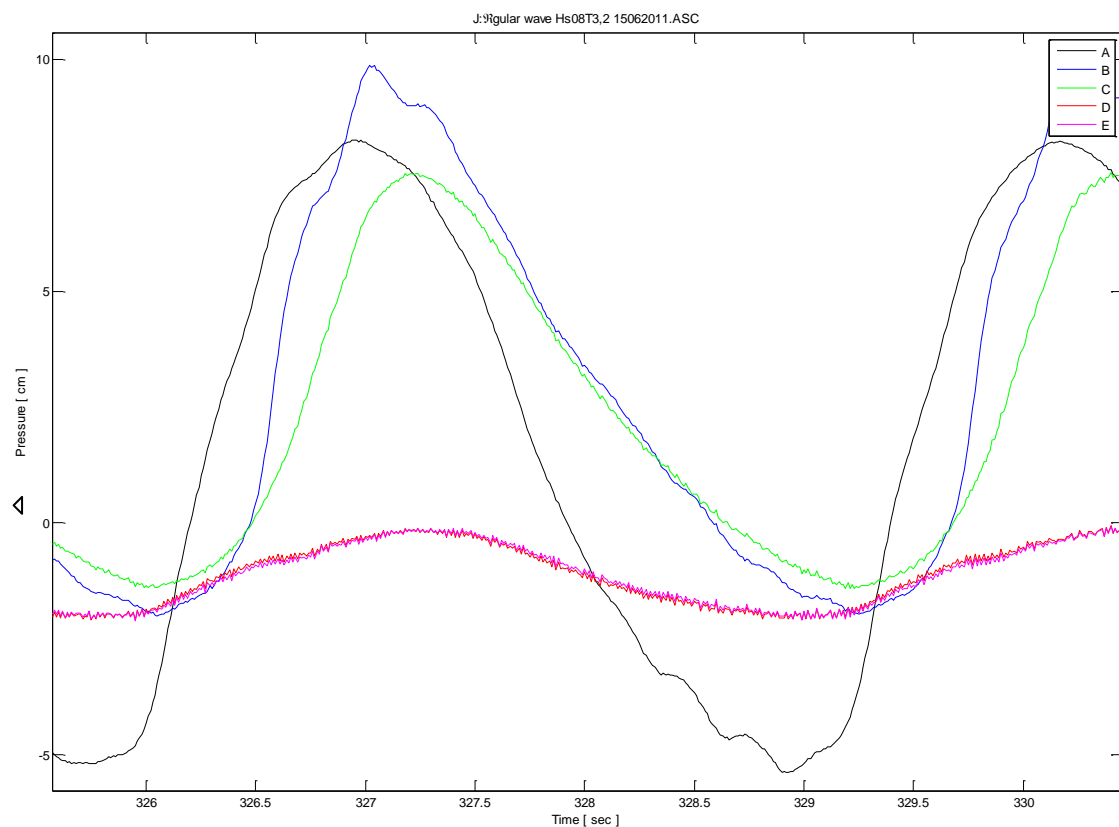


Figure 47 Pressure difference in time T=3.2s

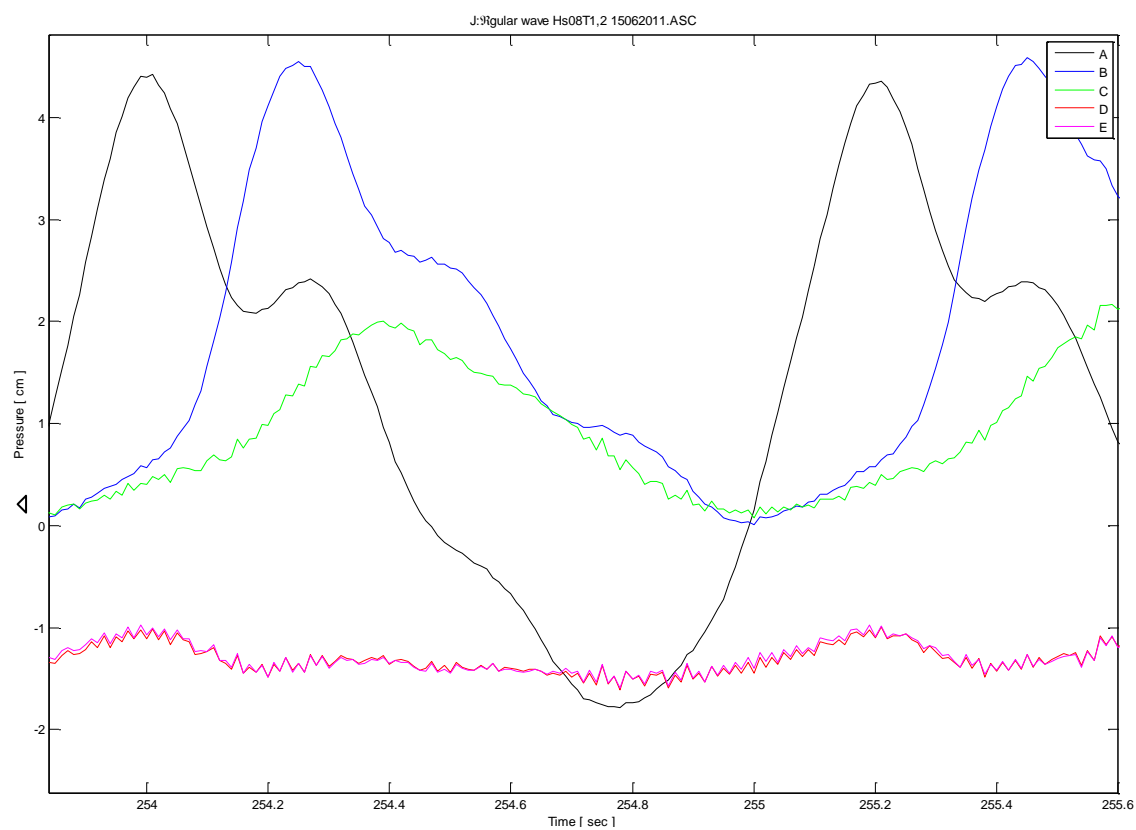


Figure 48 Pressure differences in time T=1.2s

In previous two figures the internal response to the regular wave can be seen. In the first figure the wave period was long, resulting in a more gentle water movement. In the second figure the wave period was very short, which leads to bigger internal water level differences.

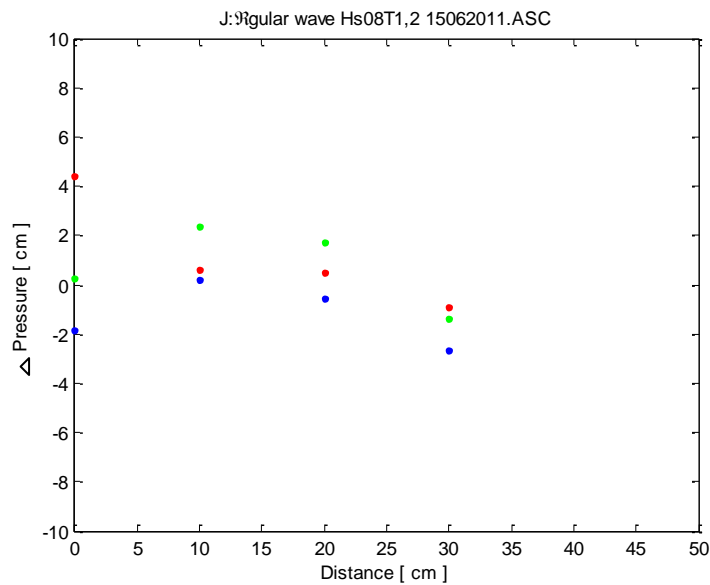


Figure 49 Measured pressure differences inside structure 3 T=1.2s

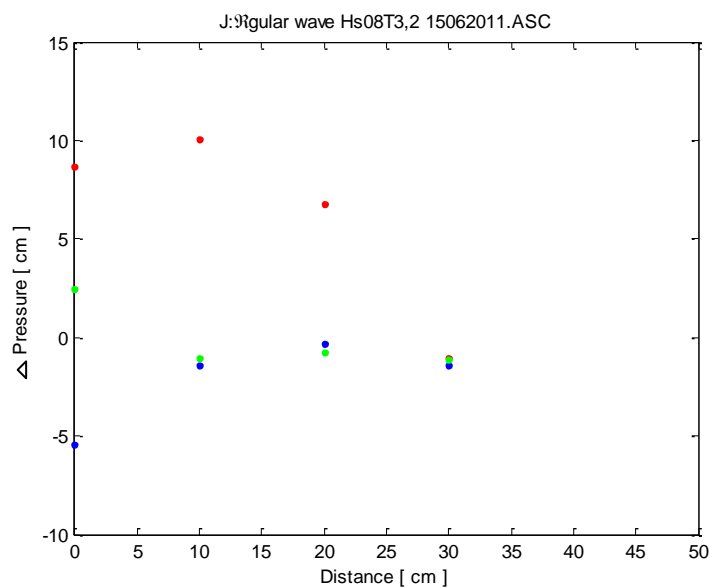


Figure 50 Measured pressure difference inside structure 3 T=3.2s

With these pressures inside the structure and assumed Forchheimer constants (see chapter 2) an estimate of the occurring flow velocities is made.



Using the relation from Burcharth with a  $\beta'$  coefficient of 2.9 then the pore velocity inside the structure (starting after the armour layer) becomes:

Position	Pressure diff. max	$l_x$	$n$	$d_{n50}$	$u$	$Re_p$
<b>Armour layer</b>	10	1	0.45	40.5 mm	0.1632 m/s	4406
<b>Filter layer 1</b>	6.5	0.65	0.49	21.8 mm	0.111 m/s	1613
<b>Filter layer 2</b>	0	0	0.5	6.67 mm	0.0 m/s	0

Table 22 Pressure and velocities structure 3 regular waves  $H=0.1$   $T=3.2$

Position	Pressure diff. max	$l_x$	$n$	$d_{n50}$	$u$	$Re_p$
<b>Armour layer</b>	4.5	0.45	0.45	40.5 mm	0.109 m/s	2943
<b>Filter layer 1</b>	2	0.2	0.49	21.8 mm	0.064 m/s	930
<b>Filter layer 2</b>	0	0	0.5	6.67 mm	0.0 m/s	0

Table 23 Pressure and velocities structure 3 regular waves  $H=0.1$   $T=1.2$

The analysis of the pressure gauges made clear that over the last filter layer (first layer from the core) hardly any significant pressure difference was recorded. The biggest changes in water levels inside the structure were recorded at the armour layer and the first filter layer, especially in the situation with short periodic waves. The video analysis supports this finding. During one test with regular waves dye was injected into this filter layer. After three waves no significant horizontal movement of the dye was observed. This in contrary to the dye in the armour – and first filter layer.

Conclusively there can be said that hardly any flow was observed in the second filter layer. The flow that did occur clearly doesn't result into turbulent flow over this layer. It is highly likely that scale effect arise over this second layer. The measure and significance of these effects are however not known at this moment. Further research of the effects on armour layer stability and therefore permeability, due to Reynolds scale effects, in scale model tests is recommended.

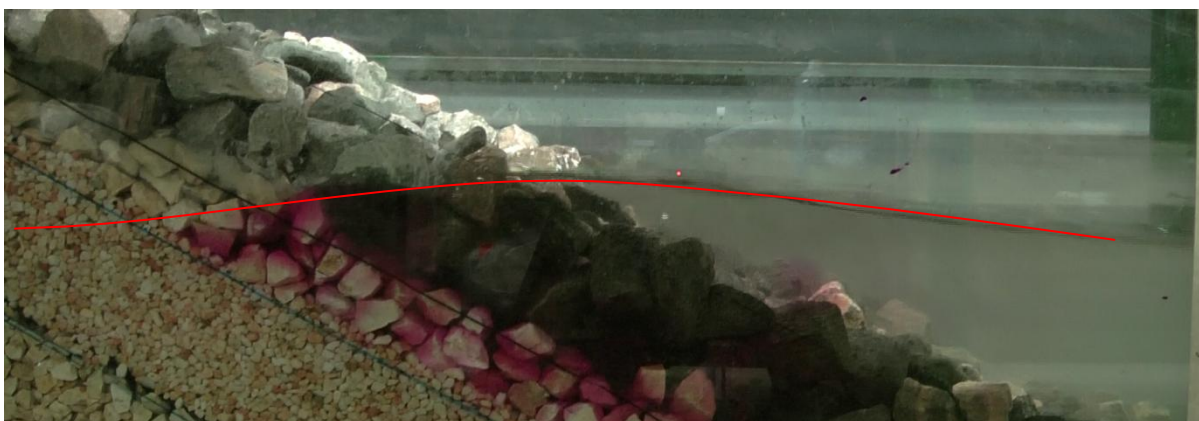


Figure 51 H max regular waves T3.2



Figure 52 H min regular waves T3.2

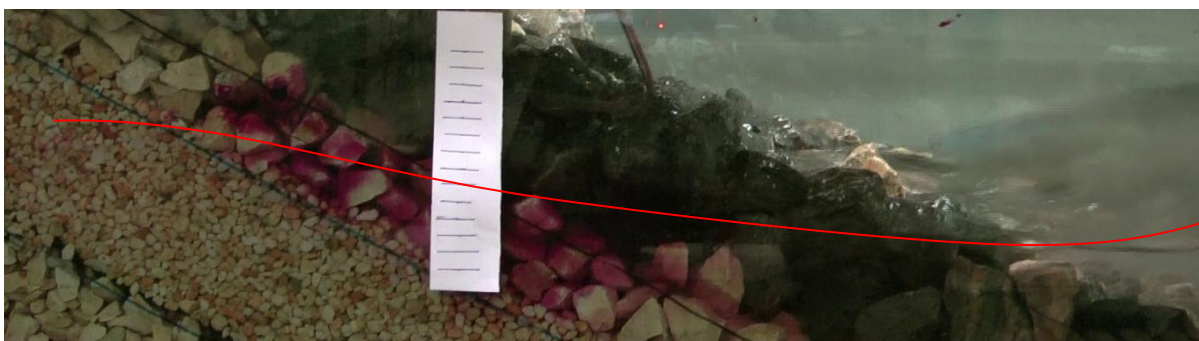


Figure 53 H min regular waves T1.2



Figure 54 H max regular waves T1.2

## 6. Discussion

After conducting and analysing all the experiments planned within this thesis some other questions arose. The questions that will be discussed in this chapter involve earlier made assumptions in this and other studies. The first question concerns the assumption that  $P$  is a function of Iribarren, as defined by JUMELET [2010]. Secondly another comparison is made between the Hudson formula, the Van Gent formula and the stability formulae of Van der Meer, this is additional to the comparison already executed by VAN DER MEER [1988].

### 6.1 $P$ as a function of the Iribarren number

BROEKHOVEN [2011] found from his experiments that the permeability is not only dependent on the structural parameters but also on the Iribarren number.

The acquired data from this research was used to find an individual value of  $P$  for each individual test, in such a way that the calculated and measured damage match. In the tables below the individual values per test are presented.

Test	$H_{m,0}$ [m]	$T_m$ [s]	$\xi_m$ [-]	$P$
<b>1b</b>	0.161	3,82	5,95	0.45
<b>2</b>	0.142	1,49	2,47	0.41
<b>3</b>	0.153	3,39	5,42	0.36
<b>4</b>	0.150	2,79	4,50	0.46
<b>5</b>	0.147	1,91	3,12	0.71
<b>6</b>	0.138	2,22	3,73	0.58
<b>6b</b>	0.150	2,23	3,60	0.58
<b>7</b>	0.180	2,42	3,55	X
<b>6a</b>	0.158	2,24	3,52	0.64
<b>6b</b>	0.163	2,31	3,57	0.66
<b>6c</b>	0.158	2,34	3,68	0.63
<b>6d</b>	0.158	2,23	3,51	0.65
<b>6e</b>	0.159	2,26	3,55	0.62
<b>3a</b>	0.175	3,27	4,89	0.45
<b>3b</b>	0.174	3,26	4,88	0.46
<b>3c</b>	0.175	3,25	4,85	0.45

Table 24  $P$  determined for each individual test structure 1

Test	$H_{m,0}$ [m]	$T_m$ [s]	$\xi_m$ [-]	P
8	0,09	1,18	2,44	0,11
9	0,10	1,81	3,57	0,27
10	0,11	4,18	7,80	0,09
11	0,10	3,59	6,96	0,07
12	0,10	2,42	4,83	0,13
13	0,10	2,11	4,21	0,25
14	0,09	1,16	2,36	0,09
15a	0,10	1,36	2,74	0,16
15b	0,10	1,39	2,79	0,10
15c	0,10	1,40	2,81	0,10
16a	0,11	4,21	7,89	0,06
16b	0,11	4,21	7,89	0,06
16c	0,11	4,21	7,93	0,06

Table 25 P determined for each individual test structure 2

The remark must be made that for the impermeable structure in some cases the calculated and measured damage were not equal. This is caused by the fact that the range of p was not sufficient to adjust the calculated damage. This was especially the case for large Iribarren numbers (5~7).

Test	$H_{m,0}$ [m]	$T_m$ [s]	$\xi_m$ [-]	P
17	0,13	1,77	3,12	0,39
18	0,12	1,49	2,67	0,54
19	0,14	3,71	6,11	0,30
20	0,13	2,27	3,96	0,47
21	0,12	2,80	4,95	0,36
22	0,14	3,42	5,74	0,32
23	0,11	1,27	2,39	0,21
24	0,12	2,53	4,56	0,41
25	0,12	2,01	3,62	0,37
26	0,11	1,18	2,26	0,19
31	0,16	1,11	1,74	0,19
27	0,125	2,30	4,06	0,49
27b	0,12	2,29	4,12	0,50
27c	0,12	2,25	4,06	0,43
28	0,14	1,42	2,41	0,36
29	0,13	1,42	2,42	0,27
30	0,13	1,41	2,43	0,31

Table 26 P determined for each individual test structure 3

With these individual values of the notional permeability a mean value and a standard deviation can be extracted. This analysis should lead to a similar resulting P value as the method in chapter 4. For the first and the third structure this is the case. However the second structure results into a higher value than found in chapter 4, an explanation for this is that the high damage values were not equal to the calculated damage because the range of P was insufficient.

Structure	Mean value	Standard deviation
Structure 1: permeable core	0.54	0.11
Structure 2: impermeable core	0.12	0.07
Structure 3: impermeable+filter	0.36	0.11

Table 27 Mean and standard deviation of P, data Kik[2011]

In the figure below the individual P values plotted against the Iribarren number. This could possibly prove the theory that the notional permeability is related to the Iribarren number. When the data from VAN DER MEER [1988] is combined with the data acquired in this study we get the following figure.

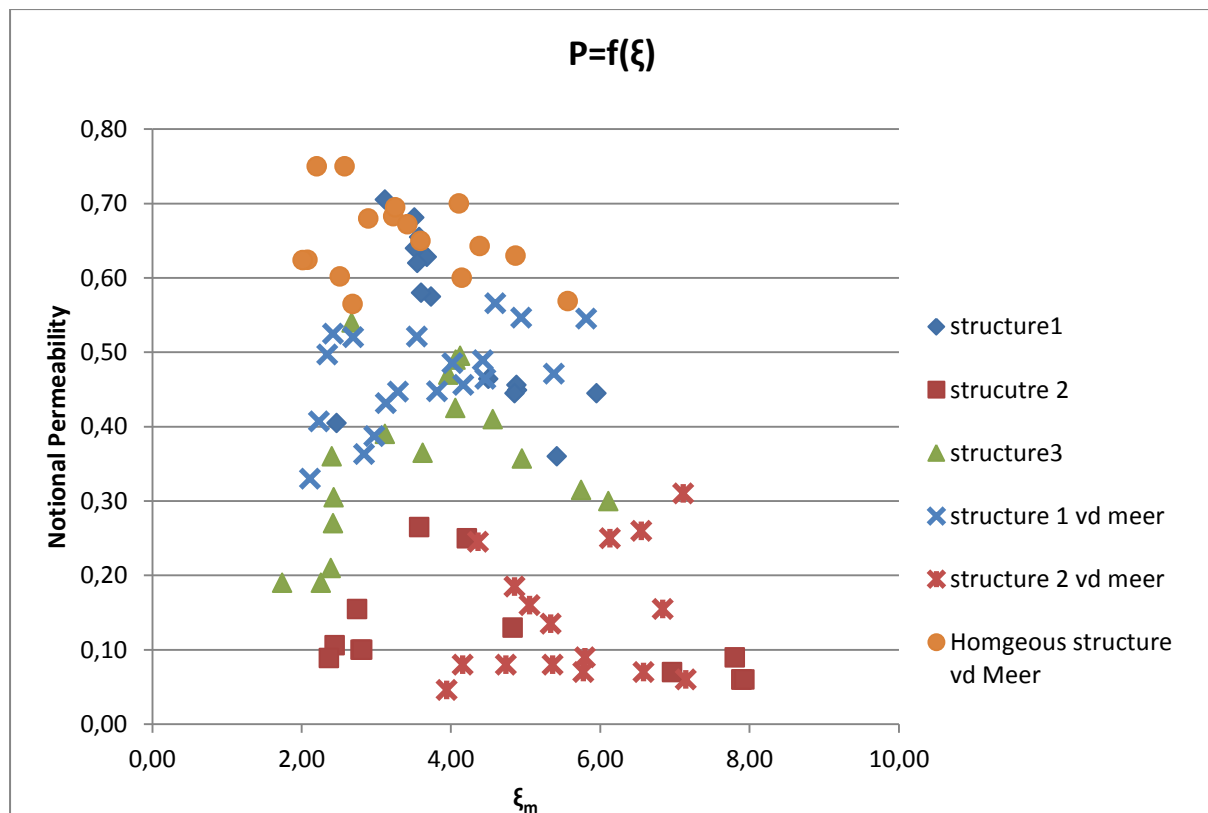


Figure 55 P as a function of Iribarren

Considering the second and the third structure no obvious trend can be recognized in the test data. For the first structure which has a completely permeable core the increase of permeability is not observed. When only looking at the data obtained in this research one could in fact recognize a decreasing trend. When looking at the data from VAN DER MEER [1988] of the homogenous and permeable structure an almost constant value of P can be observed.

On the basis of this plot no distinct relation can be extracted from the data points. And therefore no relation between P and Iribarren number can be found.

Another theory regarding the notional permeability is not based on the exchange of fluids between in the internal and external area of the breakwater but looks at the energy dissipation. The incoming energy of the wave spectrum is partially dissipated and partially reflected by the breakwater. This ratio of dissipation vs. reflection could depend on the structural properties of the breakwater and the Iribarren number. A less permeable structure has a lower ability to dissipate energy and should therefore result into a higher reflection coefficient. More reflection implies less penetration and thereby less dissipation and thus less permeability.

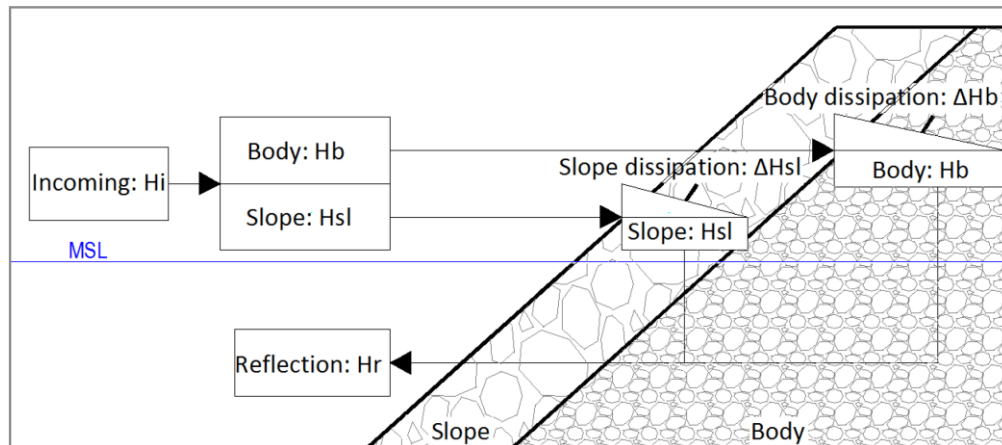


Figure 56 Energy scheme from JUMELET 2010

Within this research both the incoming and the reflected waves are measured. With means of this data the theory briefly described above can be partially supported or rejected. When this theory is correct the average reflection coefficient should be higher for the impermeable core (structure 2) and lowest for the permeable core (structure 1).

#	$H_{m,0}$	$T_m$	$\xi_m$	Reflection coefficient
1b	0.161	3.04	4.74	0.59
2	0.142	1.40	2.32	0.23
3	0.153	2.98	4.76	0.55
4	0.150	2.50	4.03	0.53
5	0.147	1.82	2.97	0.31
6	0.138	2.11	3.55	0.41
6b	0.150	2.08	3.36	0.38
7	0.180	1.84	2.71	0.32
6a	0.158	2.08	3.27	0.42
6b	0.163	2.14	3.31	0.44
6c	0.158	2.14	3.36	0.43
6d	0.158	2.10	3.31	0.43
6e	0.159	2.10	3.29	0.43
3a	0.175	2.80	4.19	0.54
3b	0.174	2.83	4.24	0.54
3c	0.175	2.83	4.23	0.55

Table 28 Measured reflection coefficients structure 1

#	$H_{m,0}$	$T_m$	$\xi_m$	Reflection coefficient
8	0.091	1,18	2,44	0.26
9	0.100	1,81	3,57	0.37
10	0.112	4,18	7,80	0.71
11	0.104	3,59	6,96	0.67
12	0.098	2,42	4,83	0.61
13	0.098	2,11	4,21	0.61
14	0.094	1,16	2,36	0.22
15a	0.096	1,36	2,74	0.28
15b	0.096	1,39	2,79	0.28
15c	0.097	1,40	2,81	0.28
16a	0.111	4,21	7,89	0.72
16b	0.111	4,21	7,89	0.73
16c	0.110	4,21	7,93	0.71

Table 29 Measured reflection coefficients structure 2

#	$H_{m,0}$	$T_m$	$\xi_m$	Reflection coefficient
17	0.125	1,77	3,12	0.29
18	0.122	1,49	2,67	0.25
19	0.144	3,71	6,11	0.63
20	0.128	2,27	3,96	0.46
21	0.125	2,80	4,95	0.58
22	0.138	3,42	5,74	0.61
23	0.110	1,27	2,39	0.21
24	0.120	2,53	4,56	0.51
25	0.120	2,01	3,62	0.38
26	0.106	1,18	2,26	0.18
31	0.158	1,11	1,74	0.20
28	0.136	2,30	4,06	0.25
29	0.134	2,29	4,12	0.22
30	0.131	2,25	4,06	0.20
27a	0.128	1,42	2,41	0.48
27b	0.120	1,42	2,42	0.47
27c	0.120	1,41	2,43	0.47

Table 30 Measured reflection coefficients structure 3

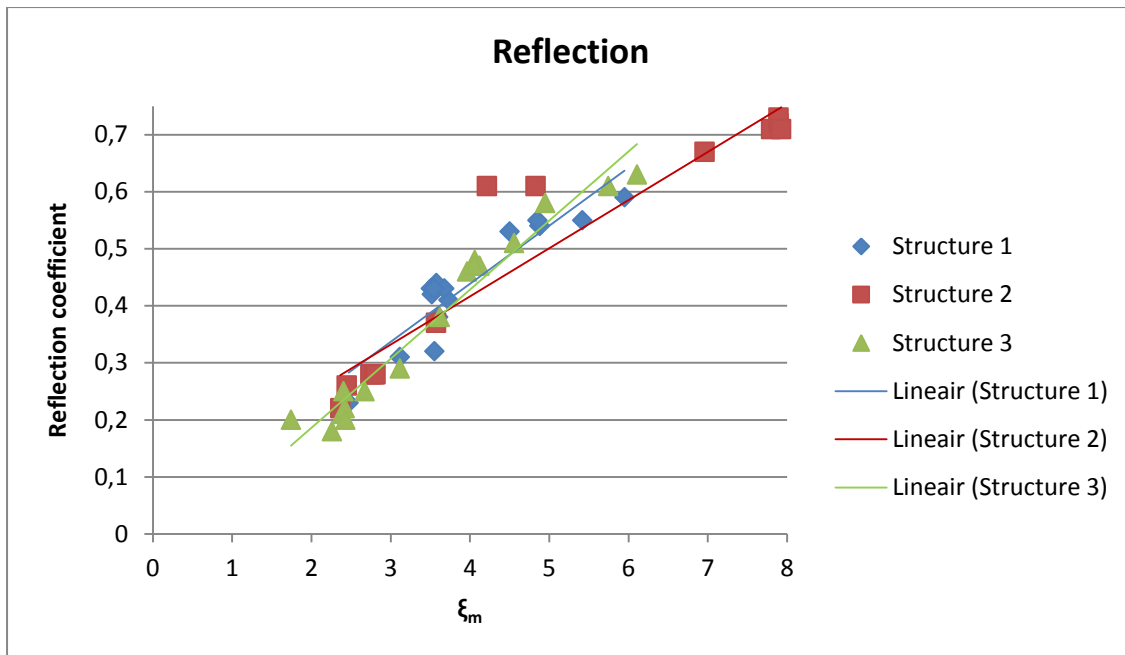


Figure 57 Measured reflection coefficient

In the figure above just the opposite of the expected results is shown. The permeable structure has a slightly higher reflection coefficient as compared to the impermeable structure. Apparently the notional permeability is not directly linked to the reflection coefficient. Perhaps the structure has more effect on the ratio between dissipation on the slope and inside the body of the structure.



## 6.2 Other stability formulae

### 6.2.1 Hudson type formula

Although the formulae of VAN DER MEER is considered as the most accurate for breakwater stability still a lot of people all over the world use the Hudson formula. The reason for this is the simplicity and familiarity of the formula.

When looking at the results of the experiments conducted within this study a clear difference can be seen with regard to the stability of the different types of structures. It might be an option to supplement the Hudson formula with an additional coefficient representing the permeability of the structure.

To compare the results a modified Hudson formula is needed because the initial Hudson formula is limited to the no damage criteria (in the order of 0 to 5 % damage). The rock manual provides a table with the influence of the damage on the  $K_D$  value. Van der Meer used these values to derive the following formula which has the addition of the damage factor  $S$ .

Armour type	Wave height factor	Damage percentage with corresponding damage level $S$						
		0-5 $S=2$	5-10 $S=6$	10-15 $S=10$	15-20 $S=14$	20-30 $S=20$	30-40 $S=28$	40-50 $S=36$
Smooth armour stone	$H_s/H_{s,D=0}$	1.00	1.08	1.14	1.20	1.29	1.41	1.54
Angular armour stone	$H_s/H_{s,D=0}$	1.00	1.08	1.19	1.27	1.37	1.47	1.56

Table 31 Wave height factor as a function of damage: From Rock Manual 2007

After curve fitting the table above the following Hudson type formula is derived:

$$\frac{H_s}{\Delta D_{n50}} = 0.7 \sqrt[3]{K_D \cot(\alpha)} * S^{0.15} \quad 6-1$$

According to the Rock Manual the  $K_D$  value is 2.0 for breaking waves and about 4.0 for non-breaking waves in the case of natural rock. The rock manual also gives values for impermeable and permeable structures. These values represent the lower limit of the formula and are therefore considered as conservative. The values are  $K_D=1$  for impermeable structures and  $K_D=4$  for permeable structures.

To compare the test data with the modified Hudson formula a plot with on the x-axis the stability parameter  $H_s/\Delta \cdot d_{n50}$  and on the y-axis the damage  $S$  has been made. Initially this comparison is only done for the 1:2 slopes and with the data from this study, VAN DER MEER [1988] and THOMPSON & SHUTTLE [1975]. This results in the following plot.

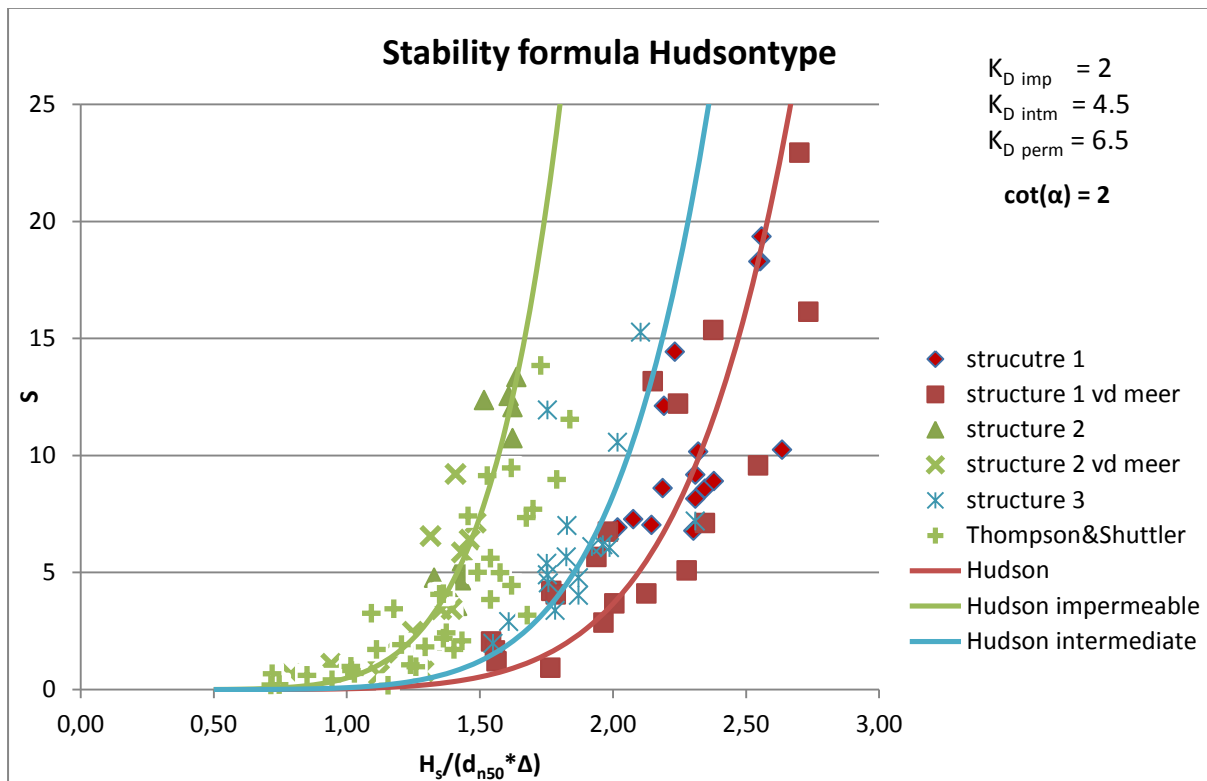


Figure 58 Stability Hudson with difference  $K_D$  values. Slope 1:2

In general gives the Hudson formula a good representation of the measured damage. When comparing the calculated data with the measured data on the basis of MAE (mean absolute error), then the accuracy is in the same order as the Van der Meer formula. With these results in mind one can say that the influence of the permeability on a 1:2 slope is more significant than the effect of the wave period.

However when adding the other tests with different slope angles executed by VAN DER MEER [1988], then the Hudson formula starts to deviate from the measured data. Big differences arise on slopes milder than 1:3, as one can see in the figure below. These milder slopes are plotted in blue. The permeable structure which was only tested on slopes in the range from 1:1.5 - 1:3 doesn't show this deviation. The Hudson formula clearly doesn't take the effect of mild slopes enough into account.

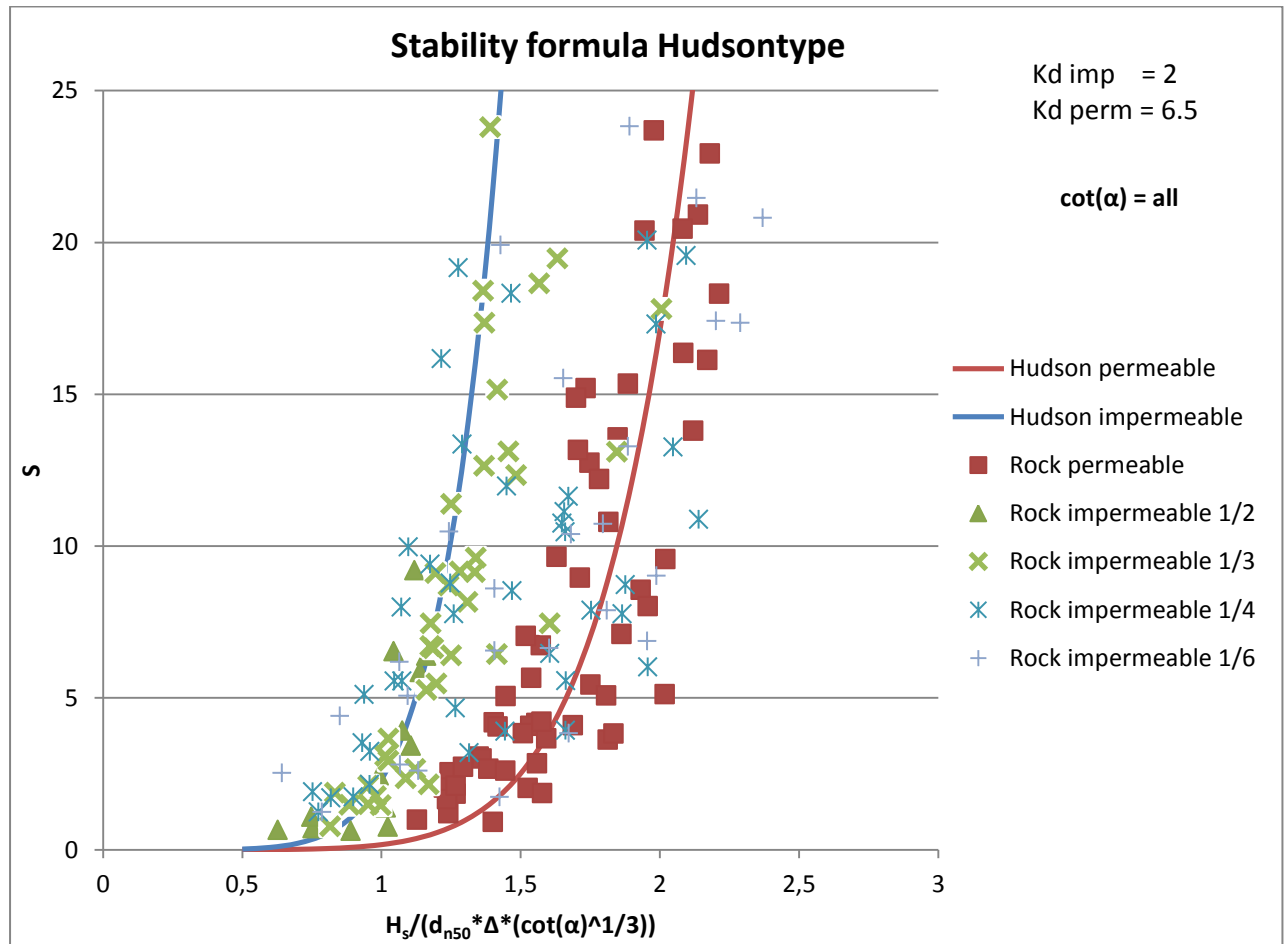


Figure 59 Stability Hudson with difference  $K_D$  values. Slope 1:1.5 ~ 1:6

To improve the shortcomings of the Hudson formula some additions are needed. First of all the effect of the number of waves or in other words the progression of damage under on-going wave attack should be added. This can be done quite easily with means of the data from the test executed by THOMPSON AND SHUTTLE [1975]. They found the relation  $S/V(N)$  with  $N$  for the number of waves. This expression can replace the  $S$  in formula 6-1.

The effect of the permeability can be included by adding an extra factor to the formula. The idea is that a basic  $K_D$  value should be chosen on the basis of the top layer material. Together with a factor representing the design of the structure will this result into a lower or higher stability.

The most important shortcoming based on the plot presented on this page is the inability of good predictions in the situation with mild slopes. Therefore the usage is limited to slopes up until 1:3 or extensive research about implementing the effect of the slope should be done to extend its range of applicability.

Additions needed to the Hudson formula:

- Number of waves
- Permeability factor
- Improved slope effect

### 6.2.2 Van Gent formula

Besides the two earlier mentioned stability formulae there are two more stability formulae. These two formulae are developed with shallow foreshores. The first one is an adjusted formula of Van der Meer but using  $H_{2\%}$  and the spectral period  $T_{m-1,0}$  the coefficients  $c_{pl}$  and  $c_s$ . VAN DER MEER [1988] already proposed to use the  $H_{2\%}$  in case of shallow water conditions and adjusted the coefficients on the basis of the relation between  $H_s$  and  $H_{2\%}$ . For a Rayleigh distribution this ratio is 1.4, ending up at 8.7 and 1.4 for the plunging and respectively the surging coefficients.

VAN GENT [2004] executed a large number of experiments with shallow foreshores and adjusted the formula of Van der Meer. Van Gent used the spectral  $T_{m-1,0}$  instead of the time signal  $T_m$  and used his experiments to define the coefficients.

These modified Van der Meer formulas are:

$$\frac{H_{2\%}}{\Delta d_{n50}} = c_{pl} P^{0.18} \left( \frac{S}{\sqrt{N}} \right)^{0.2} \xi_{m-1,0}^{-0.5} \quad (\text{plunging waves}) \quad 6-2$$

$$\frac{H_{2\%}}{\Delta d_{n50}} = c_s P^{-0.13} \left( \frac{S}{\sqrt{N}} \right)^{0.2} \xi_{m-1,0}^P \sqrt{\cot \alpha} \quad (\text{surging waves}) \quad 6-3$$

	Mean	Standard deviation
$c_{pl}$	8.4	0.7
$c_s$	1.3	0.15

Table 32 Modified coefficients Van der Meer formulae

Van Gent observed a significant decrease of the influence of the period when shallow foreshores are considered. For that reason he tried to develop a more simple stability relation for situations in which less information is available.

The Van Gent stability formula reads:

$$\frac{H_s}{\Delta d_{n50}} = 1.75 \sqrt{\cot \alpha} \left( 1 + \frac{d_{n50-core}}{d_{n50}} \right)^{\frac{2}{3}} \left( \frac{S}{\sqrt{N}} \right)^{0.2} \quad 6-4$$

A comparison between the original Van der Meer stability formulae, the Hudson formula and the Van Gent formula was made with the data of this research, the 1:2 tests of VAN DER MEER [1988] and the tests of THOMSON AND SHUTTLE [1975].

The comparison was done by comparing the calculated and measured damage. The Hudson formula was used with three different  $K_D$  as described in the beginning of this chapter. For the Van der Meer formula the values  $P=0.5$ ,  $P=0.35$  and  $P=0.1$  are used.

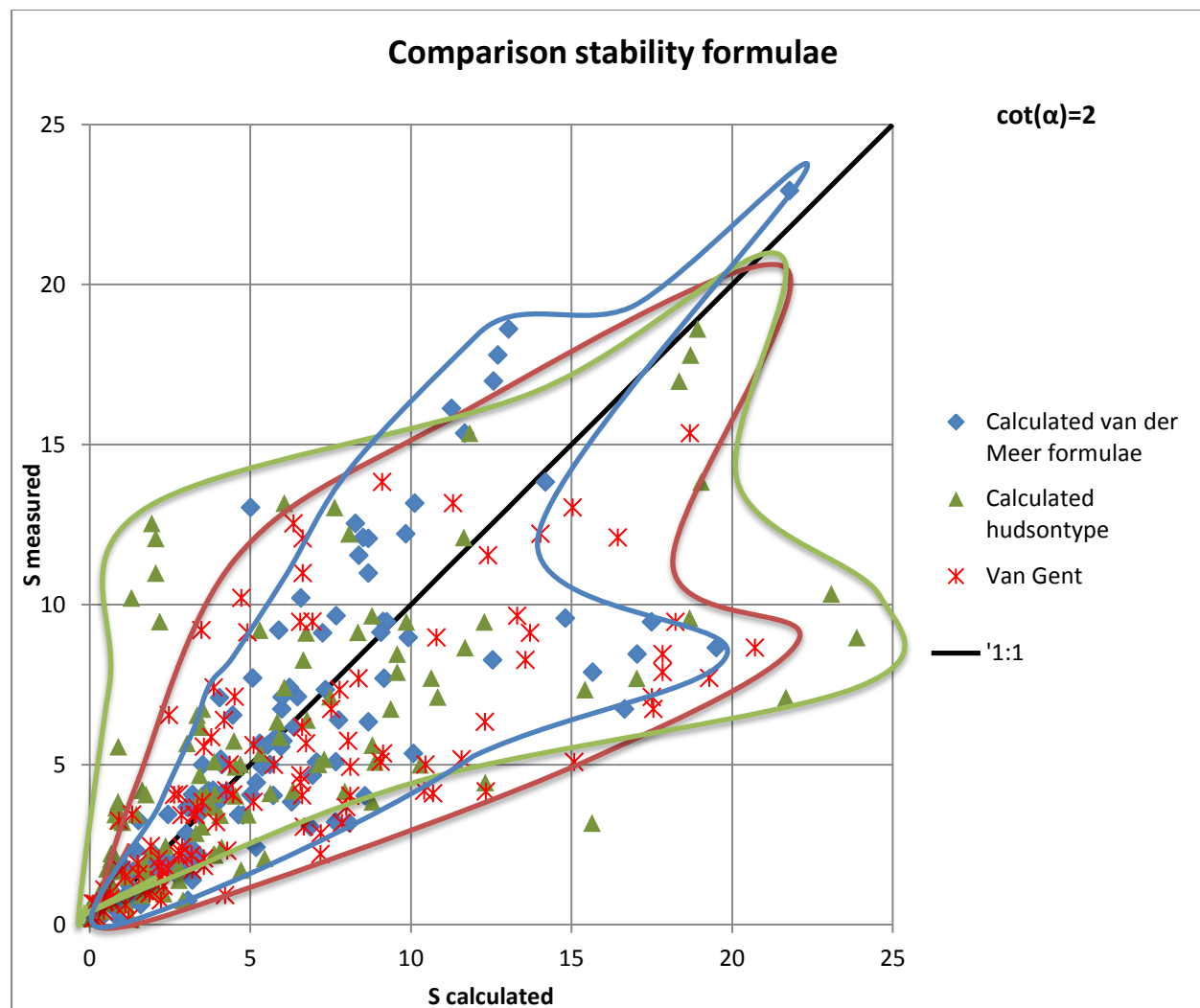


Figure 60 Comparison different stability formulae

In the figure above a larger spreading in the results of the Hudson type formula can be observed. Also the Van Gent formula shows a considerable amount of spreading in the results. From the figure it is clear that the Van der Meer formulae show the least amount of spreading which is also proven by the statistical parameters in the table below.

Formula	BIAS	MAE	RMSE
Van der Meer	0,46	1,99	3,51
Hudson	0,62	2,84	4,57
Van Gent	2.33	3.59	5.78

Table 33 Statistical performance stability formulae

The fact that the Van Gent formula doesn't show good results is probably caused by the hydraulic conditions. The ROCK MANUAL [2007] states that the Van Gent formula is not applicable in situations with an  $h/H_s$  larger than 3. In the experiments of this research this ratio is between 3.16 and 7.15. Also in the experiments of Van der Meer and Thompson and Shuttler is this ratio larger than 3. Furthermore according to the Rock manual the Van Gent formula is not recommended for constructions with an impermeable core. Analysing the different types of structures however shows that the impermeable structure gives a better result compared to the permeable structures.

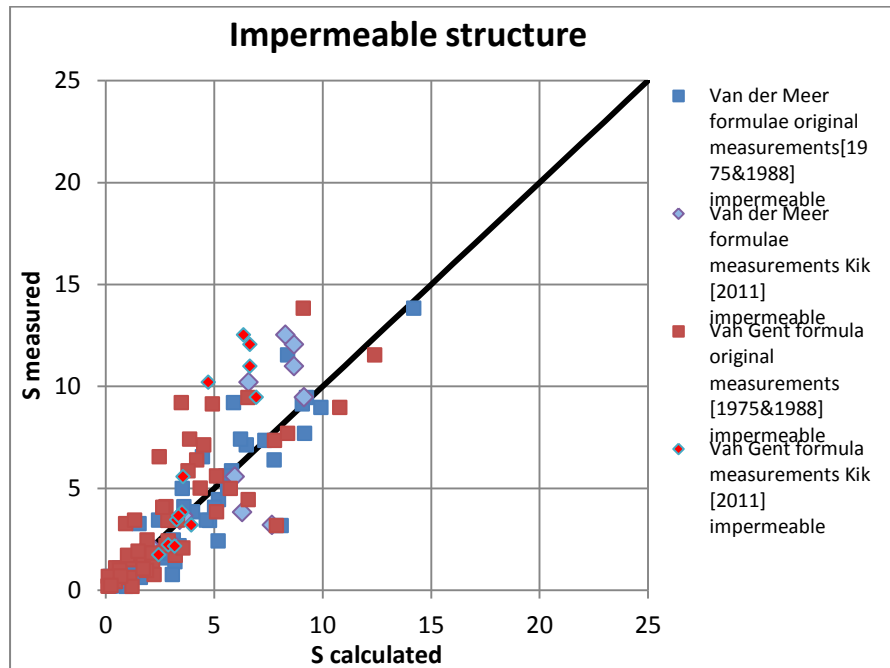


Figure 61  $S_{\text{calculated}} / S_{\text{measured}}$  for impermeable structures comparison Van Gent and Van der Meer formulae

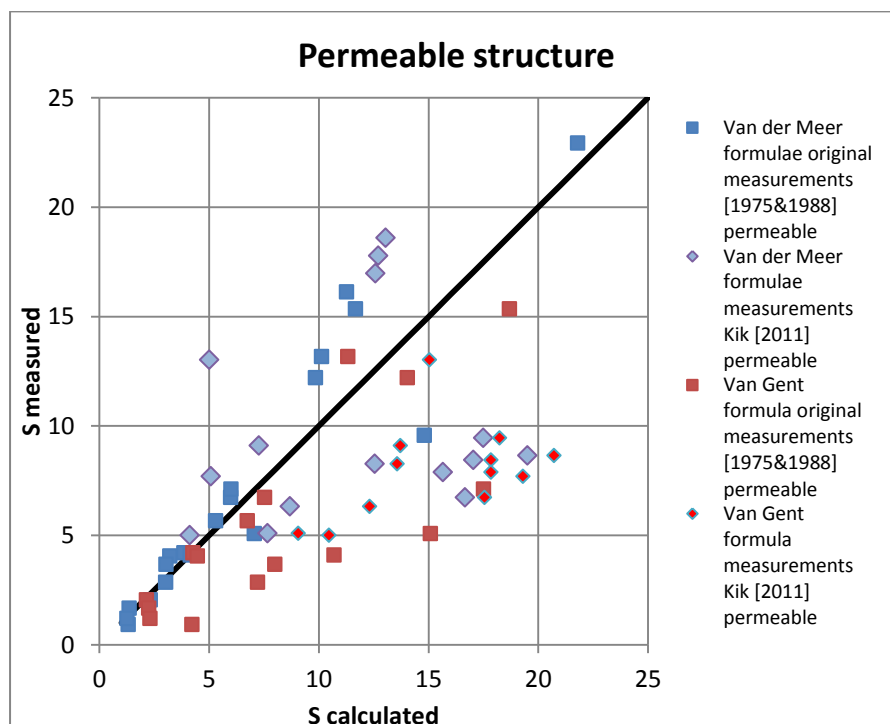


Figure 62  $S_{\text{calculated}} / S_{\text{measured}}$  for permeable structures comparison Van Gent and Van der Meer formulae

Unfortunately the data and report of Van Gent is not public. Therefore no details about the method of ending up at his final formula are known. During the analysis a mistake was made when entering the formula. The power of  $2/3$  for the term representing the permeability was forgotten and accidentally quite good results were achieved. By removing this power the permeability of the structure was given more weight.

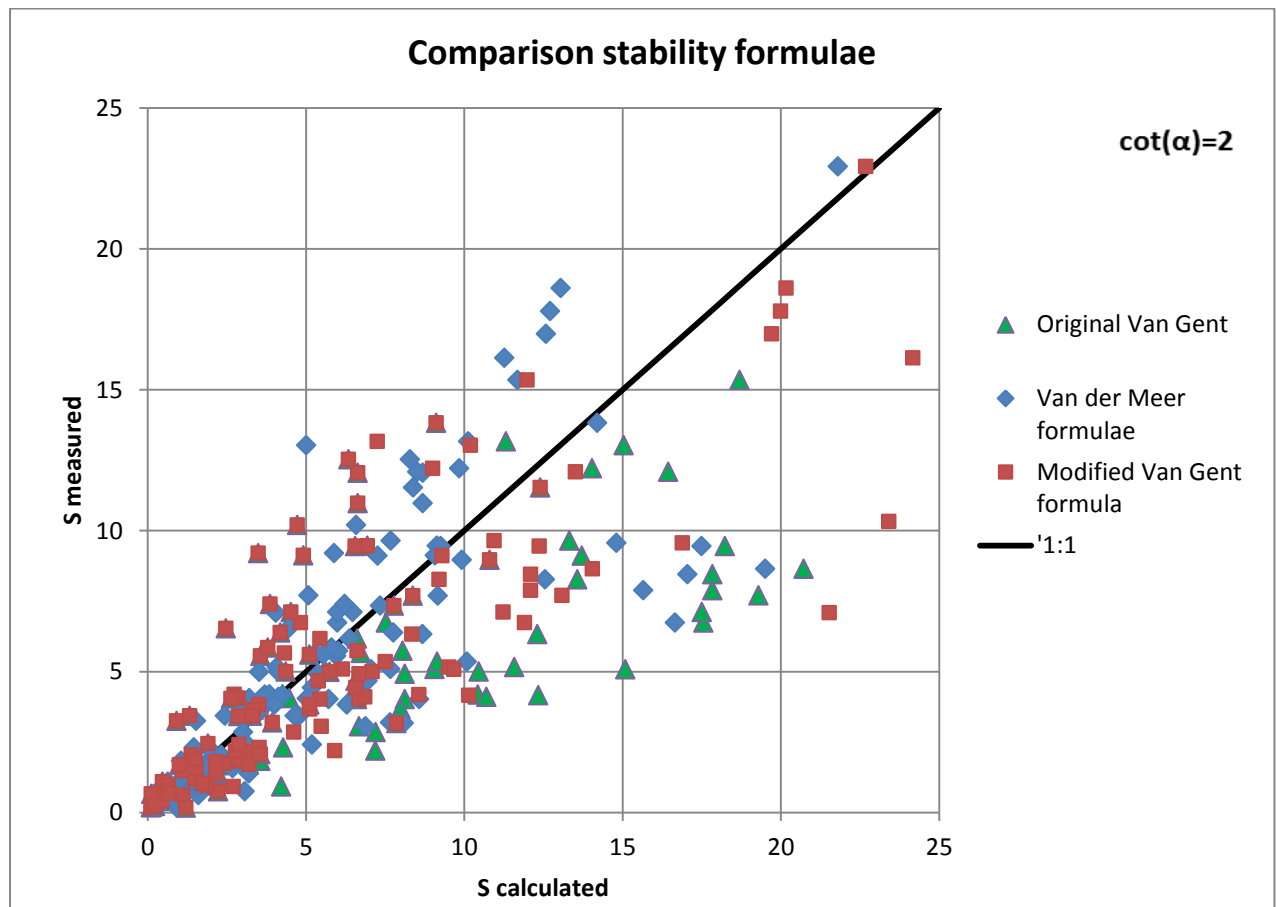


Figure 63  $S_{\text{calculated}} / S_{\text{measured}}$  for all structures comparison Modified Van Gent, original Van Gent and Van der Meer formulae

Combining all the data of the 1:2 slope tests provides like the figure on page 78 the graph above. The spreading in the results of the Van Gent formula is considerably reduced. This can also be seen in the RMSE of the formula which after removing the power of  $2/3$  is 3.19 instead of 5.78, correspondingly the BIAS has been reduced from 2.33 to 0.54.

This change has no physical base at all. Furthermore the modification give better results in deep water conditions on 1:2 slopes, while the original formula was developed for shallow water conditions. The performance on different slopes was not investigated during this study but it is recommended to have a further look into this matter.

## 7. Conclusions and recommendations

After analysing all the data a number of conclusions are drawn. In this chapter all the conclusions found will be summarised. But above all will this chapter give the answer to the research objective. The main focus of this study is to find a way to measure the permeability in a practical way.

### 7.1 Conclusions

A method to determine a specific coefficient within an existing formula can be done by fixating all the variables influencing the outcome of the formula. In this situation the coefficient to be determined is the Notional permeability, which is used in two stability formulas describing the stability of a rubble mound breakwater in surging and respectively plunging wave conditions developed by VAN DER MEER[1988].

In this situation all the variables in the formula are measured except the notional permeability (P) itself. After conducting the experiments the measured data was used to calculate a specific damage level (S), in order to end up with a value of S an assumption of P has to be made. This calculated damage level is compared to the measured damage level, the comparison is done for all tests of a specific structure and the results are averaged. The assumed value for the coefficient of interest, the notional permeability P, was fine tuned in order to end up with the lowest difference between calculated and measured damage (lowest RMSE).

Analysing whether this method and the work method of the experiments produce valid results can be done by conducting experiments on reference structures. The experiments on the reference structures showed results that are positioned within the scatter of the original measurements done by VAN DER MEER [1988] and THOMPSON & SHUTTLE [1975]. Hereby the conclusion can be drawn that the work method produces similar results as the test on which the formulae are based.

Choosing the RMSE instead of the mean absolute error (MAE), which describes the average difference of the magnitude of the error, was done to give more weight to larger errors. Adjusting the value of P in such a way that the root mean squared error (RMSE) between the calculated and measured result is as small as possible results in values of P in the order of the values defined by Van der Meer.

The first structure with a permeable core showed after analysis the lowest RMSE for a P value of 0.55. The second structure, with an impermeable core, had the lowest RMSE for the P value of 0.08. These values are very close to the recommended values for the notional permeability  $P=0.5$  and respectively  $P=0.1$ .

The previous conclusions prove that the work method and the method of analysis provide correct answers to the question: "What is the notional permeability of a specific structure". With this conclusion it can be said that similar tests on "new" structures can provide reliable values for the notional permeability.

This new structure consists out of; a double layered armour layer, a coarse filter layer (thickness:  $1 \cdot d_{n50,A}$ ) a thick second filter layer (thickness:  $2 \cdot d_{n50,A}$ ) with fine material and an impermeable core. The ratios in stone size are similar as the  $P=0.4$  structure defined by Van der Meer, namely 1:2:8 with respect to the armour layer.

The analysis of the experiments showed the lowest RMSE and BIAS for a P-value of 0.37. However the number of tests conducted on this structure is still limited, especially with regards to different slopes and wave heights. The advice at this time is to use the conservative value of  $P=0.35$  for design purposes.



The repetition tests executed together with D. Papadopoulos showed a low spreading in damage for tests with the same hydraulic load. The standard deviation of the repetition tests is 0.8. Furthermore Papadopoulos showed that measuring the cross section every 5 cm instead of 10 cm results in a higher accuracy of the final averaged profile and therefore final damage number  $S$ .

Measurements of the wave run up were done to possibly validate parts of the Volume Exchange Model regarding the reduced wave run up. The Volume Exchange Model, which was developed to mathematically determine the notional permeability, assumes that the permeability of the structure influences the wave run up. The run up compared to the run up with no permeability at all was said to be a measure of the notional permeability  $P$ . During the normal irregular wave spectra a good list of wave run up values could be made wherefrom a significant or 2% value can be deducted. However the reference level, for which BROEKHOVEN [2011] found a relation, is not suitable for irregular waves.

For the regular waves executed on the third “new” structure the measured run up reduction coefficient showed quite some scatter but the average value of the calculated Notional Permeability determined with means of this  $C_r$  value, with the exclusion of one value, was about  $P=0.28$ . The individual values are within the scatter of the found permeability coefficients.

Analysis of the pressure differences measured during the regular wave on the third structure show hardly any motion in the second filter layer. This is also supported by the video recordings. The absence of turbulent flow could lead to scale effects regarding the Reynolds scaling.

Measuring the total amount of energy dissipation caused by the structure on the basis of reflection didn't show the desired result. No clear difference between the permeable and impermeable structure was recognized during this study.

The results of this study together with the measurements of VAN DER MEER [1988] and THOMPSON & SHUTTLE [1975] were used to compare the Hudson formula with the Van der Meer formula. An attempt was made to couple a  $K_D$  value to a type of structure. This resulted into a  $K_D$  value of 2 for the impermeable structure and a value of 6.5 for the permeable structure. Comparing the measured damage with the calculated damage shows a good correlation for the Hudson formula, despite the absence of the period in the formula. However for other slopes as the 1:2 slope, and more specifically slopes milder than 1:3 the error became much larger as the Van der Meer formula. Clearly the slope effect is not good enough described in the Hudson formula.

The Van Gent formula, containing the ratio between armour stone size and core stone size, showed a larger BIAS and RMSE with respect to the Hudson and the Van der Meer formula. This is probably caused by the fact that this is an equation valid on shallow water ( $h/H_s < 3$ ). However when the power of  $2/3$  was removed from the term representing the permeability a considerable decrease of spreading occurred and the BIAS and RMSE correspondingly decreased.

## 7.2 Recommendations

Although a number of studies have been conducted on the topic of notional permeability, the subject is far from completely understood. With the experimental approach and the limited time available of this study concessions had to be made. To gain more insight into the matter and to produce better founded results a number of recommendation have been made. The recommendations basically concern the following three main topics; the scale effects, the experimental factor P and the issues regarding the Volume Exchange Model.

To gain insight in the flows occurring inside the structure pressure differences were measured. However the pressure differences of the measurements with irregular waves are hard to analyse. In this study only the regular waves on the third structure were analysed.

- **An analysis of the irregular pressure difference measurements.**

The velocities inside the layers were calculated based on the pressure differences measured with the regular waves on structure 3. To calculate these velocities assumptions regarding the Forchheimer constants had to be made.

- **Measure the Forchheimer constants to improve the accuracy of the calculated pore velocities.**

Burcharth proposed a method to scale the core differently from the total structure to ensure turbulent flow in the scale model. The impact on the resulting damage is however not known. It would be interesting to analyse the effect of the flow effect on the damage. This can only be done by measurements on different scales. In which the ratios between the stone sizes of the different layers remain constant.

- **Analyse the effect of hydraulic vs. turbulent porous flow on the resulting damage.**

As mentioned in the report some concessions regarding the used wave conditions had to be made. Only commonly recorded wave steepness's were applied. It is however good for the determination of the notional permeability to extend the wave conditions to higher Iribarren numbers.

- **Execute experiments with higher Iribarren numbers.**

Only small variations in wave height were applied and variations with period were used to change the Iribarren number. This is done because the Iribarren number is the most important variable in the stability formulae of Van der Meer. It is nevertheless good to also analyse the results of the found value for P on different wave heights to check its applicability outside the limited tested conditions.

- **Execute experiments with a variety on wave heights.**

During the experiments only one slope angle of the structure was applied. To guarantee an applicability of the value of the parameter P found for the new structure also tests on a wider range of slopes should be executed. For instance on a 1:4 and a 1:6 slope.

- **Execute tests on a wider range of structure slope angles.**

The observation method showed that the slopes can be measured quite accurately. When this is known now the experiments with low damage values can be executed. In the current study only a few tests had damage values lower than three. It would be wise to also test conditions which should lead to lower damages and prove that the notional permeability coefficient also produces reliable results in these regions.

- **Execute tests with more low damage values.**

A structure which is in all the books regarding rock slope design but is never tested with respect to the actual permeability coefficient is the  $P=0.4$  structure. From the interpolation between the tested structures done by Van der Meer a value of  $P=0.4$  was found. Now with the value of  $P=0.37$  for the third structure the interest of  $P=0.4$  structure is even larger because the stone ratios are equal, the only difference is the presence of an impermeable layer at a certain distance from the armour layer.

- **Test the  $P=0.4$  structure with respect to its real notional permeability value.**

Another experimental program which could increase the insight of the core permeability is the following. One should start with a certain known configuration with an impermeable core and gradually increase the thickness of the filter layer. Up until the moment that the core is completely permeable. In that way the one could observe at which layer thickness the presence of an impermeable core is no longer felt by the incoming wave.

- **Increase the filter layer to find the point upon which the impermeable core has no effect anymore.**

The rock balance as discussed in chapter 4 was not “closed”. On average there was a difference between the eroded and accreted area of about 30%. It will be good to analyse this difference and find a valid explanation for it. This can be done by comparing methods of measuring damage, for instance by measuring the same slope with measuring rods in combination with spheres and the method of laser and echo-sounder used in this research. Furthermore the hypothesis which says that a possible compaction of the armour layer causes the difference can be validated by measuring the in-situ density of the armour layer before and after the test.

- **Investigate the difference between eroded and accreted area.**

On the subject of the Volume Exchange model a few recommendations can be made. Especially because this concept is currently based on regular waves. A closer look has to be taken into the transformation from regular to irregular waves. At this moment the relation found by BROEKHOVEN [2011] for the reference level of the wave run up below the armour layer is only applicable on regular waves. More research on the effect of the irregular waves on the reference level has to be made.

- **Make the reference run up level as defined by Broekhoven suitable for irregular waves.**

Another way to calibrate the Volume Exchange model is to make it run for a structure like the third structure from this study. In the past only the three structures tested by Van der Meer were used to calibrate the model. Now additional data, even with internal processes like the wave run up at the core, is available. This can be used to further tune the Volume Exchange model.

- **Run the Volume Exchange model for the third structure and compare the calculated results with the measured results from this study.**

The main focus of this thesis was to investigate the possibility to measure the permeability and look into possible scale effects. With this kept in mind it is advised to start with the additional measurements regarding the Forchheimer constants and the effects of laminar instead of turbulent flow. The second focus of this study was to determine the  $P$  value for a “new” structure. For practical purposes it is advised to do additional experiments on this structure as advised on the previous page, together with the recommendation to test the  $P=0.4$  structure. The remaining recommendations involve the volume exchange model which actually is not directly in line with this research but can be considered as a study with cross references to this research. Therefore from this point of view these recommendations have to lowest priority.

### 7.3 Points of attention

Because of practical reasons a number of items deviate from the study of VAN DER MEER [1988] which is the basis of this study. These differences do not show large deviations between the expected result and the acquired results, but should be kept in mind using the results of this report. Below a brief summary of differences and points of attention of this study are given.

The water depth applied in this study was 65 cm while the water depth in the original research of VAN DER MEER [1988] was 80 cm. The available wave flume was 20 cm lower compared to the wave flume used by Van der Meer, therefore it was not possible to use the same water depth. The ratio  $h/H_s$  was during this research above three, what in the ROCK MANUAL [2007] is considered as the limit of the applicability of the Van der Meer formulae.

As mentioned in the recommendations above there is no variation of wave height applied in the test series of this study.

Measuring the profile of the structure was done by combining the measurements of the echo sounder below the water level and the laser above the water level. The advantage of this method is the digital processing of the measured signal which is less time consuming than manual measurements with measuring rods. It is however a difference between the original reference scenario.

Measuring the profile with a laser and echo sounder means that also the pores between the rocks are measured. In the study of VAN DER MEER [1988] spheres were used to measure the top of the armour layer instead of measuring between the pores.

At the end of chapter 4 it is mentioned that the rock balance is not closed. There are differences between the eroded and accreted area. There are however no values of the accreted area of the experiments of Van der Meer available, therefore the general trend of less accretion than erosion cannot be compared to the original research.

## References

Author	Year	Title	Publisher
<b>BROEKHOVEN, P.J.M</b>	2011	The influence of armour layer and core permeability on the wave run up	<i>Delft university of Technology</i>
<b>BURCHARTH, H.F ET AL</b>	1999	Scaling of core material in rubble mound breakwater model tests	<i>COPEDEC V Cape Town South Africa</i>
<b>BURCHARTH, H.F. AND ANDERSEN, O.H.</b>	1995	On the one dimensional steady and unsteady porous flow equations	<i>Coastal Engineering 24, 233-257</i>
<b>CIRIA; CUR; CETMEF</b>	2007	The Rock Manual. The use of rock in hydraulic engineering (2nd edition)	<i>C683, CIRIA, London</i>
<b>D'ANGREMOND, K VERHAGEN, H.J. ROODE VAN, F. GENT VAN, M.R.A.</b>	2009	Breakwaters and closure dams	<i>VSSD, Delft</i>
	1995	Wave Interaction with Permeable Coastal Structures	<i>Delft university of Technology</i>
<b>HOLTHUIJSEN, L. H.</b>	2008	Waves in oceanic and coastal waters	<i>Cambridge University Press</i>
<b>HEIJ DE, J.E.J.</b>	2001	The influence of structural permeability on armour layer stability of rubble mound breakwaters	<i>Delft university of Technology</i>
<b>HUGHES, S.A.</b>	1993	Physical models and laboratory techniques in coastal engineering	<i>World Scientific Publishing Co.</i>
<b>JUMELET, H.D.</b>	2010	The influence of core permeability on armour layer stability	<i>Delft university of Technology</i>
<b>MERTENS, M.</b>	2007	Stability of rock on slopes under wave attack	<i>Delft university of Technology</i>
<b>PAPADOPOULOS, D</b>	2011	Damage on rock slopes under wave attack	<i>Delft university of Technology</i>
<b>SCHIERECK, G.J.</b>	2004	Introduction to Bed, bank and shore protection	<i>VSSD, Delft</i>
<b>THOMPSON AND SHUTTLE</b>	1975	Riprap design for wind-wave attack	<i>Hydraulic research station, Wallingford</i>
<b>TROCH, P</b>	2000	Experimentele studie en numerieke modellering van golfinteractie met stortsteen golfbrekers	<i>Universiteit van Gent</i>
<b>VAN DER MEER, J.W.</b>	1988	Rock slopes and gravel beaches under wave attack	<i>Delft university of Technology</i>
<b>VILAPLANA DOMINGO, A.M.</b>	2010	Evaluation of the volume-exchange model with Van der Meer laboratory tests results	<i>Delft university of Technology</i>

## Appendix A: Rock properties

This appendix concerns the different properties of the materials used during this research.

Determining the density of the armour material was done by weighing the material both dry and submerged. The results can be seen in the table below. The average density is used in the stability calculations and to determine the  $d_{n50}$ .

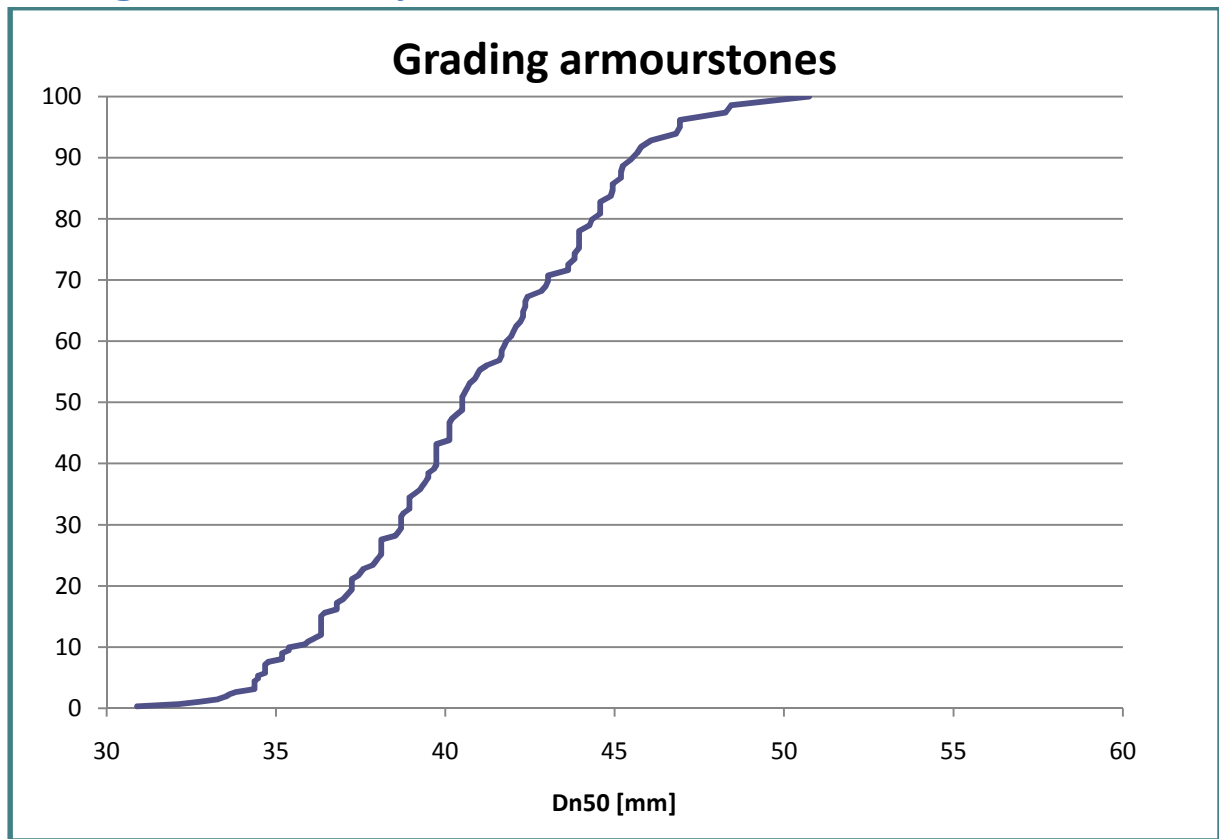
Stone	Weight dry	Weight submerged	Density
1	237.7	146.95	2.62
2	154.95	97.40	2.69
3	98.6	61.6	2.66
4	228.56	144.2	2.71
5	144.6	97.4	3.06
6	161.65	99.9	2.61
7	99.6	61.4	2.61
8	129.25	81.9	2.73
Average density			2.71

Average density of armour material

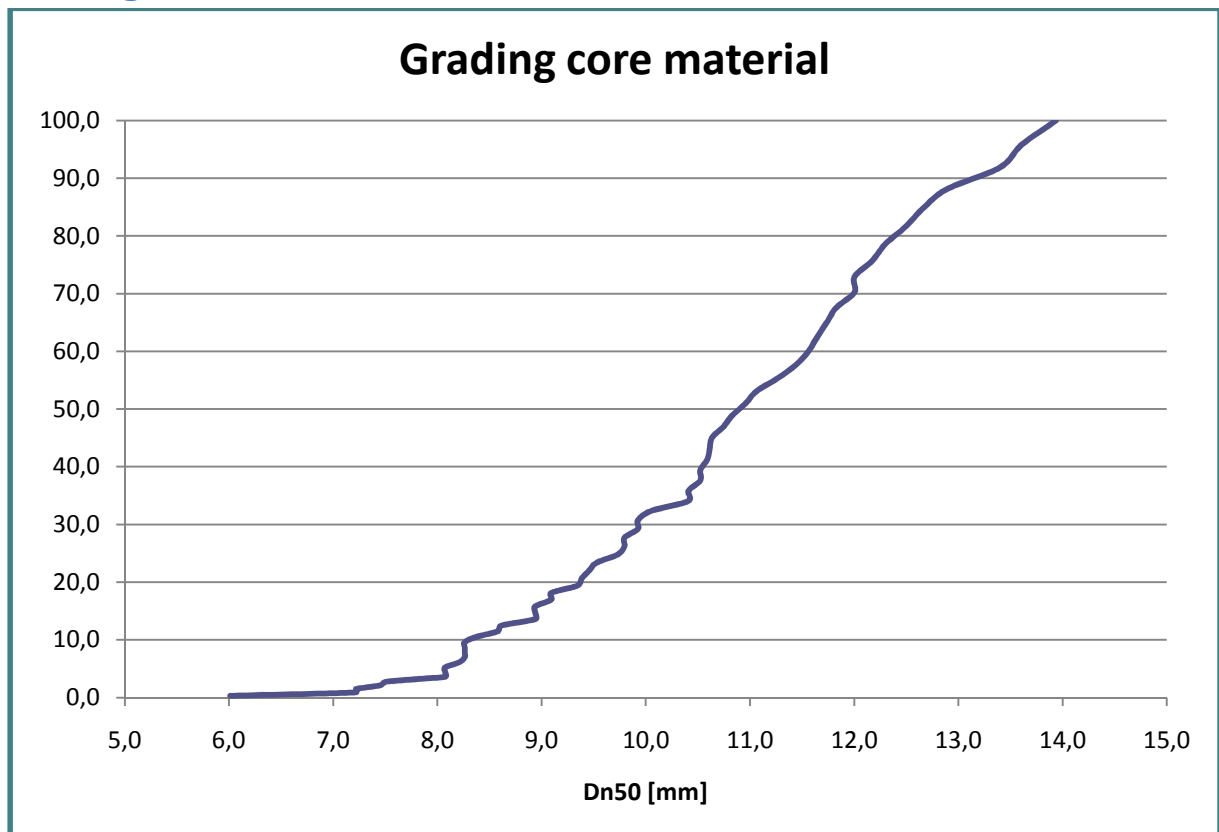
Name	Structure	Grading
Armour	All	
Core	Structure 1	11-16 mm
Filterlayer 1	Structure 2	8-11 mm
Filterlayer 2	Structure 3	4-8 mm
Filterlayer 3	Structure 3	20-40 mm

Used gradings

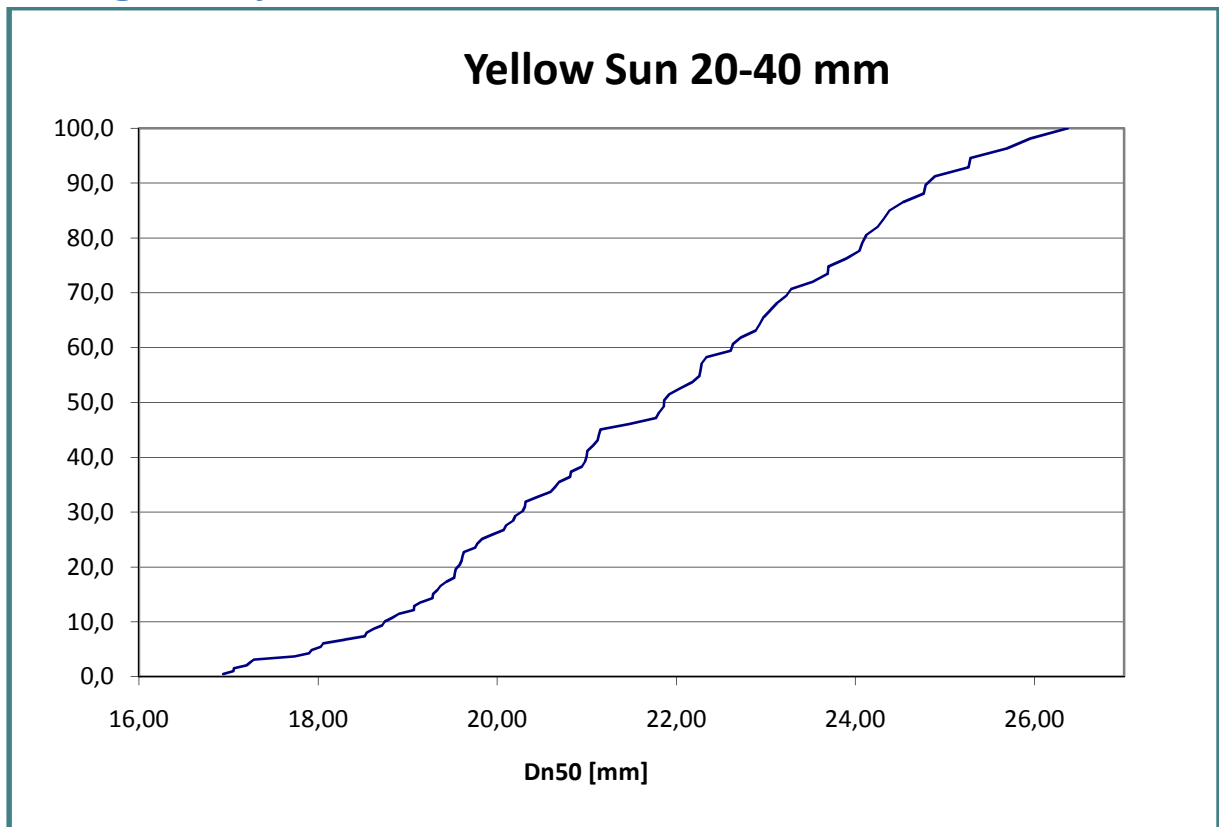
## Grading of the armour layer material



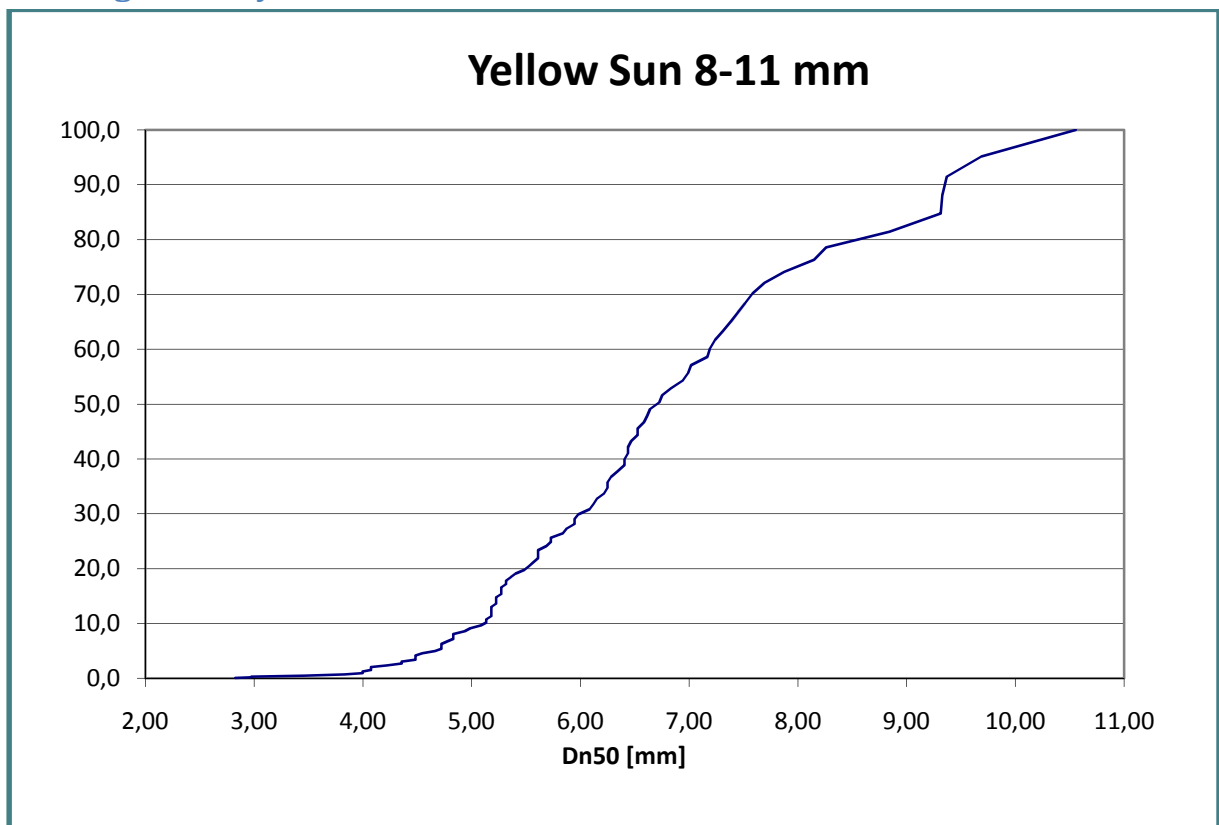
## Grading core material structure 1



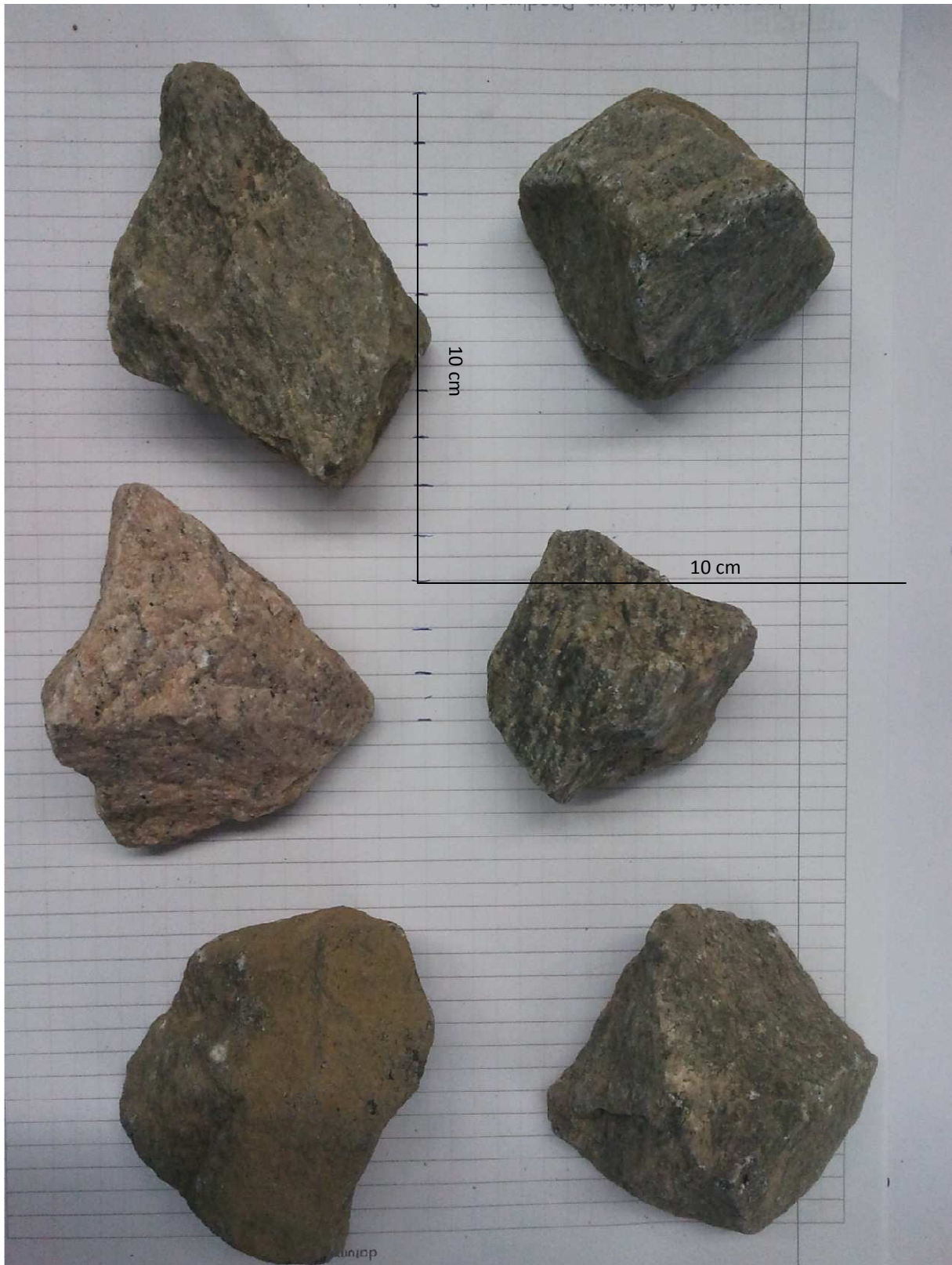
### Grading filter layer structure 3



### Grading filter layer structure 2







Comparison different methods for S structure 2

x	y	z	W	dn50	V	Blockyness	Longest	Shortest	Elongation
5	6	5,5	164,8	3,93	60,81	<b>0,37</b>	6,5	3,5	<b>1,9</b>
6,5	7	4,5	190	4,12	70,11	<b>0,34</b>	7,5	3,5	<b>2,1</b>
8,5	5	4,5	253	4,54	93,36	<b>0,49</b>	9	4	<b>2,3</b>
5,5	5,5	5	174,5	4,01	64,39	<b>0,43</b>	6	4	<b>1,5</b>
4,5	4	4,5	128,3	3,62	47,34	<b>0,58</b>	5,5	3,5	<b>1,6</b>
7	6	3,5	192	4,14	70,85	<b>0,48</b>	8	3,5	<b>2,3</b>
6,5	6	5	181	4,06	66,79	<b>0,34</b>	8	3,5	<b>2,3</b>
8,5	3,5	5,5	183	4,07	67,53	<b>0,41</b>	9	3	<b>3,0</b>
<b>Average</b>						<b>0.43</b>			<b>2.1</b>

Determining blockyness and Elongation

## Appendix B: Calibration & signal registration

All the measured signals are stored over one test in two files. The first file contains the measurements regarding the wave height, wave run up and pressure gauges which are measured during one test. The data from the wave gauges was used to calculate the incoming and reflected wave in front of the structure, this was done by means of the Matlab script decomp.m provided by the Laboratory of fluid mechanics.

Before and after a test the profile is measured which leads to a file containing the signal from the laser and echo sounder.

In the table below the different columns in the data files are explained.

Daq. board channel	Device number	Type	Daisylab entry canal	File wave measurements	File profile measurements
0	1	Wave gauge 1	2	2	
1	2	Wave gauge 2	3	3	
2	3	Wave gauge 3	4	4	
3	4	Wave gauge 4	5	5	
4	5	Wave gauge 5	6	6	
5	6	Wave gauge 6	7	7	
6	7	Wave runup	8	8	
7	8	Laser	9		3
A	9	Echo sounder	10		4
B	10	Pressure gauge A	11	9	
C	11	Pressure gauge B	12	10	
D	12	Pressure gauge C	13	11	
E	13	Pressure gauge D	14	12	
F	14	Pressure gauge E	15	13	
G	15	Wave gauge behind structure	16	14	

The first column in the daisylab file is reserved for a counter. In the profile measurement file the second column is used for a device measuring the position of the carriage, the device give a pulse every rotation. One pulse equals 0.02509 cm.

## Calibration pressure gauges

Calibration of the measurement devices was done by measuring a certain water level and measure the voltage that is displayed by the device. This results in a linear calibration factor.

Water level	Pressure gauge 1
[cm]	[V]
75	-6,5
70	-4,45
65	-2,25
55	2,1
45	6
40	8,5

Pressure gauge 2			
Water level	tube		
[cm]	[cm]	difference[cm]	[V]
66	75	9	-0,19
66	70	4	2,35
66	65	-1	4,81
66	60	-6	7,12
66	55	-11	9,5

Pressure gauge 3			
Water level	tube		
[cm]	[cm]	[cm]	[V]
68	75	7	3,55
68	70	2	1,41
68	65	-3	-0,69
68	55	-13	-5,238

Pressure gauge 4			
Water level	tube		
[cm]	[cm]	[cm]	[V]
68	80	12	4,4
68	75	7	2,5
68	70	2	0,7
68	65	-3	-1,8
68	55	-13	-5,5
68	50	-18	-7,4

Pressure gauge 5			
Water level	tube		
[cm]	[cm]	[cm]	[V]
66	75	9	6
66	70	4	3,66
66	65	-1	1,28
66	60	-6	-1,1
66	55	-11	-3,7

## Calibration wave run up gauge

Water level [cm]	Voltage
40	-9,39
45	-7,79
50	-6,16
55	-4,89
60	-3,4
65	-2,16
70	-0,91
75	0,28
80	1,73
85	3,12
90	4,83

## Wave gauge behind the structure

Water level [cm]	Voltage
55,5	-5,2
65,15	-1,37
64,9	-1,49
69,3	0,268

## Calibration wave gauges

	ADC nr	Matlab column	Calibration	+10cm	0	-10cm	[cm/V ]
<b>G18</b>	0	2		4,018	-0,003	-4,027	2,49
<b>G20</b>	1	3		3,899	-0,012	-3,959	2,55
<b>G21</b>	2	4		4,318	-0,038		2,32
<b>G23</b>	3	5		4,068	0,002	-4,003	2,48
<b>G26</b>	4	6		3,912	-0,003	-3,977	2,54
<b>G27</b>	5	7		4,199	0,005	-4,199	2,38

## Appendix C: Method of damage level

The method used in the main report is the same as used by other authors. In addition a comparison is made between other possible methods. These methods are using a discrete signal, first determine the damage and average that value and draw a polyline through the measured profile. In this appendix these three methods are compared. Furthermore the data acquired in this study was used to determine the value of  $P$  combined with the data of the test of Van der Meer 1988.

### Comparison damage methods

During a test 13 profiles were measured. For each of those measured profiles the difference between the initial and the final profile was determined, which leads to a damage number  $S$  per measured cross section. The resulting damage number of a test is average value of the damage numbers  $S$  of 13 cross sections.

A different way to determine the damage based on eroded area is to fit a poly line (very high order) through the data points. The idea is to discard the pores measured by the laser which should lead to a smoother profile with a better accuracy. In figure xx the poly line of the same cross section of figure xx is shown.

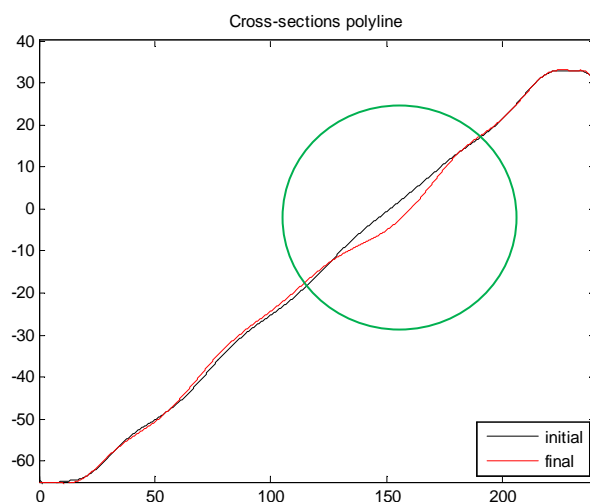


Figure 1 Measured profile test#7 poly line cross section-b,  $S=9.2$

However it appeared that the average difference between the original measurement and the poly line was considerable with an average value of  $S=2$  lower. Also the difference between the calculated result and the measured result with the poly line was much higher with respect to the original measurement. Because of the higher deviation from the calculated result the poly line will not be used in the data analysis.

In the table below the results of the different methods of damage determination is presented for the two reference cases  $P=0.5$  and  $P=0.1$ .

Test number #	P-value	S calculated	S average cont.	S average discr.	S per cross sections
<b>1b</b>	0.5	8.97	8.57	8.64	10.39
<b>2</b>	0.5	3.53	7.27	8.66	7.89
<b>3</b>	0.5	6.91	14.42	15.67	15.31
<b>4</b>	0.5	9.54	12.11	12.06	12.94
<b>5</b>	0.5	7.69	7.03	7.25	8.78
<b>6</b>	0.5	8.7	6.92	5.89	8.16
<b>6b</b>	0.5	11.55	8.6	8.22	10.44
<b>7</b>	0.5	17.12	10.24	9.62	12.23
<b>6a</b>	0.5	14.18	9.17	8.88	11.35
<b>6b</b>	0.5	17.03	8.9	9.07	11.18
<b>6c</b>	0.5	15.22	8.14	8.75	9.58
<b>6d</b>	0.5	14.35	6.78	7.24	8.64
<b>6e</b>	0.5	14.77	10.15	9.86	9.85
<b>3a</b>	0.5	18.71	18.29	17.63	20.69
<b>3b</b>	0.5	17.9	18.28	18.19	19.39
<b>3c</b>	0.5	18.42	19.34	19.95	21.24

Comparison different methods for S structure 1

Test number #	P-value	S calculated	S average cont.	S average discr.	S per cross sections
<b>8</b>	0.1	2.48	4.77	4.82	5.11
<b>9</b>	0.1	7.15	5.13	5.09	7.14
<b>10</b>	0.1	9.66	13.34	13.82	18.48
<b>11</b>	0.1	6.70	12.35	12.82	12.90
<b>12</b>	0.1	5.70	5.47	5.30	8.80
<b>13</b>	0.1	6.35	4.66	4.83	7.64
<b>14</b>	0.1	1.99	2.10	2.21	3.56
<b>15a</b>	0.1	3.02	2.45	3.65	5.44
<b>15b</b>	0.1	3.08	3.69	3.80	6.21
<b>15c</b>	0.1	3.14	3.56	3.55	5.41
<b>16a</b>	0.1	9.20	12.05	11.88	14.47
<b>16b</b>	0.1	9.20	10.73	11.04	13.84
<b>16c</b>	0.1	8.77	12.53	13.06	16.27

Comparison different methods for S structure 2



Method	Discrete(4 cm)	Continuous	Per cross section
<b>BIAS</b>	1.63	1.72	<b>0.23</b>
<b>MAE</b>	4.27	3.97	<b>3.71</b>
<b>RMSE</b>	5.34	5.06	<b>4.56</b>

Statistical performance measurements structure 1

Method	Discrete(4 cm)	Continuous	Per cross section
<b>BIAS</b>	-1.49	<b>-1.26</b>	-3.76
<b>MAE</b>	2.11	<b>1.95</b>	3.76
<b>RMSE</b>	2.73	<b>2.53</b>	4.50

Statistical performance measurements structure 2

Although the method in which for each cross section the damage is calculated and subsequently averaged gives the best fit with the calculated results for the first structure it will not be used because the basic concept is not equal to the method of earlier studies. The continuous measurement is a more accurate measurement with the same concepts of averaging the profiles before determining the damage. For the second structure the continuous measurement is clearly the most accurate way to describe the damage with respect to the calculated results. The averaged continuous measurement method will be used within this report.

## Combined P with original data

Combining all the data of Van der Meer with the data acquired during this research provides the following tables.

P	BIAS	MAE	RMSE
0.48	1.12	2.86	4.05
0.49	0.76	2.67	3.88
0,5	0.41	2.63	3.79
0.51	0.07	2.69	3.75
0.52	-0.25	2.79	3.77
0.53	-0.56	2.90	3.83
0.54	-0.85	2.99	3.93

Statistical values damage structure 1(data measurements KIK[2011]& measurements VANDERMEER[1988])

P	BIAS	MAE	RMSE
0.06	-0.18	1.47	1.91
0.07	-0.22	1.43	1.87
0.08	-0.30	1.41	1.89
0.09	-0.39	1.44	1.94
0.10	-0.54	1.48	2
0.11	-0.69	1.52	2.08

Statistical values damage structure 2 (data measurements KIK[2011]& measurements VANDERMEER[1988])

## Appendix D: Test planning

A rough estimate for the time required for one test is given below:

Action	Required time [min]
Profile measurement	45 min
3000 waves	120 min
Profile measurement	45 min
Restoring profile for next test	60 min
Restore pressure gauges	15 min
<b>Total duration per test</b>	<b>285 min</b>

Table 1 Rough time estimate of a test

This results in one test a day. For the first few test approximately one test a day is reasonable value to use in the planning.

The first week is reserved for preparations of the rock material and calibrating the measurement equipment.

With a total available time in the laboratory of 8 weeks, this leaves 7 weeks available for actual testing. Because physical model testing is a very depending on technique one should account for setbacks as well. Therefore one week is extra time for unforeseen delays. Finally six weeks will be available for testing.

The constructing of a new structure will take up about one day. When conducting experiments on three structures this thus implies 3 days required for the construction of the breakwaters.

Therefore in six weeks 27 tests could be executed. Every structure will be tested with 5 different wave steepness's. After every test the armour layer and if necessary the first under layer will be rebuild.

### Statistics

In order to have some information about the spreading of the results of the experiments, a number of repeating tests have to be executed. One should expect the same results for every test, however the irregularity of the waves, the position of the stones and other small processes which might influence the stability can result in a slightly different result.

All of the three structures will be submitted to repetition tests.

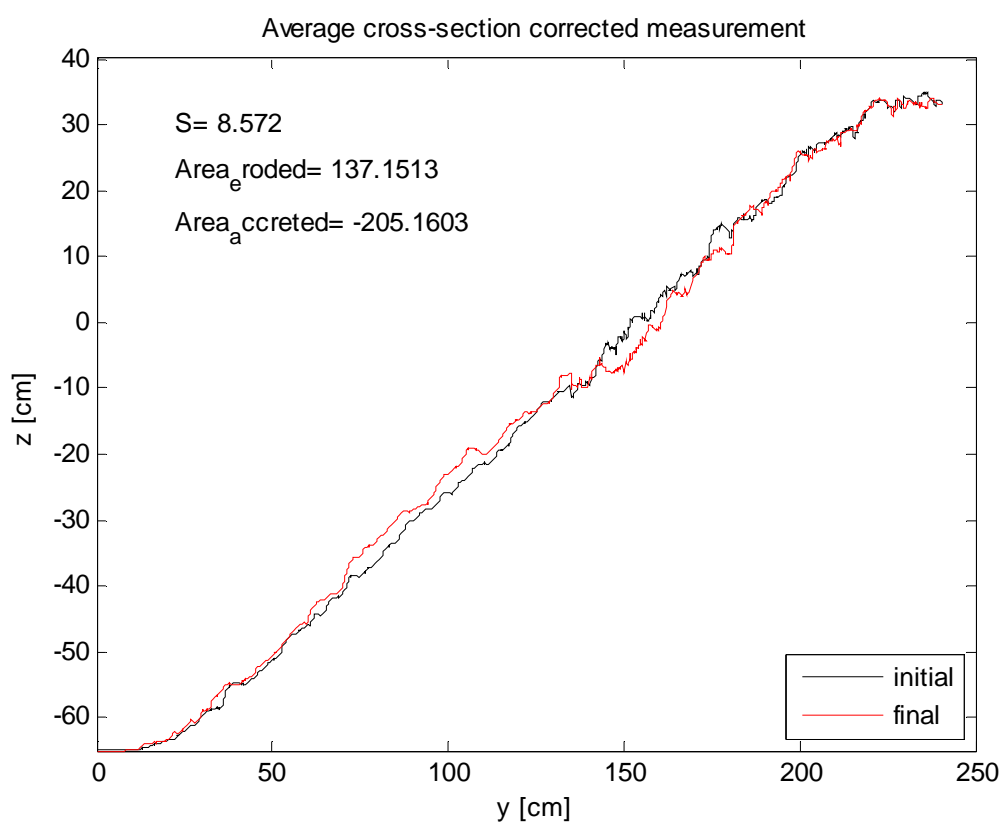
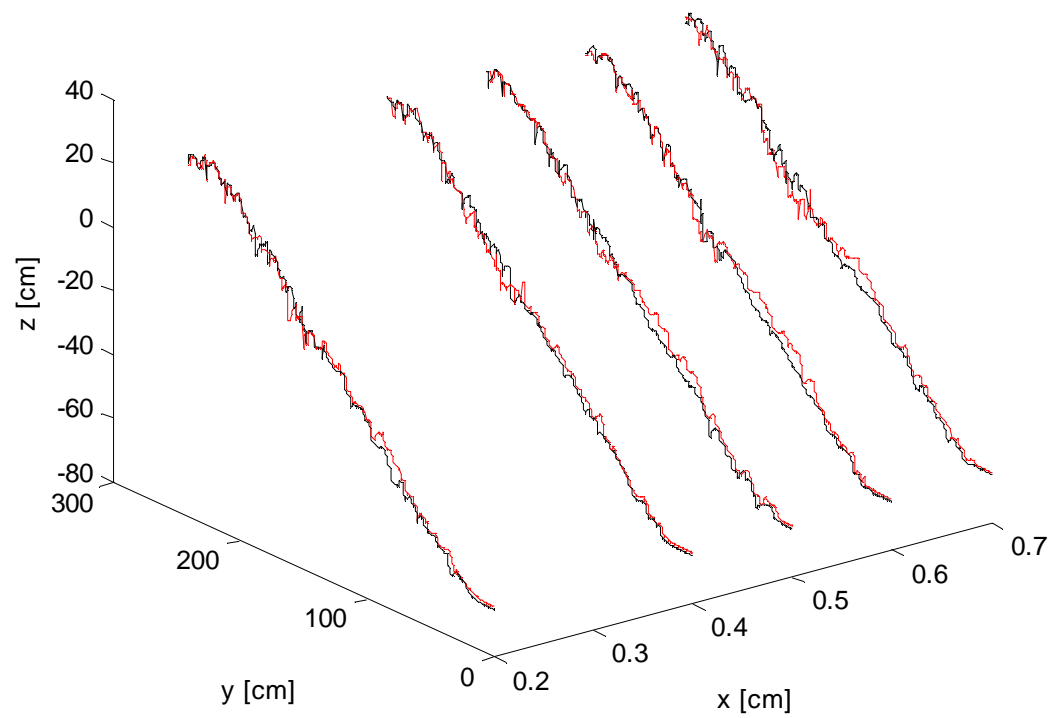
Monday, 4 April 2011	Sorting rock	Week 1
Tuesday, 5 April 2011	Sorting rock	
Wednesday, 6 April 2011	Sorting rock	
Thursday, 7 April 2011	Sorting rock	
Friday, 8 April 2011	Sorting rock	
Saturday, 9 April 2011		
Sunday, 10 April 2011		
Monday, 11 April 2011	Building structure 1	Week 2
Tuesday, 12 April 2011	Test1	
Wednesday, 13 April 2011	Test2	
Thursday, 14 April 2011	Test3	
Friday, 15 April 2011	Test4	
Saturday, 16 April 2011		
Sunday, 17 April 2011		
Monday, 18 April 2011	Test5	Week 3
Tuesday, 19 April 2011	Repetition test	
Wednesday, 20 April 2011	Building structure 2	
Thursday, 21 April 2011	Test6	
Friday, 22 April 2011	Boat trip river dynamics	
Saturday, 23 April 2011		
Sunday, 24 April 2011		
Monday, 25 April 2011	Easter	Week 4
Tuesday, 26 April 2011	Test7	
Wednesday, 27 April 2011	Test8	
Thursday, 28 April 2011	Test9	
Friday, 29 April 2011	Repetition test	
Saturday, 30 April 2011		
Sunday, 1 May 2011		
Monday, 2 May 2011	Building structure 3	Week 5
Tuesday, 3 May 2011	Test10	
Wednesday, 4 May 2011	Test11	
Thursday, 5 May 2011	Test12	
Friday, 6 May 2011	Test13	
Saturday, 7 May 2011		
Sunday, 8 May 2011		
Monday, 9 May 2011	Test14	Week 6
Tuesday, 10 May 2011	Test15	
Wednesday, 11 May 2011	Repetition test	
Thursday, 12 May 2011	Repetition series	
Friday, 13 May 2011	Repetition series	
Saturday, 14 May 2011		
Sunday, 15 May 2011		
Monday, 16 May 2011	Repetition series	Week 7
Tuesday, 17 May 2011	Repetition series	
Wednesday, 18 May 2011	Repetition series	
Thursday, 19 May 2011	Repetition series	
Friday, 20 May 2011		
Saturday, 21 May 2011		
Sunday, 22 May 2011		
Monday, 23 May 2011	Unforeseen delays	Week 8
Tuesday, 24 May 2011	Unforeseen delays	
Wednesday, 25 May 2011	Unforeseen delays	
Thursday, 26 May 2011	Unforeseen delays	
Friday, 27 May 2011	Unforeseen delays	
Saturday, 28 May 2011		
Sunday, 29 May 2011		

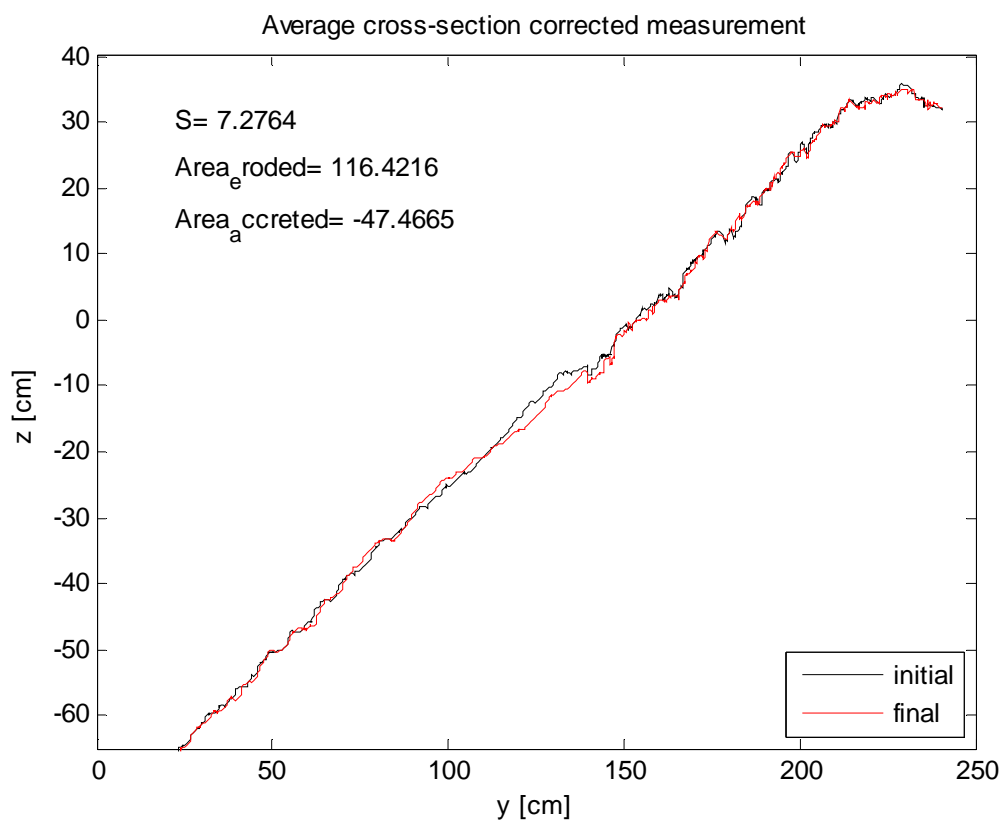
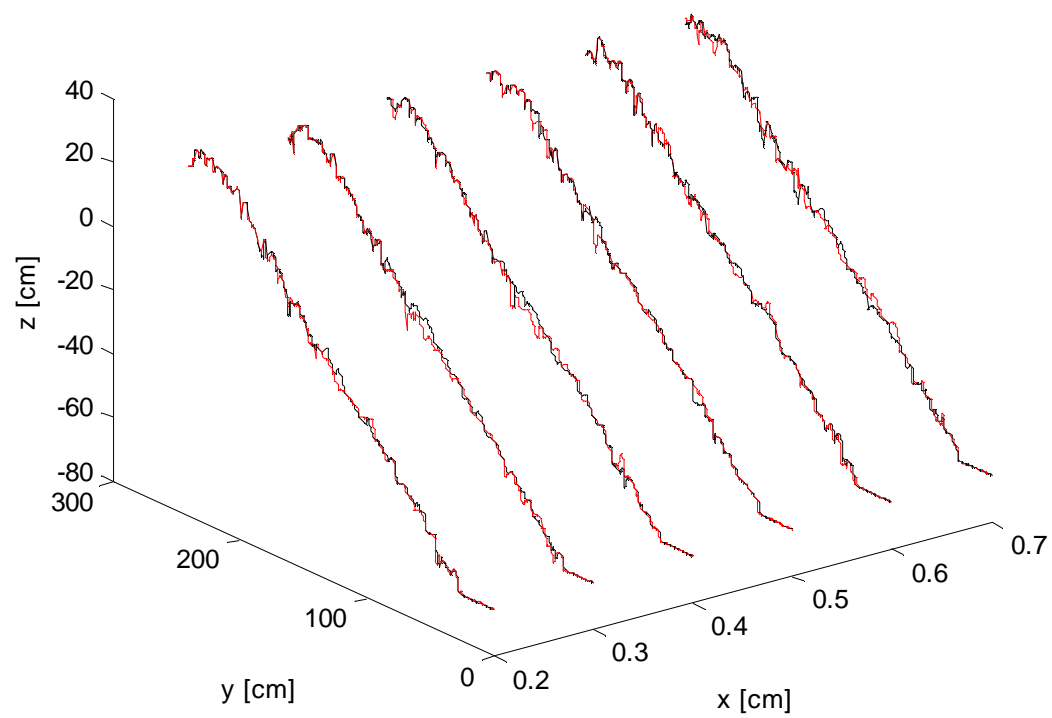
## **Appendix E:      Averaged damage profiles per test**

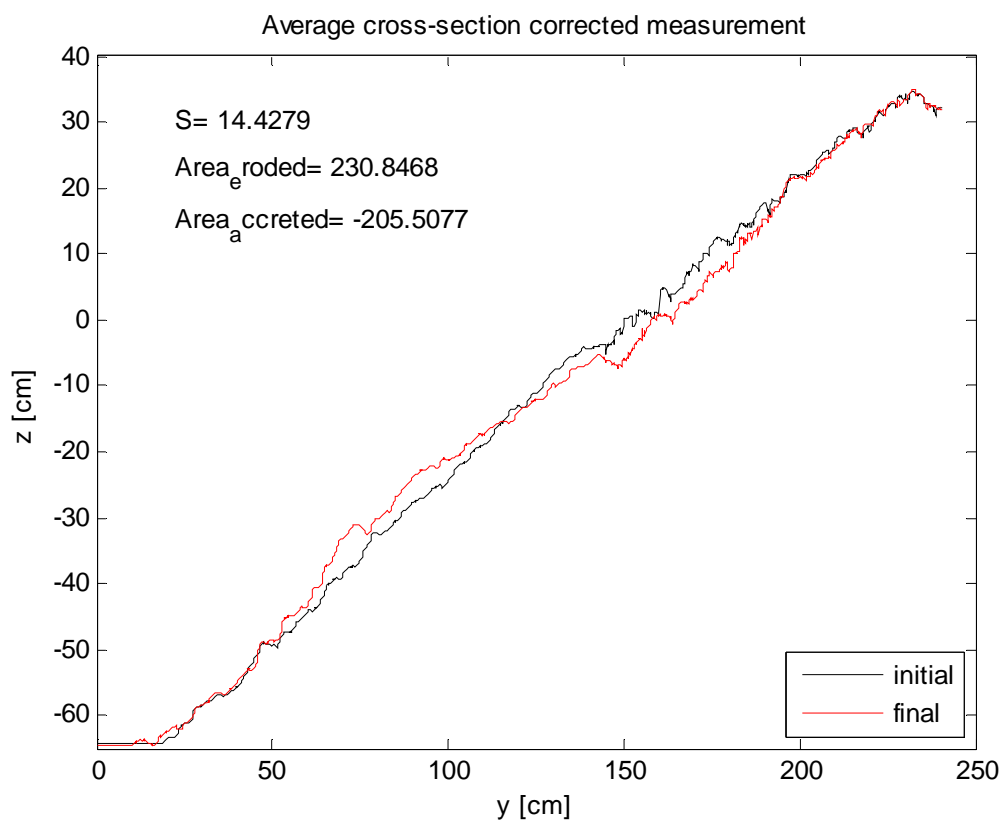
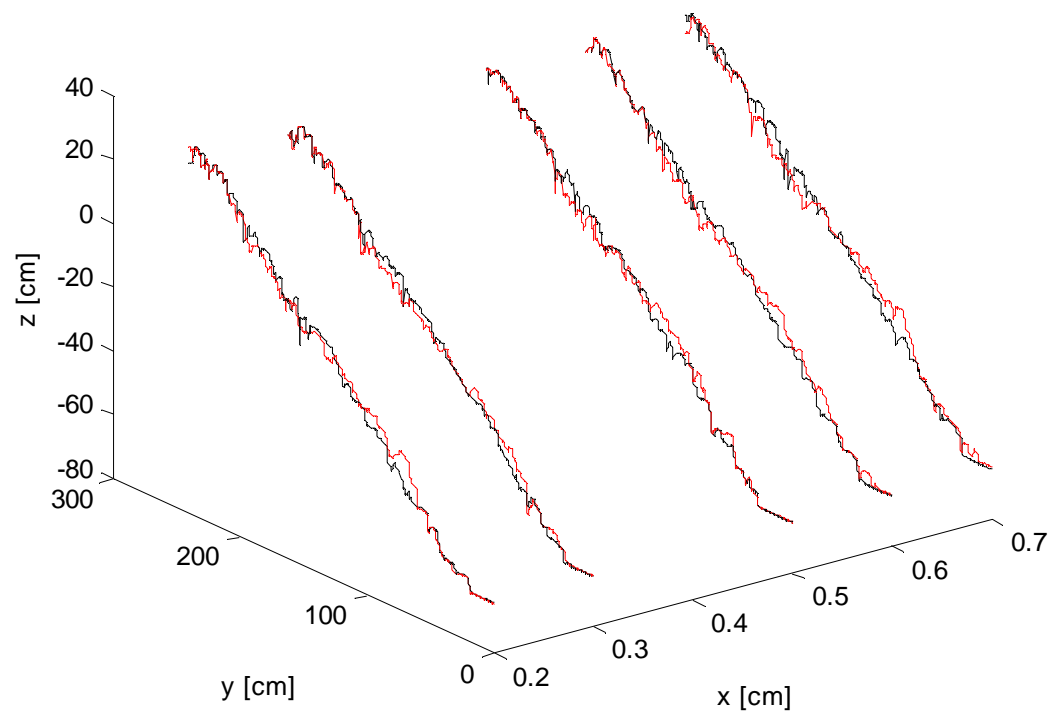
As mentioned in the report each structure is measured by a number of profiles. The measurements of the first structure were except for the repetition tests carried out every 10 cm. The other structures were measured every 5 cm. After analysis it showed that some measurements contained errors, therefore for some structures less profiles are used. Besides the measured eroded area also the accreted area was determined. In case of a closed stone balance these values should be equal to each other. This was however not always the case. A possible explanation for this observation can be that the different devices used to measure the profile. The echo sounder has the tendency to smoothen out the signal a bit because of the bigger footprint of measuring signal in contrary to the laser which has a much smaller footprint. Another explanation can be that displaced rocks are positions right in between two measuring rays.

## Structure 1

1b

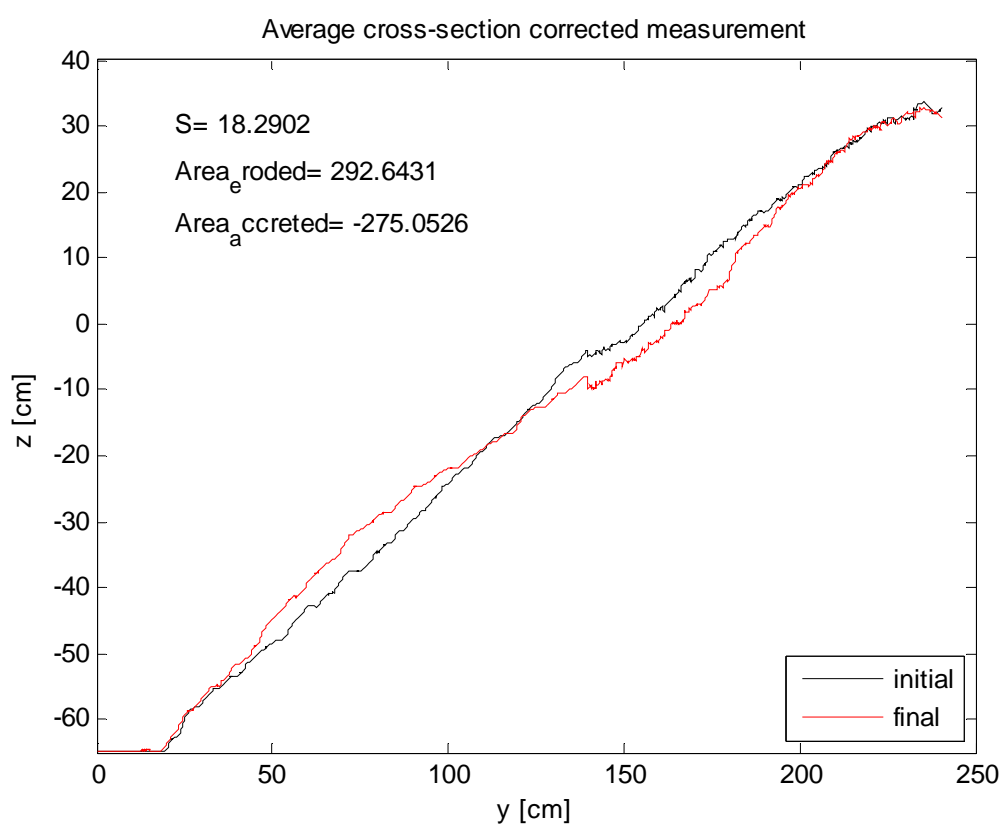
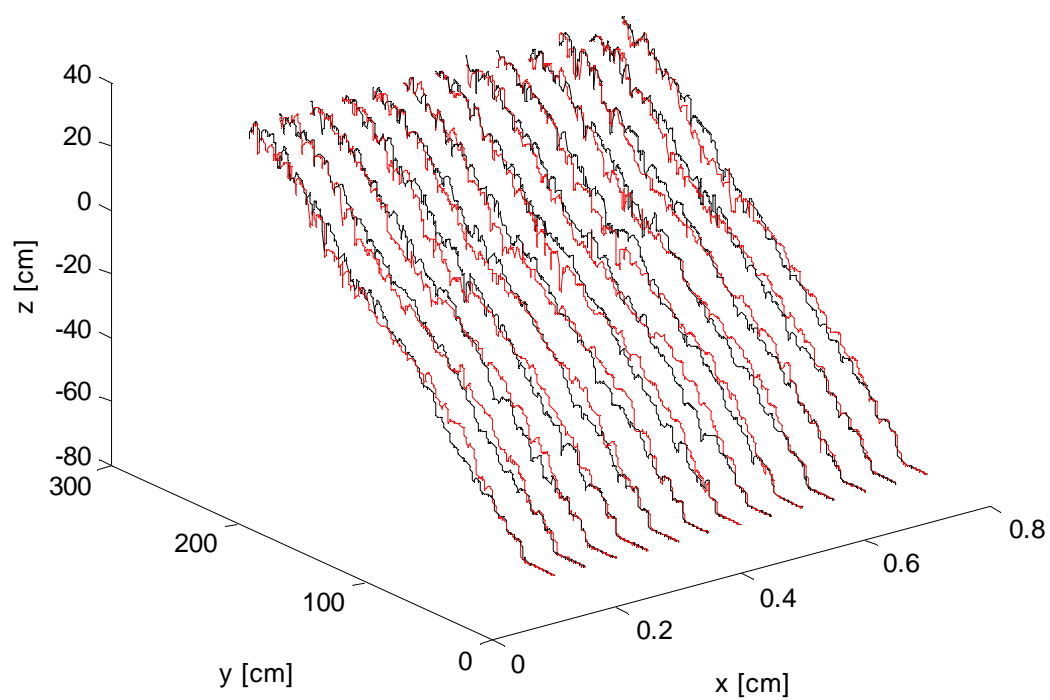




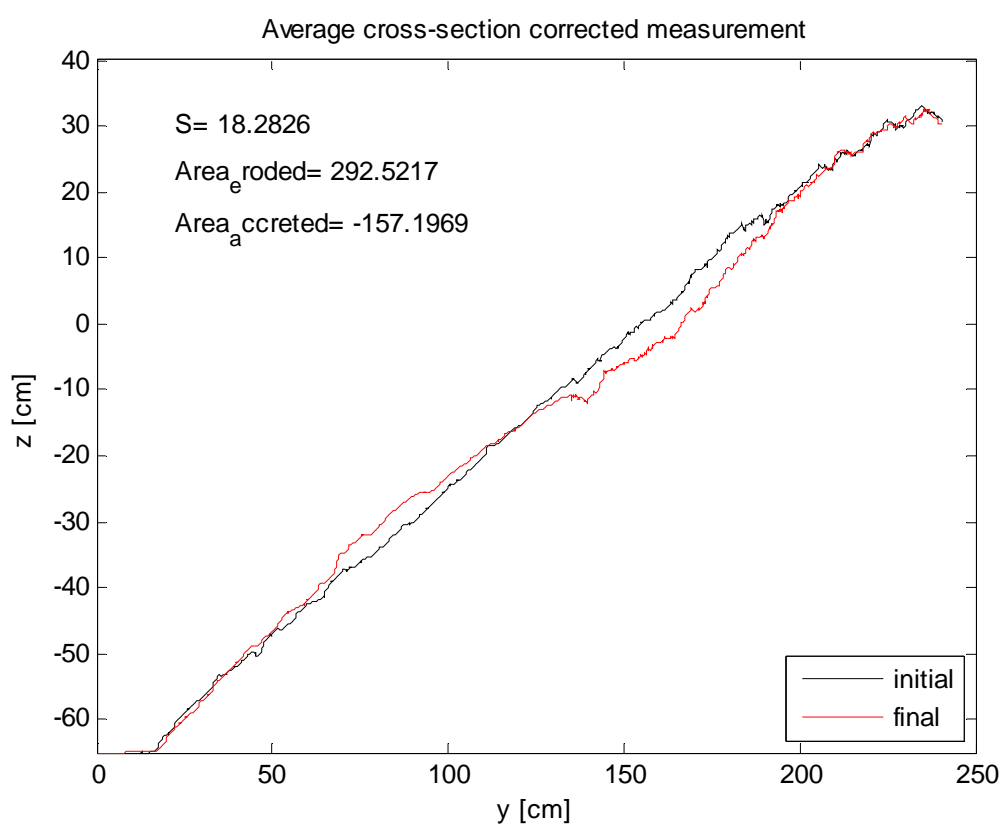
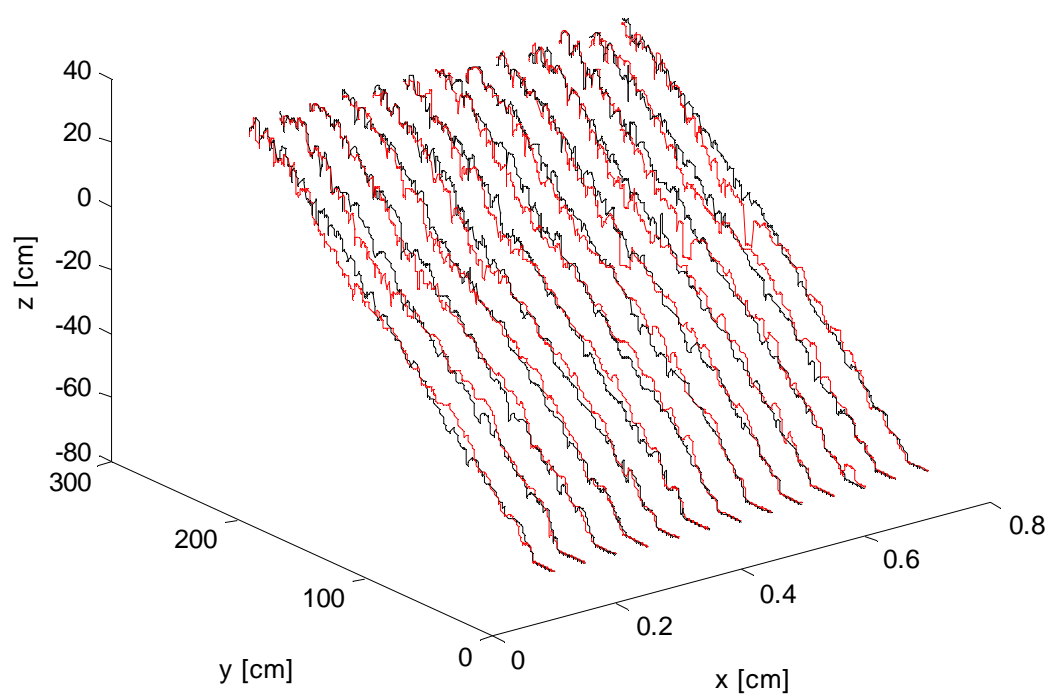




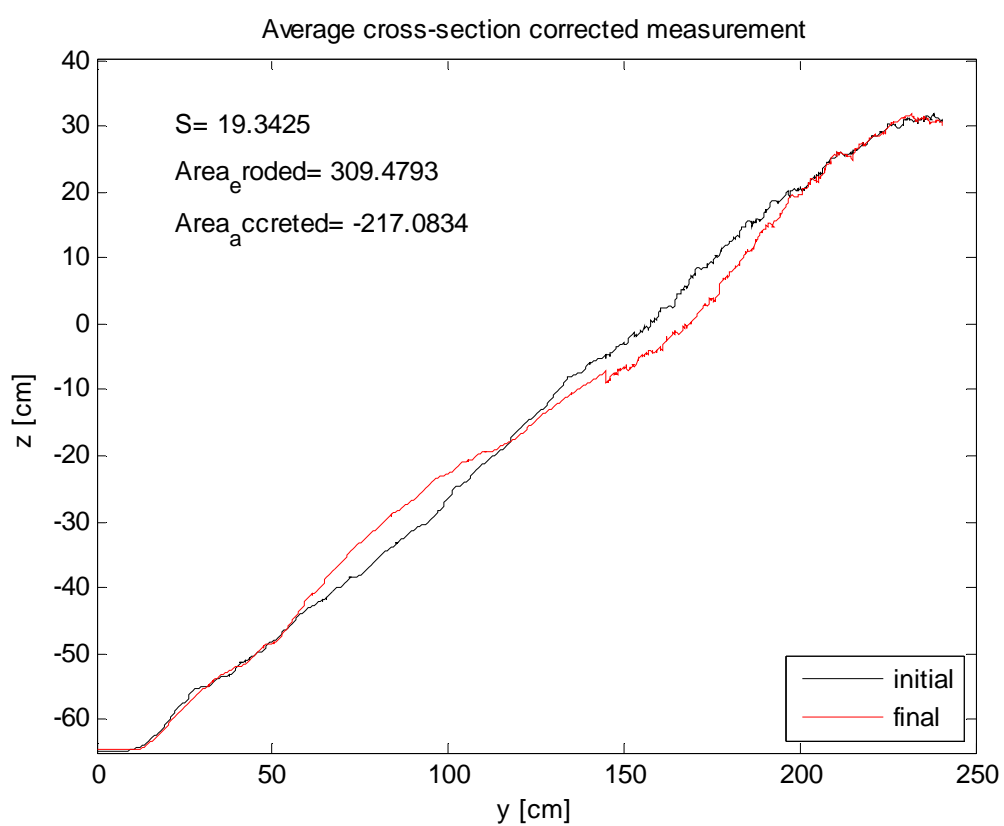
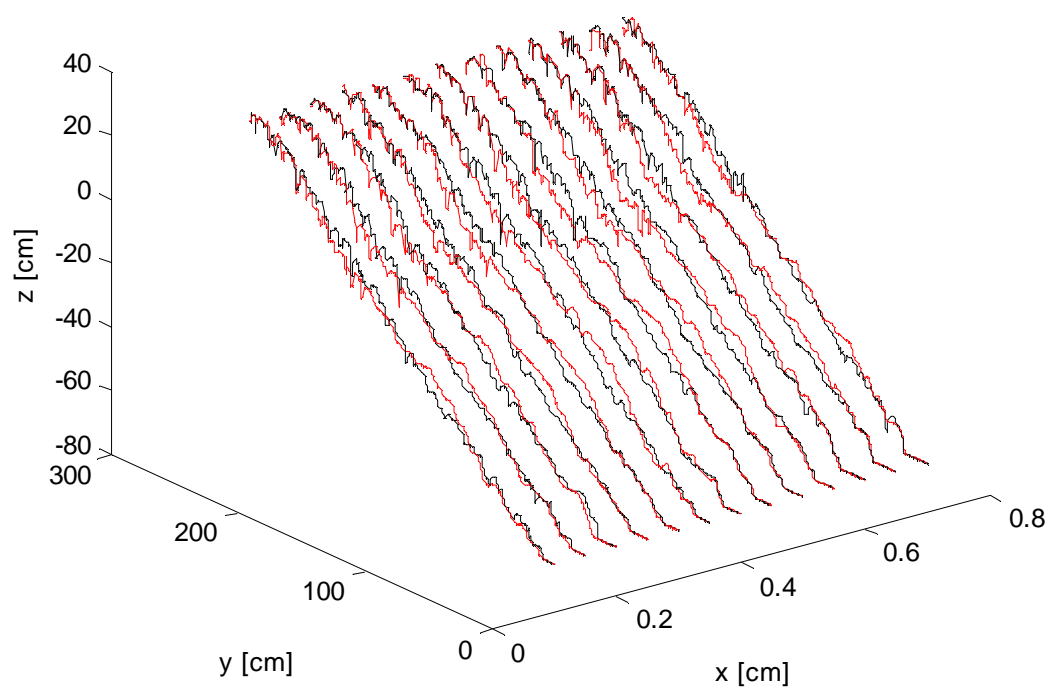
3a

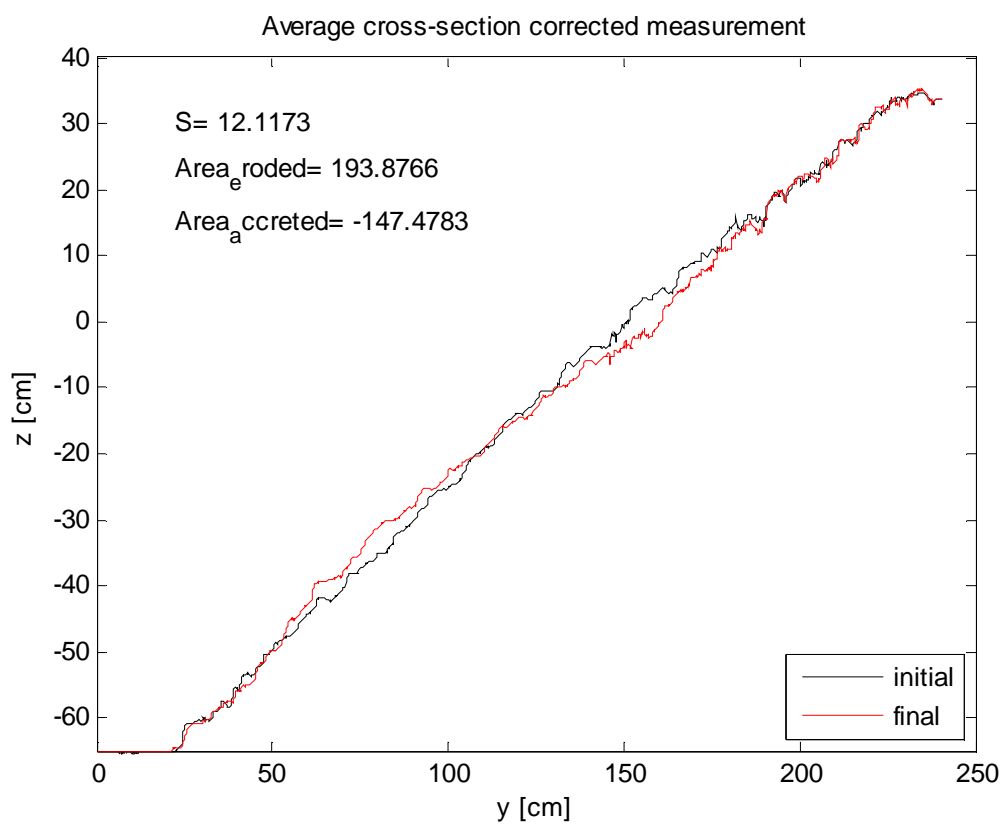
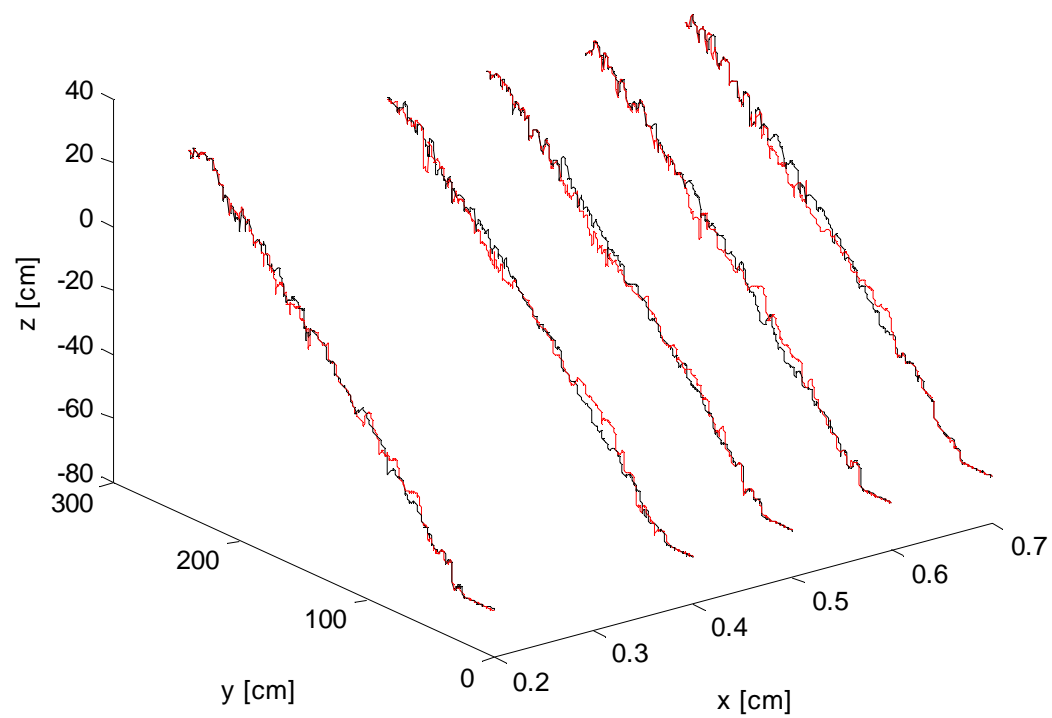


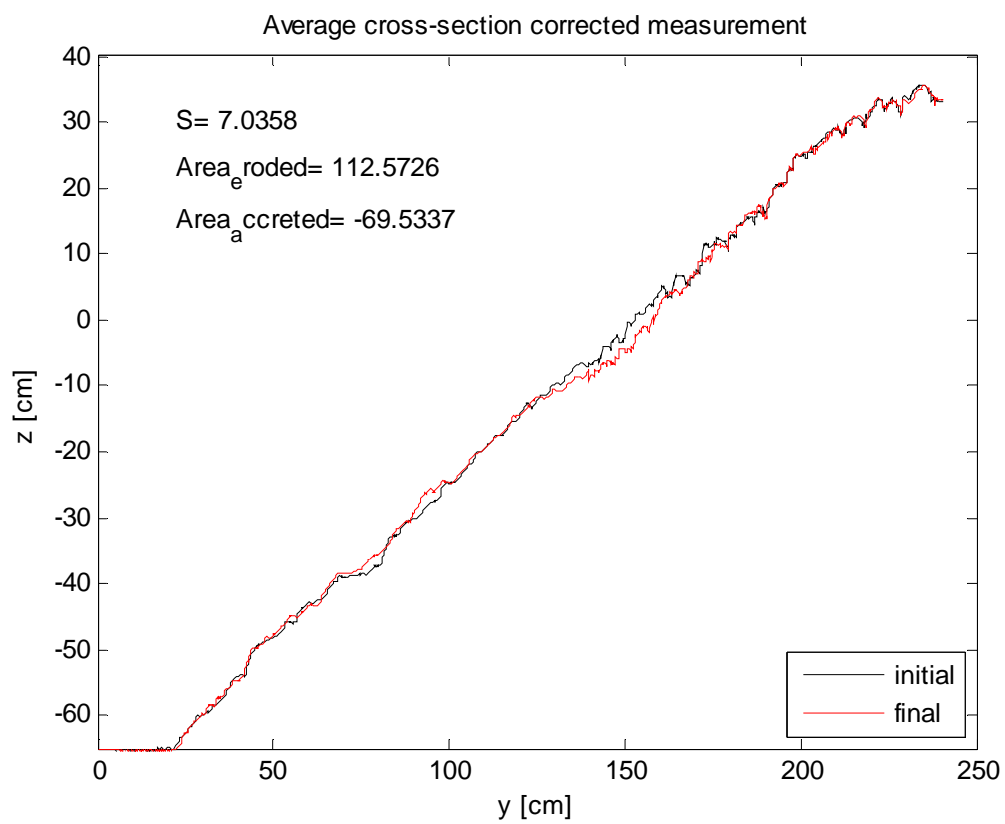
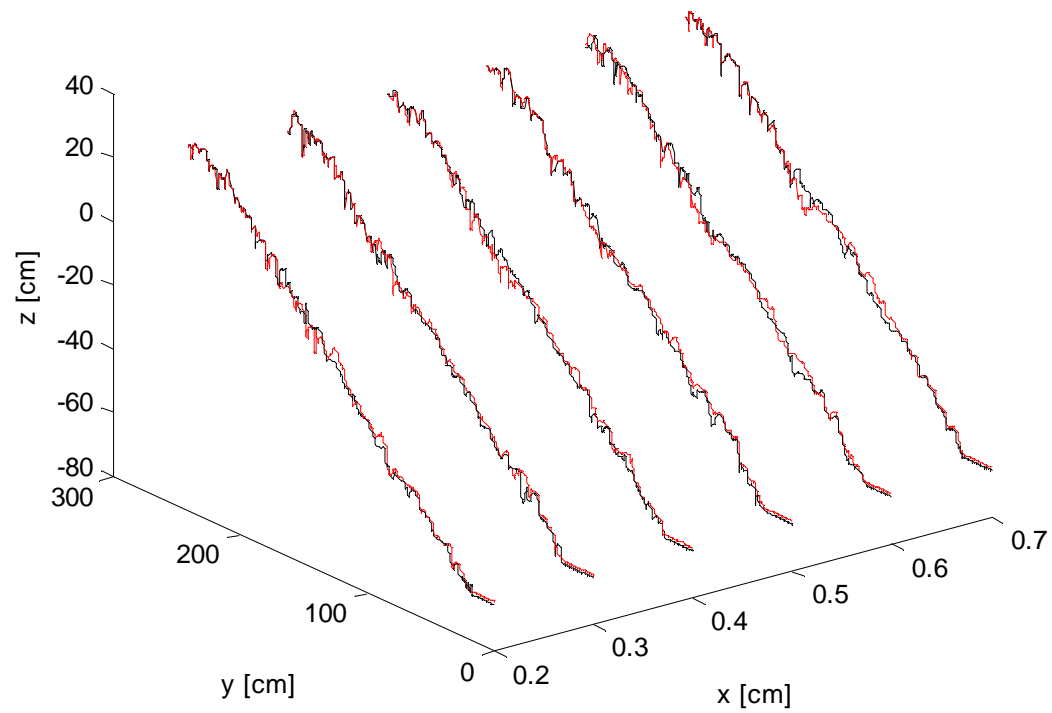
3b

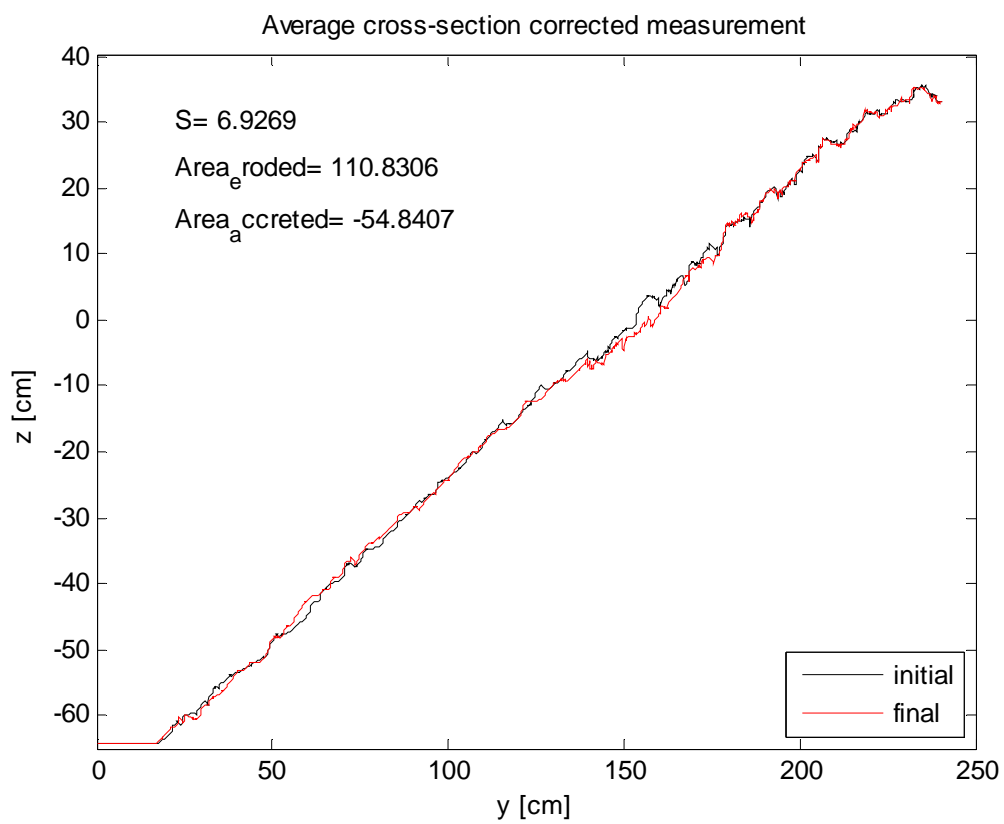
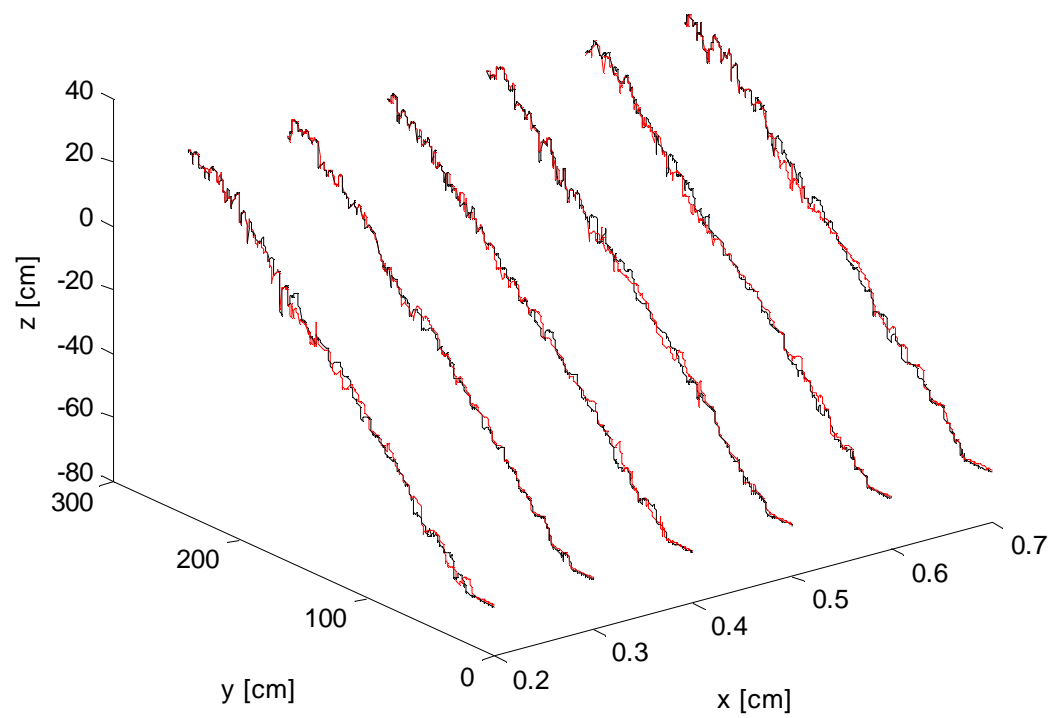


3c

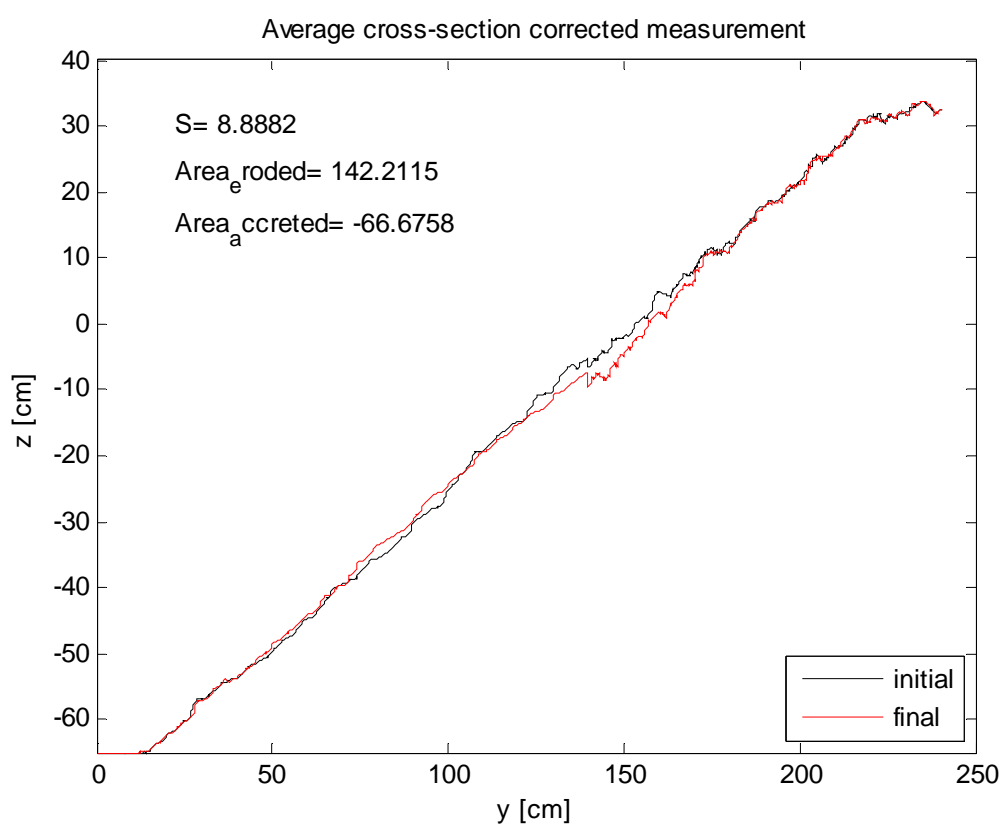
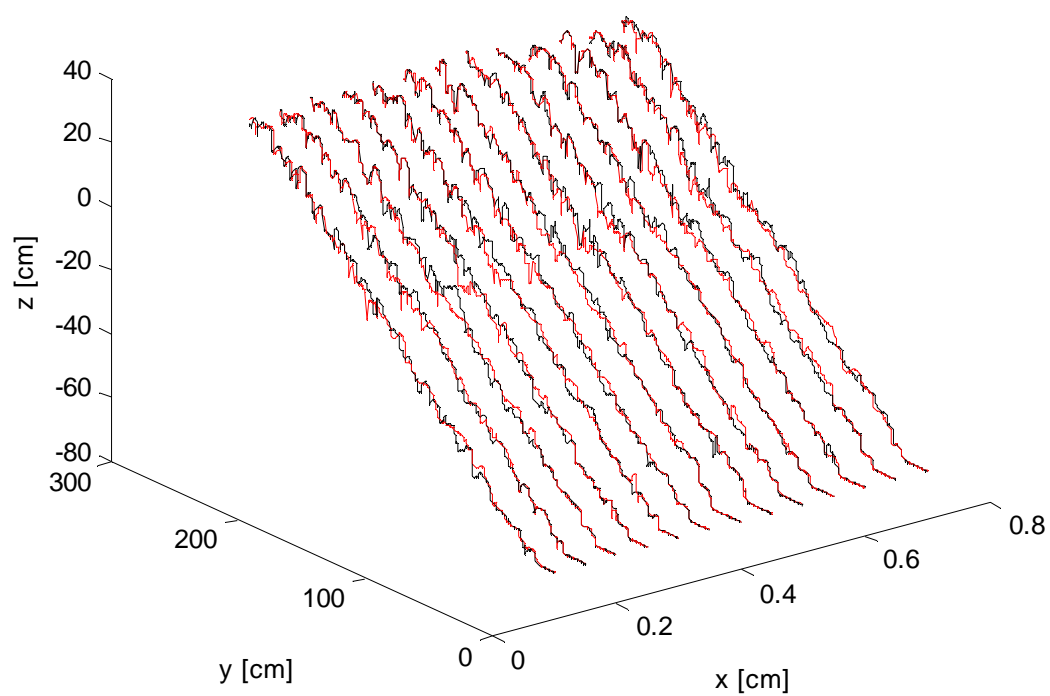




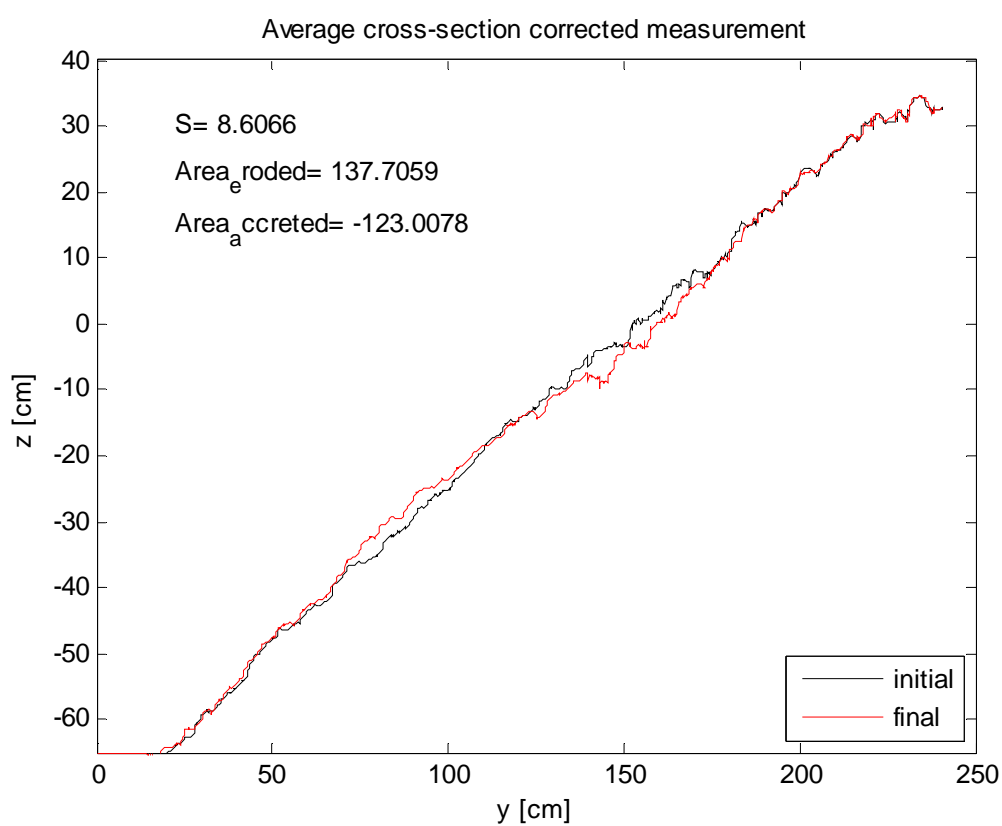
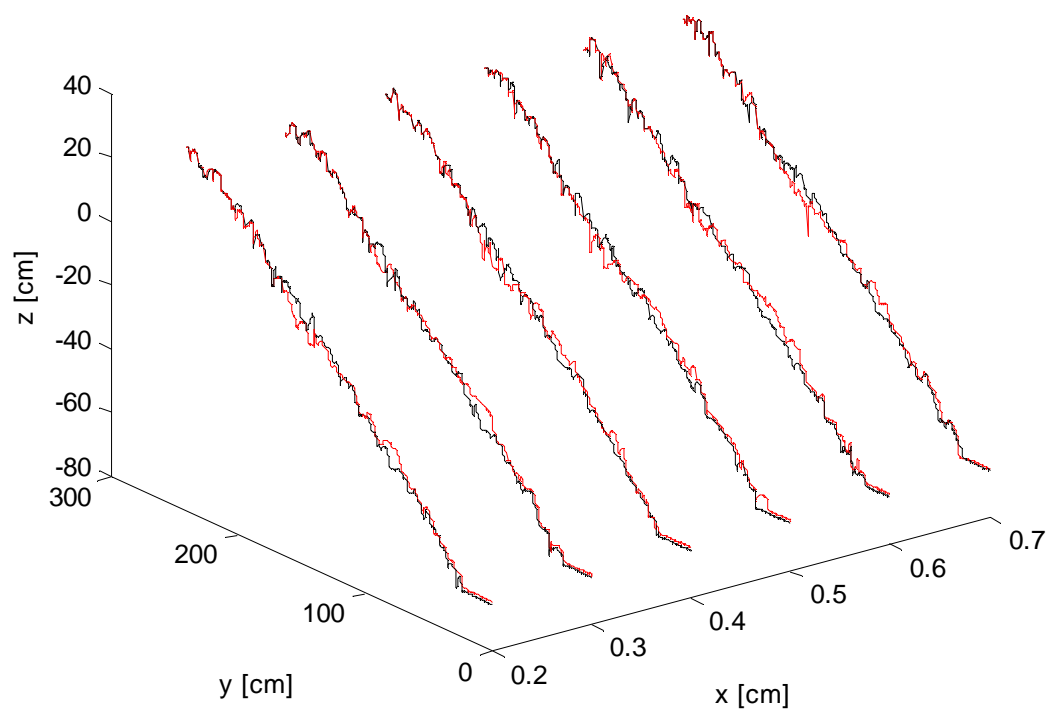




6a

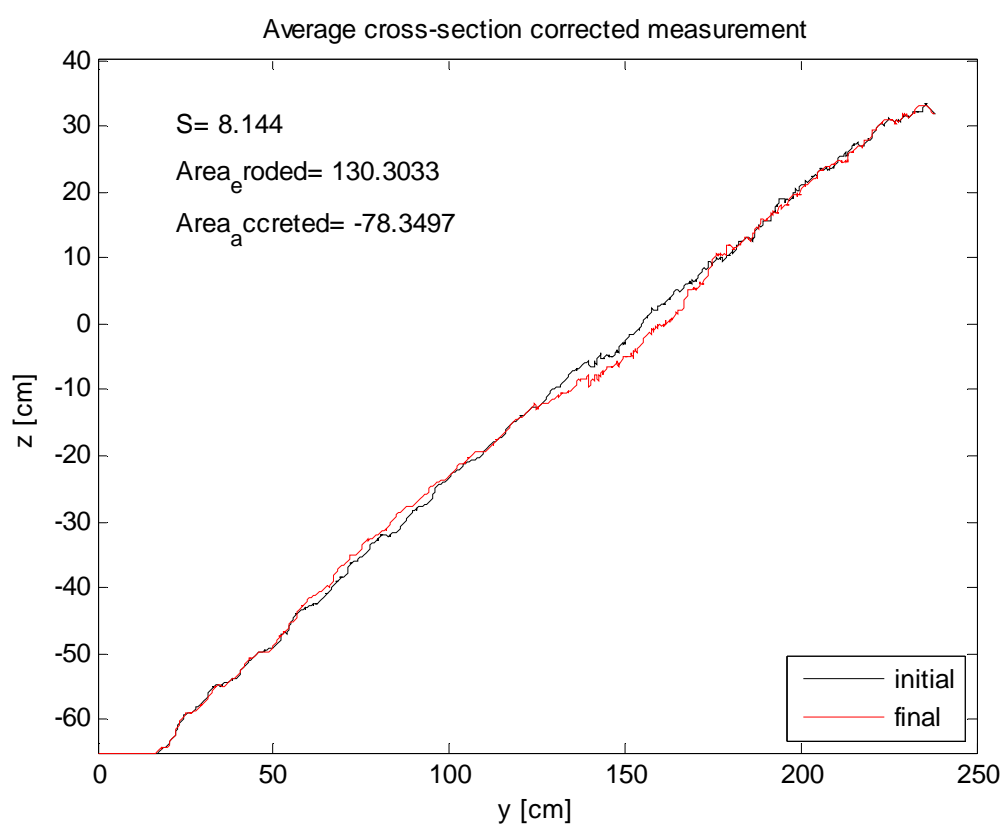
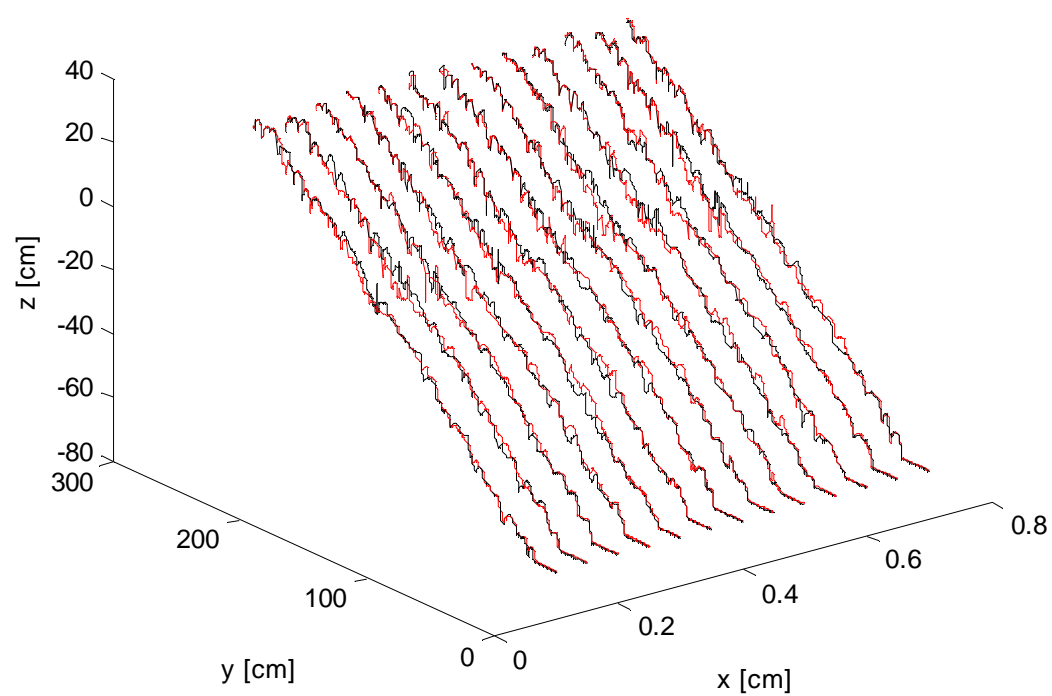


6b

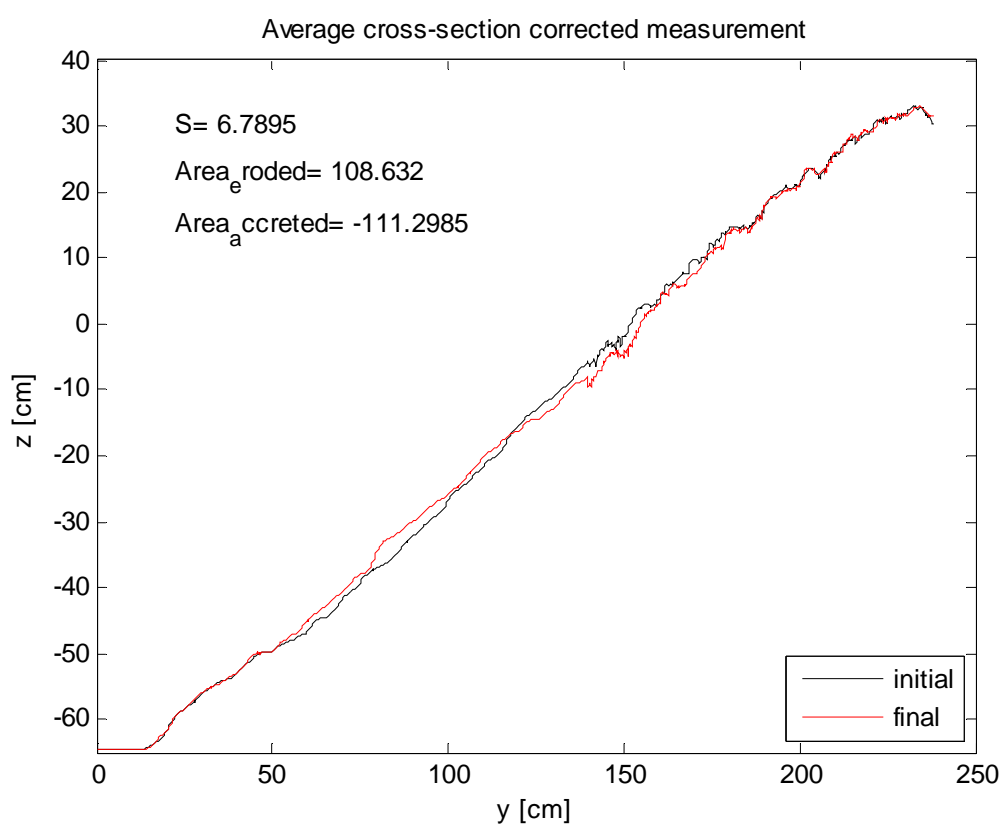
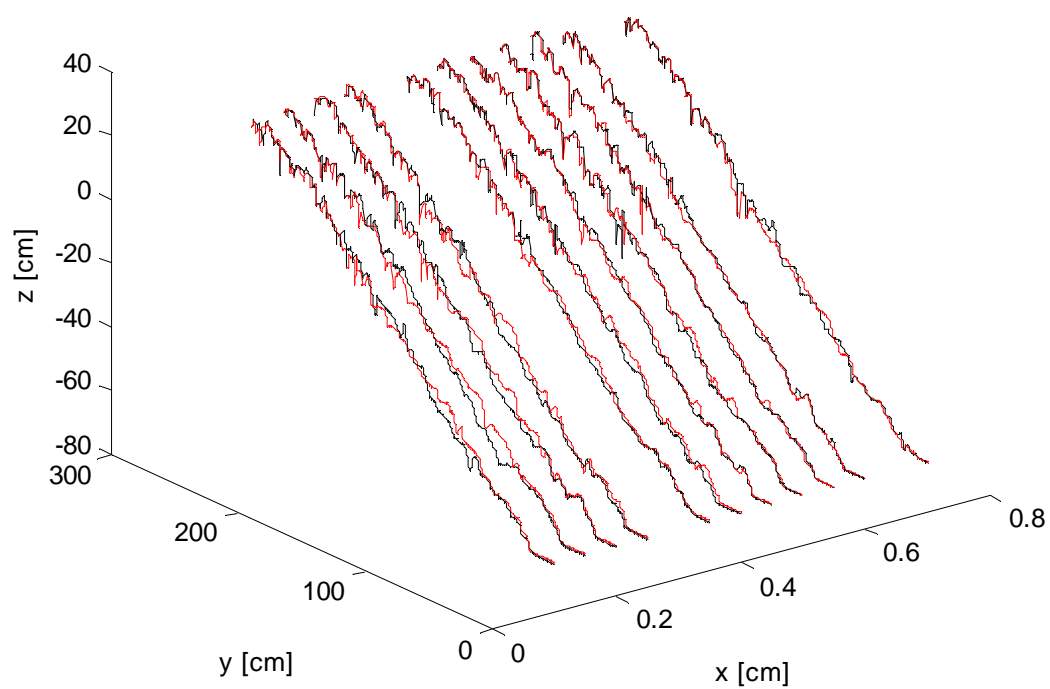


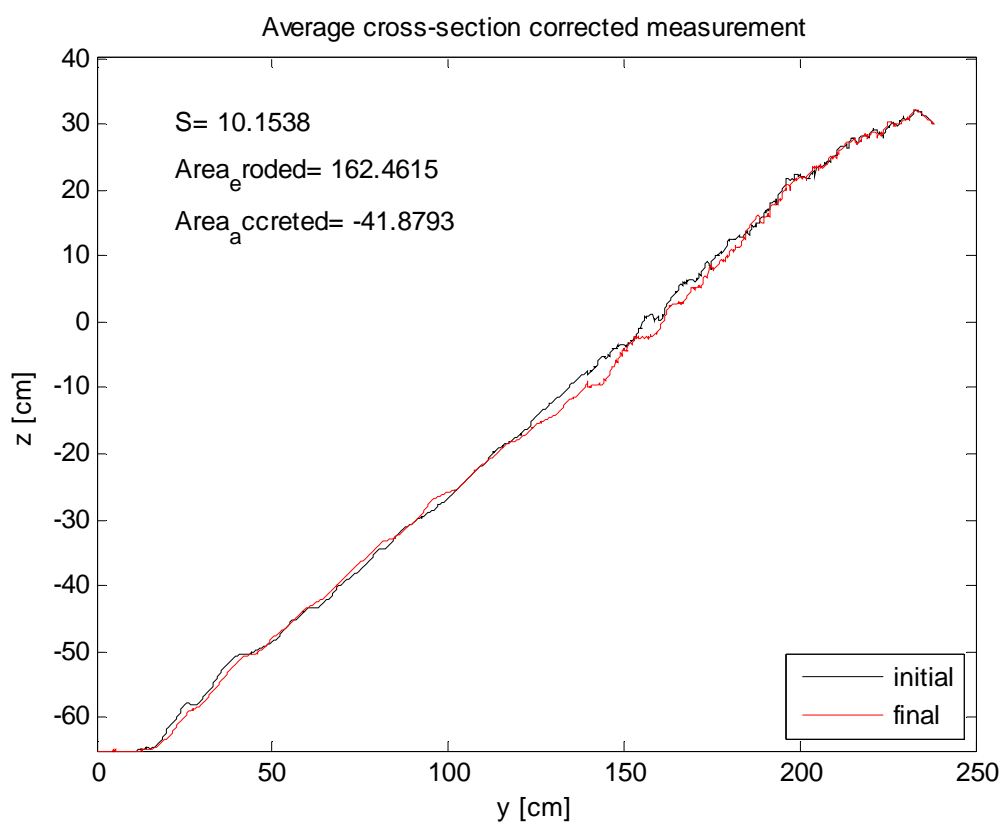
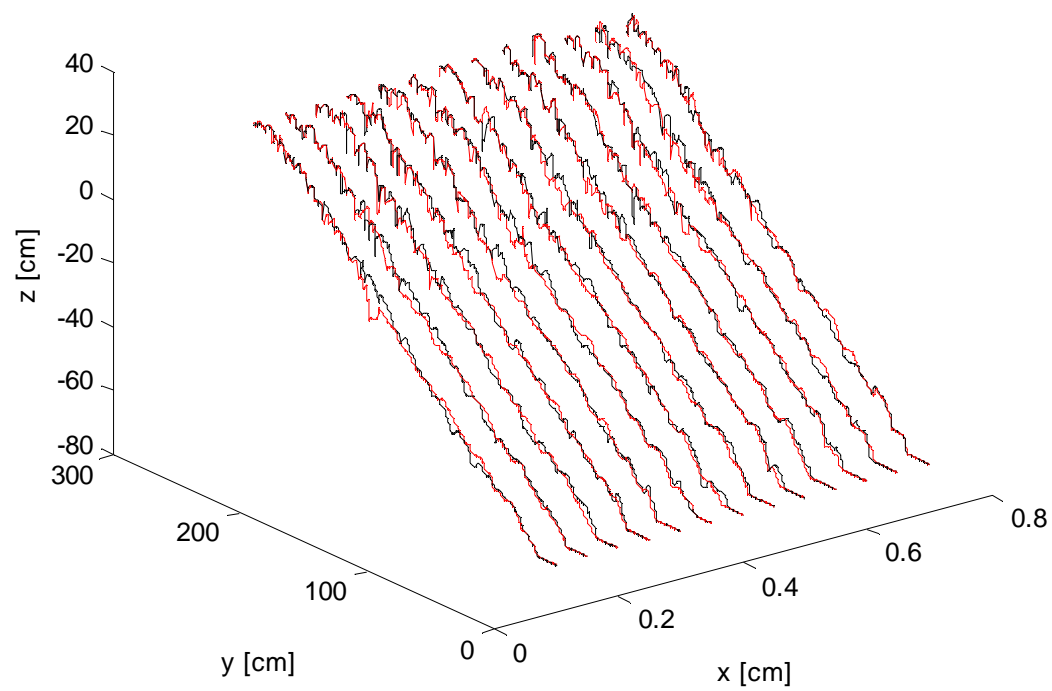


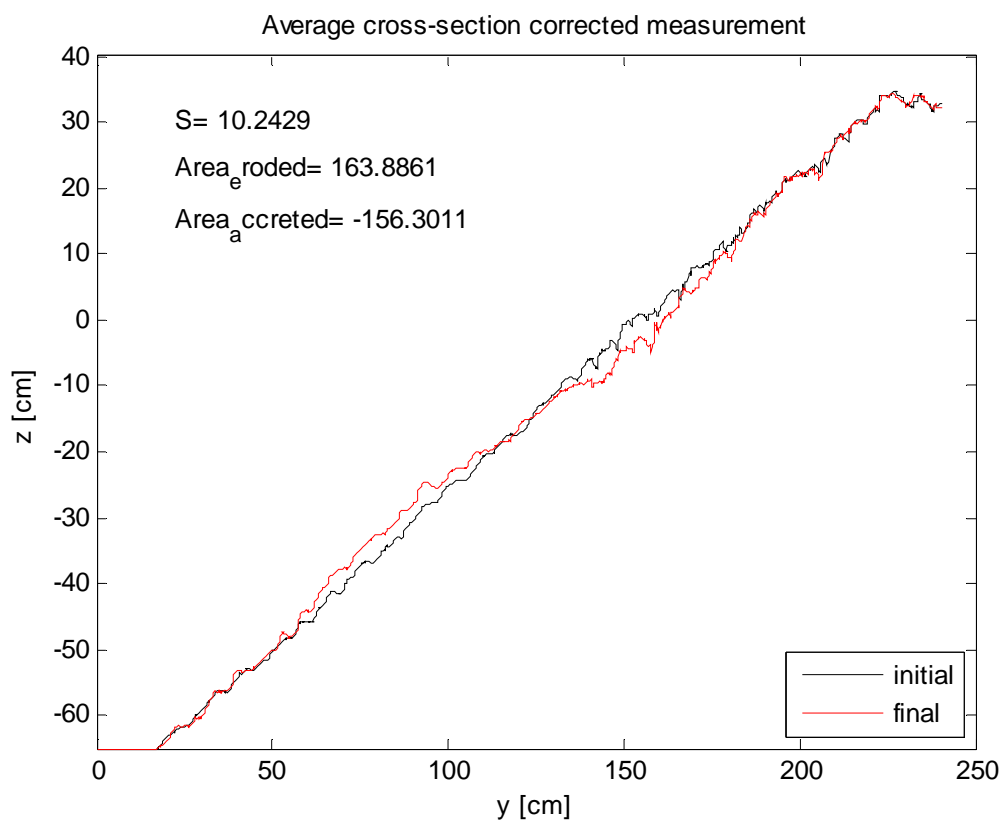
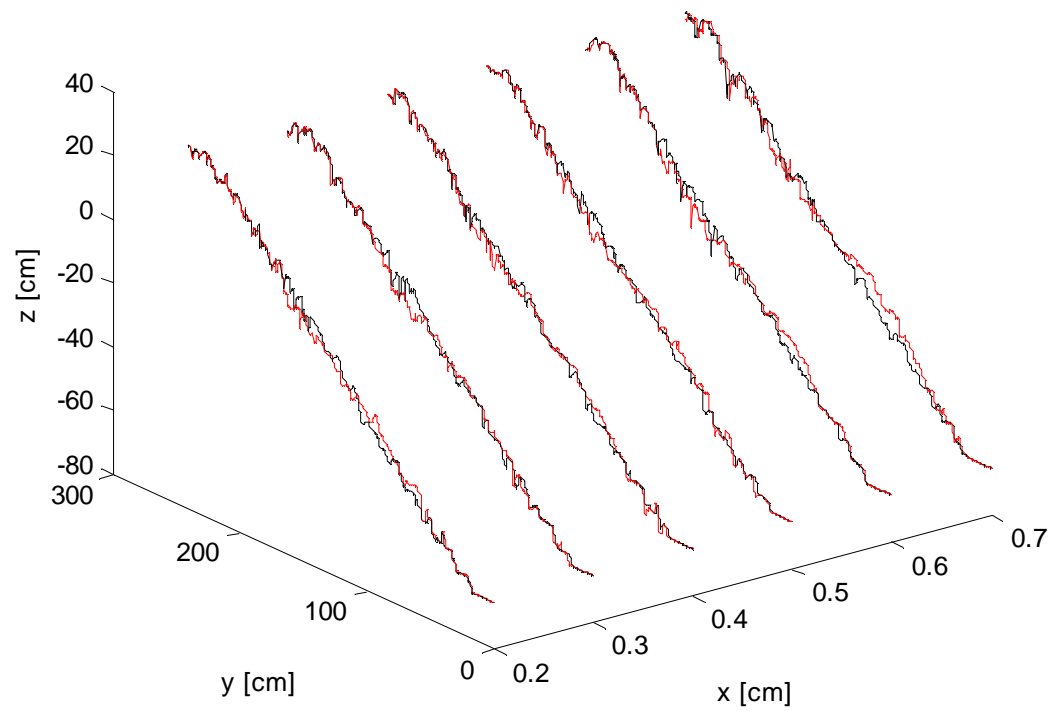
6c



6d

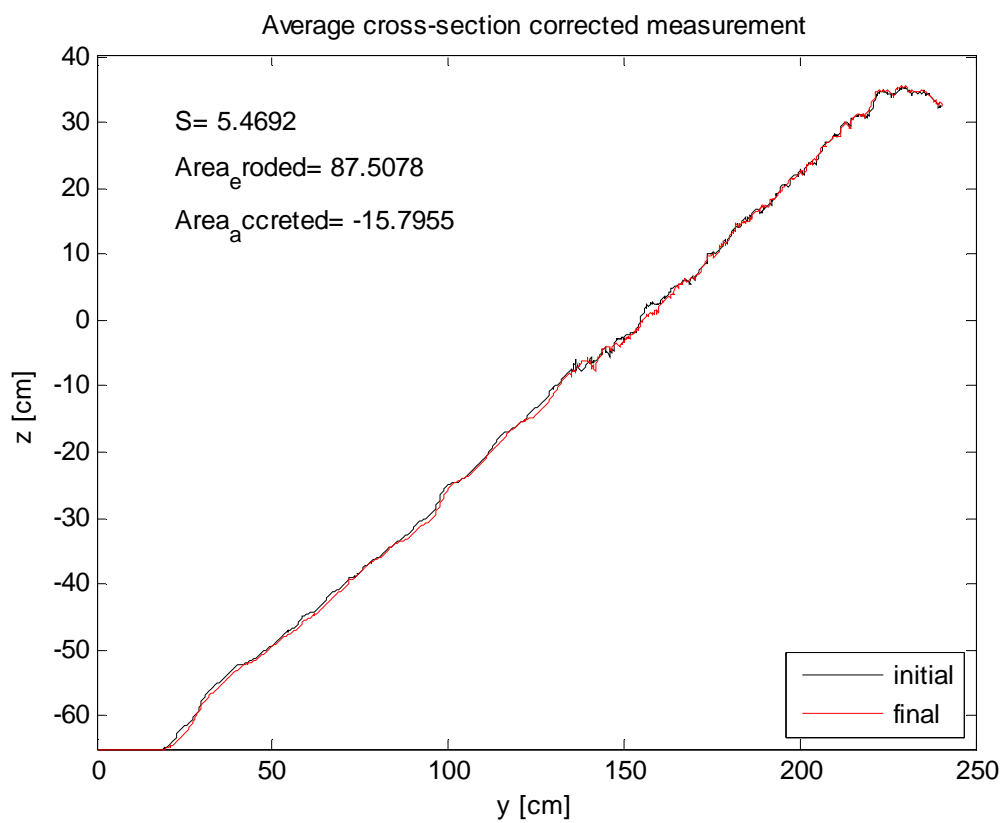
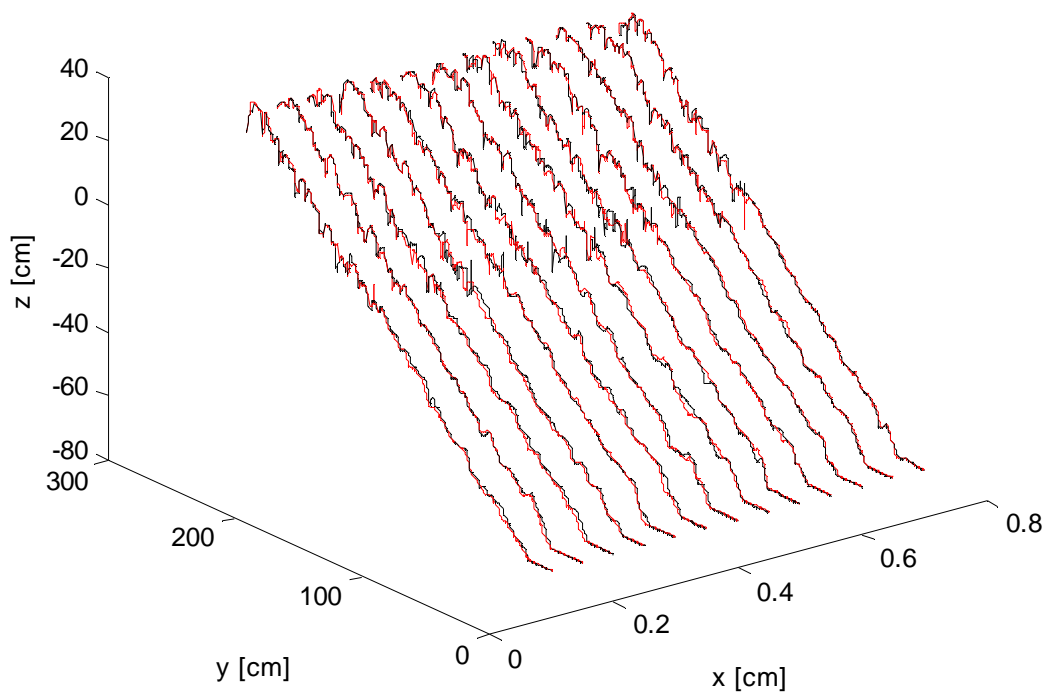


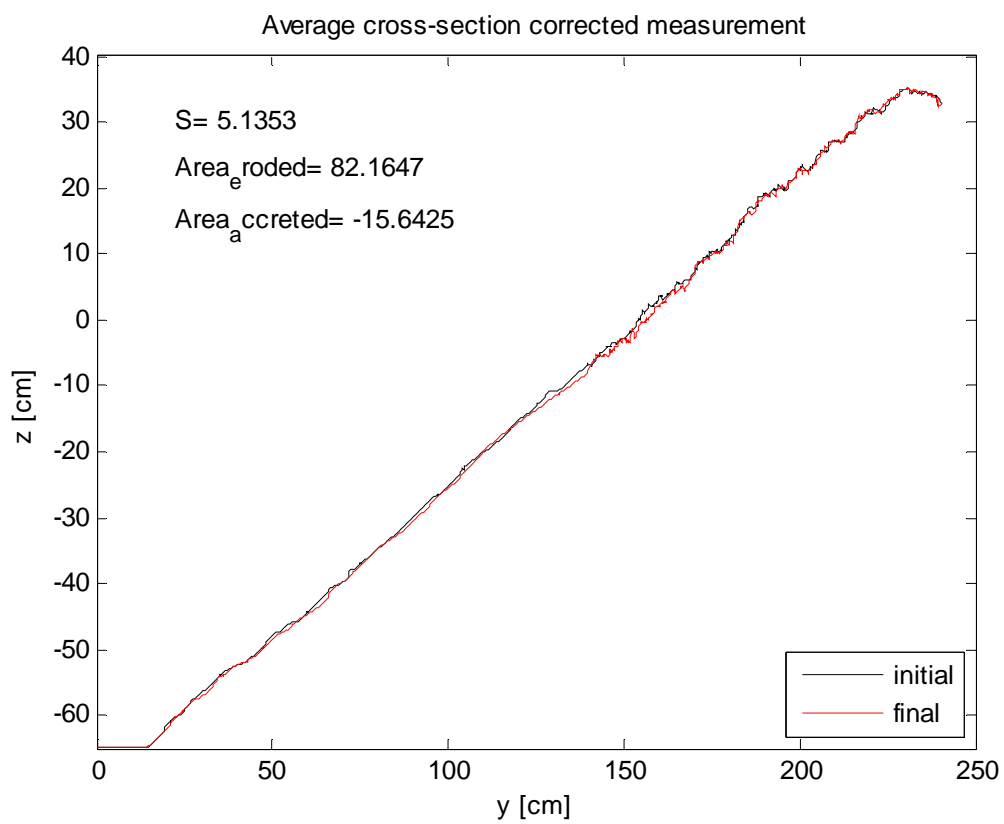
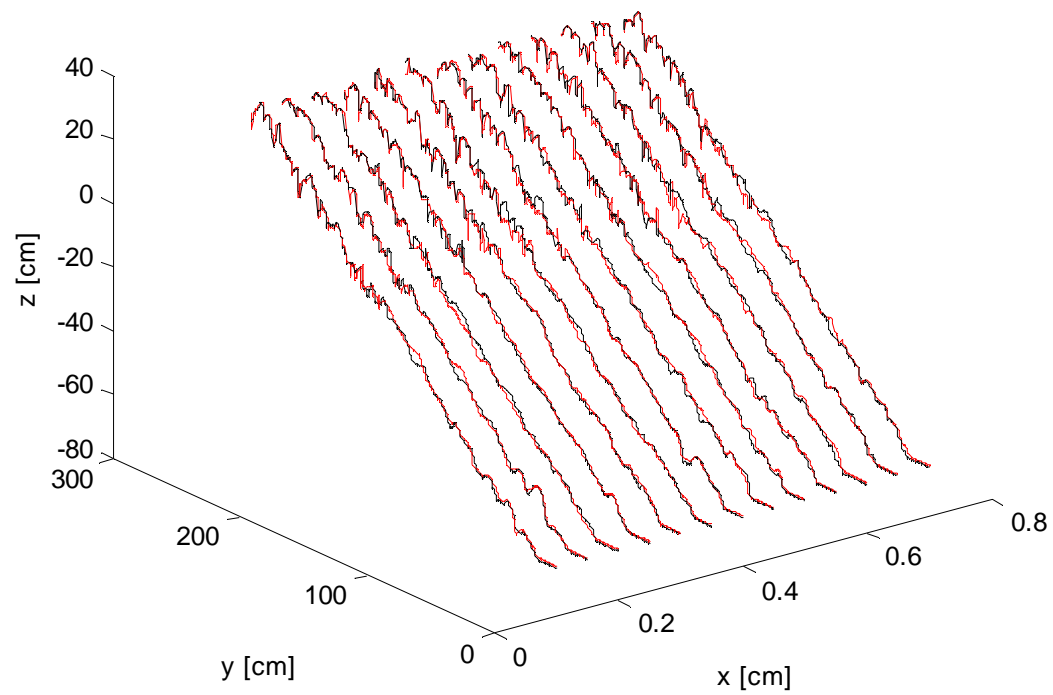


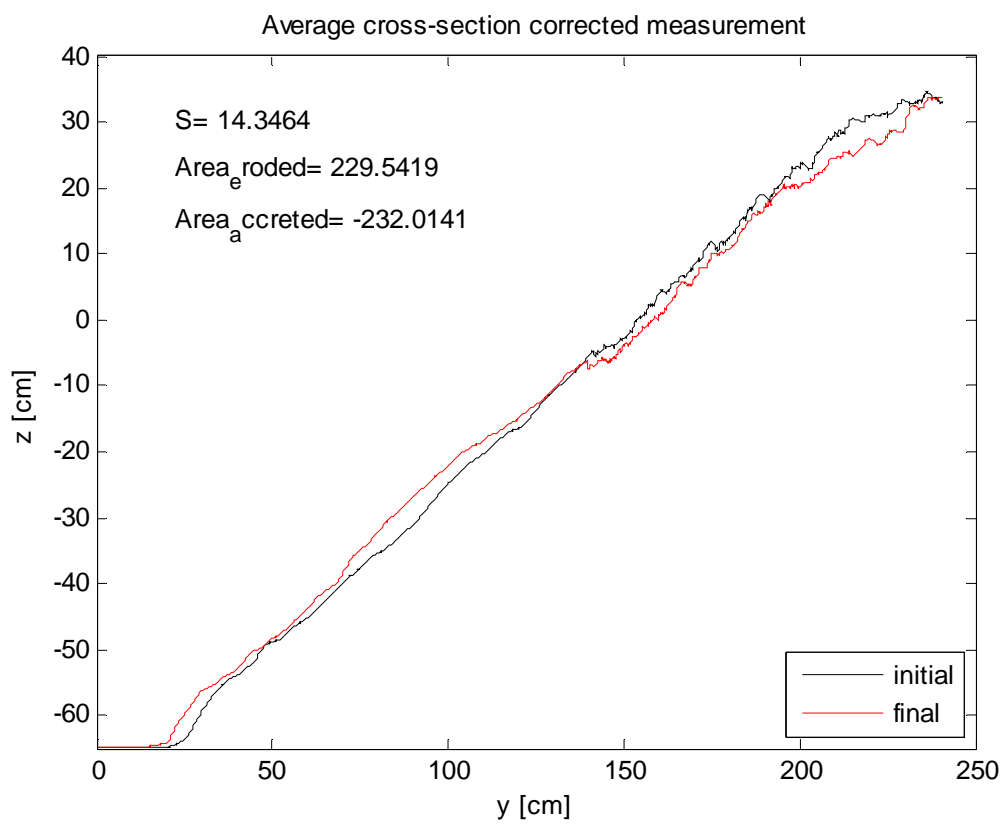
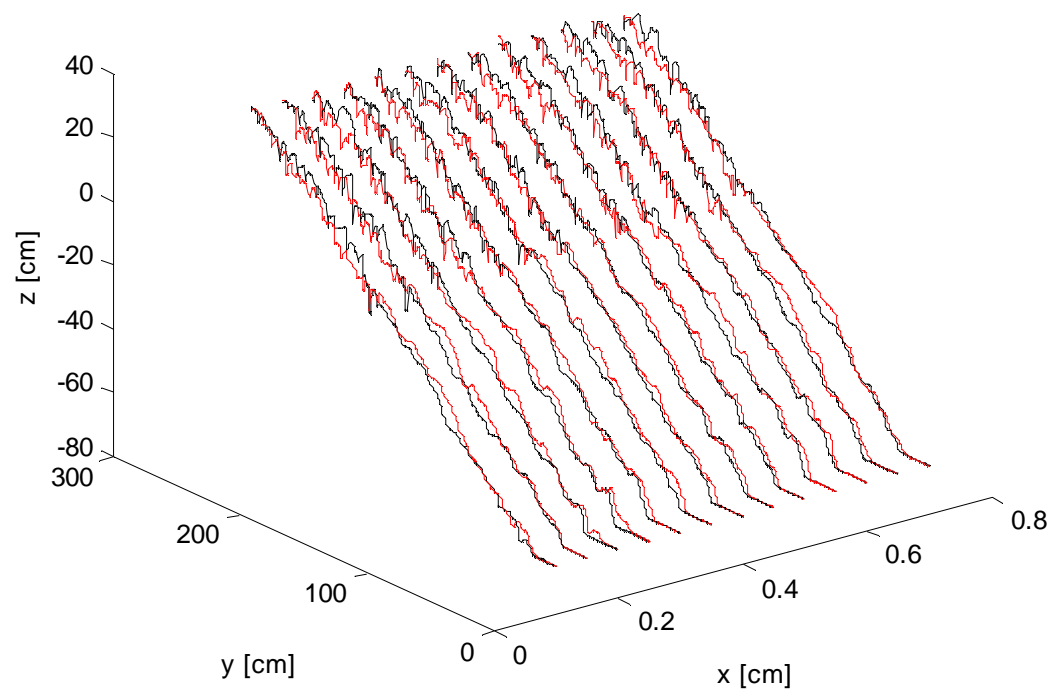


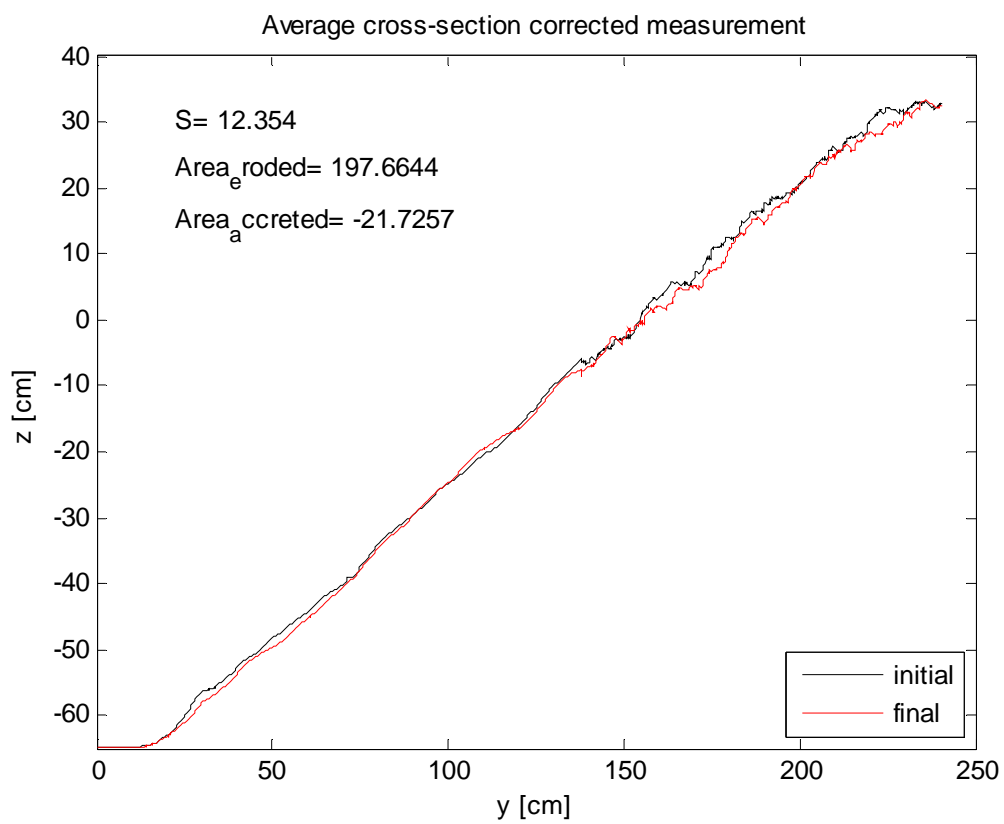
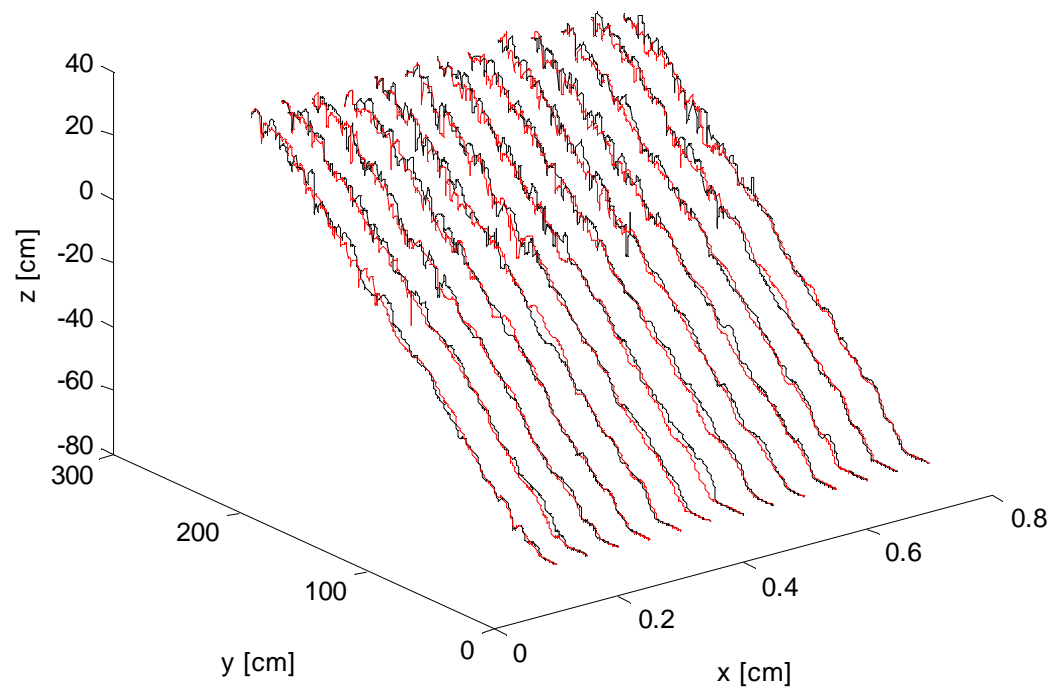
## Structure 2

8

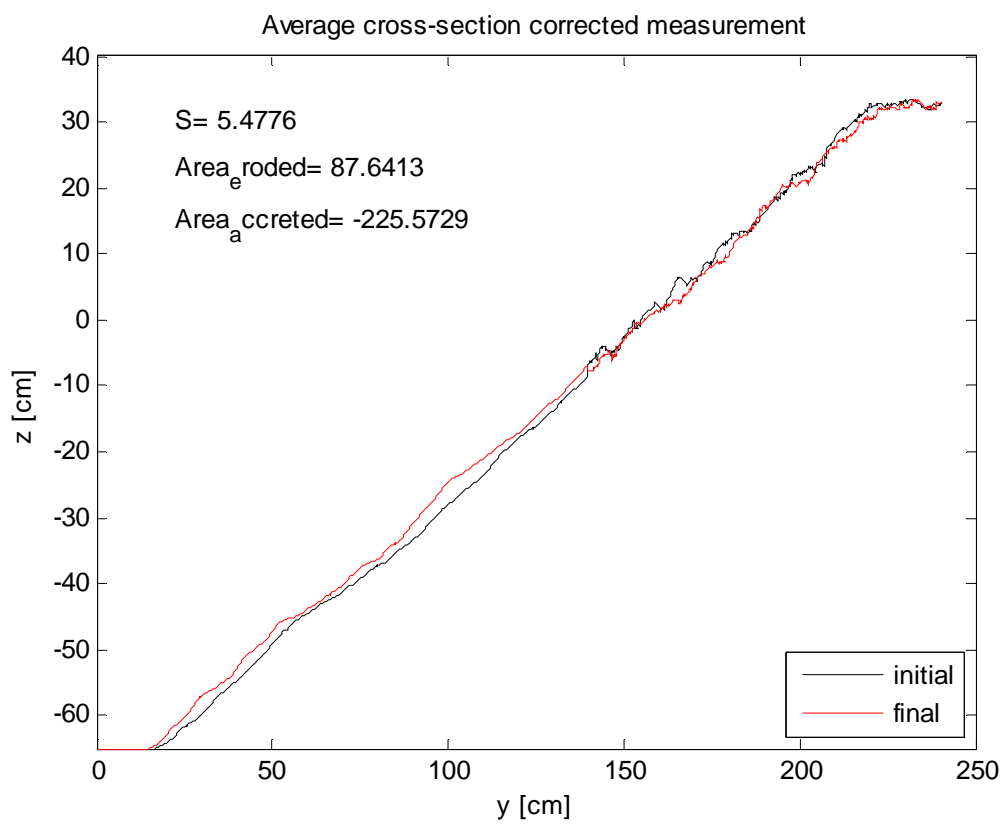
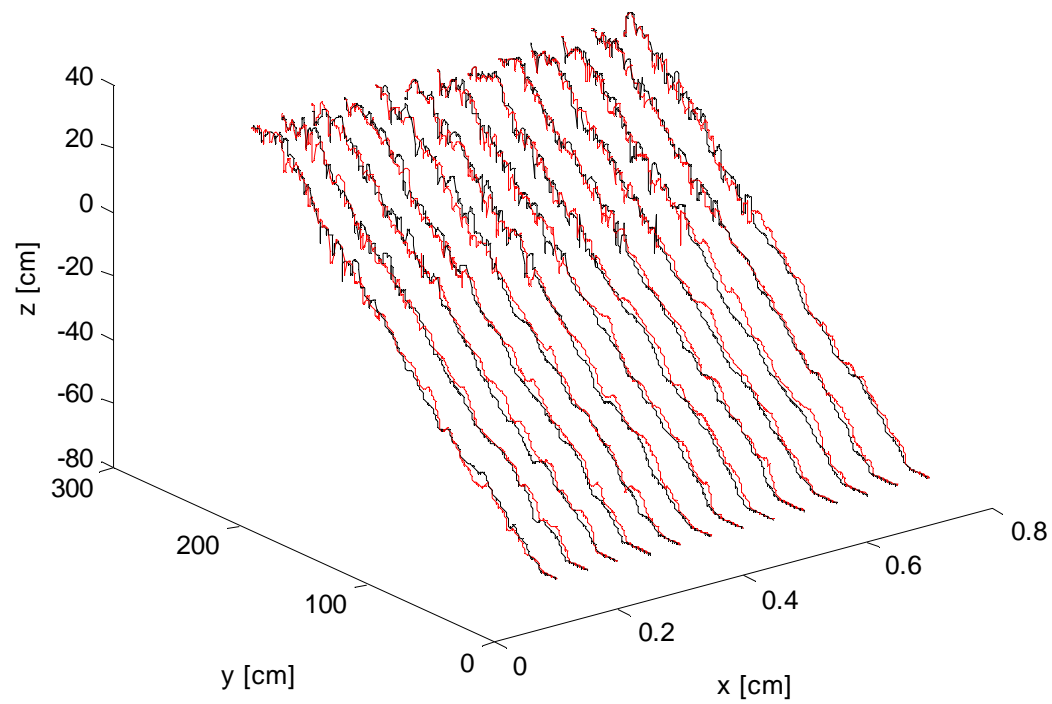


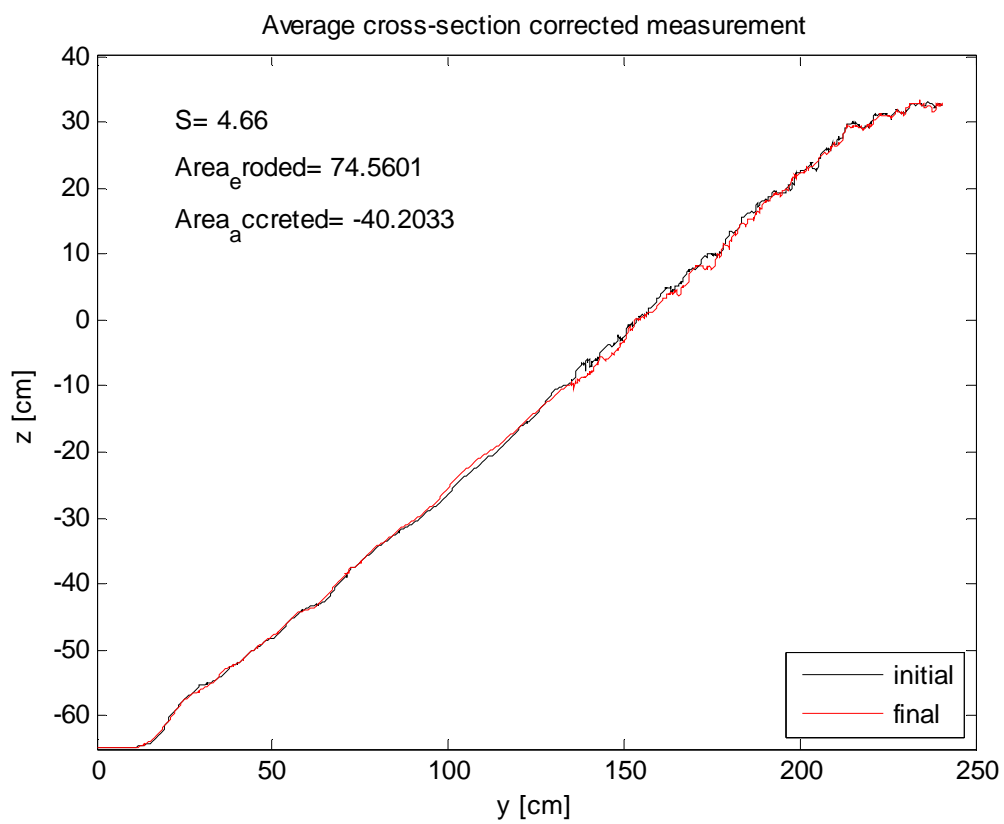
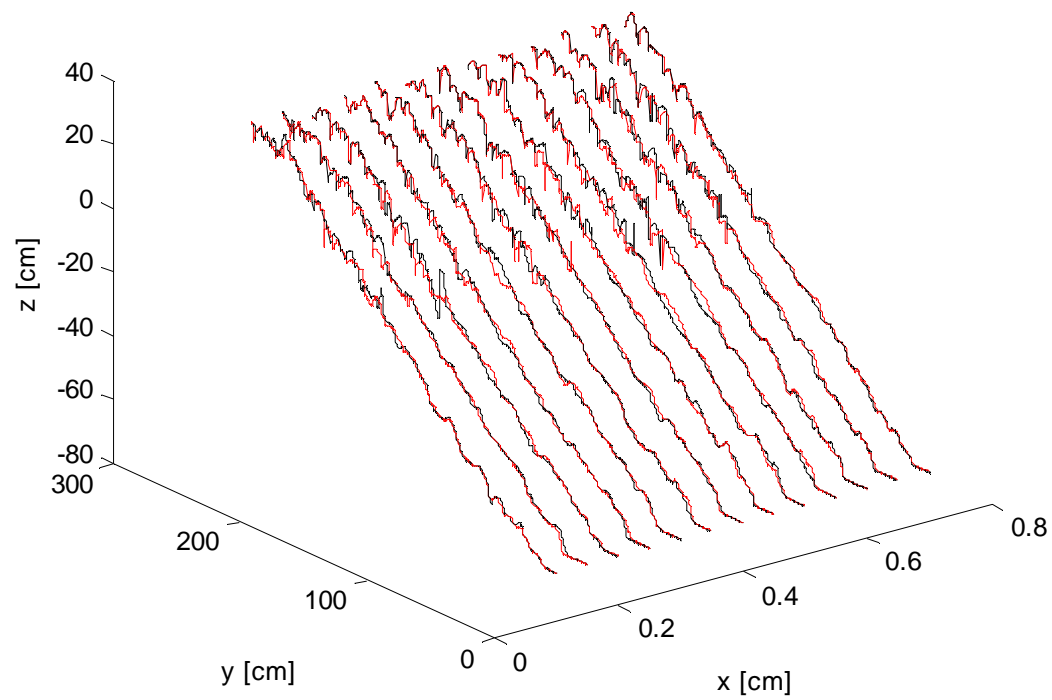


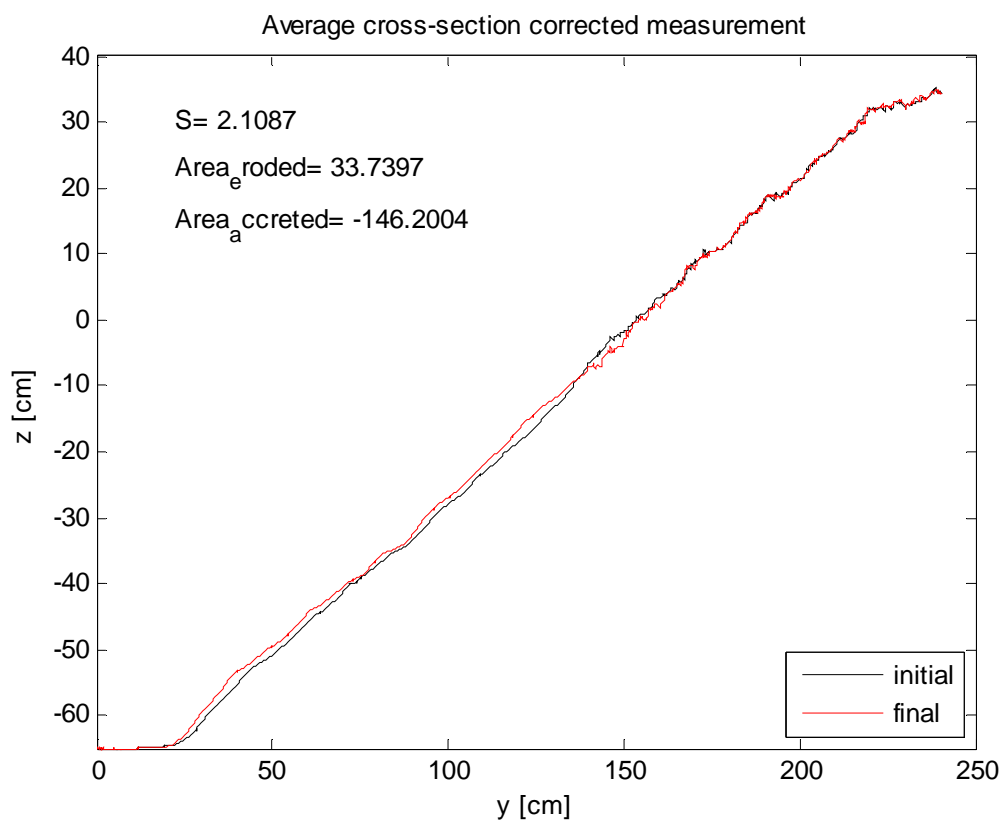
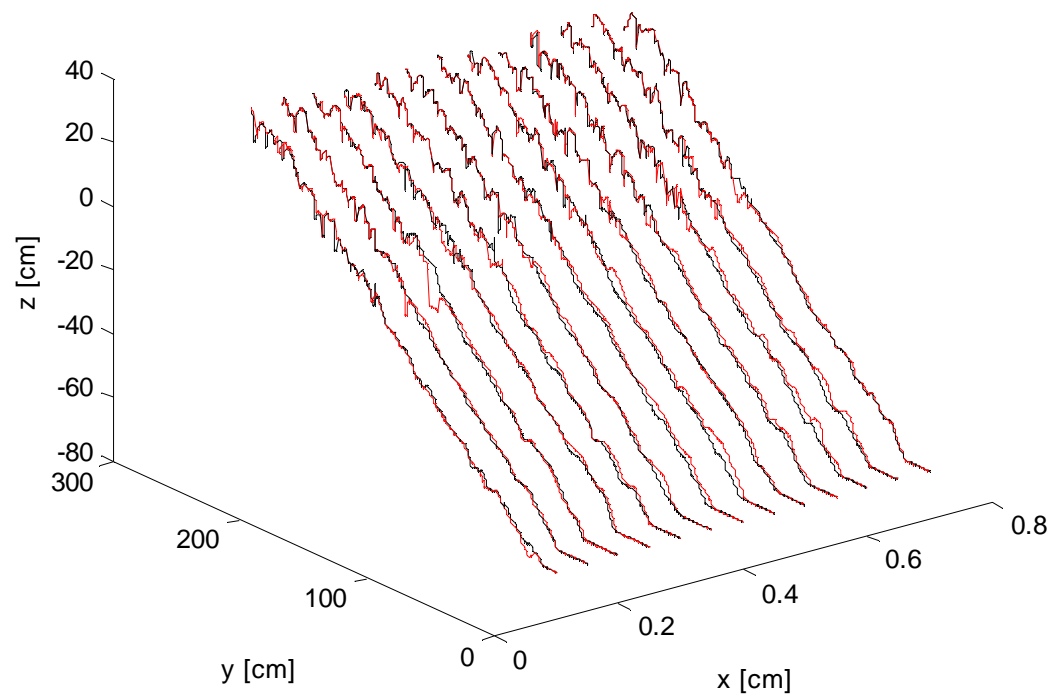




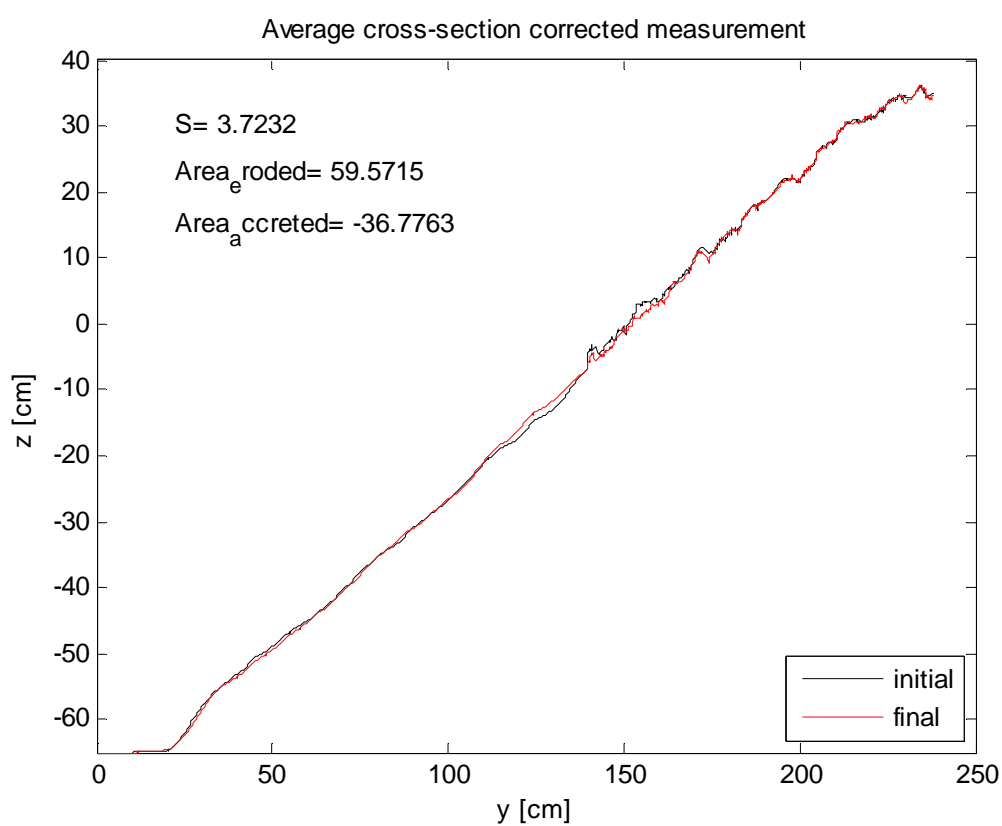
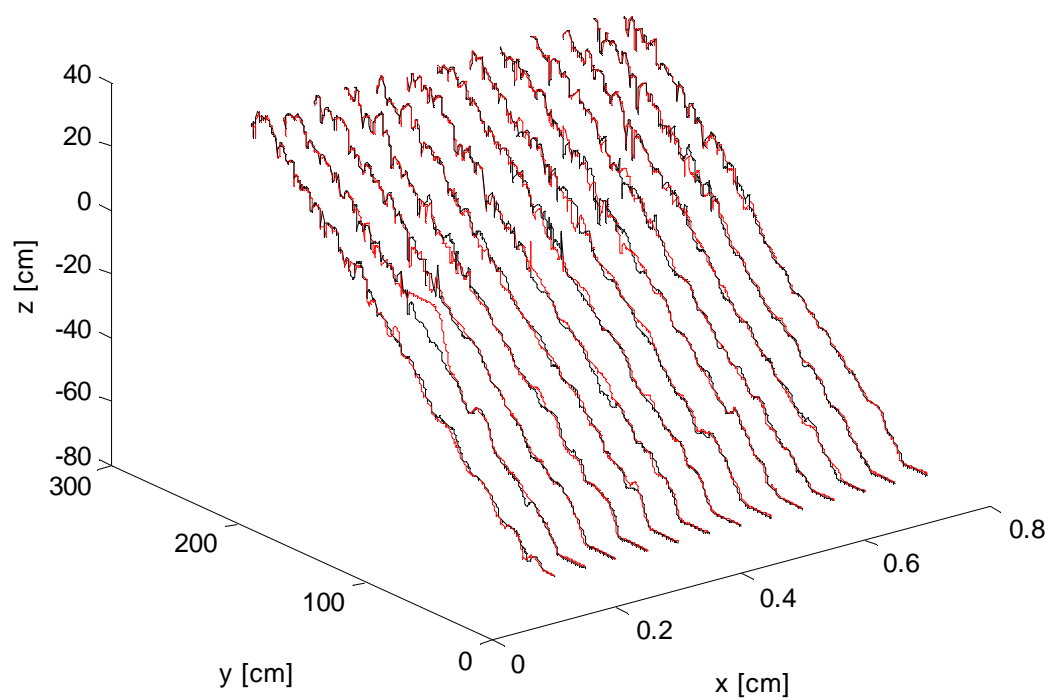




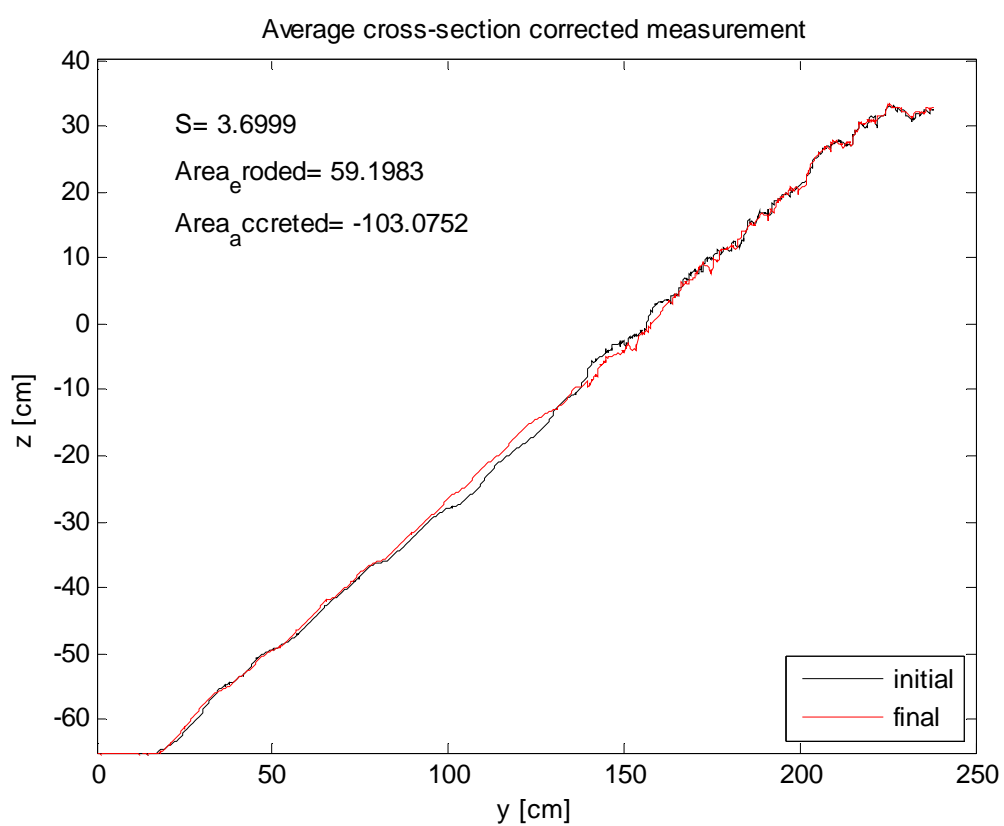
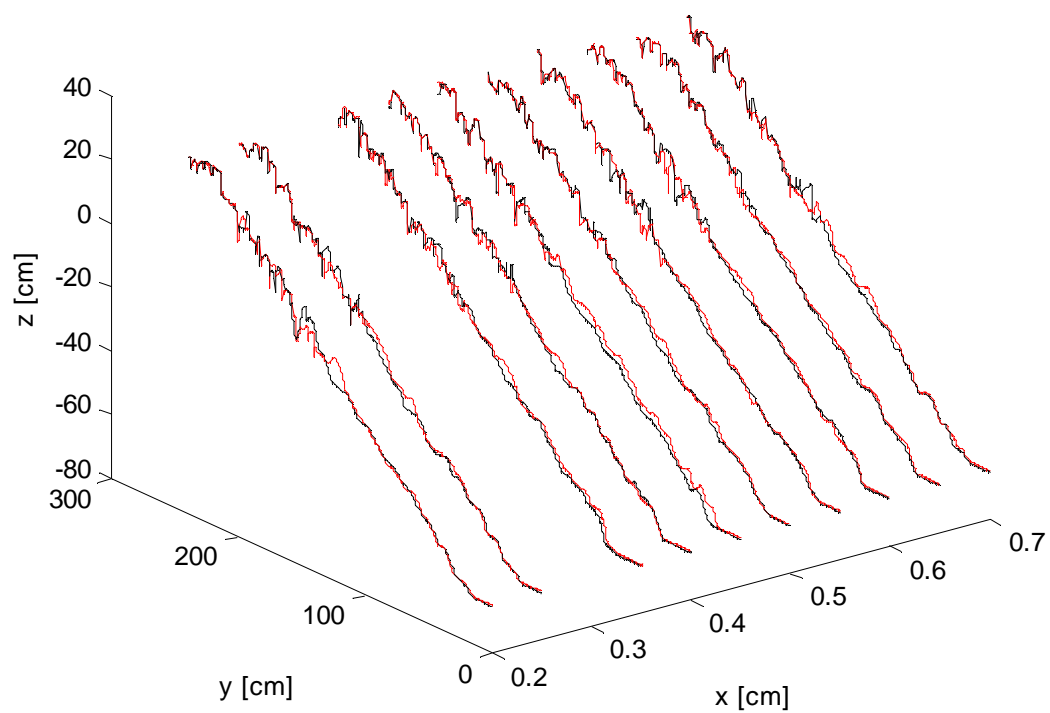




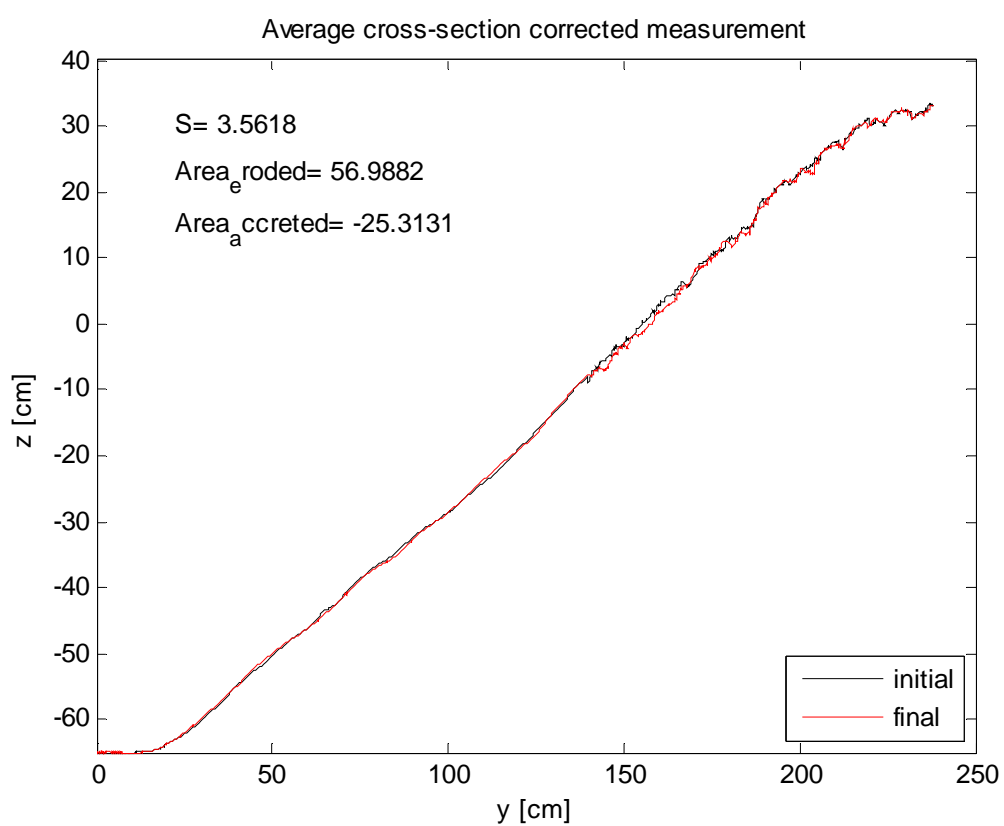
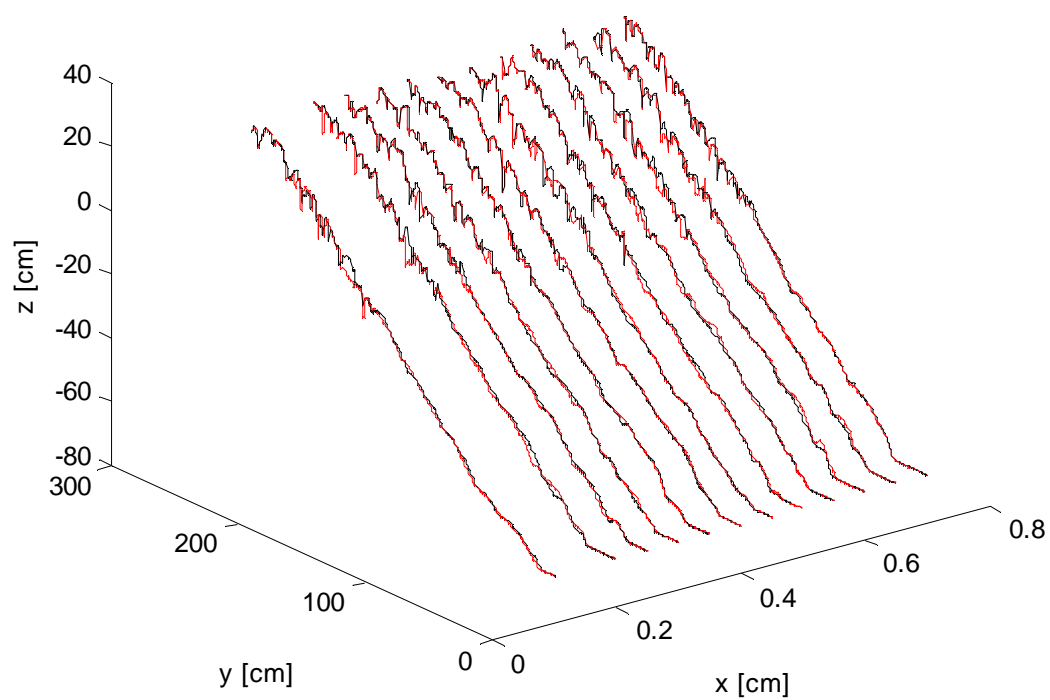
15a



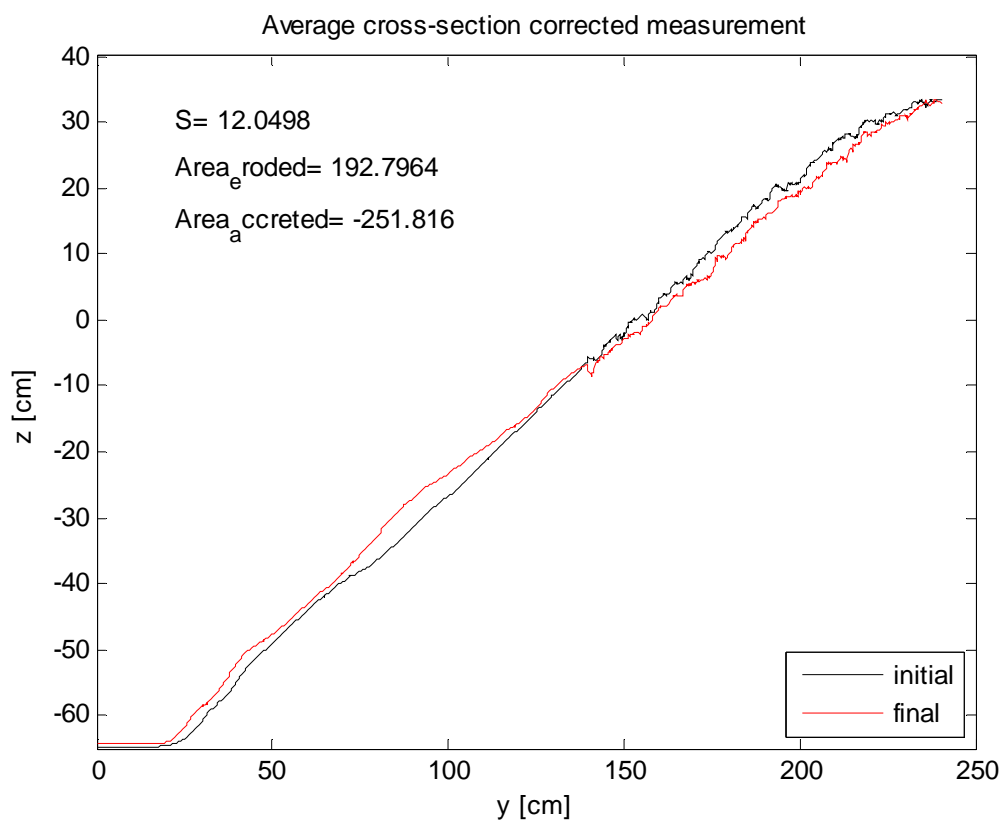
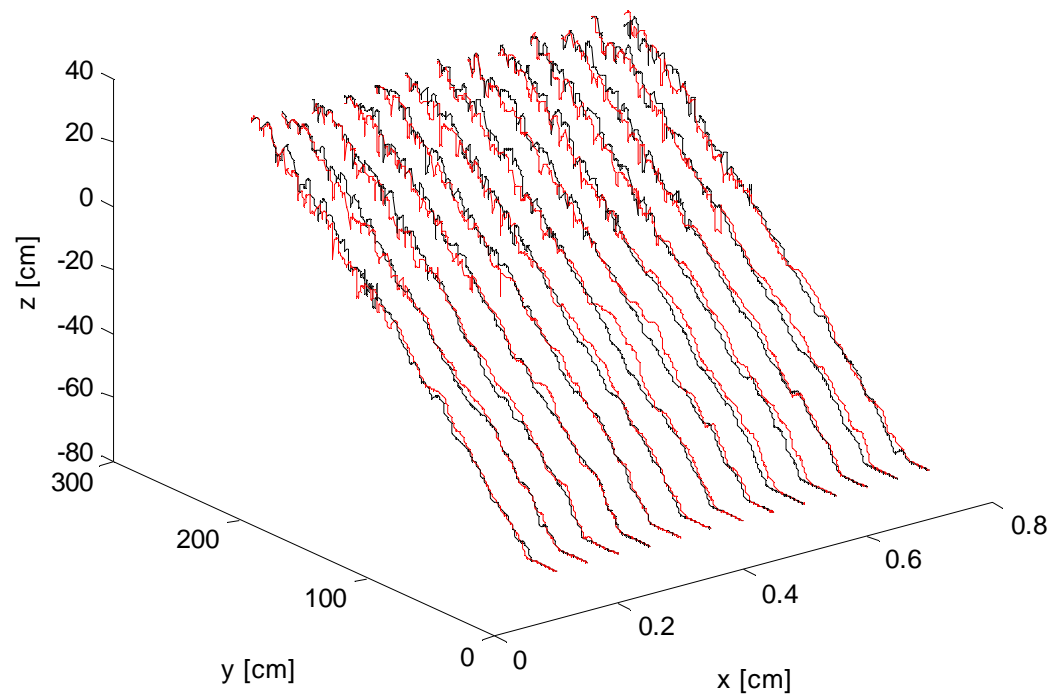
15b



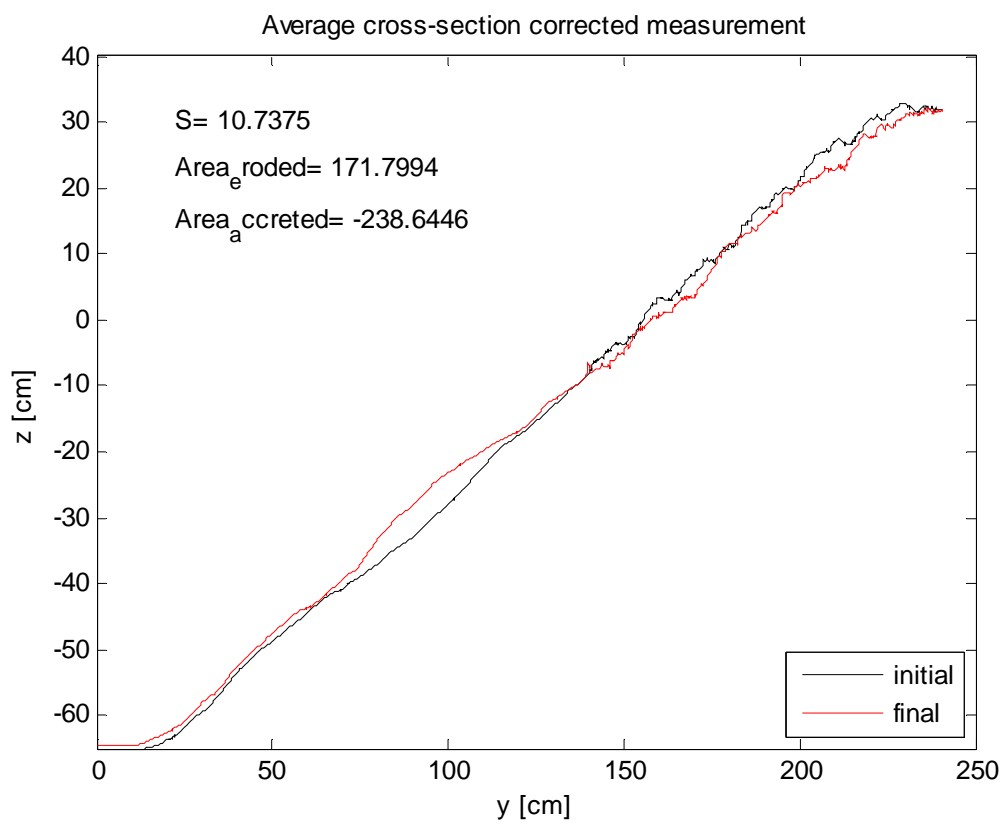
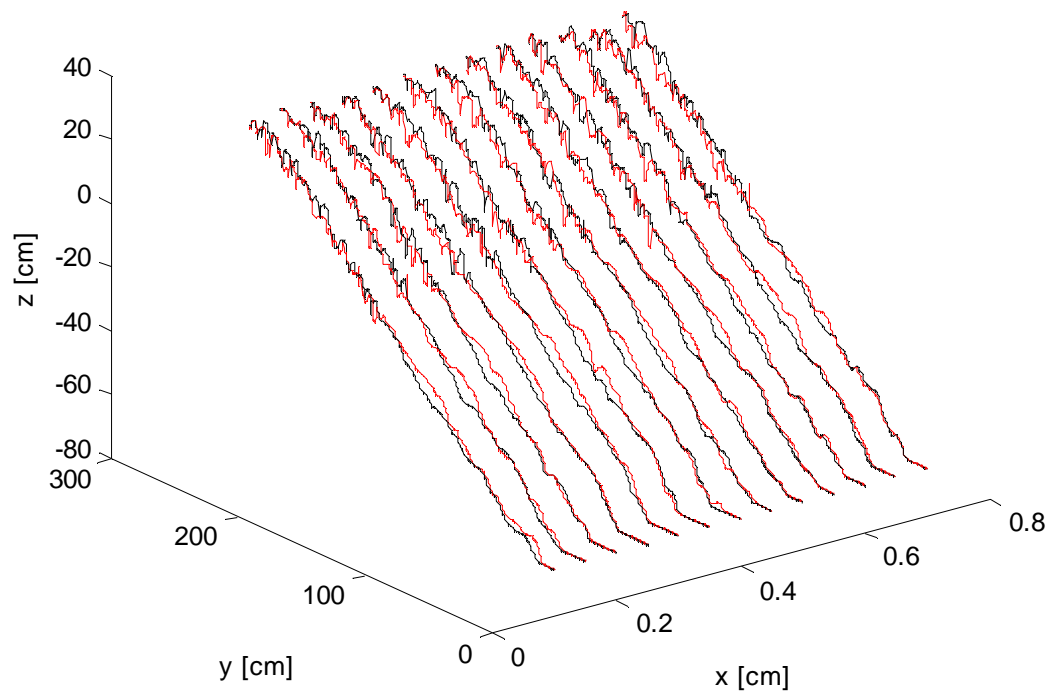
15c



16a

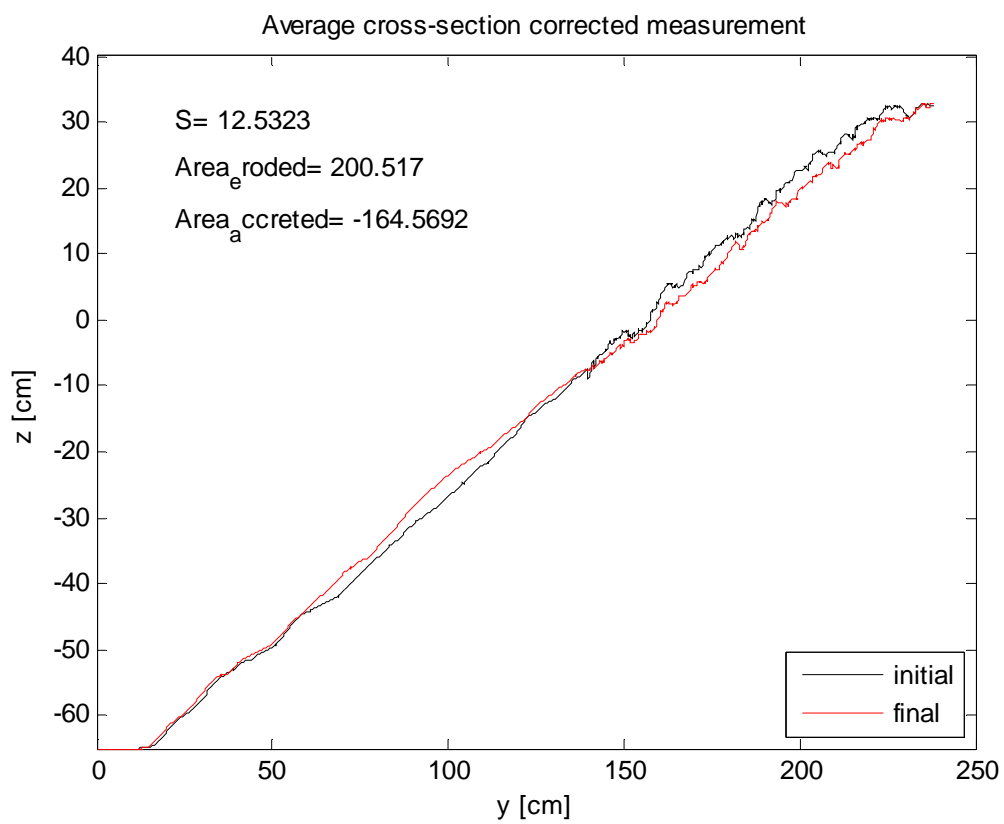
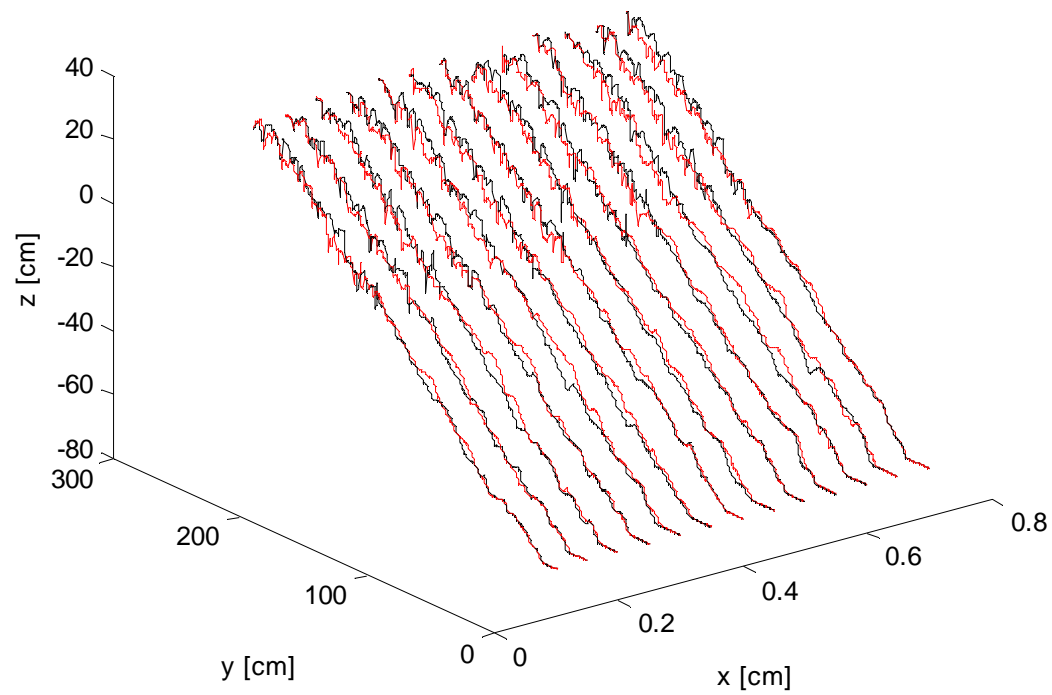


16b



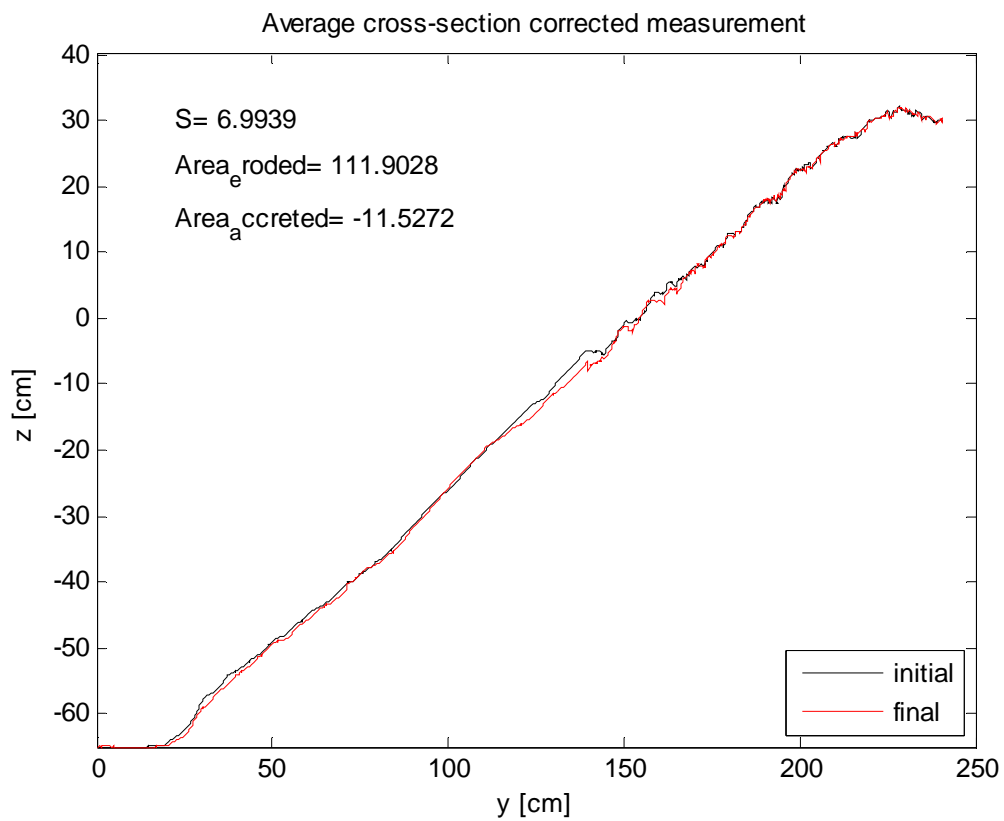
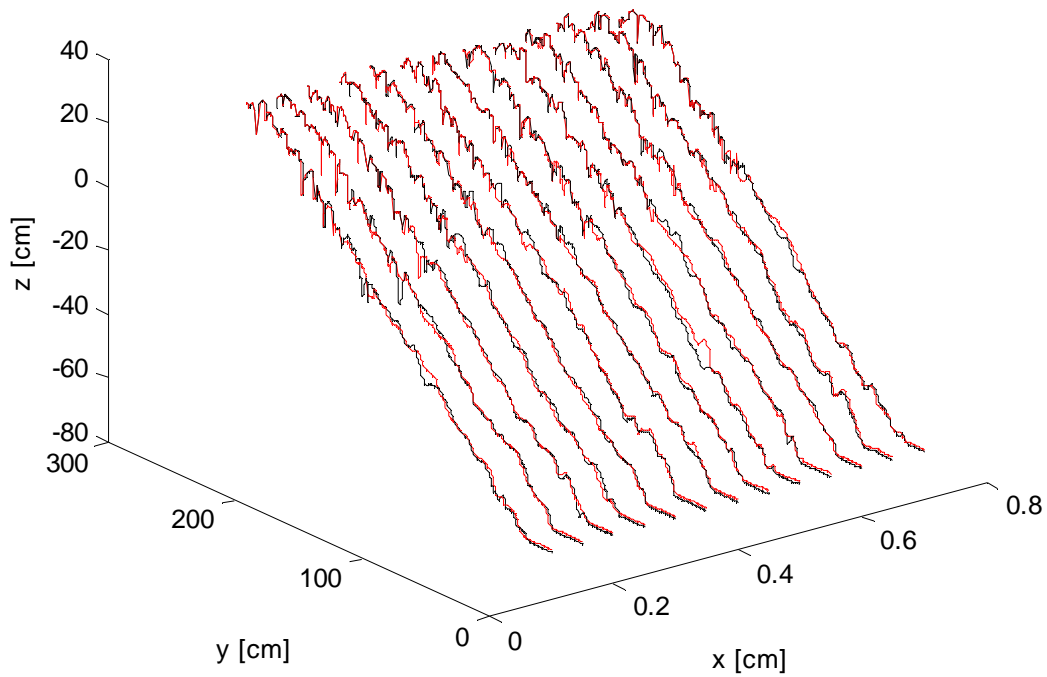


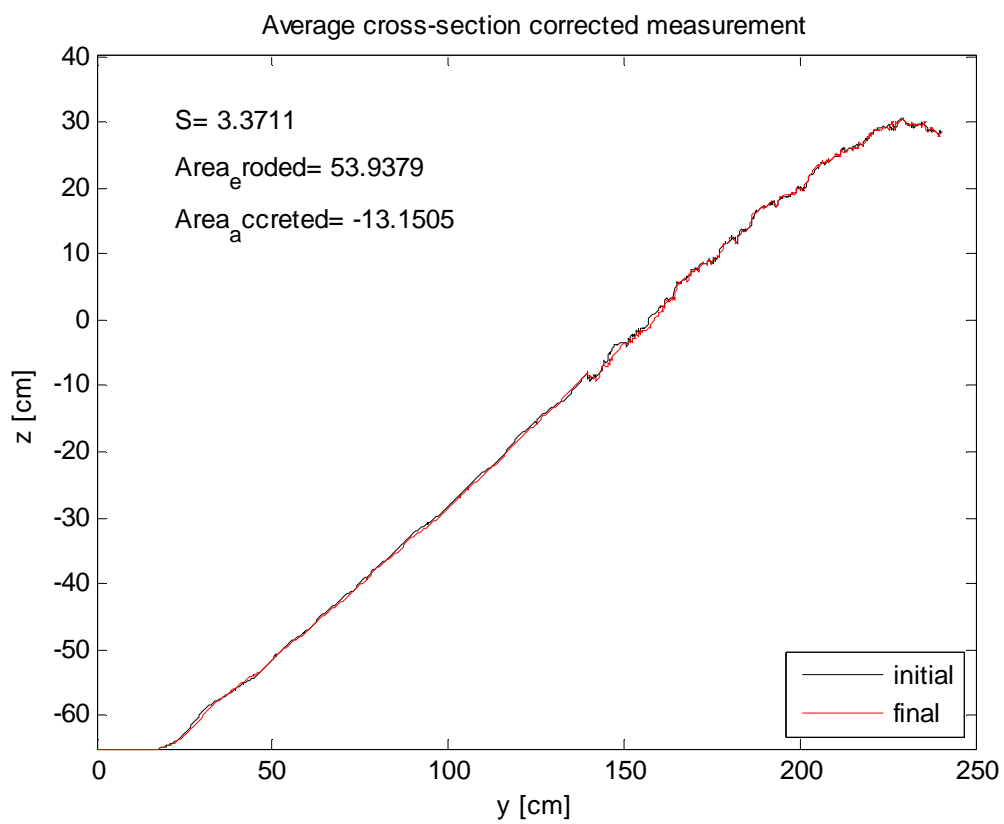
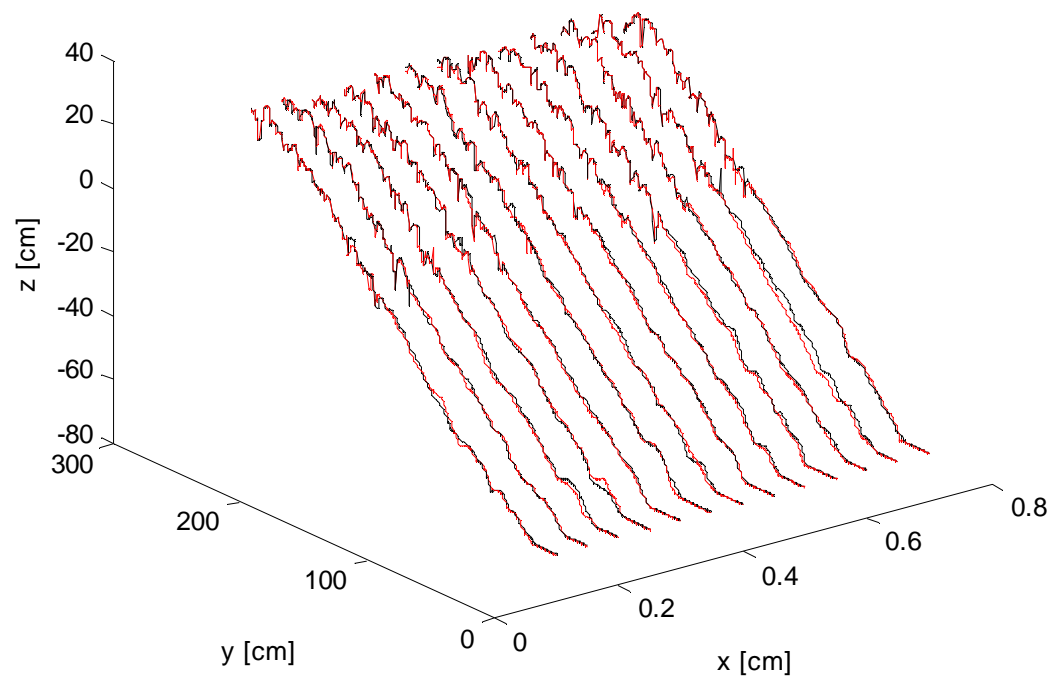
16c

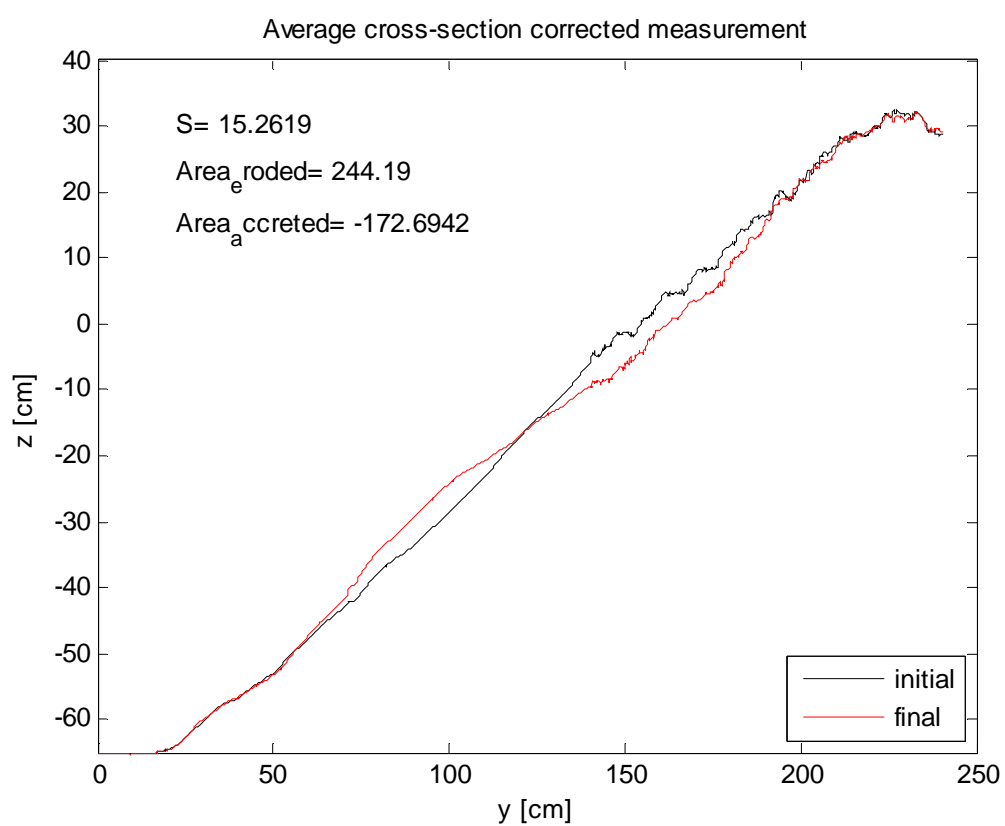
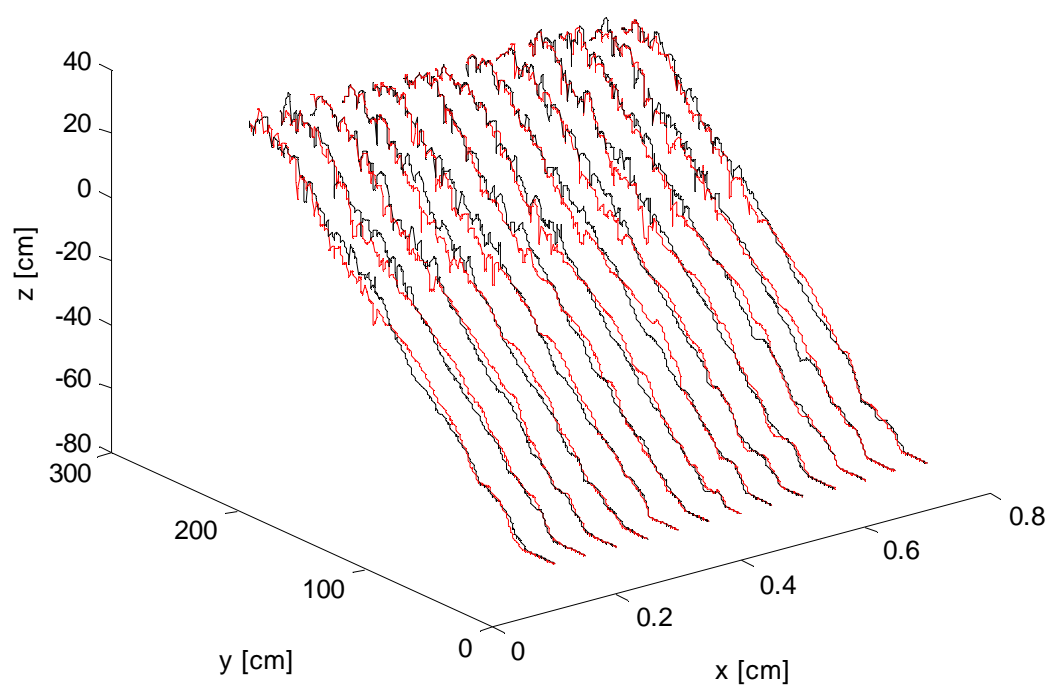


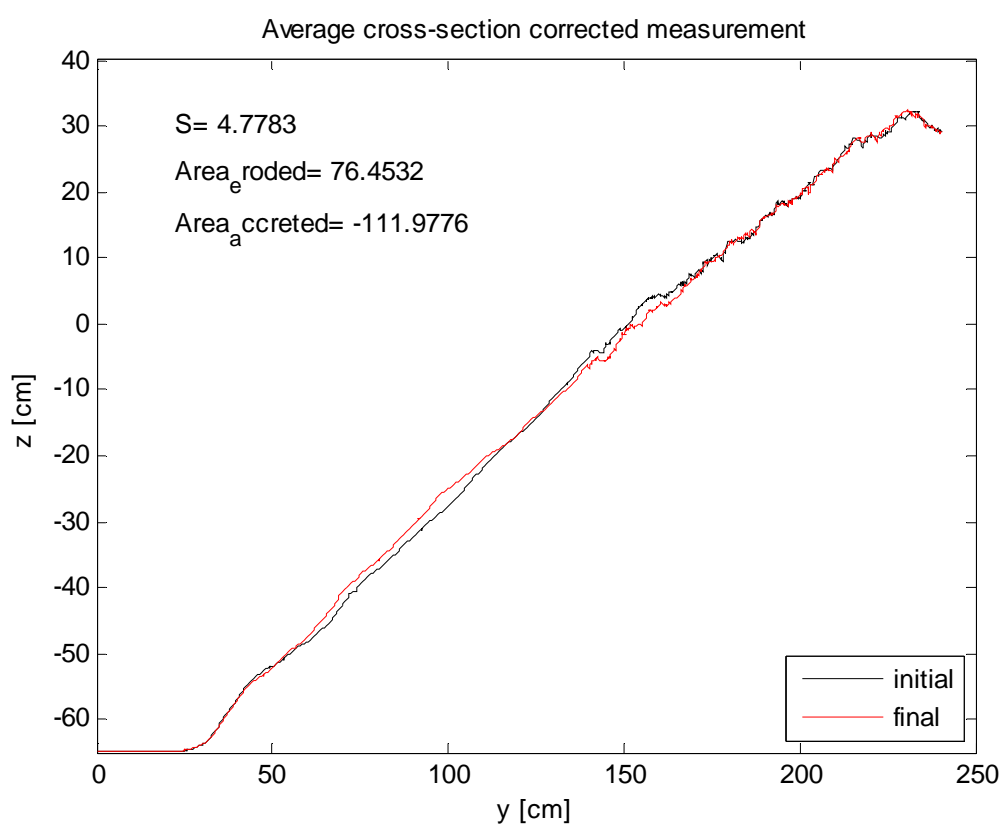
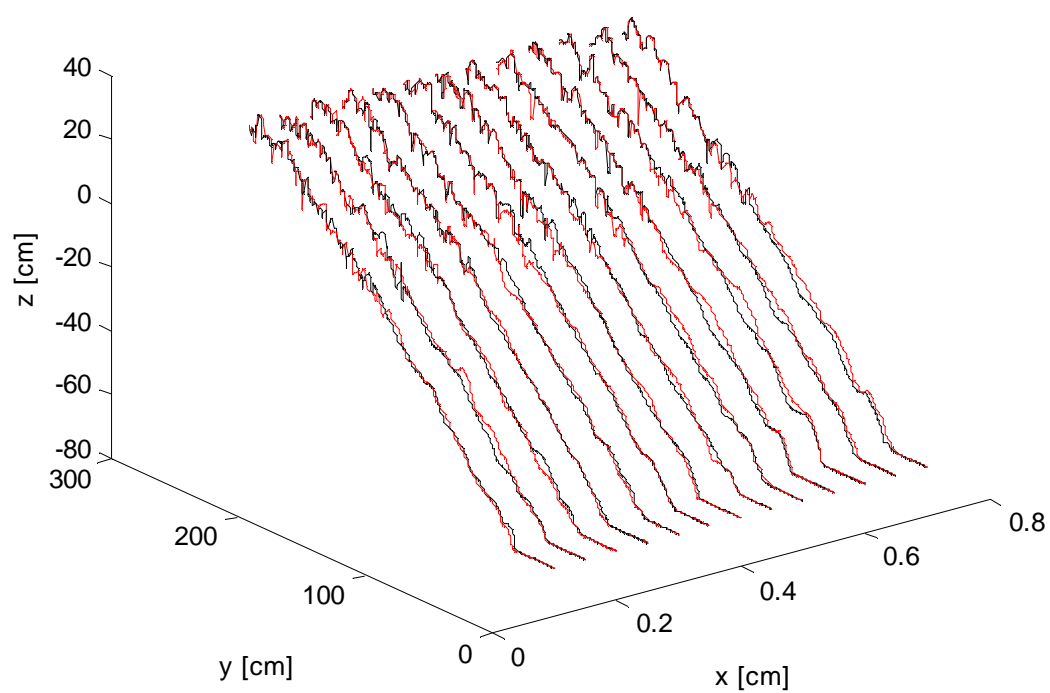
### Structure 3

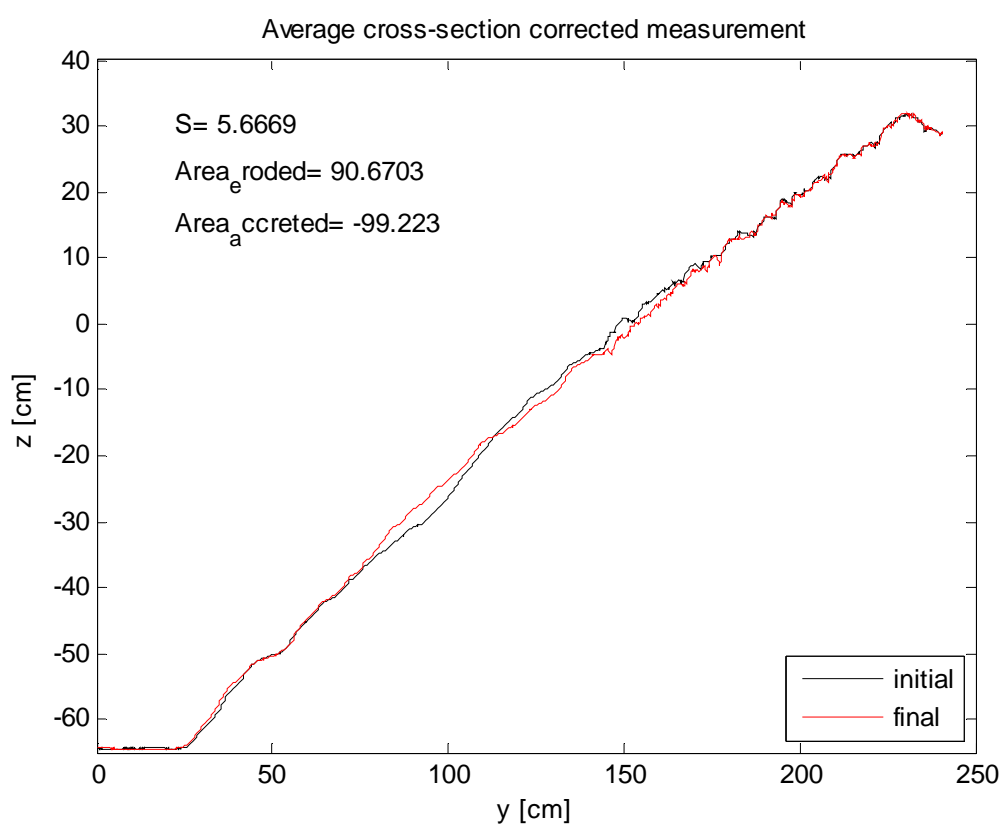
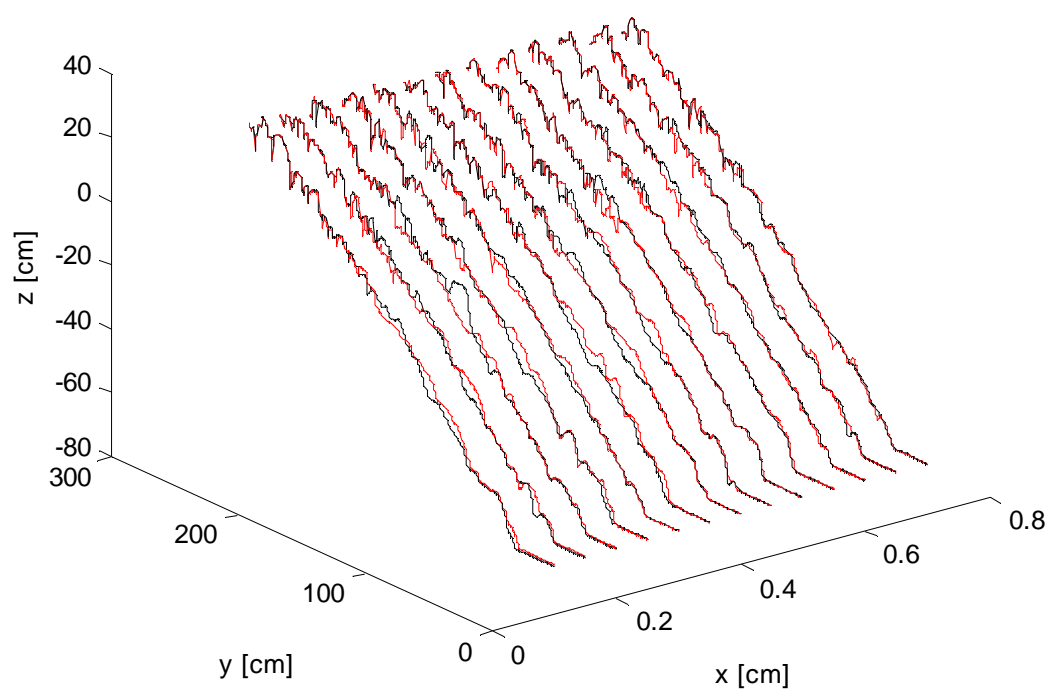
17

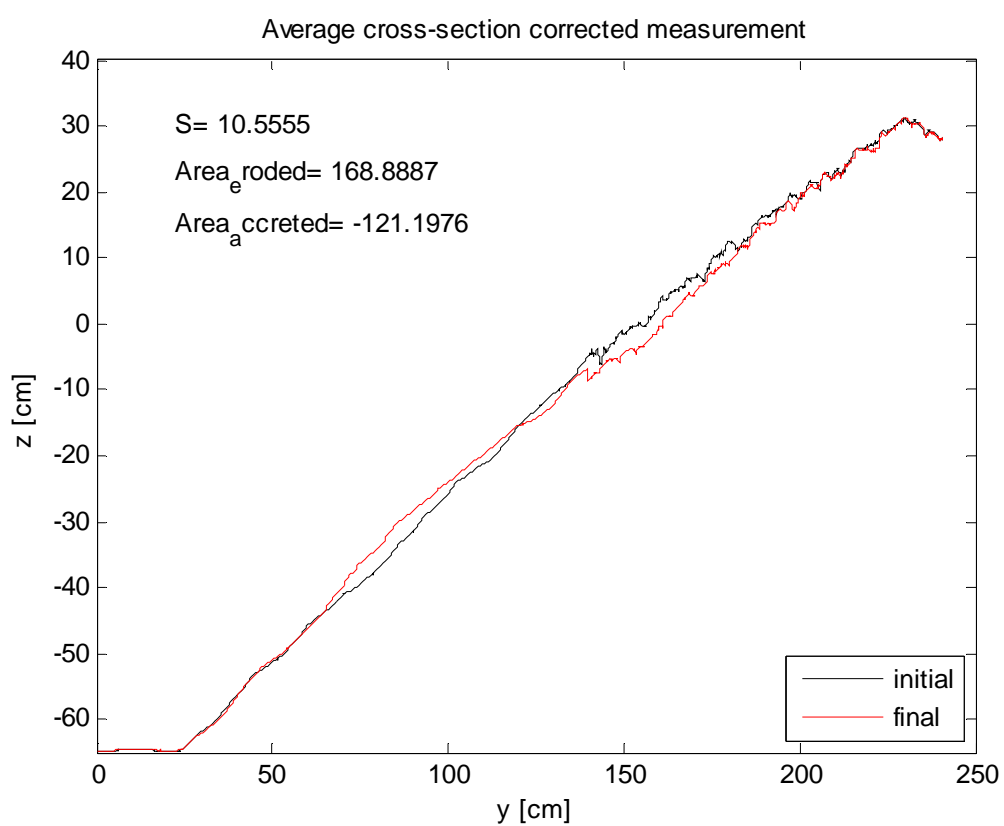
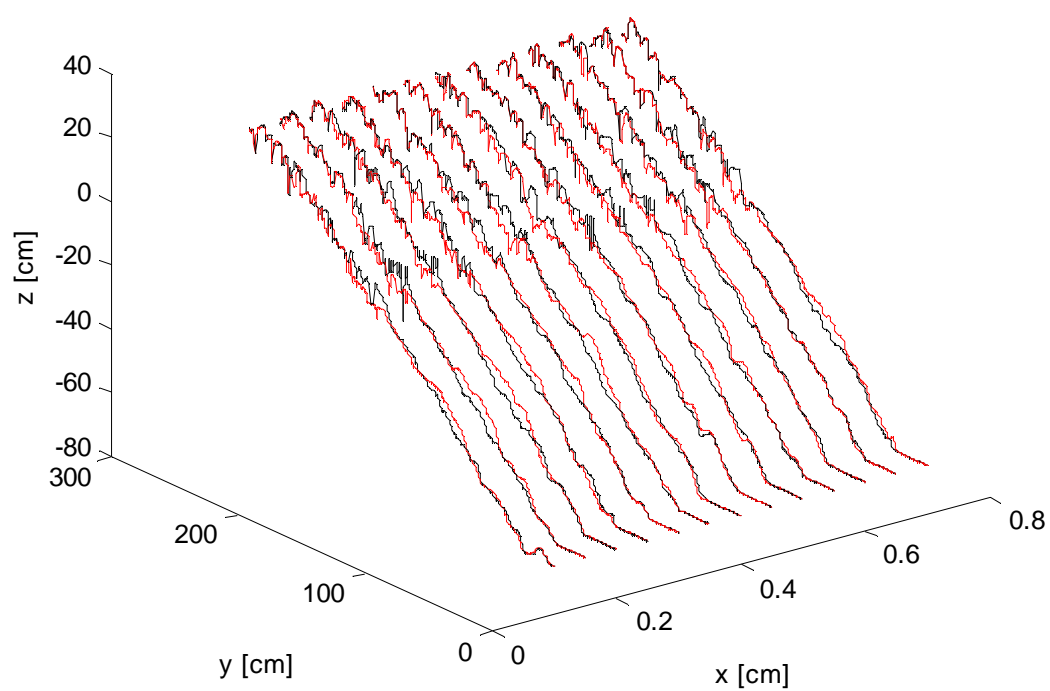


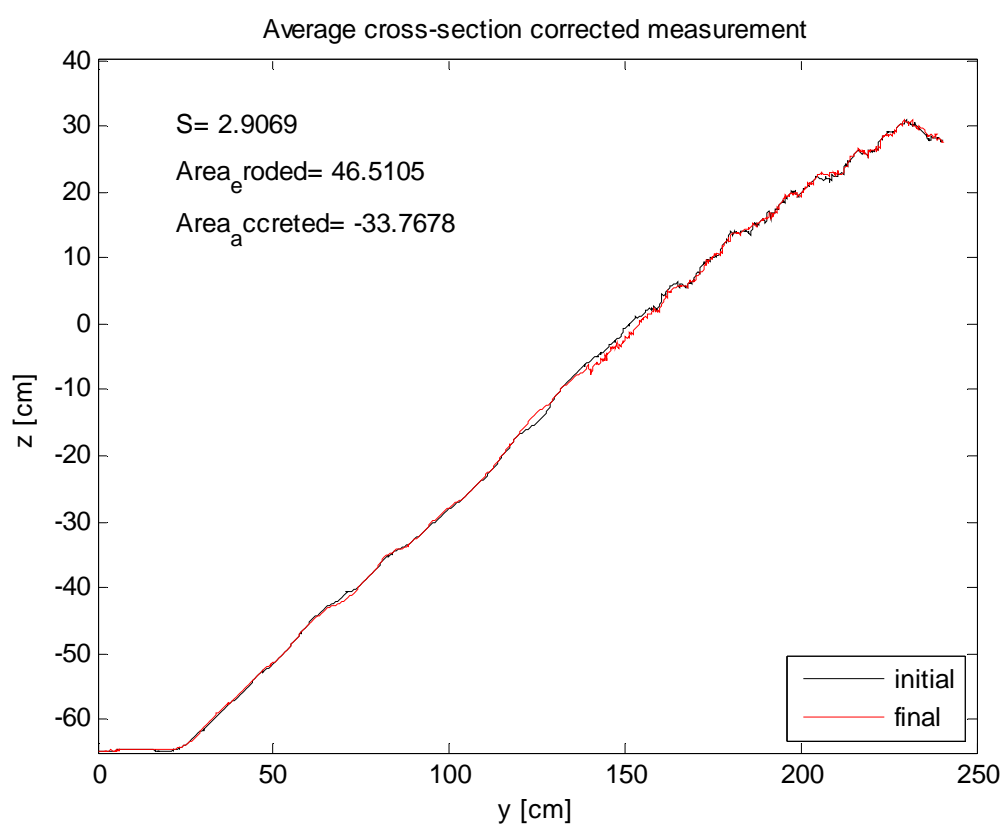
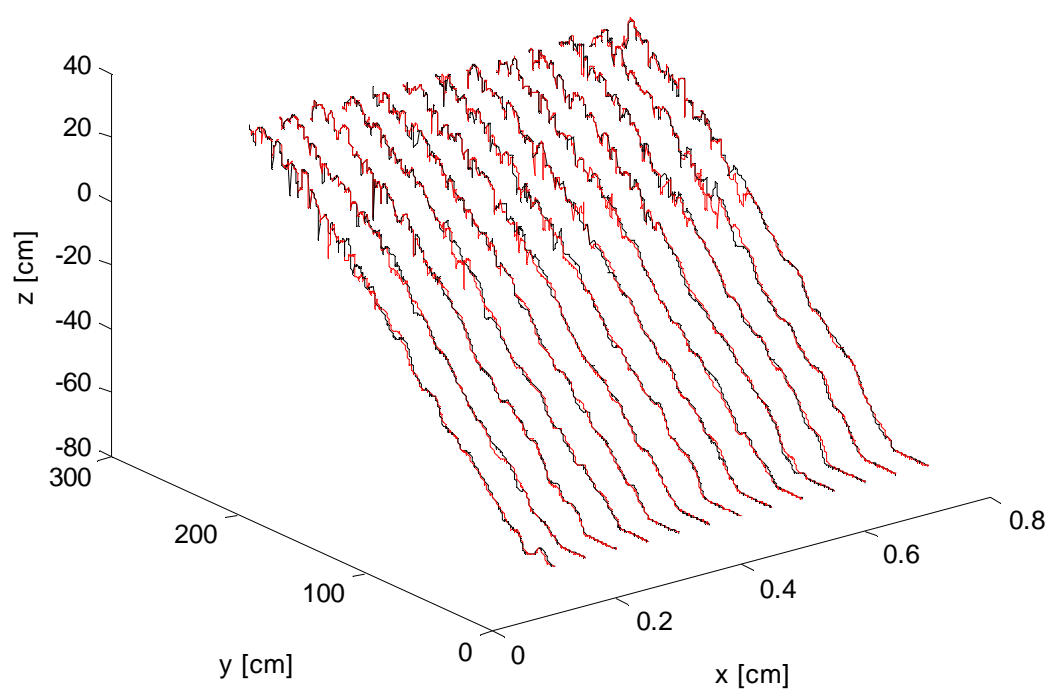




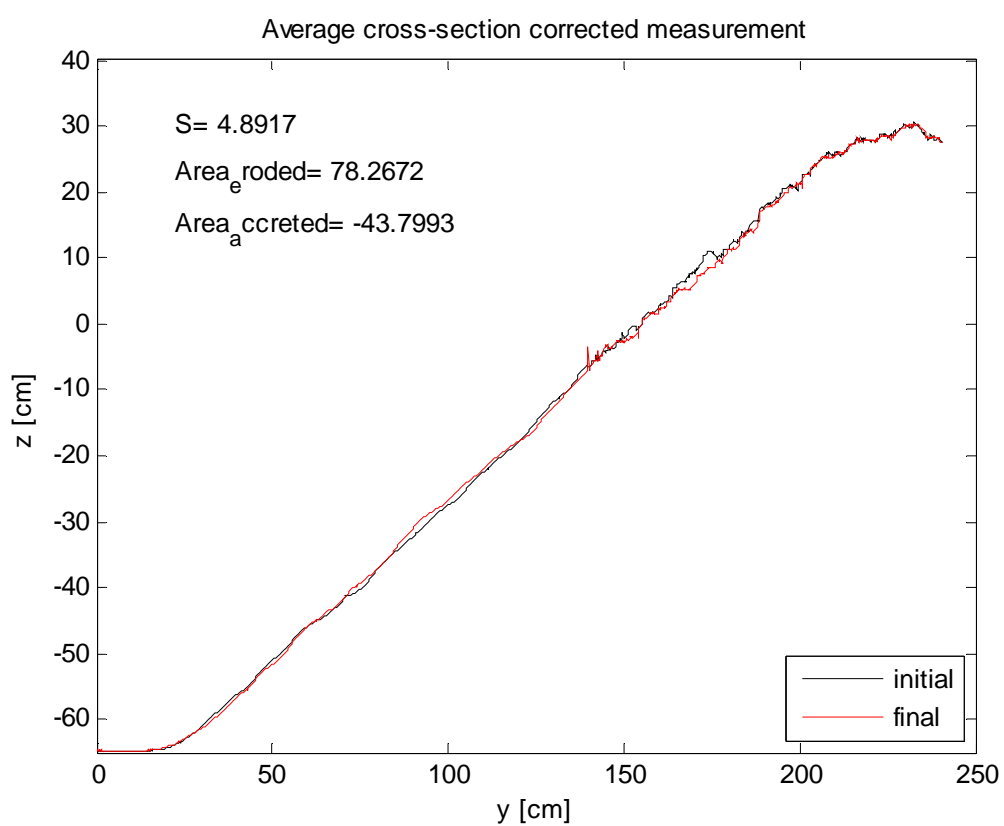
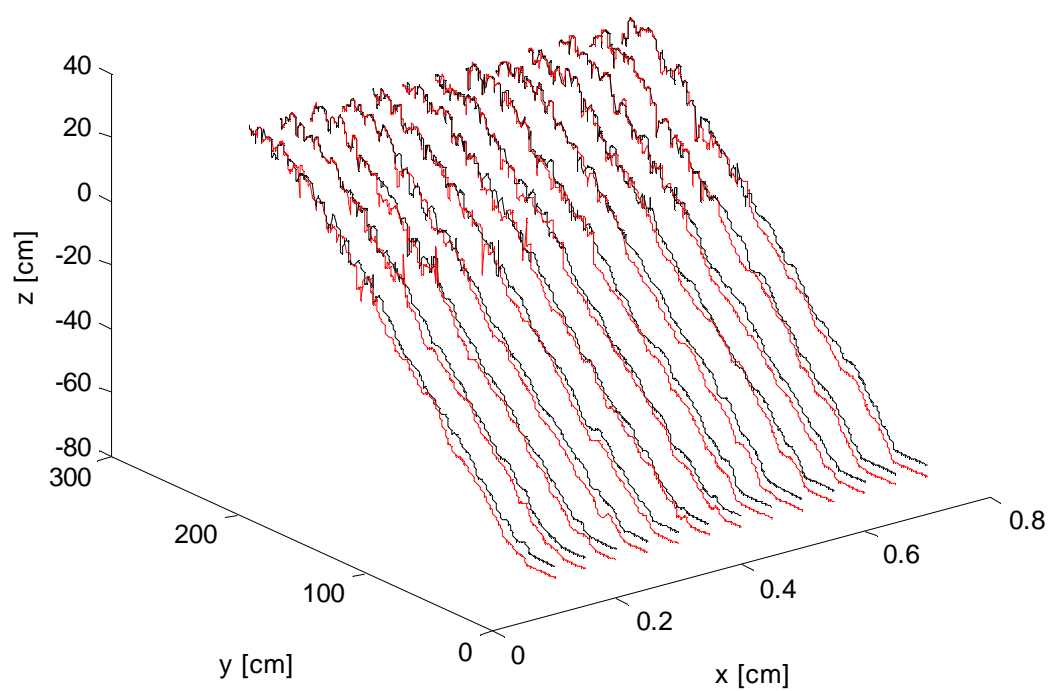


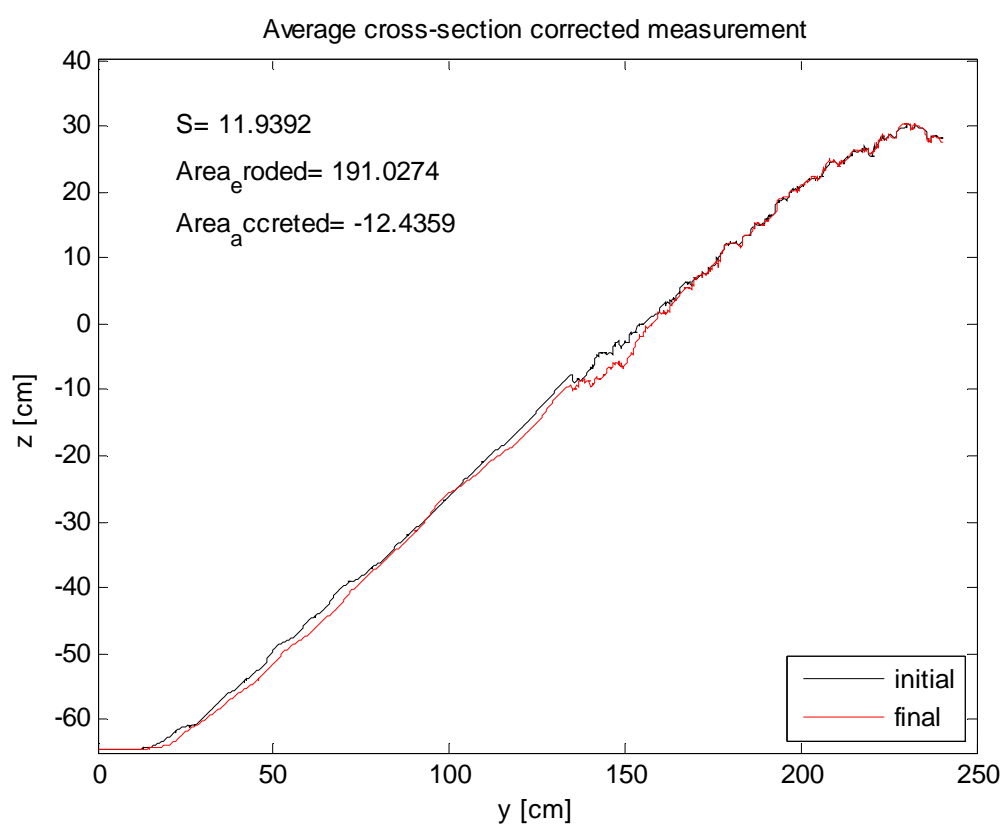
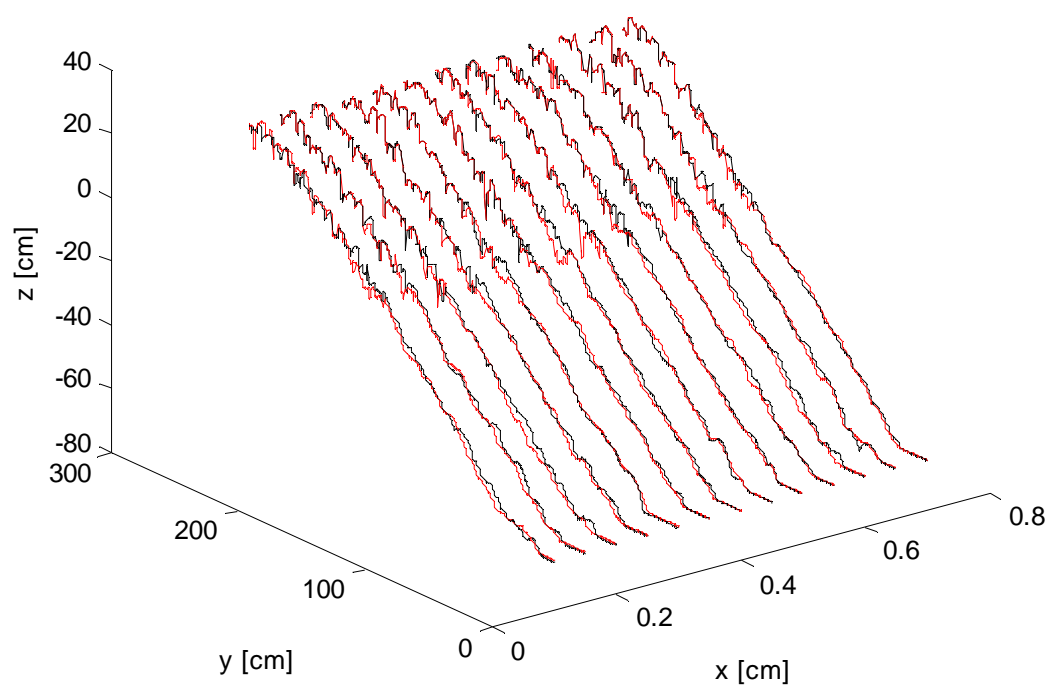


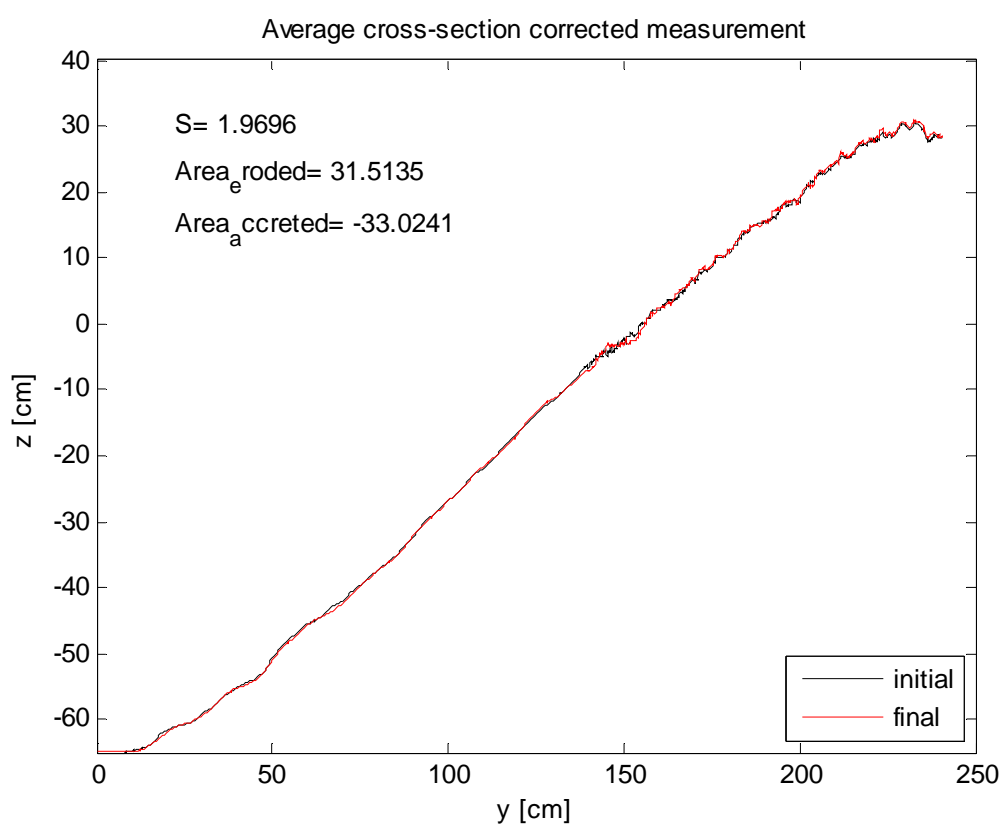
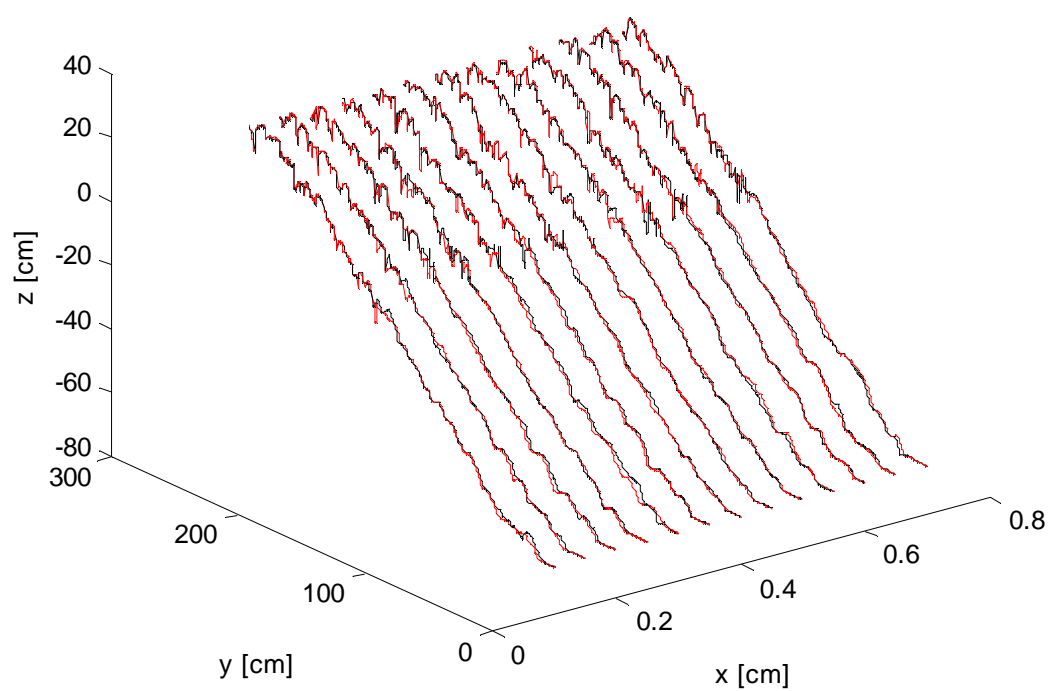


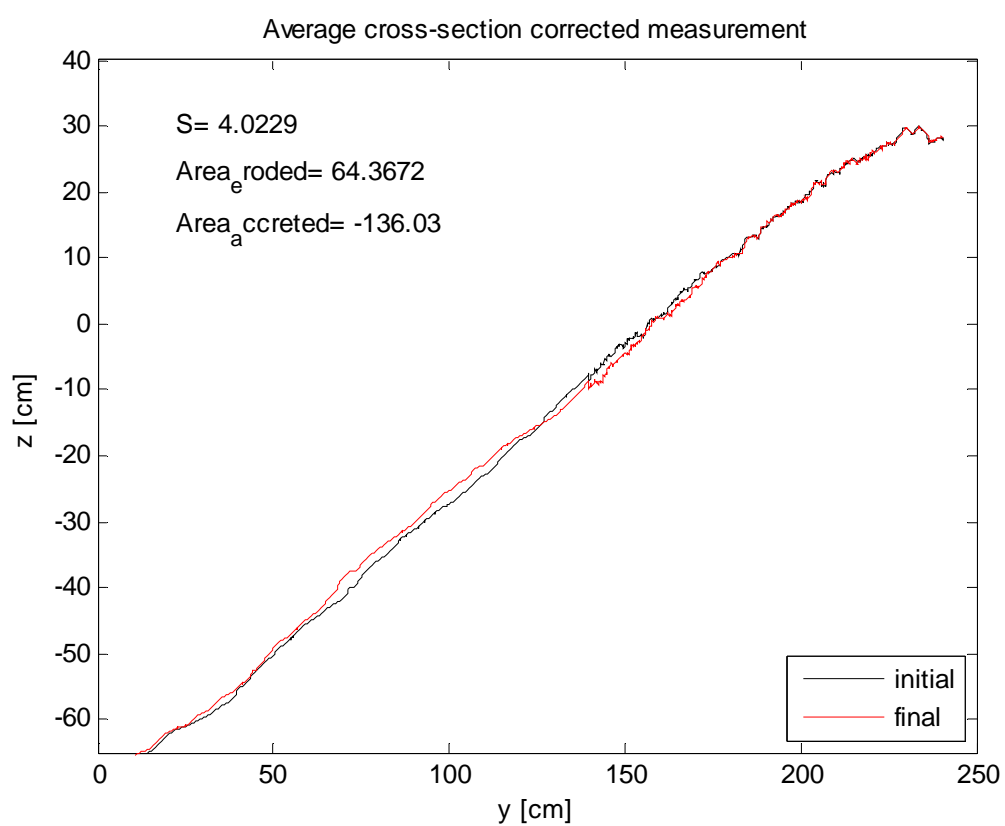
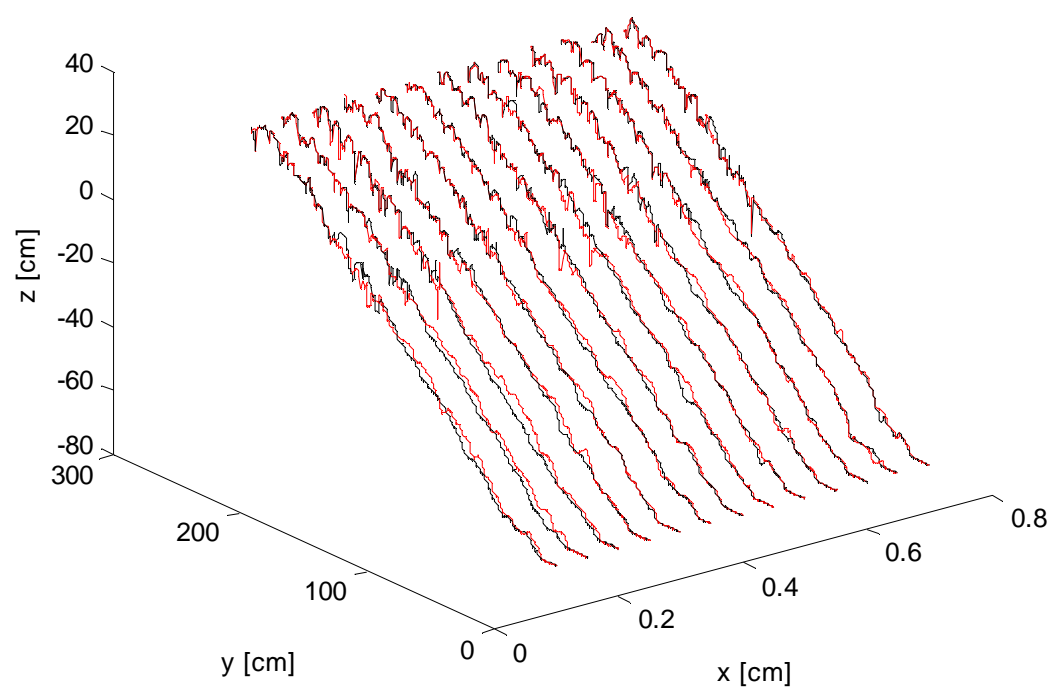




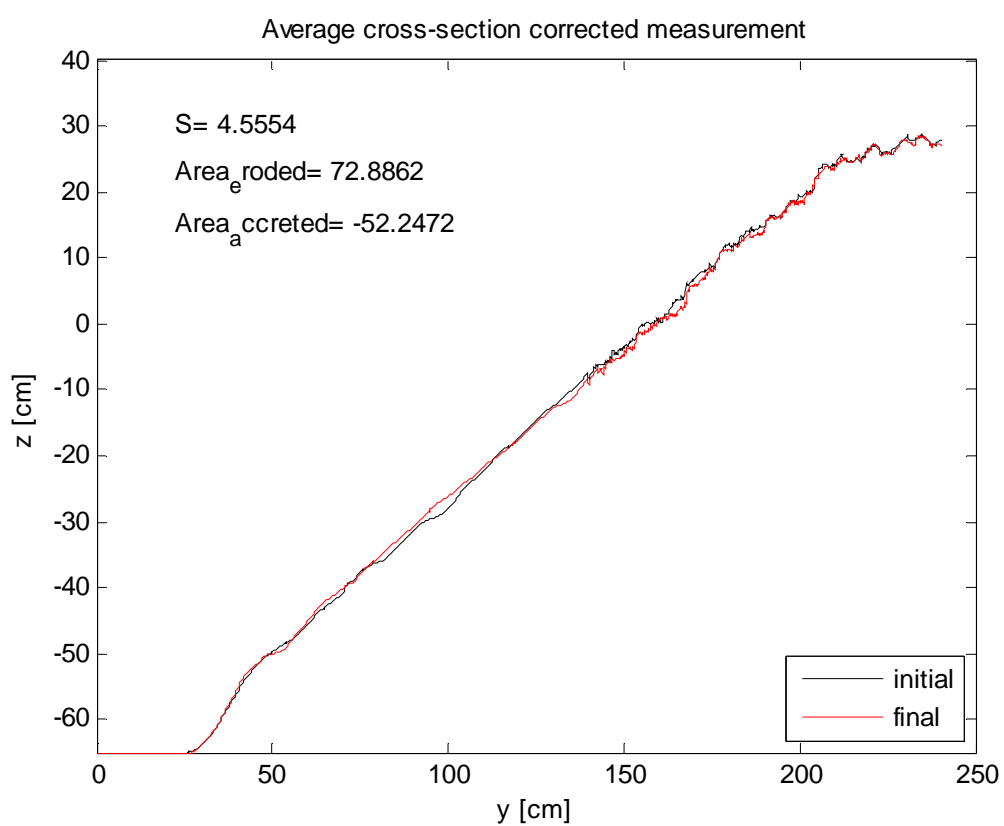
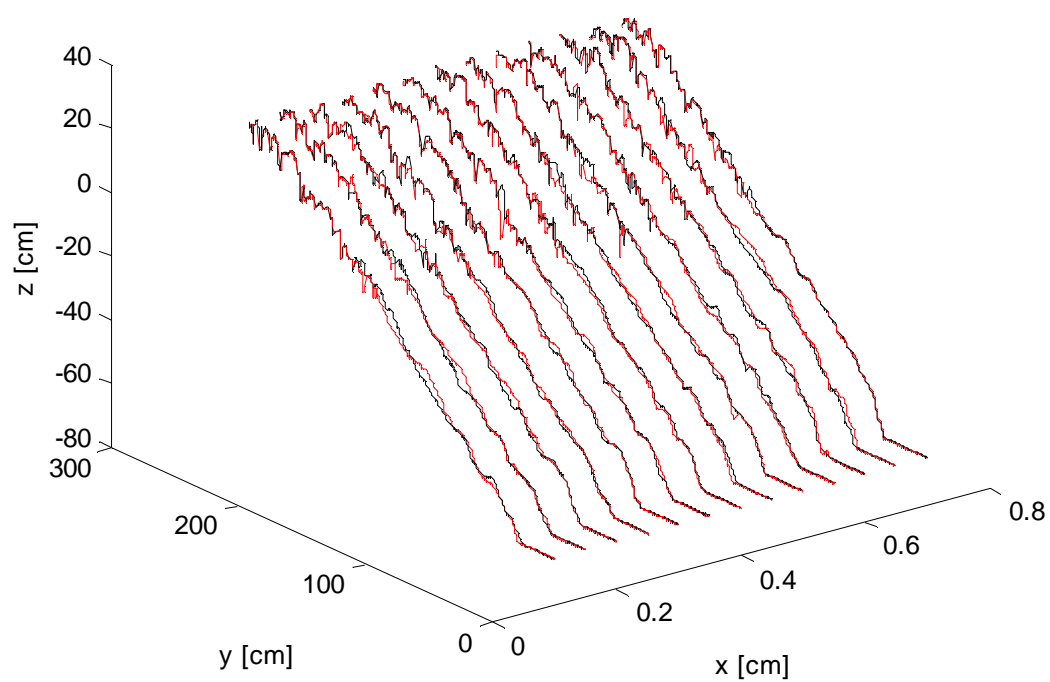




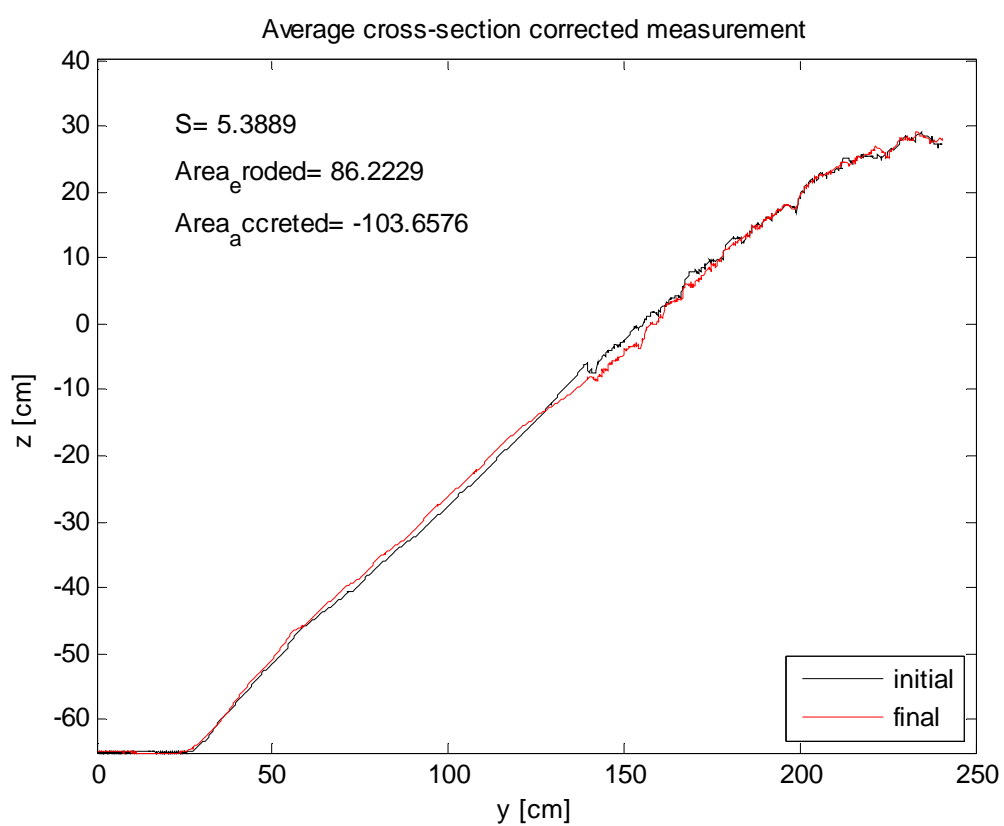
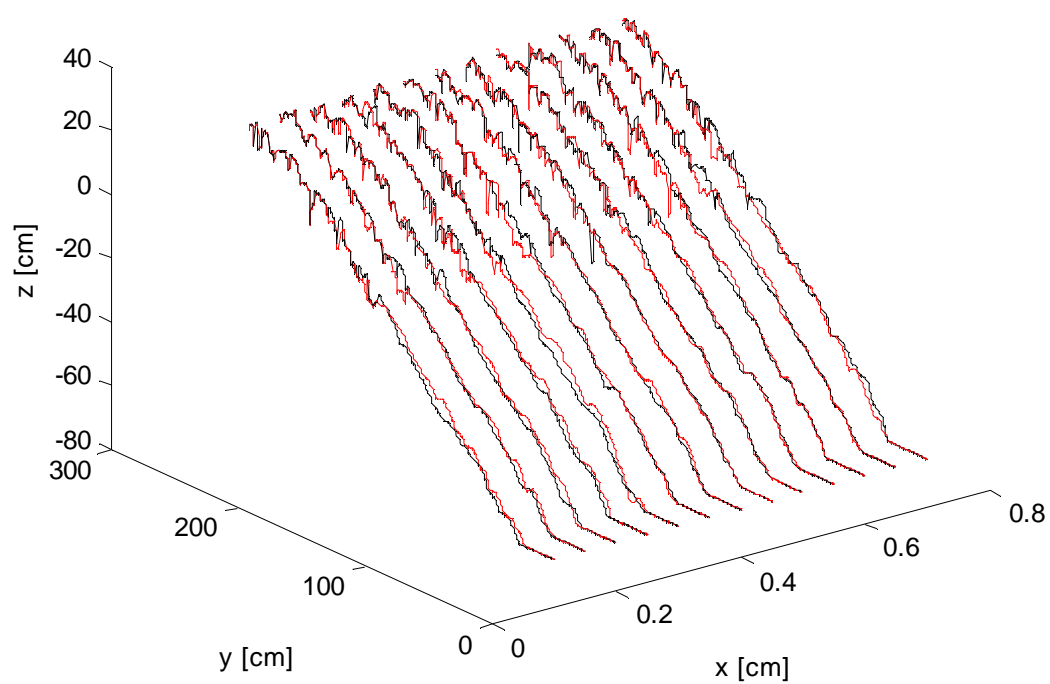


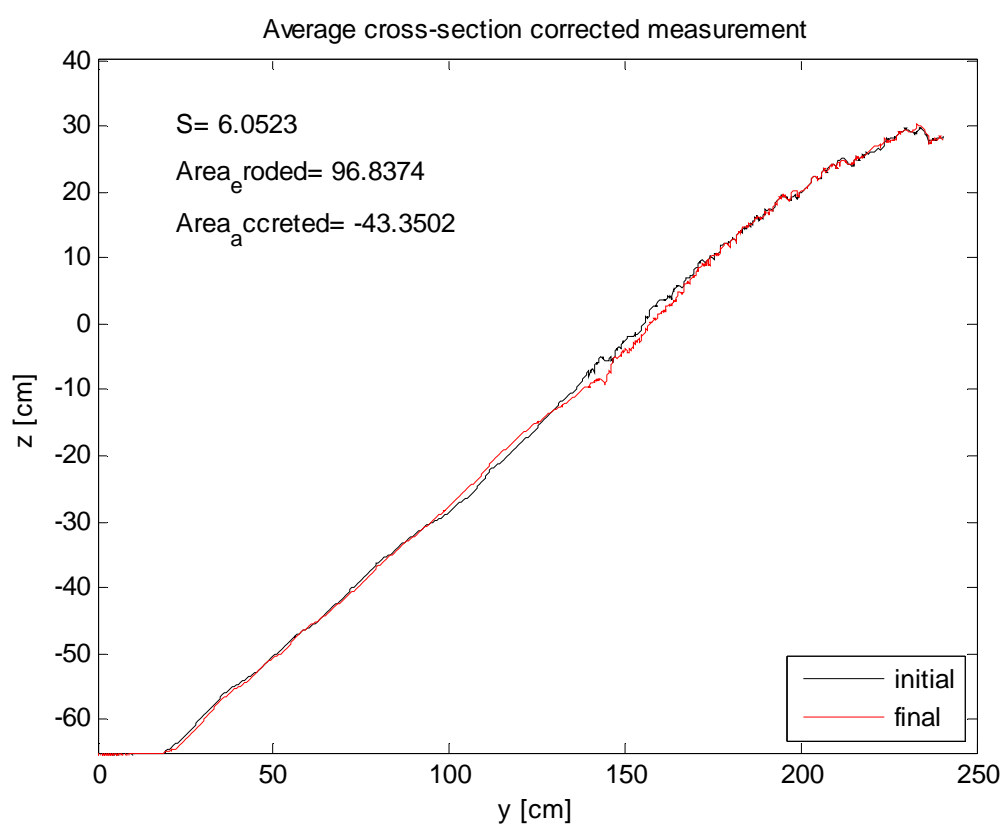
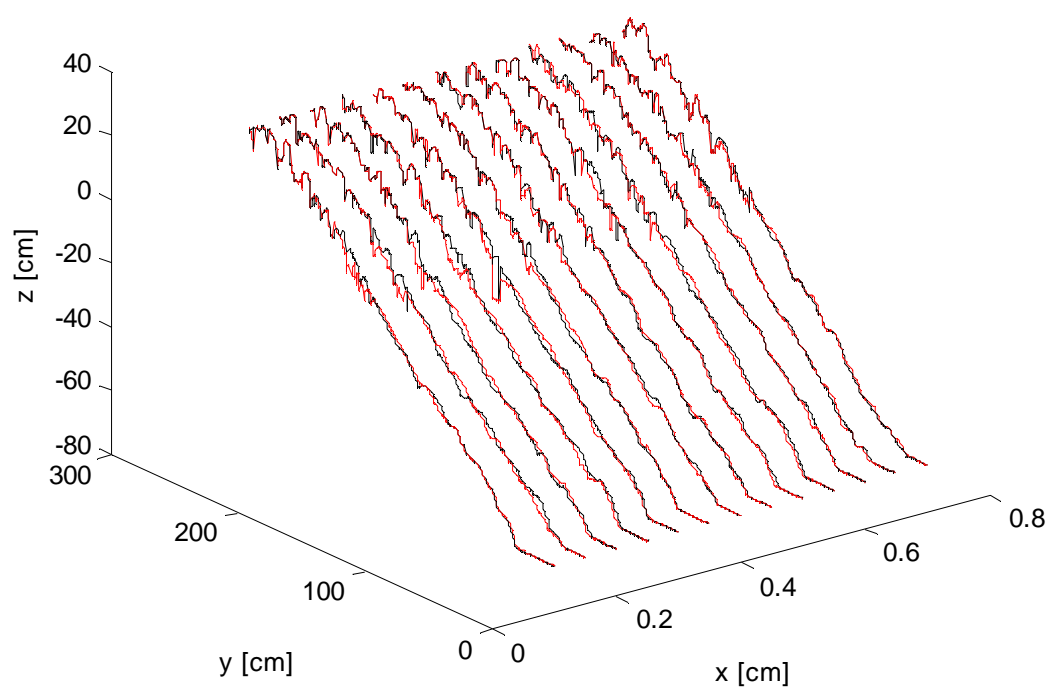


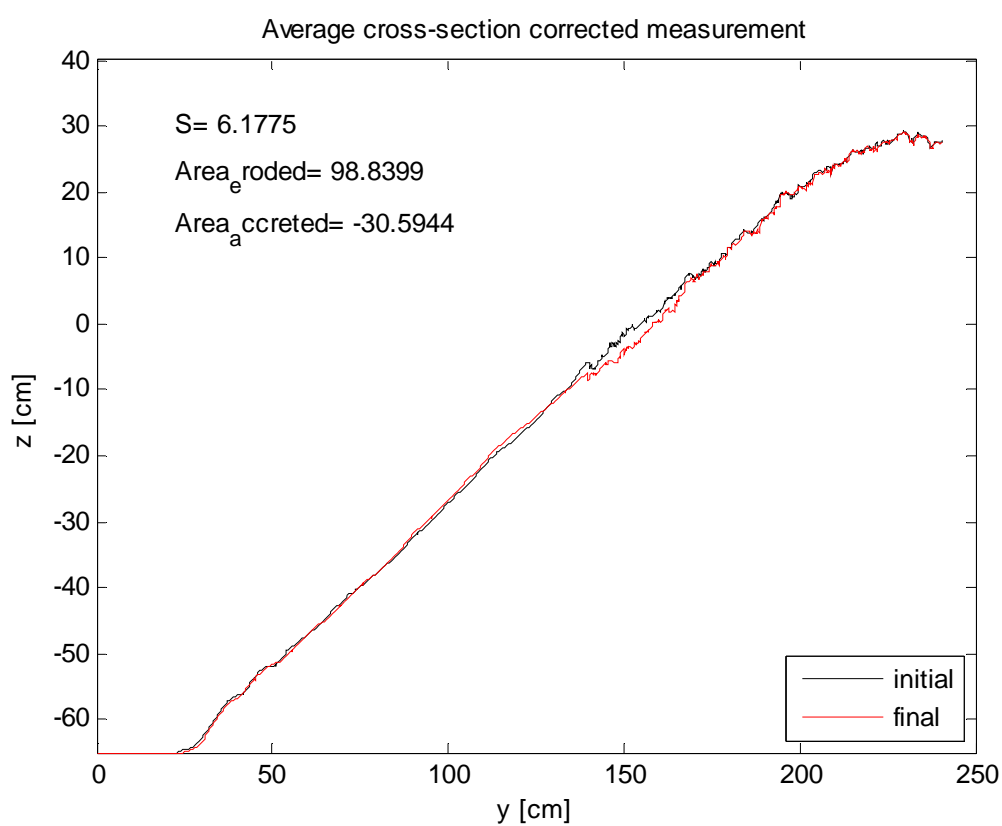
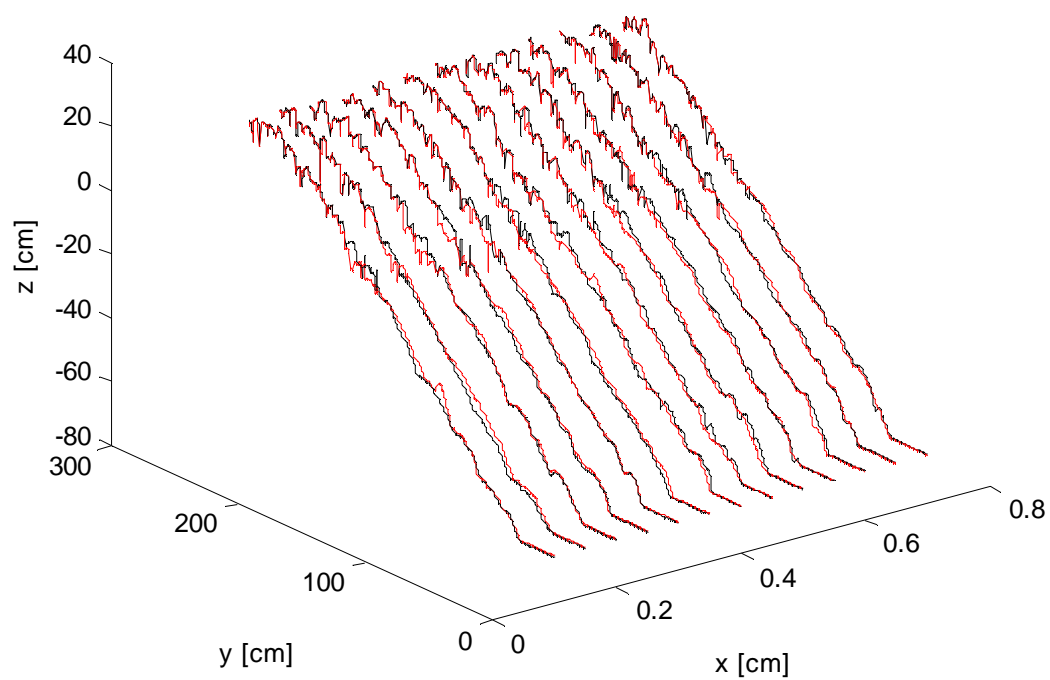
27b



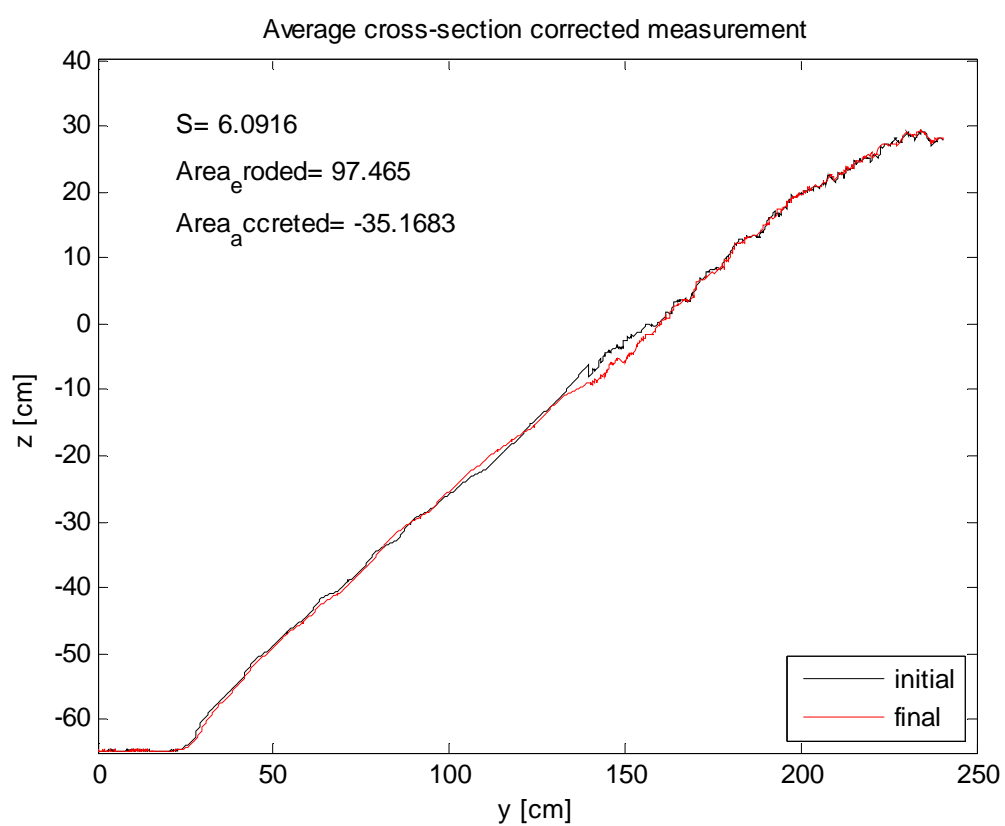
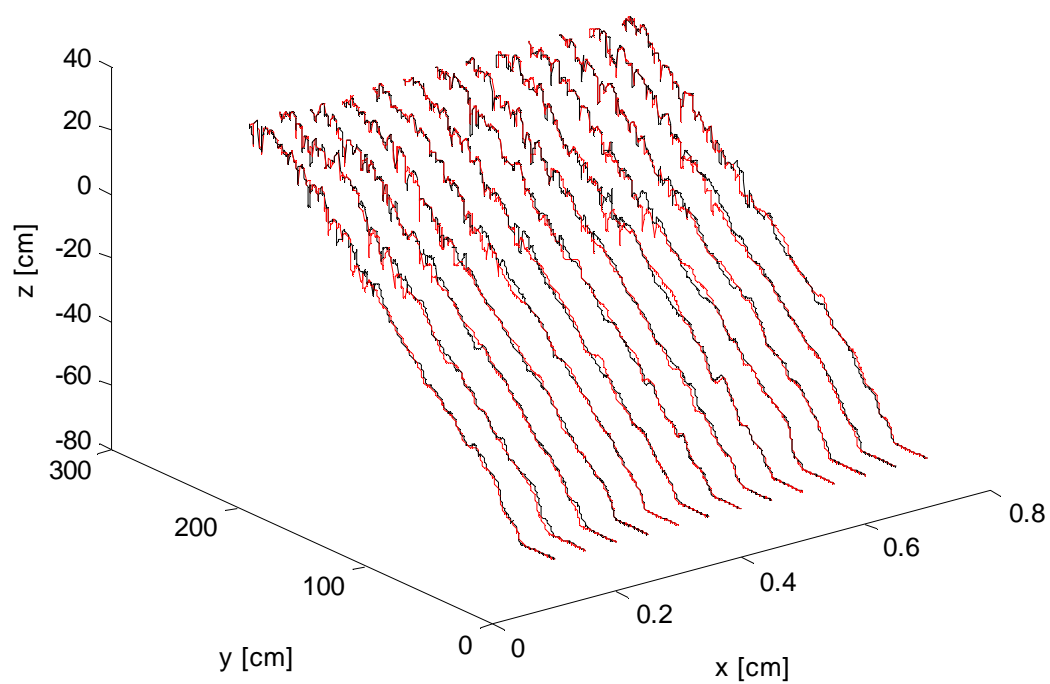
27c

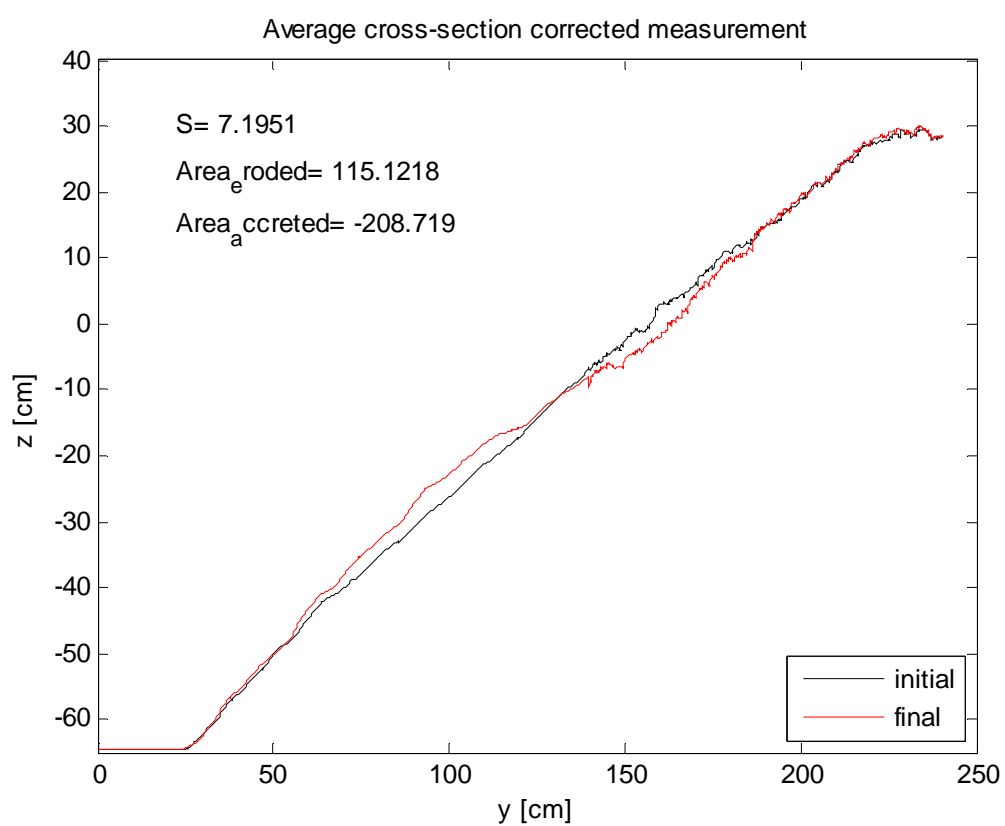
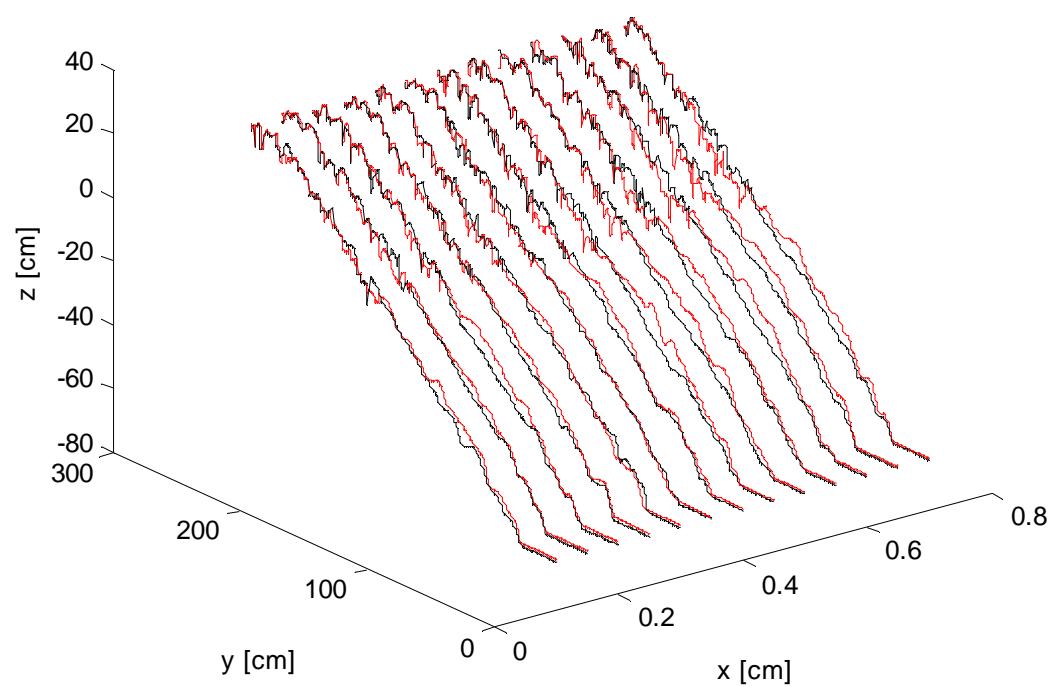












## Appendix F: Specifications Laser and Echo sounder

### Specifications laser ILD 1700-750

Type	ILD 1700-	2	10	20	40	50	100	200	250VT	500	750
Measuring range	mm	2	10	20	40	50	100	200	250	500	750
Start of measuring range	mm	24	30	40	175	45	70	70	70	200	200
Reference distance (MR)	mm	25	35	50	195	70	120	170	195	450	575
End of measuring range	mm	26	40	60	215	95	170	270	320	700	950
Linearity	FSO	±0.1 %	±0.08 %					±0.1 %	±0.25 %	±0.08 %	±0.1 %
Resolution <sup>1</sup>	µm	0.1	0.5	1.5	4	3	6	12	50	30	50
Measurement frequency programmable		2.5 kHz (1); 1.25 kHz (1/2); 625 Hz (1/4); 312.5 Hz (1/8)									
Light source (laser diode)		Wave length 670 nm, red, max. power 1 mW, laser class 2									
Permissible ambient light (at 2.5 kHz)		10.000 lx							15.000 lx	10.000 lx	
Spot diameter	SMR	80	110	320	230	570	740	1300	1500	1500	1500
	MR	35	50	45	210	55	60	1300	1500	1500	1500
	EMR	80	110	320	230	570	700	1300	1500	1500	1500
Temperature stability	% FSO/°C	0.025	0.01					0.025		0.01	

Type	ILD 1700-	2	10	20	40	50	100	200	250VT	500	750
Operating temperature		0 ... +50 °C							0 ... +55 °C	0 ... +50 °C	
Storage temperature		-20 ... +70 °C									
Protection class		IP 65 (with plugged connection)									
Power supply U <sub>B</sub>		24 V (11 ... 30 V) DC; max. 150 mA									
Measurement value output	selectable	4 -20 mA; 0 -10 V; RS422									
Voltage output		R <sub>i</sub> = 100 Ohm, I <sub>max</sub> = 5 mA, short-circuit proof									
Load current output		R <sub>Load</sub> < (U <sub>B</sub> -6 V) / 20 mA, R <sub>Load</sub> ≥ 250 Ohm for U <sub>B</sub> = 11 VDC									
Switching outputs	programmable	Error or/and limit values, short-circuit proof									
Switching inputs		Laser ON/OFF; Zero									
Synchronization	programmable	Simultaneous or alternating									
Sensor cable	Standard Extension	0.25 m (with cable jack) 3 / 10 m									
Elektromagnetic compatibility (EMC)		EN 61326-1: 2006-10 DIN EN 55011: 2007-11 (Group 1, class B) EN 61 000-6-2: 2006-03									
Vibration (acc. to IEC 60068-2-6) <sup>2</sup>		2 g / 20 ... 500 Hz									
Shock (acc. to IEC 60068-2-29) <sup>2</sup>		15 g / 6 ms									
Weight (with 25 cm cable)		550 g			600 g		550 g			600 g	

## Specifications echo sounder

Equipment types	ULTRALAB® UWS <ul style="list-style-type: none"> <li>• Specification xM : one measurement channel</li> <li>• Specification xM2 : two measurement channels</li> <li>• Specification 1Mx : 1 MHz</li> <li>• Specification 2Mx : 2 MHz</li> </ul>
Sensors	<ul style="list-style-type: none"> <li>• UWS2M : 2MHz, IP 68, M30x1.5, without temperature sensor</li> <li>• UWS1M : 1MHz, IP 68, M30x1.5, without temperature sensor</li> </ul>
Parameter settings	<ul style="list-style-type: none"> <li>• Via operating buttons, digitally using display, or</li> <li>• via serial interface (optional)</li> <li>• Code protected access</li> </ul>
Display	Integrated, 4-digit 12mm LCD display
Measurement range	Adjustable, max. travel time: 32 ms (approx. 23 m in water)
Technical resolution	1% of measurement range, max. +/- 1 mm (at constant ambient conditions)
Accuracy	4-digit (1mm to 9.999m measurement range)
Measurement repetition rate	max. 10 Hz
Voltage output	BNC socket: 0/2 – 10 V data output with zoom function
Switch outputs	(optional) <ul style="list-style-type: none"> <li>• 2 independent switch outputs for limit values</li> <li>• 1 switch output for error signals</li> </ul> max. switch voltage 50 V (optionally 250 V), max. switch current 5 A
Interface	(optional)  serial, RS-485 for data inquiry and parameter setting

	(semi-duplex operation, max. 32 devices on bus)
Power supply	230 VAC (110 VAC optional), 250 mA
Housing	approx. 330 / 115 / 260 mm width / height / depth IP 50
Temperature range	-20 ... +70°C
Scope of delivery	Laboratory device UWS, ultrasound sensor UWS, 10 m sensor cable, operating instructions, power cable